DESIGN AND SYNTHESIS OF TRIAZENE-SUBSTITUTED PUSH-PULL
DYES USING FORMAL [2+2] CYCLOADDITION-
RETROELECTROCYCLIZATION REACTIONS

A THESIS SUBMITTED TO
THE GRADUATE SCHOOL OF NATURAL AND APPLIED SCIENCES
OF
MIDDLE EAST TECHNICAL UNIVERSITY

BY

FLORA MAMMADOVA

IN PARTIAL FULFILLMENT OF THE REQUIREMENTS
FOR
THE DEGREE OF MASTER OF SCIENCE
IN
CHEMISTRY

JANUARY 2022

Approval of the thesis:

DESIGN AND SYNTHESIS OF TRIAZENE-SUBSTITUTED PUSH-PULL DYES USING FORMAL [2+2] CYCLOADDITION-RETROELECTROCYCLIZATION REACTIONS

submitted by **FLORA MAMMADOVA** in partial fulfillment of the requirements for the degree of **Master of Science** i**n Chemistry, Middle East Technical University** by,

Prof. Dr. Halil Kalıpçılar
Dean, Graduate School of **Natural and Applied Sciences**   _____

Prof. Dr. Özdemir Doğan
Head of the Department, **Chemistry**   _____

Assist. Prof. Dr. Çağatay Dengiz
Supervisor, **Chemistry, METU**   _____

Examining Committee Members:

Prof. Dr. Cihangir Tanyeli
Chemistry, METU   _____

Assist. Prof. Dr. Çağatay Dengiz
Chemistry, METU   _____

Prof. Dr. Özdemir Doğan
Chemistry, METU   _____

Prof. Dr. Metin Zora
Chemistry, METU   _____

Assist. Prof. Dr. Yunus Emre Türkmen
Chemistry, Bilkent University   _____

Date: 26.01.2022

I hereby declare that all information in this document has been obtained and presented in accordance with academic rules and ethical conduct. I also declare that, as required by these rules and conduct, I have fully cited and referenced all material and results that are not original to this work.

Name Last name : Flora Mammadova

Signature :

ABSTRACT

DESIGN AND SYNTHESIS OF TRIAZENE-SUBSTITUTED PUSH-PULL DYES USING FORMAL [2+2] CYCLOADDITION-RETROELECTROCYCLIZATION REACTIONS

Mammadova, Flora
Master of Science, Chemistry
Supervisor : Assist. Prof. Dr. Çağatay Dengiz

JANUARY 2022, 144 pages

Conjugated push-pull chromophores are valuable due to intramolecular electron charge transfer band (ICT), second and third order nonlinear optical properties. These extraordinary features allow to use them in the area of optoelectronics where advanced applications are possible. Organic light emitting diodes (OLEDs), solar cells, organic field effect transistors (OFETs) are some examples. Synthesis of push-pull chromophores is possible by click-type [2+2] cycloaddition-retroelectrocyclization (CA-RE) reactions. In this thesis, triazene-substituted terminal and non-terminal alkyne substrates are used as electron-donors which react with strong electron-acceptors TCNE and TCNQ. Optoelectronic properties of obtained push-pull dyes are characterized via UV/Vis spectroscopy and theoretical calculations.

Keywords: [2+2] cycloaddition-retroelectrocyclization, push-pull chromophores, triazene, optoelectronics.

ÖZ

İT-ÇEK TİPİ BOYALARIN KLİK-TİPİ [2+2] SİKLOKATILMA-RETROELEKTROSİKLİZASYON TEPKİMELERİ ARACILIĞIYLA DİZAYNI VE SENTEZİ

Mammadova, Flora
Yüksek Lisans, Kimya
Tez Yöneticisi: Dr. Öğr. Üy. Çağatay Dengiz

OCAK 2022, 144 sayfa

Konjuge it-çek tipi kromoforlar, molekül içi yük transfer özelliği, ikinci ve üçüncü mertebe doğrusal olmayan optik özellikleri nedeniyle oldukça değerli bileşiklerdir. Bu özellikler, gelişmiş uygulamaların mümkün olduğu optoelektronik alanında kullanılmalarına imkan verir. Organik ışık yayan diyotlar (OLED'ler), güneş pilleri, organik alan etkili transistörler (OFET'ler) bu bileşiklerin kullanım bulduğu örneklerden bazılarıdır. İt-çek tipi kromoforların sentezi, klik-tipi [2+2] siklokatılma-retroelektrosiklizasyon tepkimeleri ile mümkündür. Bu tezde, triazen ile türevlendirilmiş terminal ve terminal olmayan alkinlerin, güçlü elektron çekiciler TCNE ve TCNQ ile tepkimeleri incelenmektedir. Elde edilen it-çek tipi boyaların optoelektronik özellikleri UV/Vis spektroskopisi ve teorik hesaplamalar ile çalışılmıştır.

Anahtar Kelimeler: [2+2] siklokatılma-retroelektrosiklizasyon, kromofor, triazen, optoelektronik

This thesis is dedicated to *my family* for their endless support and love.

ACKNOWLEDGMENTS

TABLE OF CONTENTS

LIST OF TABLES

TABLES

LIST OF FIGURES

FIGURES

LIST OF ABBREVIATIONS

CA: Cycloaddition

CA-RE: Cycloaddition–Retroelectrocyclization

OLED: Organic light emitting diode

DFT: Density functional theory

CPCM: Conductor-like Polarizable Continuum Model

DDQ: 2,3-Dichloro-5,6-dicyano-1,4-benzoquinone

EDG: Electron donating group

ICT: Intramolecular charge-transfer

TD-DFT: Time-dependent density functional theory

TCNE: Tetracyanoethylene

TCNQ: 7,7,8,8-Tetracyanoquinodimethane

TCBD: Tetracyanobutadiene

D-A: Donor-Acceptor

DMA: Dimethylaniline

DEA: Diethylaniline

HDA: Hetero-Diels-Alder

HT: Head to Tail

HH: Head to Head

LIST OF SCHEMES

SCHEMES

xx

CHAPTER 1

INTRODUCTION

Organic chemistry allows designing, synthesizing, and improving different types of molecules to be used in a wide range of areas. Extensive studies have demonstrated that organic structures have optical, photoelectric, and electrical properties in their solid states.[1] The control of morphology, modifiability of chemical structures, and electron flow of advanced organic structures make them great candidates for application in electronic and optoelectronic devices. In addition to these properties, low fabrication costs and easy processing increased the interest in organic electronics in the last 50 years.[2]

Push-pull chromophores possess distinguished charge-transfer abilities, and that being the case, they have recently become the subject of attention. The fundamental molecular structure of push-pull chromophores possesses a strong electron donor part (D), and electron acceptor part (A) are connected through a π-conjugated spacer.[3] Push-pull chromophores are essential and desired structures for their optoelectronic properties in molecular and oligomeric[4] and polymeric platforms.[5] Intense intramolecular charge transfer (ICT) bands,[6,7] second and third-order nonlinear optical properties,[8,9,10] absorption and emission properties that lead to bathochromic shift,[11] tuning ability[12] are characteristics for the popularity of push-pull chromophores. These salient properties of push-pull chromophores make them promising candidates for optoelectronic and electronic applications,[11,13] such as in solar cells,[14,15] organic light-emitting diodes (OLED)[16]. ICT properties of push-pull chromophores result in a small Highest Occupied Molecular Orbital (HOMO) and Lowest Unoccupied Molecular Orbital (LUMO) gap in the structures, and tunability of the gap allows increasing application areas of these types of molecules.[17,18]

HOMO-LUMO frontier orbital energies can be calculated using computational chemistry methods and further approved by electrochemical methods such as cyclic voltammetry (CV).[19] Photophysical properties of push-pull chromophores can be investigated by considering absorption maxima (λ_{max}) values obtained from UV-Vis spectroscopy measurements.[20,21]

More than one structural key point affects ICT properties of push-pull chromophores, such as conjugation type, planarity, attached functional groups, the capability of electron donor and acceptor parts in the structure.[6] In this thesis, all these features will be investigated meticulously to give a clear idea.

Diverse synthetic methods can be used to obtain push-pull chromophores based on desired molecular structure types. Many of them contain cross-coupling reactions which require a large volume of solvents and the usage of toxic metals.[22,23] Besides, problems such as long reaction times, and high costs made researchers look for new methods to synthesize chromophores. Click chemistry covers complete environmentally friendly reactions with short reaction times, and in this thesis, click-type reactions have been used to prepare targeted structures.[24]

Click-type [2+2] cycloaddition (CA) and [2+2] cycloaddition-retroelectrocyclization (CA-RE) reactions are widespread methods to utilize for the synthesis of push-pull chromophores. These reactions are facile, cost-effective, and environmentally friendly, easy to purify and can be performed at ambient conditions.[24] The previously mentioned characteristics of click-type [2+2] CA and [2+2] CA-RE reactions motivated us to select and use them as our synthetic routes to obtain push-pull chromophores.

1.1 Conjugated Push-Pull Chromophores

Three types of conjugation can be encountered in the synthesis of push-pull chromophores, homoconjugation, spiroconjugation, and π-conjugation. Homoconjugated push-pull chromophores are separated by a spacer that is not conjugated (Figure 1). Spiroconjugation is a special case of homoconjugation with mutually perpendicular π electron systems that are connected. (Figure 1).[25]

Spiroconjugation   Homoconjugation π-conjugation
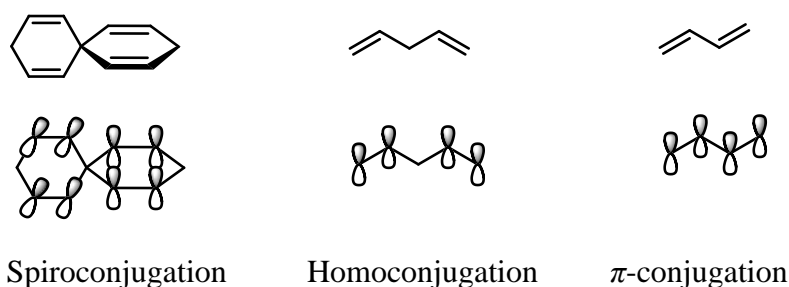
Figure 1. Representations of spiroconjugation, homoconjugation and π-conjugation.

In π-conjugated systems, donor and acceptor groups are conjugated through π electrons, alternating single and double or triple bonds (Figure 1). For each system, similar reactions are used to synthesize the desired molecule, but those molecules might have distinct electronic properties due to differences in electron delocalization or interactions. Conjugation type and length have a controlling impact on the properties of push-pull chromophores.[26] Herein, we will be focusing on the synthesis and analysis of π-conjugated and homoconjugated push-pull chromophores.

1.2   Non-planar Push-Pull Chromophores

Planar and non-planar push-pull chromophores can differ in their electronic and physical properties, such as solubility, sublimation ability, and thermal stability.[27]

3

It was assumed that molecular planarity is essential to obtain perfect electron charge transfer, but this idea was disproved by Diederich research group. There are many reported works on this issue.[28,29,30] Diederich and co-workers have done remarkable research related to the effectiveness of non-planar push-pull chromophores, and they have revealed that the physical properties of well-designed non-planar chromophores can predominate their planar-analogs.[29] The following DMA-substituted structures are examples of planar 4-(4-(dimethylamino)phenyl)but-1-en-3-yne-1,1,2-tricarbonitrile (**1**),[30] 2,3-bis((4-(dimethylamino)phenyl)ethynyl)fumaronitrile (**2**),[31] and non-planar **3**,[30] **4**,[32] **5**,[32] push-pull chromophores, respectively (Figure 2). The synthesis of non-planar push-pull chromophores is the main focus of this thesis. Comprehensive research on planar and non-planar push-pull chromophores proves their outstanding optoelectronic properties *via* UV/Vis spectroscopy, reduction potential (HOMO-LUMO gap) measurement by cyclic voltammetry, and computational chemistry.
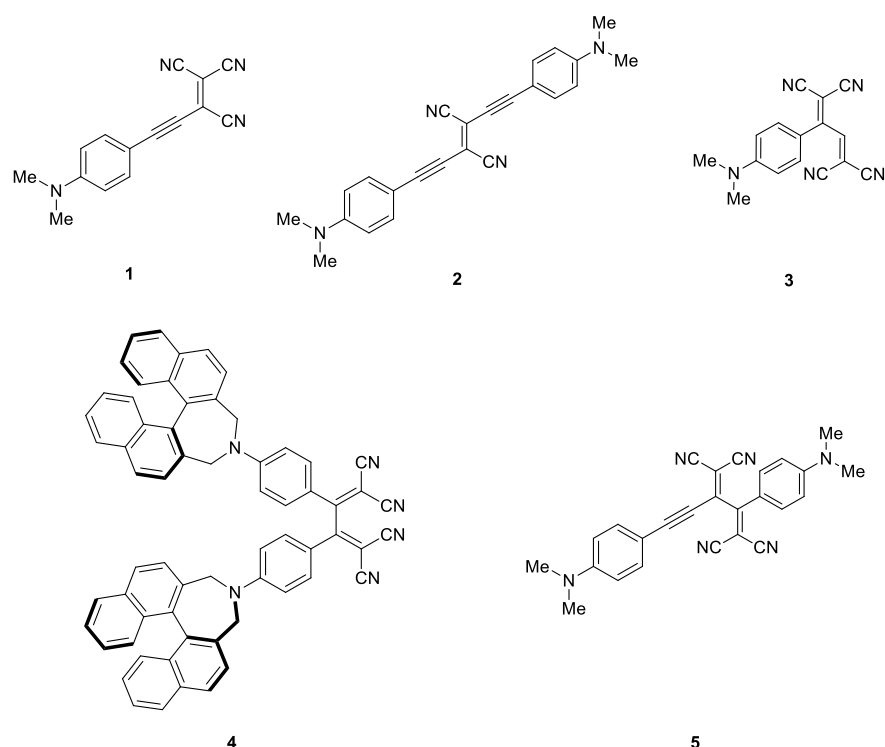
Figure 2. Planar **1,2** and non-planar **3,4,5** push-pull chromophore examples.

1.3 Click Chemistry

Click chemistry is a term that was entered into organic chemistry literature by K. Barry Sharpless in 2001.[24] According to the work, there are several criteria to call the reaction "click-type". Atom economy, variety of scope, efficiency, high reactions yields, no byproducts, or generation of harmless byproducts that can be removed easily are some of them.[24] Besides, mild reaction conditions such as room temperature, using nontoxic solvents or neatly performed reactions, and using no catalyst make a reaction to being called a "click" reaction. It is better to use simple methods for the purification process, such as distillation and crystallization.[24] Because of all points mentioned above, click-type reactions are desired and researched in organic chemistry.

In the same paper and their following works, Sharpless et al. describe several click-type reactions and the growing impact on different areas.[32,33,34] CA reactions (1,3-dipolar CA, Diels-Alder transformations), ring-opening reactions of strained heterocyclic electrophiles, oxidative cases of addition reactions can be a generalization of reactions for these reaction types. CA reactions represent click-type reactions clearly, especially the ones with heteroatoms.

1.3.1 Huisgen Dipolar CA Reaction

As previously mentioned, 1,3-dipolar CA reactions are very popular as an example of click chemistry.[35] The following scheme describes Huisgen dipolar CA reaction between bis(azide) **6** and alkyne **7**, which provides access to a five-membered ring bis(triazole) **8** (Scheme 1).[24]
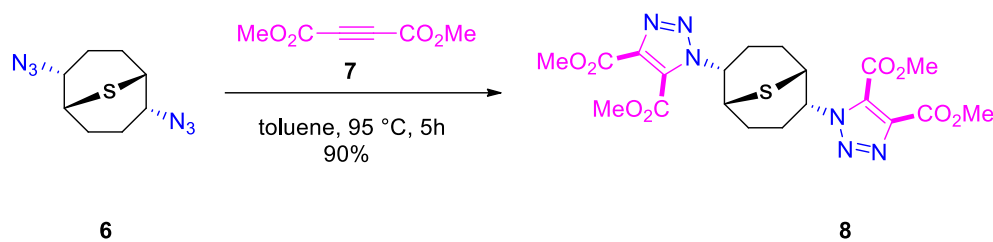
Scheme 1. Azide-alkyne 1,3-dipolar CA reaction.

1.3.2 Diels-Alder Reaction

Diels-Alder is [4+2] type pericyclic CA reaction. It is another example of CA reactions that are supposed to be a good candidate for click-type reactions according to Sharpless.[24] In 1928, Otto Diels and Kurt Alder reported a reaction between cyclopentadiene **9** and quinone **10** providing monoadduct **11** which was then transformed to diadduct **12** (Scheme 2).[36] The discovery of Diels-Alder reaction advanced scope of pericyclic reactions that are used in total synthesis of natural products.[37] Additionally, Diels-Alder click chemistry has been used in polymer synthesis in later years.[38,39]
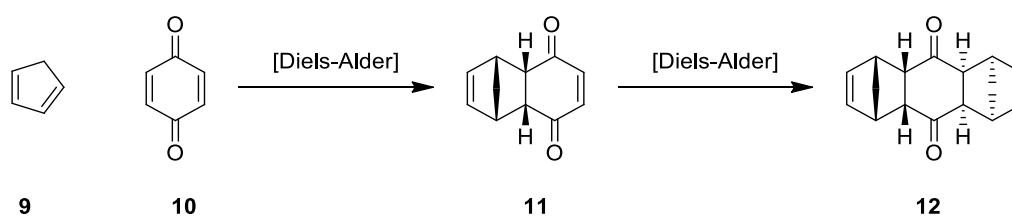
Scheme 2. Discovery of Diels-Alder reaction.

[4+2] Retro-Diels Alder reactions, such as the reaction between *trans*-cyclooctane **13** and tetrazine **14**, are also click reactions. It occurs at 25 °C and is completed after 40 minutes. The only by-product is N_2, and the reaction occurs in

water with a high quantitative yield which is desired property of a click-type reaction (Scheme 3).[40]
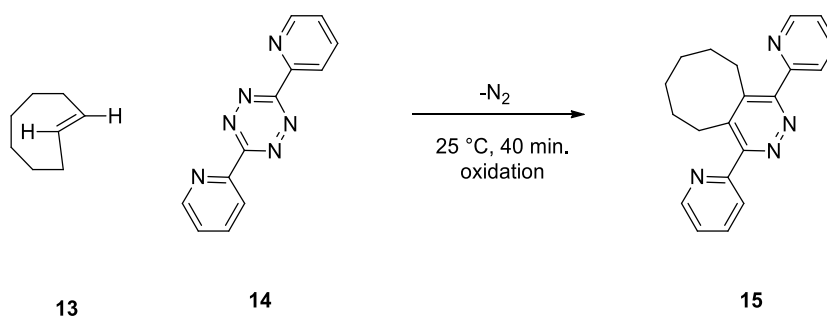
Scheme 3. [4+2] Retro-Diels–Alder reaction of *trans*-cyclooctene and tetrazine.

Besides aforementioned well-known click reactions, [2+2] CA and [2+2] CA-RE reactions are click-type reactions that allow trouble-free access to the synthesis of push-pull chromophores[41] and this will be the principal focus of this thesis.

1.4 Reactions for the Synthesis of Push-Pull Chromophores

Push-pull chromophores can be obtained by using many synthetic pathways and reaction types. Knoevenagel condensation,[42] Claisen-Schmidt condensation,[43] Horner-Wadsworth-Emmons reaction,[44] and cascade pericyclic reactions such as [2+2] CA-RE,[46] [4+2] hetero-Diels–Alder (HDA) reaction[47] are common reactions to generate desired chromophores. Among the examples mentioned earlier, pericyclic reactions attract considerable attention because of mild reaction conditions, high selectivity, a broad scope, and atom economy.[45] In this

thesis, we have utilized [2+2] CA and [2+2] CA-RE reactions to obtain intended push-pull chromophores.

1.5 [2+2] CA Reactions and Woodward-Hoffman Rules

In 1965, R. B. Woodward and Roald Hoffmann published a paper explaining stereochemistry of electrocyclic reactions.[48] In the same year they reported two more papers named "Selection Rules for "Concerted Cycloaddition Reactions" and "Orbital Symmetries and endo-exo relationships in Concerted Cycloaddition Reactions".[49,50] In these papers, Woodward and Hoffmann explained the mechanism of CA reactions and their relation with orbital symmetry. They derived "selection rules" for concerted CA reactions to occur. According to a published paper [4+2] reactions are thermally allowed, while [2+2] reactions are forbidden.[48,51] [2+2] CA reactions are possible only under photochemical conditions.[48] The orbital symmetry is a crucial factor for CA reactions, and preservation of it is decisive for the outcome of the reaction. This is related to the overlapping of HOMO and LUMO. In the following figure, HOMO and LUMO do not overlap. In a thermal [2+2] reaction, electron of π orbital has to be transferred to σ^*, which has very high energy.[52] According to Woodward-Hoffmann rules, overlapping HOMO and LUMO is possible when one of the reactants is excited photochemically (Figure 3).[53]
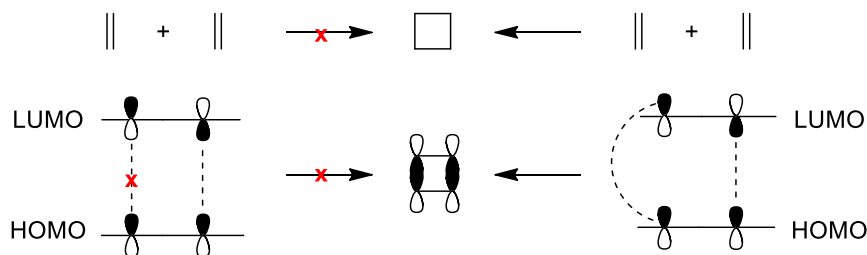
Figure 3. Thermally forbidden [2+2] CA reaction.

There are many examples of [2+2] photochemical CA reactions between two groups, enone-alkene and alkyne-alkene.[52,53,54] Scheme 4 is a general representation of [2+2] CA reactions. When alkenes with **16** and **17** with different R groups reacts cycloadduct **18** forms (Scheme 4). The second is the representation of the reaction of alkene **16** with alkyne **19** resulting in cycloalkene **20** (Scheme 4).
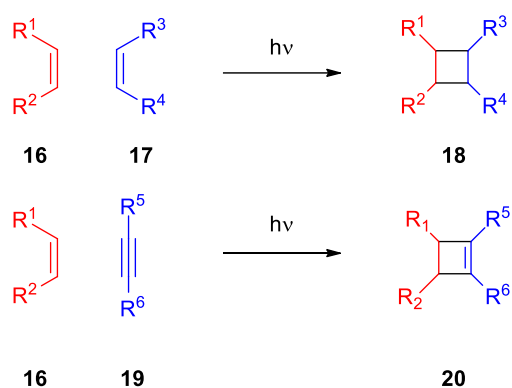
Scheme 4. [2+2] photochemical CA reactions.

In 1962, Eaton and co-workers published a paper about the reaction between enone and alkene. They revealed the photodimerization of enone **21** in 24 hours to obtain **22** in Head to Tail (HT) and **23** Head to Head (HH) fashion (Scheme 5).[54,55,56] When **21** reacts with **24** formation of **25** is observed.
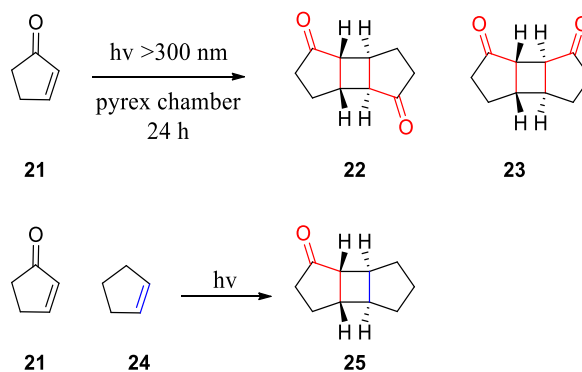
Scheme 5. Photodimerization and CA of cyclopentenone.

9

In 1964, Corey and co-workers reported a paper investigating regio-control of photochemical reactions systematically.[57] The paper contains pieces of information about photochemical CA reactions of 2-cyclohexenone with substituted olefins, such as isobutylene, 1,1-dimethoxyethylene, benzyl vinyl ether, and vinyl acetate. Subsequently, Cantrell et al. investigated and reported photocycloaddition reactions of some 3-substituted cyclohexenones and β-substituted enones.[58,59] Photochemical reaction between 3-methyl cyclohexanone **26** and 1,1,-dimethoxyetylene **27** yields products **28** and **29** along with other minor products, and acetal hydrolysis of the products with methoxyls at C-7 gives product **30** at the end (Scheme 6).
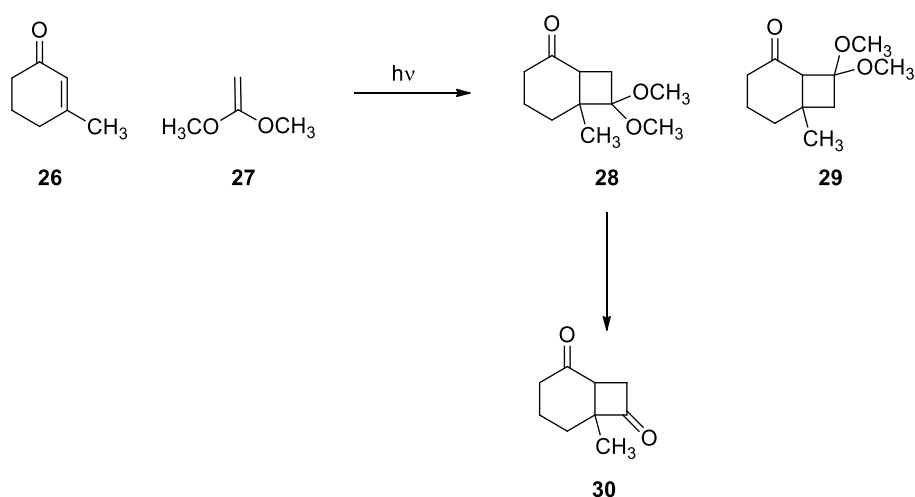
Scheme 6. Products from the reaction of 3-methylcyclohexanone with 1,1-dimethoxyethene.

Years of research and the discovery of potential of the photocycloaddition reactions gave rise to use of them in the synthesis of natural products. E.J. Corey is the first researcher demonstrated total synthesis of *d,l*-Caryophyllene and *d,l*-Isocaryophyllene by photochemical CA reaction.[58] After this early work, many groups followed the same strategy to synthesize natural products. Total synthesis of (±) Grandisol **31**,[60] β-Bourbonene **32**,[61] (±) Hippolachnin A **33**,[62] spatane diterpenes

e.g. spatol **34**,[63] are some of natural products that contain photocycloaddition reactions in their synthetic pathway (Figure 4).
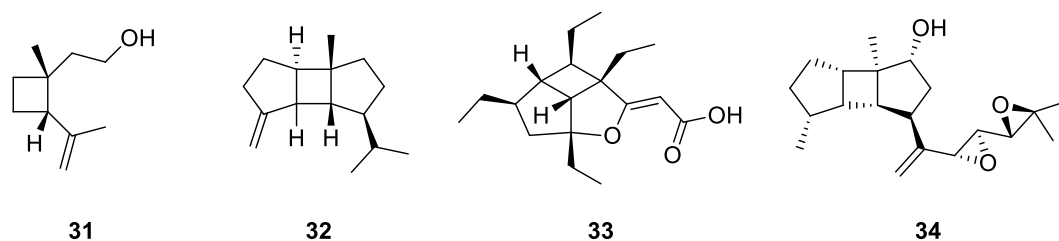
Figure 4. Natural products – grandisole, hippolachnin, spatol, and β-bourbonene synthesized *via* photochemical CA reactions.

1.5.1 [2+2] Thermal CA Reactions

The possibility of [2+2] CA reactions under only UV light was disproved by Reinhoudt in 1974.[64] During their investigation about thermal [2+2] CA reactions, Reinhoudt manifests many reactions occurring under thermal conditions depending on functional groups (Scheme 7). In Scheme 7, a formation of two σ bonds has been shown between two alkene-containing structures, and cyclobutene formation achieved *via* reaction of alkene and alkyne (Scheme 7).[64]

Mechanism of thermal [2+2] CA reactions was another issue that needed to be solved. According to Epiotis if one of the reactants is electron-rich and the other one is electron deficient, activation energy will be lowered.[64,65] This pioneering discovery led many researchers to dive into the area and to look for more reactions to widen the substrate scope for thermal [2+2] CA reactions. There are many examples of thermal [2+2] CA reactions between two groups, such as alkyne and allene,[66,67] alkene, and allene.[68]

11
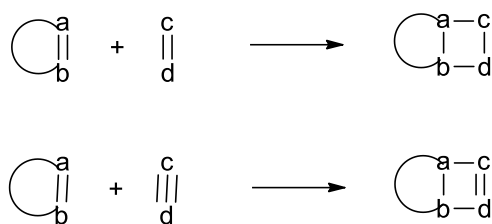
Scheme 7. General representation of cyclobutane and cyclobutene formation starting from alkenes and alkynes.

In 2010 Diederich and co-workers reported reaction between 2,3-dichloro-5,6-dicyano-1,4-benzoquinone (DDQ) **36** and acetylenic precursors **35** giving homoconjugated chromophores (Scheme 8).[69] Interestingly, upon heating of cycloadduct **37** at 80 °C in DCE, the formation of product **39** is discovered by the same group (Scheme 8). In the same year, Trofimov et al. informed about CA reaction between DDQ and alkyne as well,[70] followed by rearrangements of obtained [2+2] cycloadducts.[71]
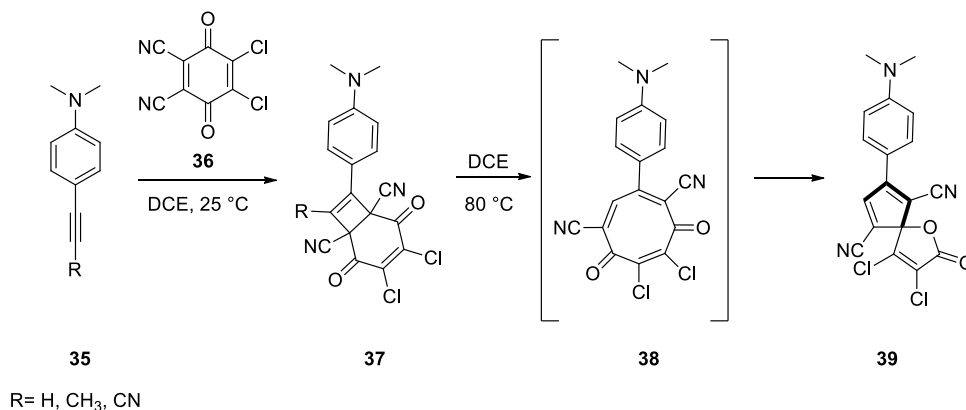
Scheme 8. Reaction between *N,N*-dialkylanilino derivatives and DDQ.

1.6   [2+2] CA-RE Reactions

As mentioned before, [2+2] CA-RE click reactions are an efficient and facile method for synthesizing push-pull chromophores. The reaction between electron-

rich alkyne and electron-deficient alkene occurs *via* the formation of cyclobutene ring followed by ring-opening retroelectrocyclization reaction (Scheme 9). Scheme 9 describes CA-RE reaction of alkyne **40** with tetracyanoethylene (TCNE) **41** and 7,7,8,8-Tetracyanoquinodimethane (TCNQ) **44**. During the course of reaction unstable cyclobutene intermediates **42** and **45** are formed. Even though [2+2] CA-RE reactions are scrutinized for decades, the exact reaction mechanism stays still unknown. The most intriguing question is related to the formation of cyclobutene structure that occurs via concerted or in two-step process.

EDG : Electron Donor Group
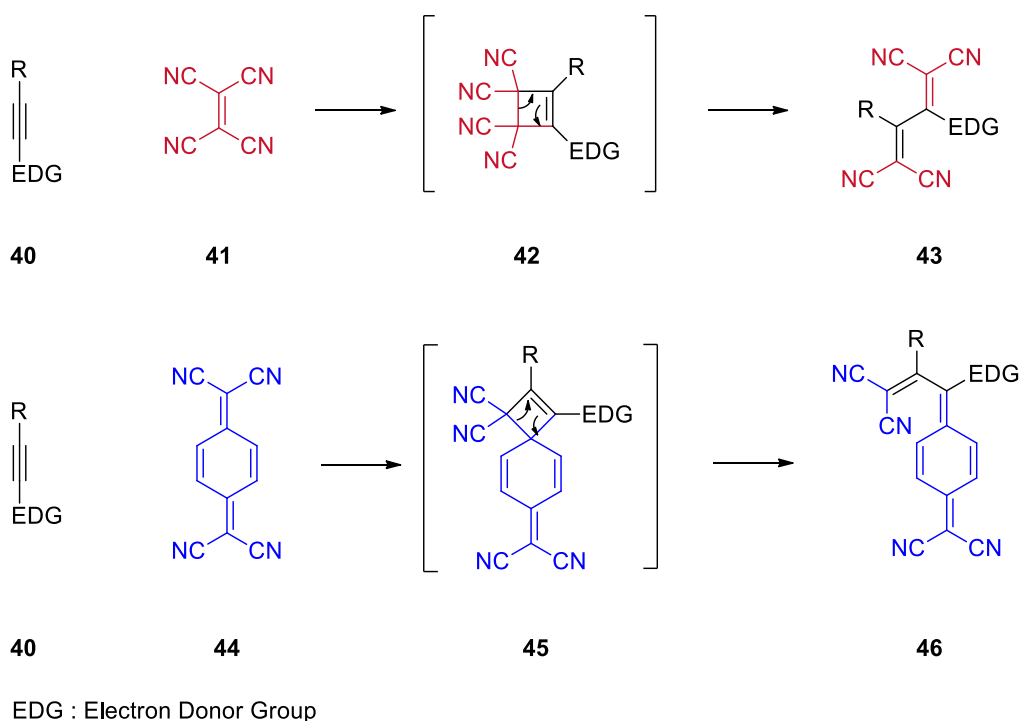
Scheme 9. General representation of [2+2] CA-RE reaction using electron-rich alkynes and electron-poor alkenes.

In 2007, Diederich and co-workers published a seminal paper proposing a mechanism for thermal [2+2] CA-RE transformations.[72,73,74] According to the proposal, reaction initially proceeds *via* zwitterionic or biradical intermediate species (Scheme 10).

13
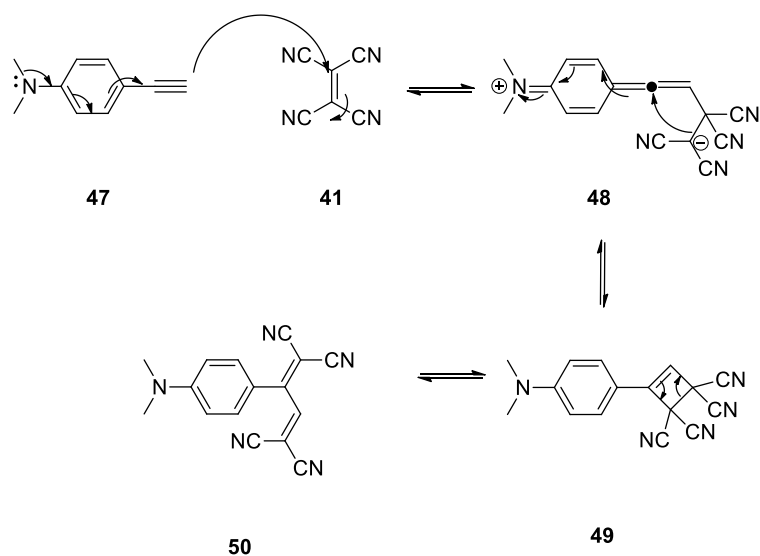
Scheme 10. [2+2] CA-RE reaction mechanism *via* zwitterionic intermediate.

The first discovery of [2+2] CA-RE dates back 1981. Bruce and co-workers reported a reaction between electron-rich ruthenium-acetylide complex **51** and TCNE **41** as an example of [2+2] CA-RE to synthesize organometallic 1,1,4,4-tetracyanobuta-1,3-diene (TCBD) derivative **53** (Scheme 11).[75]
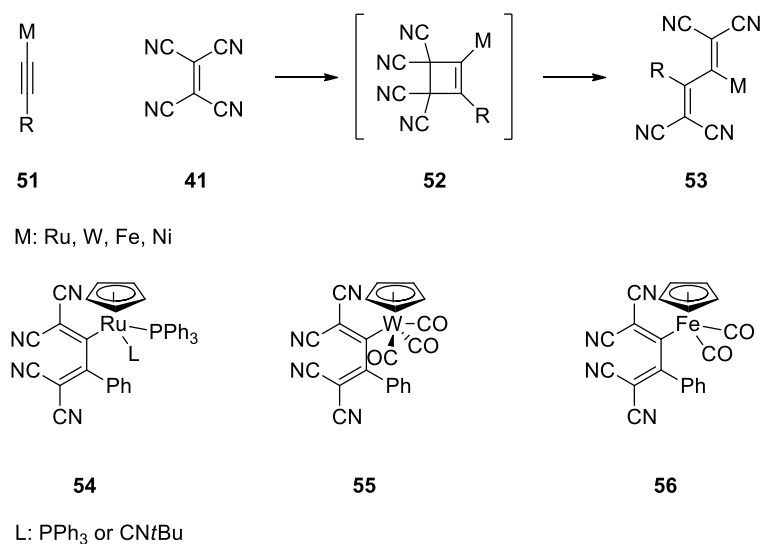
Scheme 11. Reaction between metal-substituted acetylides and TCNE to obtained TCBD products.

14

Besides, ruthenium **54**, tungsten **55**, and iron **56** complexes are among the synthesized organometallic TCBD derivatives. This pioneering work led to further investigations on this area and revealing the possibility of [2+2] CA-RE reactions between many other electron rich alkynes and electron poor alkenes. Takashi and co-workers reported a paper in 1999 to describe reaction with Pt(II) acetylides and TCNE **41** (Scheme 12).[76] μ-Ethynediyldiplatinium complex **57** was treated with TCNE **41** under reflux for 5 hours in benzene, and the products were in cis **58** and trans **59** forms. Structures were confirmed by spectral analysis and X-ray diffraction data.[76]
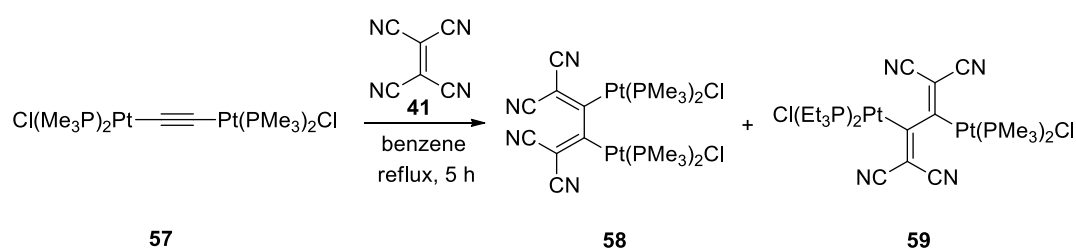
Scheme 12. Reaction between Pt(II) acetylide and TCNE.

In 1995, research group of Jen reported the first fully organic TCBD structure.[77] Later, Sutter followed this initial approach by describing the synthesis and characterization of bithiophene-containing chromophoric structures.[78] Yamashita and co-workers is another research group that reported D-π-A type systems before 2005.[79] In their work, electron donor compounds containing 1,3-dithiol-2-ylidine units react with an electron-deficient alkene TCNE at room temperature to synthesize desired donor-acceptor chromophores in good yields (45-85%). The figure shown below describes TCBD products that were obtained by Yamashita group *via* reaction between acetylene containing 1,3-dithiol-2-ylidene derivatives with cyano-rich alkene TCNE (Figure 5).[79] Products **60** and **61** are examples of mentioned TCBD structures. (Figure 5).

15
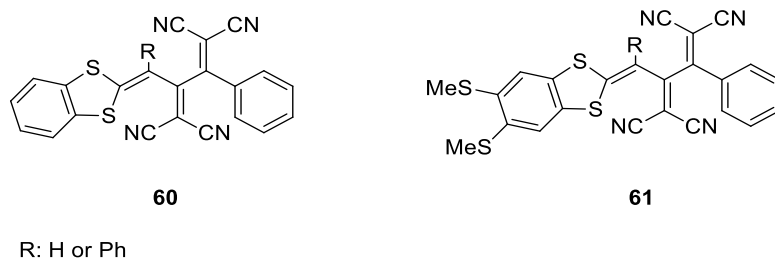
Figure 5. 1,3-dithiol-2-yldine containing TCBD products.

In 2005, Diederich and co-workers focused on synthesis of push-pull chromophores *via* thermal [2+2] CA-RE reactions by controlling reactivity of alkynes. The following Scheme 13 describes reaction between dimethylanilino substrates **35** and TCNE **41** to obtain 1,1,4,4-tetracyanobuta-1,3-diene derivatives **62a**, **62b**, and **62c**, in high yields (96-100%).[80]
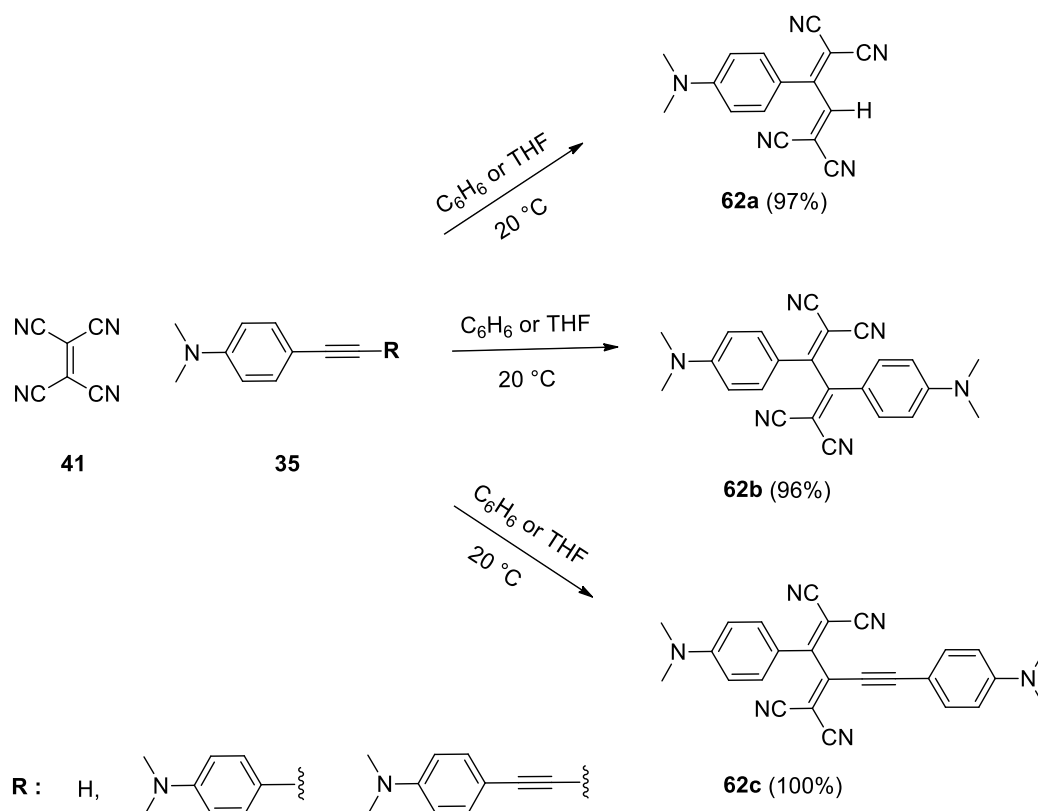
Scheme 13. Reaction between DMA-substituted alkynes and TCNE.

These reactions are usually conducted at room temperature, in mild conditions, by using nontoxic solvents or with no solvent and absence of by-products are great advantages. These characteristics make them to be regarded as "click-type" reactions.[24,41] Starting from 2005, Diederich group synthesized push-pull chromophores *via* click type [2+2] CA-RE reactions by focusing on enriching substrate scope of electron-rich alkyne. In their study, Diederich and co-workers manifested the principal impact of reactivity of alkyne groups in the reactions (Scheme 14).[72] Non-terminal alkyne group containing starting materials **63** reacted with TCNE **41** and resulted in TCBD products **64**, **65,** and **66** in good to high yields. Therefore, it was clear that with sufficient activation of alkyne group, the reaction between donor and acceptor groups occurs at mild conditions and results in high yields (Scheme 14).
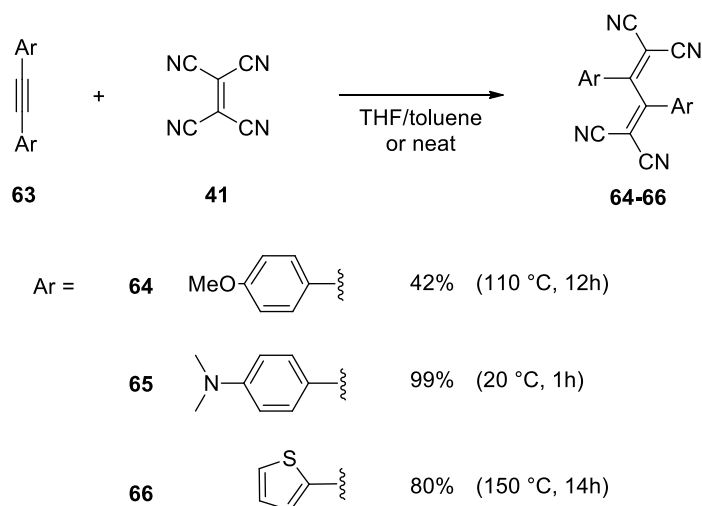
Scheme 14. Reaction between non-terminal alkynes and TCNE.

1.7 Common Electron Donor and Electron Acceptor Structures

As mentioned before, [2+2] CA-RE reactions requires electron donor alkyne and electron acceptor alkene structures to give push-pull chromophores.[41,75] For

decades, researchers have been working on improving or finding structures to obtain the most effective push-pull chromophores. Cyanide containing alkenes such as TCNE **41**,[80,81] TCNQ **44**,[80,72] 2,3,5,6-Tetrafluoro-TCNQ (F$_4$TCNQ) **67**[82] are the most used ones (Figure 6). The strong electron-withdrawing ability of cyanide groups causes them to have a great potential to be subjected to [2+2] CA-RE reactions. Exocyclic double bond of TCNQ and F$_4$TCNQ reacts with alkyne with complete regioselectivity.[82] All these structures are commercially available which is another advantage in terms of the practicality of synthesis. TCNE is the first compound that has been used for [2+2] CA-RE reaction by Takashi and co-workers in the 1990s.[83]
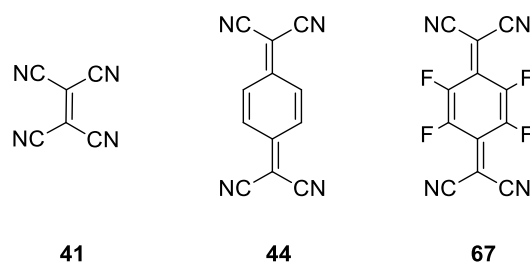
Figure 6. Common electron-deficient olefins used in thermal [2+2] CA-RE.

TCNE, TCNQ, F$_4$TCNQ are used for the synthesis of conjugated push – pull chromophores which are accessed through [2+2] CA-RE reaction. Beside its role as an oxidant (DDQ) **36** is utilized as strong electron acceptor in [2+2] CA reactions (Figure 7).[84]
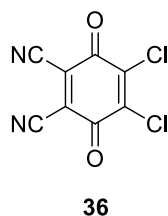
Figure 7. Electron-deficient alkene : 2,3-dichloro-5,6-dicyano-1,4-benzoquinone (DDQ).

18

DDQ reacts with alkyne and yield in homoconjugated push-pull chromophores and spiro systems *via* [2+2] CA reaction and electrocyclic ring opening reaction followed by a transannular rearrangement respectively.[69] There are examples of synthesized electron deficient alkenes to expand the scope. Some of them are (S)-ethyl 2-(4-(2,2-dicyanovinyl)benzamido)propanoate (**68**), (Z)-2-(5-(4-(diethylamino)benzylidene)-4-phenylthiazol-2(5H)-ylidene)malononitrile (**69**), 2-(4-azidobenzylidene)malononitrile **70**, 2-phenylethene-1,1,2-tricarbonitrile (**71**) (Figure 8).[85,86,87,88]
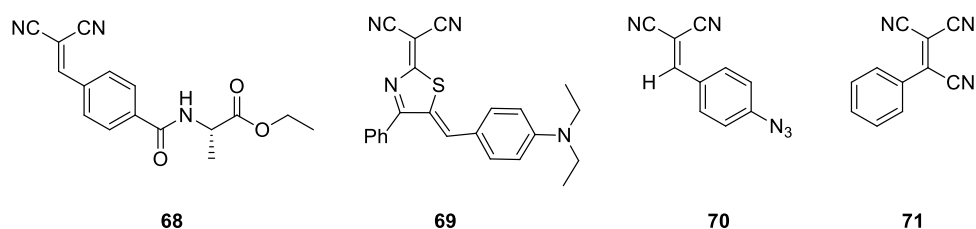
Figure 8. More of examples of electron deficient olefins.

Obviously, another focus in the synthesis of push-pull chromophores *via* [2+2] types of reactions is to improve alkyne structure by controlling its substituents. The first work by Bruce et. al.[75] was followed by many other papers to synthesize novel alkyne structures.[89] *N,N*-dimethylanilino (DMA)-substituted alkynes and their substrates have been synthesized by Diederich and co-workers in 2005.[30] In that work, 1,1,4,4-tetracyanobuta-1,3-diene moieties have been obtained with a reaction between DMA-substituted alkyne and TCNE *via* [2+2] CA-RE reacion (Scheme 13)[30] In the following years, Diederich group published papers on push-pull chromophores demonstrating reaction of different alkyne substituted structures with TCNE or TCNQ.[72,90,91] Electron donor alkynes are not limited with DMA, the following structures are some of examples that has been used to get TCBD products. Derivatives of triphenylamine **72**,[92] carbazole **73**,[93] urea **74**,[94] azulene **75**,[95] cyclopenta[b]furan-2-one (**76**),[95] ferrocene **77**,[6] with terminal alkyne groups takes part in formation of push-pull chromophores (Figure 9).
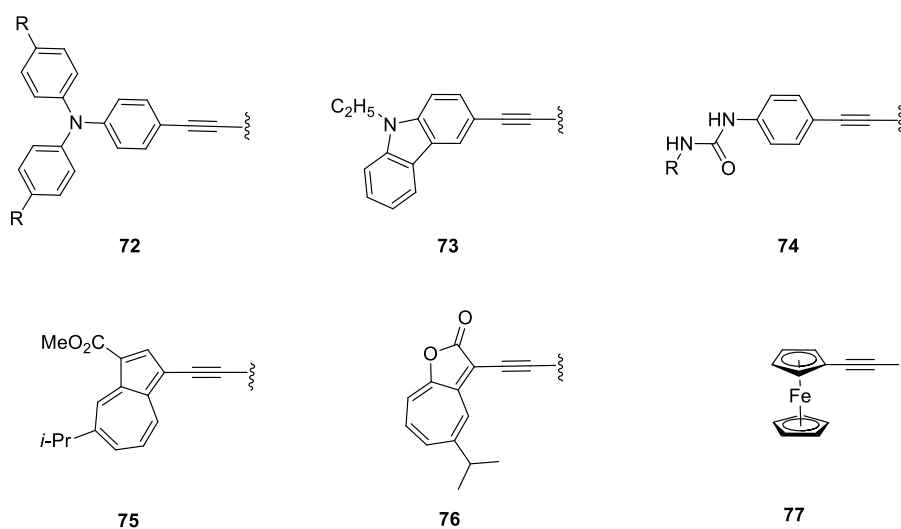
Figure 9. Electron donor alkyne derivatives used in [2+2] CA-RE reactions.

Conjugation of the system is essential in terms of increasing potential optoelectronic properties of push-pull chromophores.[17] On the grounds of this, improving conjugation in D-π-A systems is another target for the organic chemistry community. In 2005, Diederich and co-workers published a paper demonstrating non-terminal alkyne as an electon-donor substrate.[31] Figure 10 describes synehtsized and characterized electron donors **78**, **79**, and **80** (Figure 10).[31]
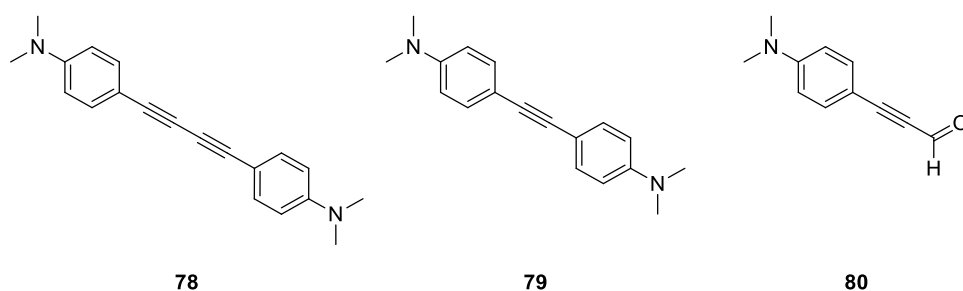
Figure 10. Non-terminal alkyne derivates used in [2+2] CA-RE reactions.

Tetrathiafulvalene (TTF) **81** and ferrocenyl (Fc) **82** substituted electron donors are other examples for non-terminal alkyne containing substrates to synthesize push-pull chromophores (Figure 11).[6]
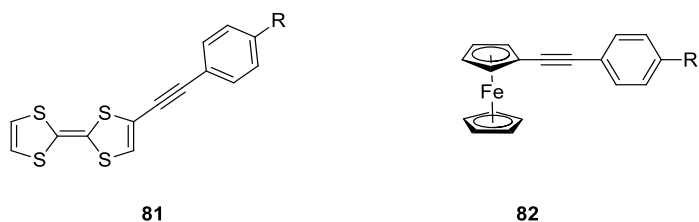
Figure 11. More of examples of non-terminal alkyne derivates used in [2+2] CA-RE reactions.

1.8 Aim of Study

Intense intramolecular charge transfer featured push-pull chromophores are studied extensively in the last few decades due to their substantial potential in optoelectronic devices. Taking advantages of pericyclic, "click chemistry"-type [2+2] CA and [2+2] CA-RE reactions chromophores can be prepared straightforwardly. For that purpose, finding new prospective electron donor substrates is a principal factor. Even though the synthesis of substrates as an electron-donor is a rather hot topic for a long time, it is still a barrier to the synthesis of push-pull chromophores. The reason behind it finding stable, sufficiently electron-donor, easily purified substrates is very challenging. The second chapter of this thesis concentrates on the synthesis of triazene group containing electron donor terminal alkyne substrates. Stable, easily purified triazene-substituted electron donor alkyne structure is novel in the literature and has been synthesized by our group. To obtain TCBD products thermal [2+2] CA-RE reaction is performed. TCNE and TCNQ were used as electron acceptor alkene structures. Throughout the chapter, experimental sections will be provided and UV/Vis spectroscopy data will be given alongside computational studies. The third chapter of the thesis holds synthesis of non-terminal alkyne substrates to expand substrate scope further. Those molecules were obtained *via* Sonogashira cross-coupling and Hay coupling reactions. Even though the reaction of two triazene group containing Sonogashira cross-coupling products and dimers were unsuccessful, replacing one triazene group with *N,N,*-diethyl-4-

aniline solved the problem. At the end, the reactions of the above-mentioned substrates with TCNE, TCNQ, and DDQ became successful and push-pull chromophores were obtained by [2+2] CA and [2+2] CA-RE reactions. All synthesized TCBD molecules are studied experimentally and characterized.

CHAPTER 2

RESULTS AND DISCUSSION

2.1 Design and the Synthesis of Triazene-based Push-Pull Chromophores

2.1.1 Synthesis of Triazene-Substituted Alkyne Substrates

Despite the efforts for decades, the insufficient substrate scope of alkynes stays the biggest challenge in [2+2] CA and [2+2] CA-RE reactions. In this chapter, our purpose was to synthesize push-pull chromophores containing a brand-new donor groups that is used in click-type CA-RE reactions. To achieve the goal, we came up with the idea of using triazene group as an electron-donor component. Triazene's function was framed to masking aryl iodide substrates for branched dendrimer synthesis.[96] Also, it has been used in medicinal chemistry,[97,98,99,100] polymer, and oligomer synthesis,[101] as a protecting group in natural product synthesis,[102] and to form heterocycles.[103] Even though it has quite a wide range of applications, until our work, there is not much in the literature related to an electron-donor capability of triazene groups. The results will be discussed in this chapter , reported in Journal of Molecular Structure in 2019.[20]

Triazene-substituted substrates were synthesized in three steps (Scheme 15). Applied synthetic pathways have been reported by Hecht[104] in 2008 and our group in 2019.[84] The first step was commenced with commercially available 4-iodoaniline (**83**), and addition of HCl, $NaNO_2$ caused to in situ formation of diazonium salts. Iodo-triazene **84a-f** were obtained by adding the required amount of dialkylamines. Sonogashira cross-coupling reaction allowed to obtain **85a-f** by adding an excess

amount of trimethylsilylacetylene at room temperature. As a last step to afford **86a-f** simple deprotection with K_2CO_3 is used. Yields for the final products were in between 30-77%.

^{1}H and ^{13}C NMR was used to characterize all products in each step. Acyclic alkyl containing molecules showed relatively broad peaks in ^{13}C NMR due to limited free rotation around N-N bond. This finding is in agreement with previously reported literature results.[105]
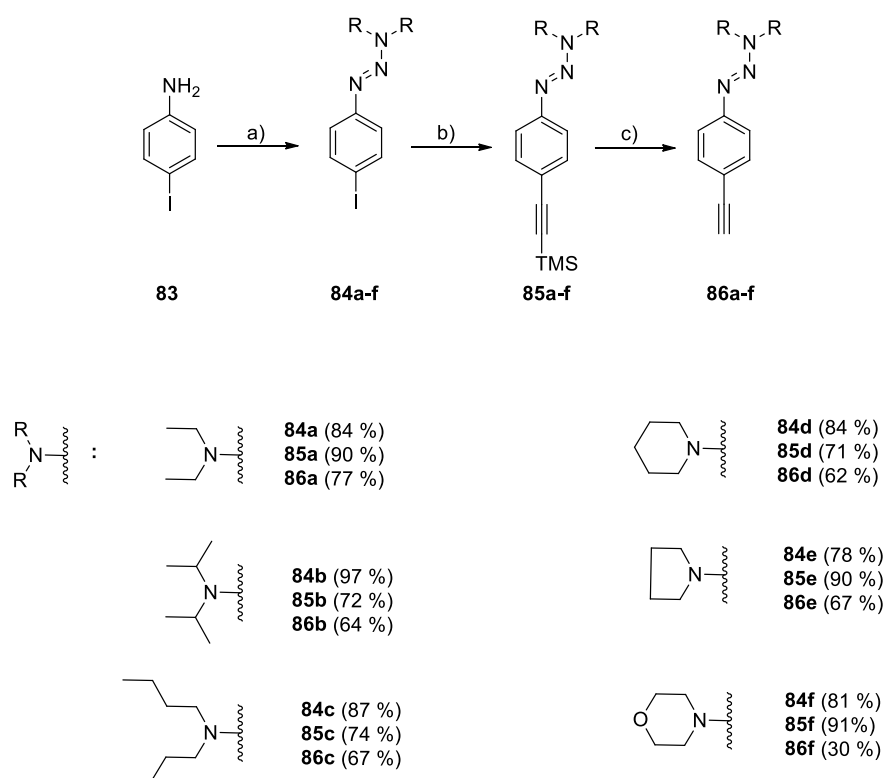
Scheme 15. Synthesis of electron-rich alkyne substrates.
a) i) HCl, $NaNO_2$; ii) MeCN, H_2O; iii) K_2CO_3, R_2NH; b) TMSA, [PdCl$_2$(PPh$_3$)$_2$], CuI, Et$_3$N, r.t. c) K_2CO_3; MeOH, r.t.

2.1.1 Synthesis of Triazene-Substituted Push-Pull Chromophores

Targeted conjugated push-pull chromophoric structures were obtained through the reactions between triazene-substituted alkyne substrates **86a-f** and TCNE **41** *via* click-type formal CA-RE reaction cascade (Scheme 16). The reported reactions were conducted in dichloromethane (DCM) at room temperature in one step, making it practically easy and very efficient (Scheme 16). Starting materials were consumed fully, and no side product formation was observed in all cases.

Even though all push-pull dyes **87-92** were obtained quantitatively, purification was a challenge. Decomposition of the products was observed while interacting with silica. This obstacle is circumvented by taking advantage of the solubility of synthesized dyes in DCM, but not in *n*-hexane. Push-pull dyes **87-92** were washed with *n*-hexane, and therefore, impurities were removed. We presumed that **87-92** are unstable in acidic and basic conditions. For this reason, column chromatography could not be applied for purification. Scheme 16 describes the overall reaction and quantitative yields for each push-pull chromophores changing from 42% to 96%. Acyclic substituents **87-89** were obtained in high yields 76-96%. However, pyrrolidine and morpholine containing adducts gave lower yields (42-46%). Interestingly, piperidine-containing push-pull chromophore was obtained in 92%. Formation of insoluble charge transfer complexes could be a reason for this difference in yields.

There was no correlation between donor strength of triazene groups and yields of push-pull dyes. All dyes **87-92** were solid and possess dark-purple color. It worth to mention that all dyes are quite stable under ambient conditions for weeks.
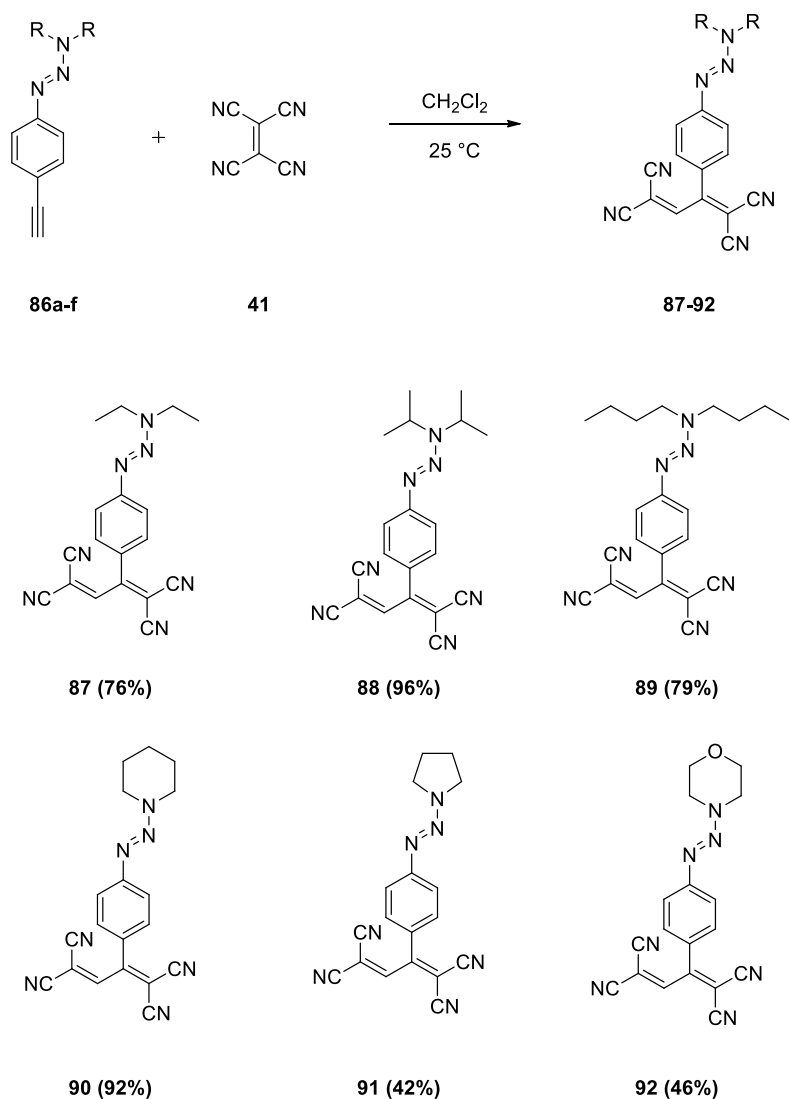
Scheme 16. Synthesis of push-pull chromophores *via* reaction between electron-rich alkynes and TCNE.

Although crude ^{1}H NMR spectra prove the quantitative formation of push-pull dyes **87-92**, we needed a method to report yields for each product. For this purpose, we utilized the quantitative NMR (qNMR) method.[106] Choosing proper internal standards was the key for this method to get accurate results. Certain requirements had to be fulfilled to perform qNMR, such as the solubility of chosen

internal standard in deuterated chloroform (CDCl$_3$) and the solvent of the reaction.[106] Also, its ^{1}H NMR peaks should not be overlapped with any of the peaks of the product.[106] And of course, internal standards cannot be reacting with any reagents in the reaction mixture.[106] Taking into account all these points, 3,4,5-trimethoxybenzaldehyde (**93**) was an excellent choice to be used as internal standard (Figure 12). It is soluble in DCM and has a distinctive peak at 9.8 ppm. Experimental procedure was simple to apply for this method. Internal standard was added with other reagents, and ^{1}H NMR was recorded. After including some properties such as molecular weight, number of hydrogens to calculations, ratio of peak of analyte to internal standard gives yield.[106]

93
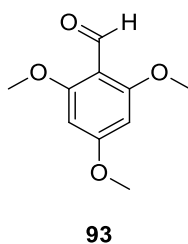
Figure 12. 1,3,5-trimethoxybenzaldehyde.

As shown in Scheme 16, the lowest yield 42% was observed for push-pull dye **91**, and the highest belongs to isopropyl containing adduct **88** which is 96%. Yet, interestingly the yield for piperidine-substituted adduct was 92%. Low yields could be due to formation of insoluble charge transfer complexes between **91**, **92**, and TCNE **41**.[107] According to the results we can say that there is no correlation between donor ability of different substrates and their yields. As indicated clearly, push-pull chromophores **87-92** are simple to synthesize and purify *via* formal [2+2] CA-RE reaction.

27

2.3   UV/Vis Spectroscopy

As mentioned earlier D-π-A systems are known for their intense intramolecular charge transfer (ICT) bands.[7,8,13] UV/Vis spectroscopy is a great tool to investigate ICT abilities of push-pull chromophores . Figure 13 describes UV/Vis data for **87-92** systems. The electronic absorption spectrum of each dye has been shown in a different color (Figure 13).
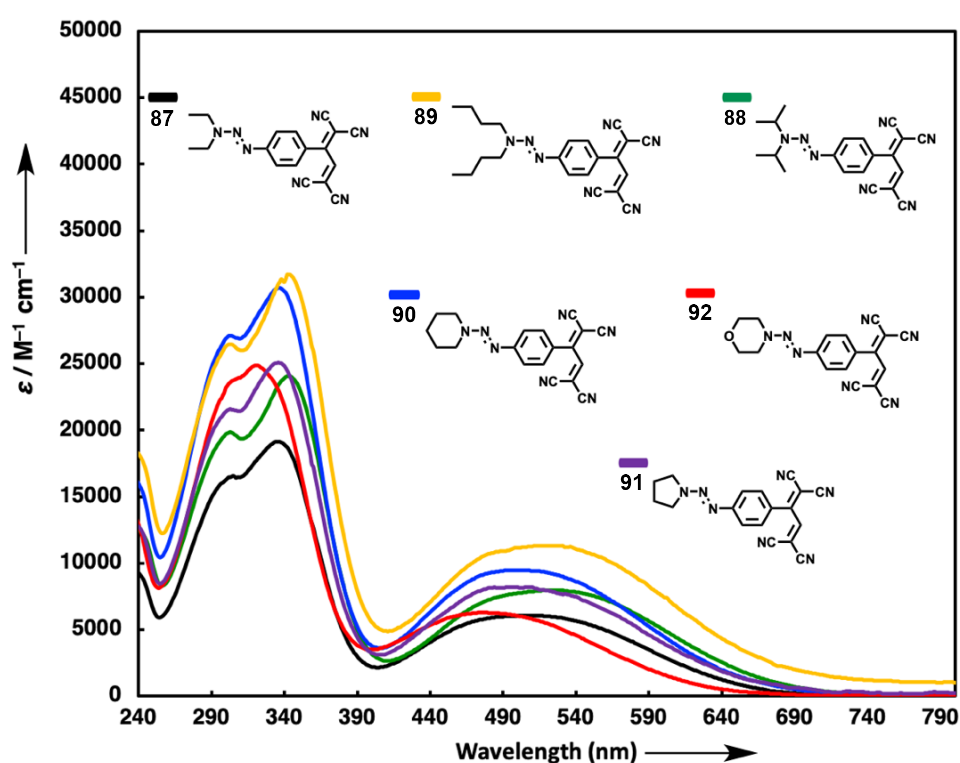
Figure 13. UV/Vis spectra of conjugated chromophores **87** (black line), **88** (green line), **89** (yellow line), **90** (purple line), **91** (blue line), and **92** (red line) in CH_2Cl_2 at 298 K.

Values of molar extinction coefficient change for **87-92** between 6080–11300 M^{-1} cm^{-1}. The following data shows the most red-shifted absorption wavelength for each chromophore **87-92**, λ_{max} = 508 nm (6080 M^{-1} cm^{-1} for **87**), 524 nm (7965 M^{-1}

28

cm^{-1} for **88**), 521 nm (11300 M^{-1} cm^{-1} for **89**), 499 nm (9451 M^{-1} cm^{-1} for **90**), 507 nm (8177 M^{-1} cm^{-1} for **91**), 476 nm (6313 M^{-1} cm^{-1} for **92**). The hypsochromic shift (blue shift) was observed for compound **92**. It can be attributed to the presence of morpholine group in the structure. Morpholine possesses weak electron donor capability compared to other structures due to the electron withdrawing effect of oxygen. Although triazene groups are not strong electron donors as dialkilanilino derivatives,[17,41] synthesized push-pull dye systems **87-92** show charge-transfer from triazenes to tetracyanobutadiene unit. Therefore, obtained UV/Vis spectroscopy data is evidence of moderate-intensity ICT bands for obtained push-pull chromophores **87-92**.
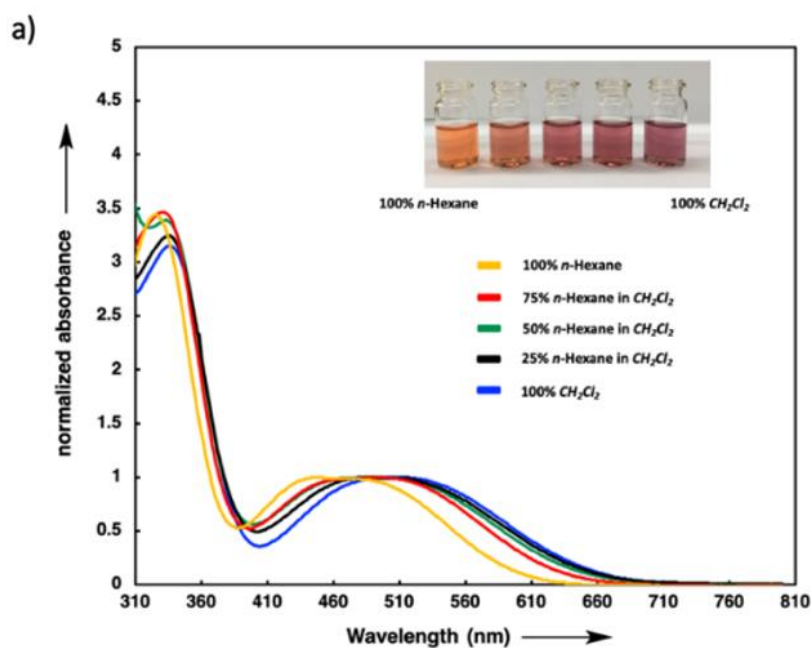
Figure 14. UV/Vis absorption spectra of push-pull dye **87** in CH$_2$Cl$_2$/*n*-hexane mixtures at 298 K.
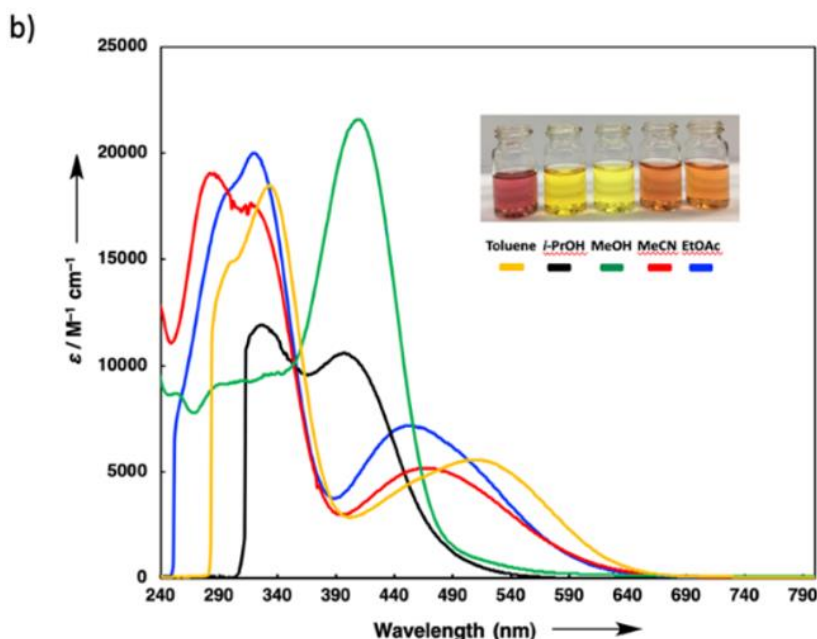
Figure 15. UV/Vis absorption spectra of push-pull dye **87** in different solvents at 298 K.

Solvatochromism is a phenomenon of changing of color of a solution due to interaction with solvents of different polarities.[108] It is another way of proving ICT properties of a given structure.[109] We used this strategy to approve the validity of ICT properties of **87-92** systems. We selected **87** as an example to investigate its color change in different solvents. Different fraction of DCM and *n*-hexane was used to see effect of polarity. Figure 14 showed positive solvatochromism as polarity increased (Figure 14). It means a bathochromic shift was observed. Changing of the color of **87** from orange to dark purple was observed as a fraction of DCM increased in a mixture. The second figure (Figure 15) describes the interaction of push-pull dye **87** with five different solvents (toluene, *i*-PrOH, MeOH, MeCN, EtOAc). Solvatochromic behavior of **87** shows a substantial increase in the extinction coefficient value in alcoholic solvents, and hydrogen bonding is assumed to be the reason for this.[110] In toluene, color of the mixture changed to purple, and the highest redshift was observed.

2.4 Theoretical Studies

Beside experimental methods, push-pull chromophores investigated through computational techniques. It allows to look into theoretical possibility of obtained data and thus, to approve the validity of it. Intramolecular charge transfer (ICT) ability of push-pull chromophores is a fundamental property of D-π-A systems.[17] Structures that possess this property have low energy transition bands. The lowest energy transition bands reflect excitation from the highest occupied molecular orbital to the lowest unoccupied molecular orbital.[20] With the help of computational chemistry, it is possible to understand ICT of the targeting molecules by analyzing the distribution of HOMO and LUMO levels. The small overlap of HOMO and LUMO orbitals is proof of efficient electron charge transfer in push-pull chromophores **87-92**. Table 1 displays HOMO and LUMO depictions of push-pull dyes **88** and **91**. Furthermore, electrostatic potential map (ESP) depictions provide an evidence for ICT properties of push-pull chromophores **87-92**.[114,115]

Table 1. HOMO-LUMO orbital depiction and ESP map of **88** and **91.** The upper plots represent the HOMOs, and the lower plots represent the LUMOs.
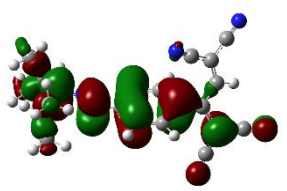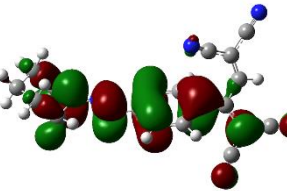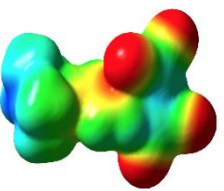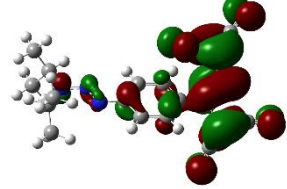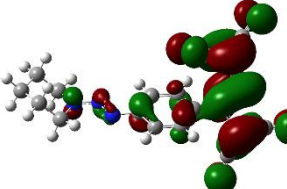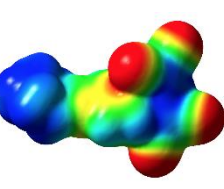
Orbital	88	91	ESP
HOMO			
LUMO			

Figure 15 exhibits theoretical calculations for the extinction coefficient value of 87. Gaussian-09 was used for DFT and TD-DFT calculations.[111] B3LYP functional using basis set B3LYP/6-31++G(d,p) was used to obtain molecular structures for push-pull chromophores **87-92**.[112] The conductor-like polarizable continuum model (CPCM) was selected as the solvation model in CH_2Cl_2. Time-dependent density theory (CAM-B3LYP/6–31++G(d,p)) was applied to calculate the vertical excitation energies at the S_o level again with CPCM solvation in CH_2Cl_2.[109] For **87-92** deviation from experimental results was observed for calculated transition energies, which was expected since similar deviations also have been reported for similar systems.[113] Theoretical value has been scaled by 2.66. Scaling was required to match computational and experimental spectra. Accordingly, extinction coefficient value is well estimated compare to experimental one. For all push-pull dyes, experimental and computed λ_{max} value differences for CT absorption bands are in the range of 0.01-0.07 eV.
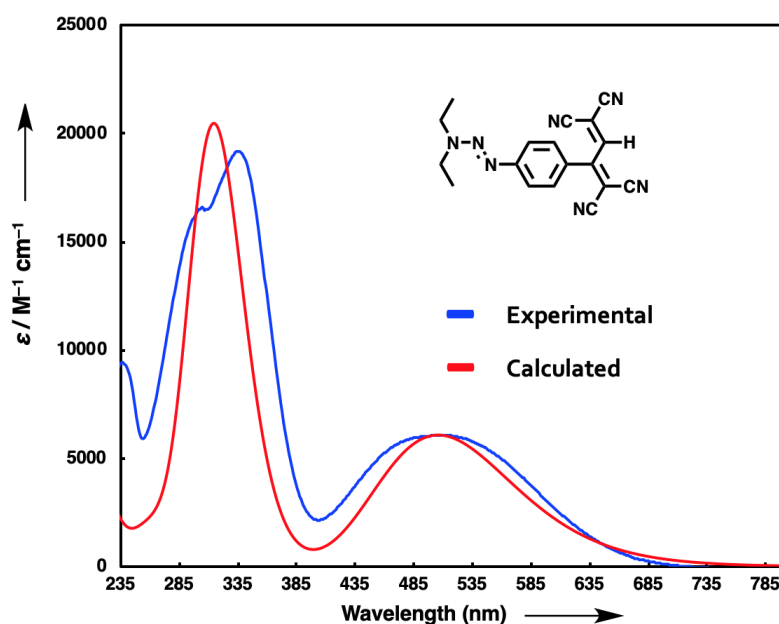
Figure 16. Calculated (not shifted, scaled by 2.66, red line) TD-DFT:CAM-B3LYP/6-31++G(d,p) level of theory in CH_2Cl_2 and experimental (blue line) UV/Vis absorption spectrum of **87**.

CHAPTER 3

RESULTS AND DISCUSSION

3.1 Synthesis of Symmetrical and Unsymmetrical Di-triazene Substituted Substrates for [2+2] CA-RE

Synthesis of non-terminal alkyne-containing substrates is another challenge commenced by Diederich and co-workers earlier in 2005.[29] In their substantial work, DMA substituted cross-coupling product **35** reaction with TCNE **41** accomplished successfully and resulted in push-pull chromophores **62** (Scheme 13).[29] Those coupling products display third-order nonlinear optical properties that were reported by Diederich group for the first time.[29] By taking this work as a reference, we synthesized triazene-substituted cross-coupling products and dimers *via* Sonogashira and Hay coupling reactions, respectively.

3.1.1 Synthesis of Symmetrical and Unsymmetrical Di-triazene Substituted Substrates *via* Sonogashira Cross-Coupling

In order to achieve the ultimate goal of the synthesis of symmetrical cross-coupling products, Sonogashira cross-coupling reaction is applied (Scheme 17). Scheme 17 describes the reaction between aryl iodides **84** and alkynes **86** yielding **94-97** in low to good yields (28-52%). The starting materials **84** and **86** were synthesized according to above mentioned synthetic route (Scheme 15).
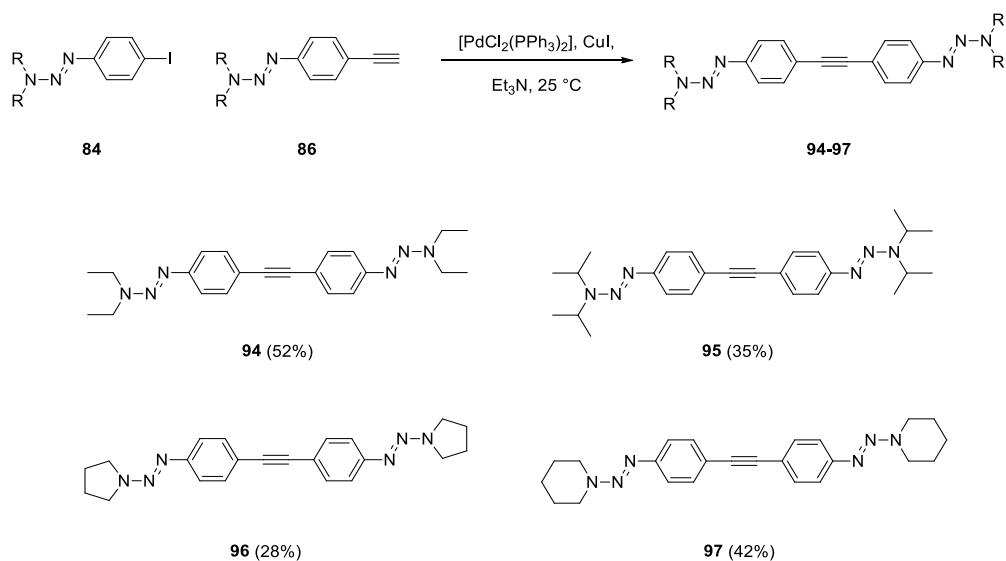
Scheme 17. Synthesis of triazene containing symmetrical cross-coupling products.

As described in scheme 18, with the intention of observing the effects of different substrate groups unsymmetrical coupling products were synthesized too (Scheme 18).
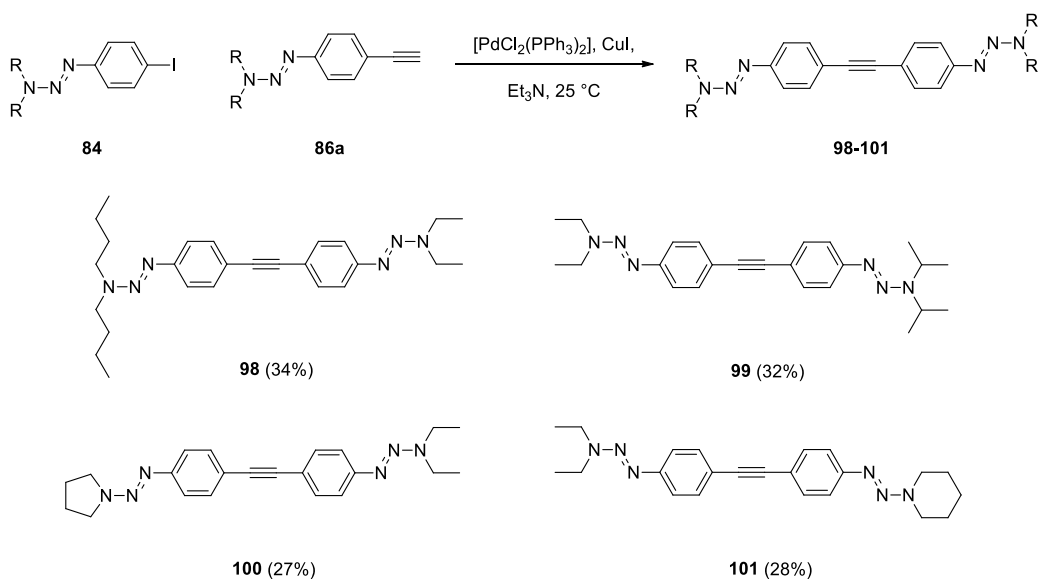
Scheme 18. Synthesis of triazene-containing unsymmetrical cross-coupling products.

Sonogashira cross-coupling reaction is used again. To synthesize unsymmetrical coupling products **98-101**, ethyl group was kept constant on one side of the structure and the other one alternated between butyl **98**, isopropyl **99**, pyrrolidine **100**, and piperidine **101**. The yields were low (27-34%) for the products, and this could be related to the dimerization of acetylene containing starting reagents (homo-coupling) due to interaction with oxygen in the presence of copper.

3.1.2 Reaction with Symmetrical Coupling Products with TCNE

The primary purpose of synthesizing of the products mentioned above is to obtain push-pull chromophores. TCNE **41** was used as an electron acceptor reagent (Scheme 19). As shown in Scheme 19, the reaction was conducted at room temperature and 75 °C, DCE was used as a solvent. However, no product formation was observed. An interesting observation was made when the same reaction was applied at 75 °C. Instead of attaining the desired CA-RE product **102**, diphenylacetylene **103** was isolated (Scheme 19). Somehow TCNE **41** causes oxidation of triazene group in the starting material instead of reacting non-terminal acetylene group. It means donor ability of the triazene group is not enough to activate alkyne unit for the [2+2] CA-RE reaction to occur either at room temperature or 75 °C.
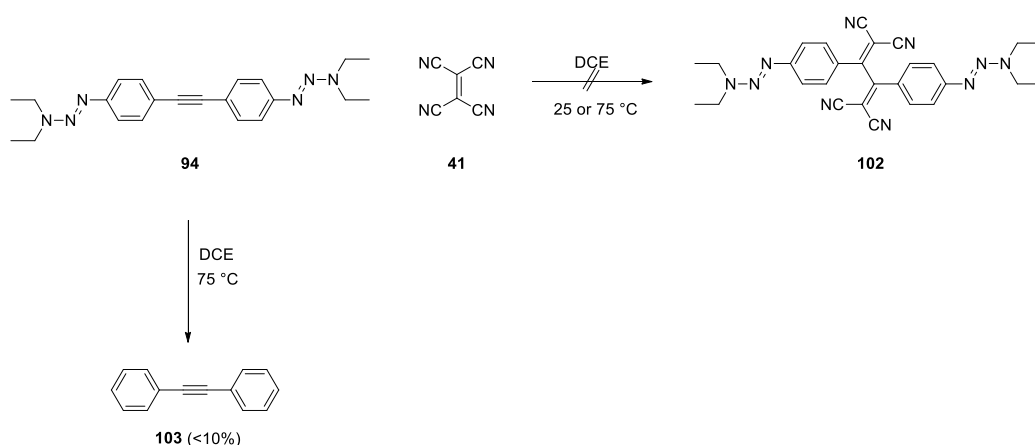
Scheme 19. Reaction between coupling product **94** and TCNE **41** at 25 and 75 °C.

35

.

In an attempt to compare this observation, diphenyl acetylene was synthesized by using Sonogashira cross-coupling reaction. Commercially available iodobenzene **104** and phenylacetylene **105** gave the product **103** at room temperature (Scheme 21). As expected, NMR spectra obtained from two different experiments matched well and this observation proved formation of **103** when **94** and TCNE **41** reacts.
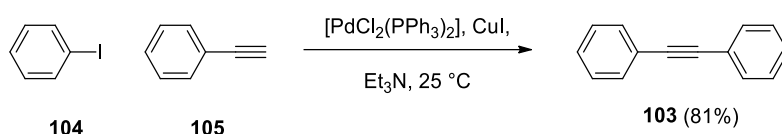
Scheme 20. Synthesis of diphenylacetylene **103**.

3.1.3 Reaction with Symmetrical Coupling Products with TCNQ

Electron-deficient alkene, TCNQ **44** is another structure with substantial electron acceptor property through four nitrile groups. Because of this reason, it has been used as an electron acceptor in the synthesis of push-pull chromophores.[72,80,116] Synthesized structure **94** was put into the reaction with TCNQ **44** at room temperature, but expected product **106** was not observed (Scheme 21). When the reaction condition was slightly changed by simply increasing temperature to 75 °C, the overall result unfortunately did not change. Interestingly, as it happened in reaction with electron-deficient TCNE **44**, formation of diphenyl acetylene **103** was once again observed (Scheme 21).

36
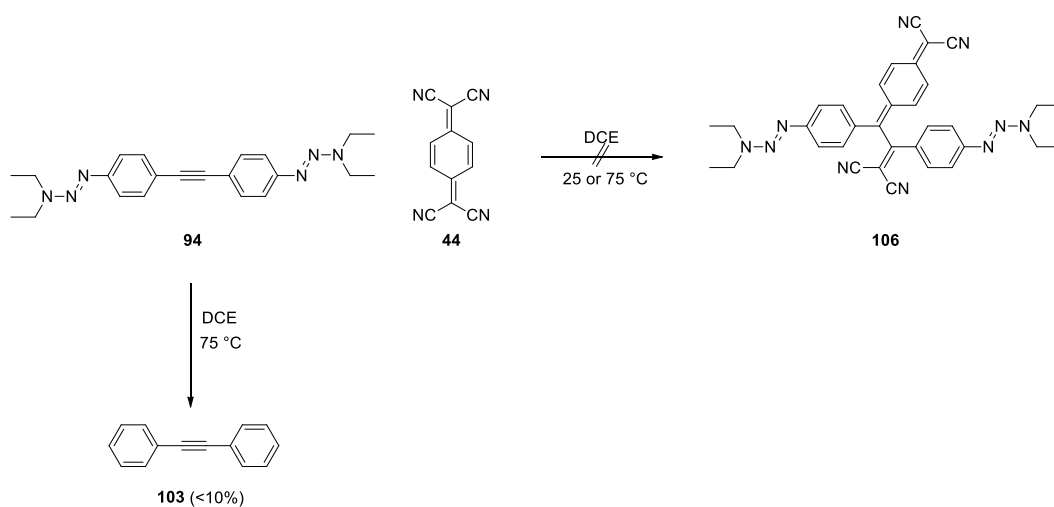
Scheme 21. Reaction between coupling product **94** and TCNQ **44** at 25 and 75 °C.

3.2. Synthesis of Symmetrical and Unsymmetrical Dimer Substrates

Issues with the reaction of TCNE **41** with coupling products as discussed in the previous section was referred to electron donating ability of triazene side groups.
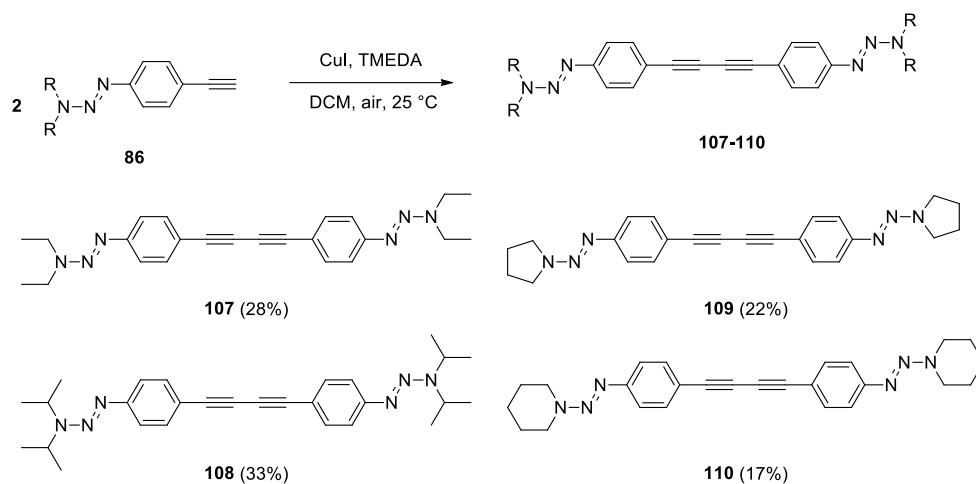
Scheme 22. Synthesis of triazene containing symmetrical dimer products.

Nevertheless, steric hindrance due to two bulky benzene groups could be another reason for the unsuccessful results obtained from previous reactions. To make a space for TCNE **41** to react with acetylene group, triazene-substituted symmetrical dimer structures **107-110** were synthesized (Scheme 22). To access these compounds, Hay coupling was used to synthesize targeted coupling products.

Unsymmetrical dimer substrate **111** was synthesized by using Hay coupling of alkynes structures **86a** and **86c** together with symmetrical dimers **112** and **107** as side products.[29]
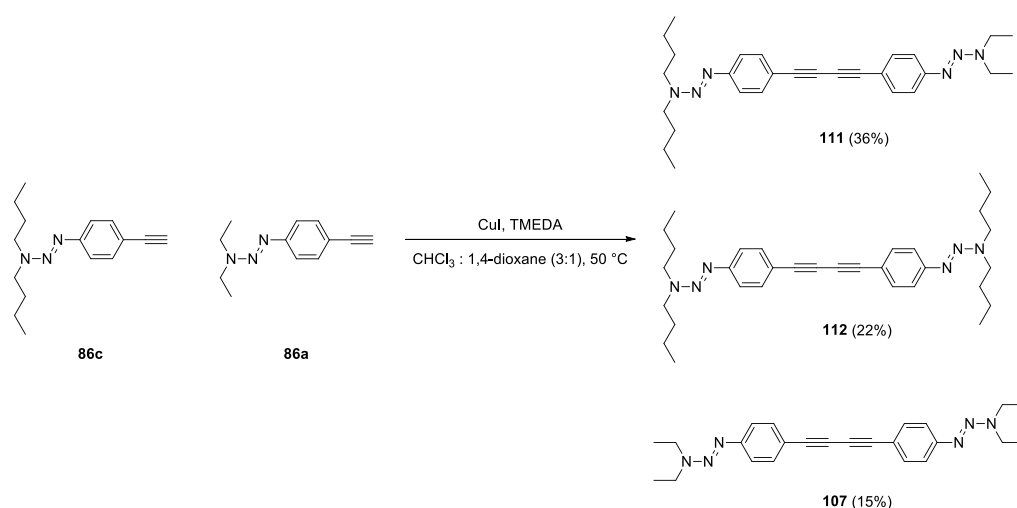
Scheme 23. Synthesis of unsymmetrical dimer **111**.

3.2.1. Reaction of Symmetrical and Unsymmetrical Dimer Substrates with TCNE

Triazene-substituted dimer **107** was put into the reaction with TCNE **41** at room temperature. Yet, the reaction did not occur under ambient conditions (Scheme 24). The reaction was expected to give product **113** at 75 °C, but as it happened with the previous reaction between **94** and TCNE **41**, unexpected another product was

38

obtained. Formation of 1,4-diphenylbuta-1,3-diyne (**114**) was observed at 75 °C (Scheme 24).
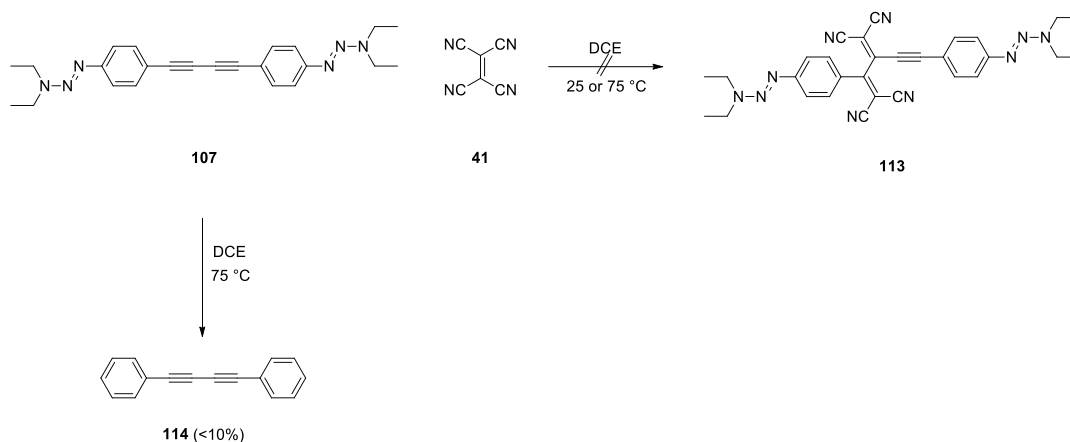
Scheme 24. Reaction between **107** and TCNE **41** at 25 and 75 °C.

According to literature procedures, Scheme 25 represents the synthesis of 1,4-diphenylbuta-1,3-diyne (**114**)[29] to compare the result obtained through the reaction on Scheme 24.
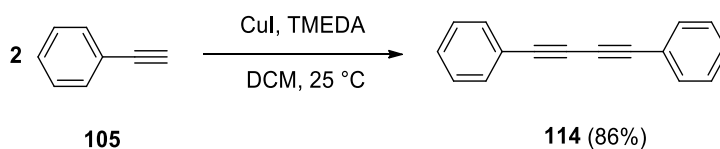
Scheme 25. Synthesis of 1,4-diphenylbuta-1,3-diyne **114**.

3.2.2. Reaction of Symmetrical and Unsymmetrical Dimer Substrates with TCNQ

The same starting materials **107-110** were attempted to have a reaction with TCNQ **44**. Nevertheless, the desired structure **115** could not be obtained in these conditions either (Scheme 26). Instead, **114** was obtained again. To understand more about the course of the reaction the following experiment was done. The starting material **94** was put into a round-bottom flask and dissolved in DCE at 75 °C. This

39

experiment aimed to investigate any possible effect of heat to obtain diphenyl acetylene **103**. After one, two, and three days TLC results demonstrate that nothing happened with the starting material **94**. No diphenyl acetylene **103** was observed even after three days. This observation gives a hint that the formation of **103** is somehow related to both heat and electron acceptor reagants TCNE **41** and TCNQ **44**. Targeted push-pull chromophores *via* [2+2] CA-RE reactions between **94-101** coupling products and TCNE were expected to have significant ICT properties.
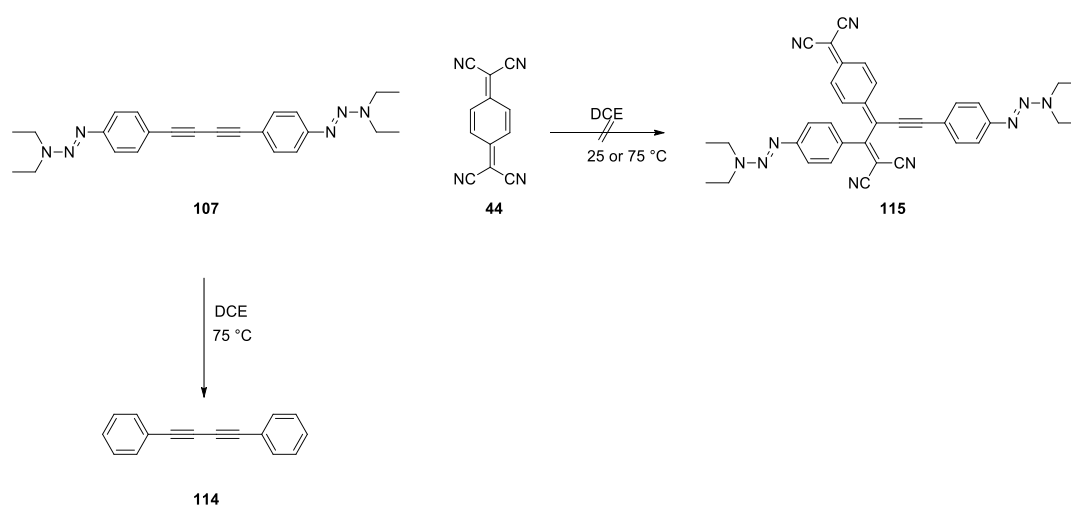
Scheme 26. The formal CA-RE reaction between symmetrical dimer **107** and TCNQ **44** at 25 and 75 °C.

For this goal , we tried to obtain the desired structure with another pathway as shown in Scheme 27. Our purpose was to synthesize 4,4'-(ethyne-1,2-diyl)dianiline **117** *via* Sonogashira cross-coupling reaction between alkyne **116** and aryl iodide **83**, then to have its reaction with electron-poor alkene TCNE **41**, which is most certainly expected to provide push-pull product **118** (Scheme 27). Then the transformation of amine to triazene group could give the desired push-pull product **119**.

40
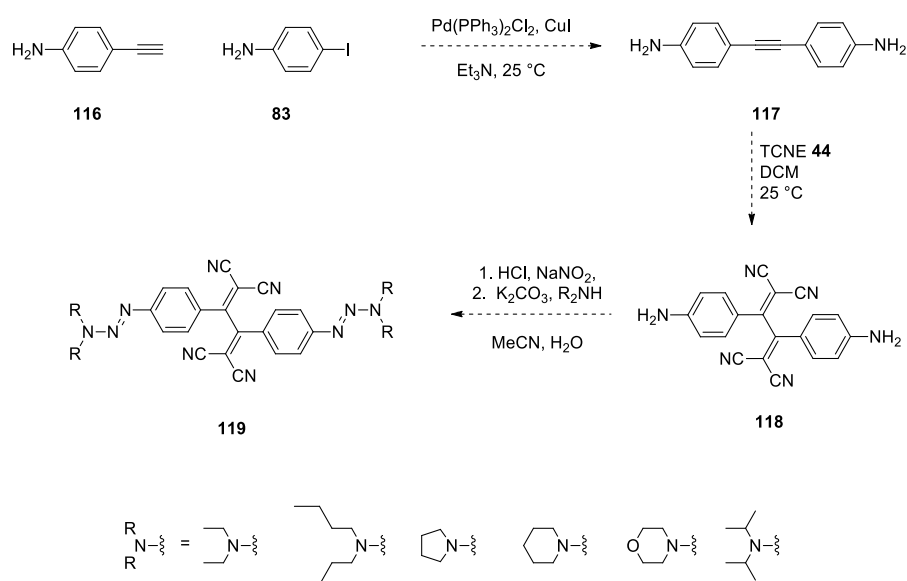
Scheme 27. General reaction scheme to obtain **119**.

The starting reagent **116** was synthesized from commercially available 4-iodoaniline **83**, as shown in Scheme 28. Sonogashira cross-coupling reaction was followed by deprotection of TMS group with K_2CO_3 (Scheme 28).
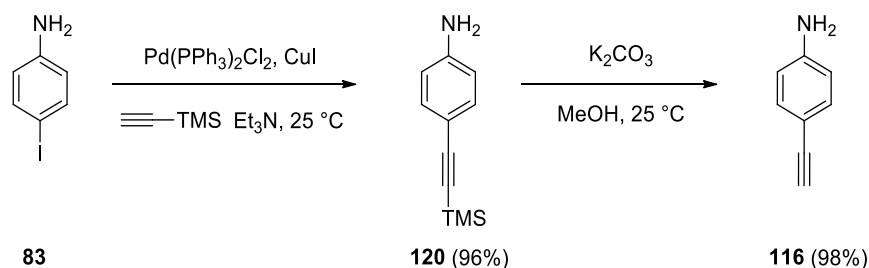
Scheme 28. Synthesis of **116**.

Before testing the target reaction (scheme 27), the following was tested with 4-ethynylaniline to ensure the triazene group formation. However, the transformation of amine group to triazene did not occur with cyano-rich substrate. As a result, the desired push-pull chromophores **86a-f** could not be attained by this pathway either.
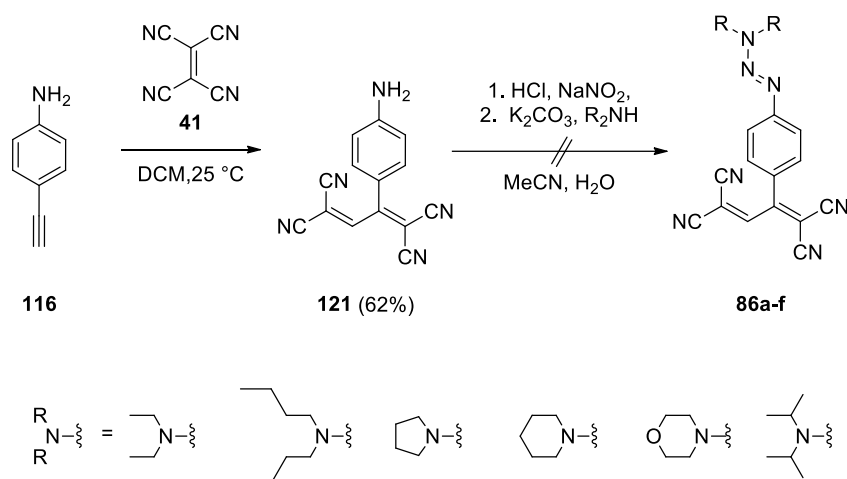
Scheme 29. Attempted synthesis of **86a-f** with another pathway.

3.3 Synthesis of DEA-substituted Triazene-containing Non-terminal Alkyne Substrates

The targeted reaction between TCNE and TCNQ with triazene-substituted non-terminal alkynes were not successful in obtaining push-pull chromophores as described in the previous section. To overcome the problem, we utilized diethylaniline (DEA) group as a strong electron donor to activate the reaction. DMA-substituted acetylene group is a well known for its strong electrong donating ability.[29,117] *N,N*-diethyl-4-ethynylaniline (**122**) was synthesized according to literature procedure (Scheme 30).[120] Sonogashira cross-coupling reaction was utilized to obtain **123**. Deprotection of TMS group with K_2CO_3 in MeOH results in formation of desired product **124**.
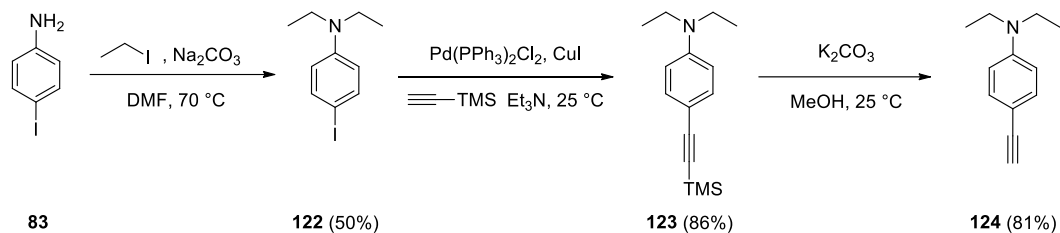
Scheme 30. Synthesis of *N,N*-diethyl-4-ethynylaniline (**124**).

Triazene-substituted reagents **84a-e** reacted with *N,N*-diethyl-4-ethynylaniline (**124**) *via* Sonogashira cross-coupling reaction and resulted in **125-129** in good yield (56-78%) (Scheme 31).
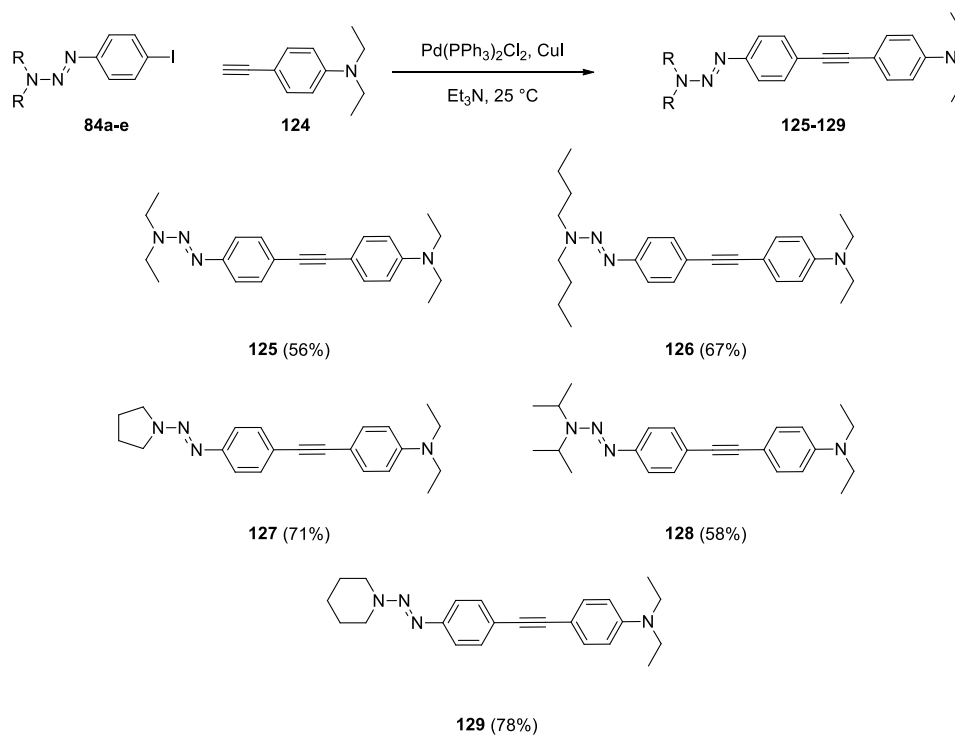
Scheme 31. Synthesis of DEA-substituted non-terminal alkynes.

3.3.1 Reactions of DEA-substituted Alkyne Substrates with TCNE

The CA-RE reaction was conducted between coupling products **125-129** and TCNE **41** at room temperature (Scheme 32). Owning to strong electron donor ability of diethylamine group assisted by a triazene group, push-pull chromophores **130-134** were sucessfully obtained. Obtained products were purified by column chromatography and isolated in a very high yields (96-99%) (Scheme 35).
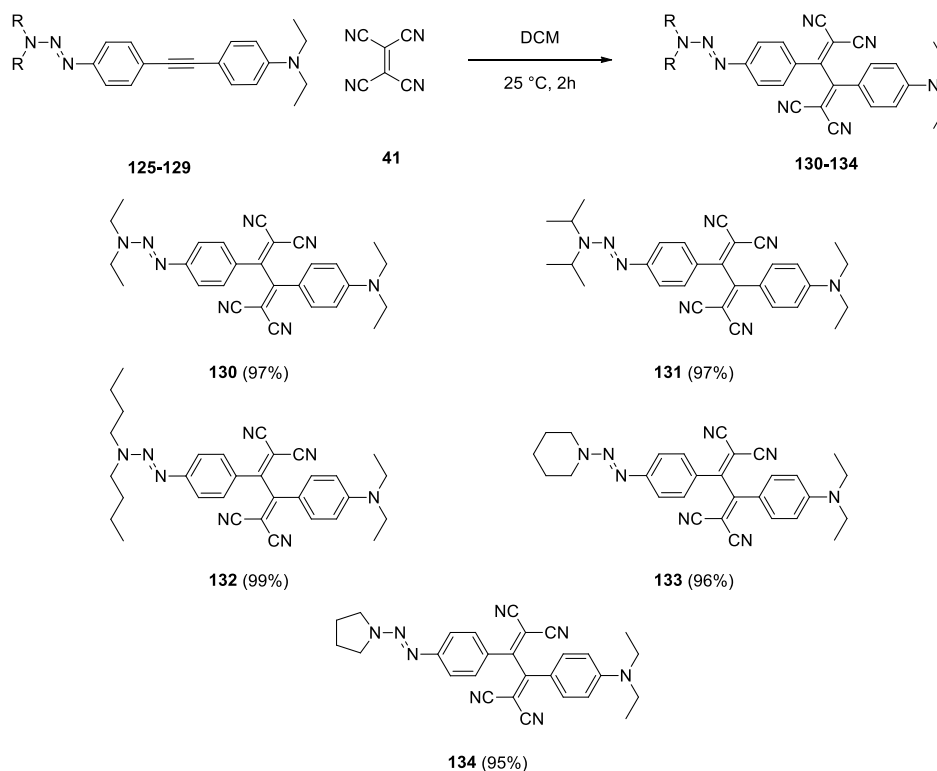
Scheme 32. Push-pull chromophores **130-134** obtained through the reactions between DEA-substituted alkynes and TCNE.

3.3.2 Reactions of DEA-substituted Alkyne Substrates with TCNQ

Since the **125-129** with TCNE **41** became successful in producing targeted push-pull chromophores **130-134**, we turned our attention to try the same reaction

44

with TCNQ **44** (Scheme 33). **125-129** was used as electron-donating alkyne, and TCNQ **44** acted as electron-acceptor to produce **135-139** in high yield (95-99%) at room temperature (Scheme 33). Completing the reaction took only 1.5 hours, making the reaction quite practical for application purposes.
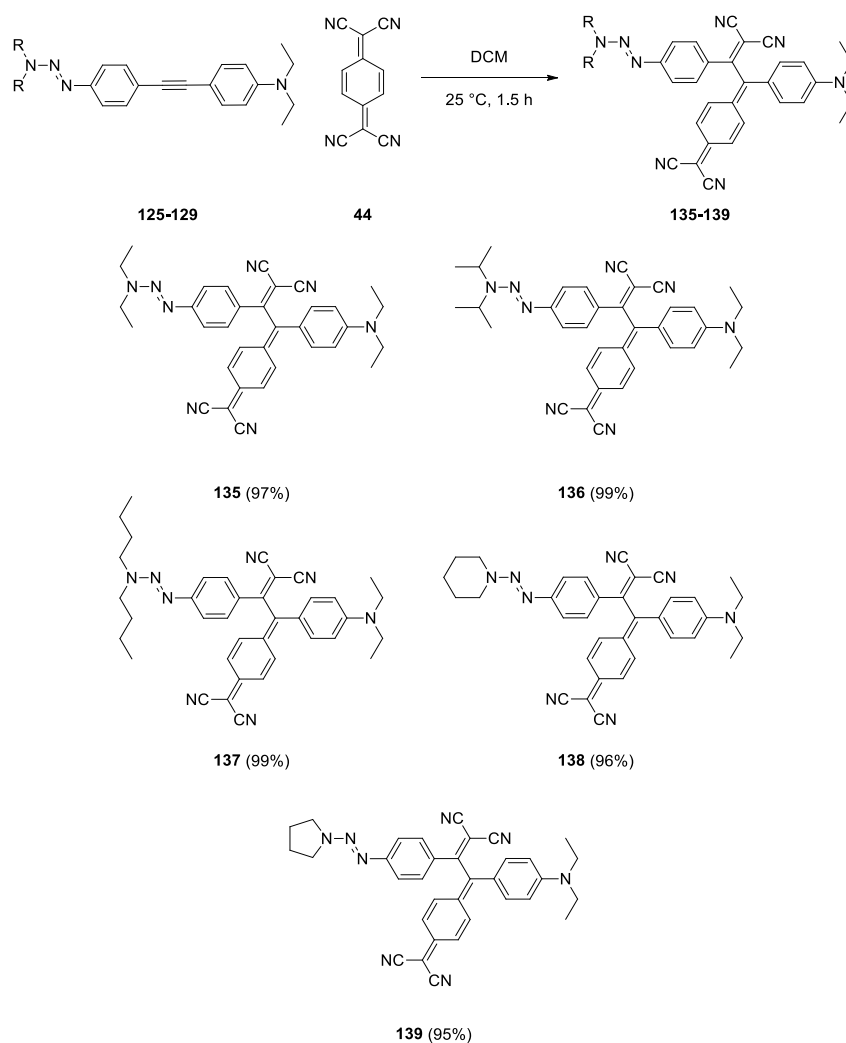
Scheme 33. Push-pull chromophores **135-139** obtained through the reactions between DEA-substituted alkynes and TCNQ.

3.4   UV/Vis Spectroscopy

As mentioned earlier in Chapter 2, UV/Vis spectroscopy is essential and valid technique to approve ICT properties of push-pull chromophores. Since we obtained our targeted push-pull chromophores **130-139** successfully, UV/Vis spectroscopy was utilized to confirm strong ICT bands of synthesized dyes. Figure 16 describes UV/Vis spectra of TCNE products. Different colors have been chosen for each dye. Molar extinction values changes for **130-134** between $44432–60652$ M^{-1} cm^{-1}. The following data shows strongest photon absorption wavelength for each chromophore **130-134**, $\lambda_{max} = 454$ nm (44432 M^{-1} $cm^{-1}$for **130**), 465 nm (55254 M^{-1} $cm^{-1}$for **131**), 467 nm (60651 M^{-1} $cm^{-1}$for **132**), 461 nm (46016 M^{-1} $cm^{-1}$for **133**), 459 nm (51149 M^{-1} cm^{-1} for **134**). There is no strong bathochromic or hypsochromic shift for compounds **130-134**. This highlights that different triazene groups have limited impact on electron delocalization.
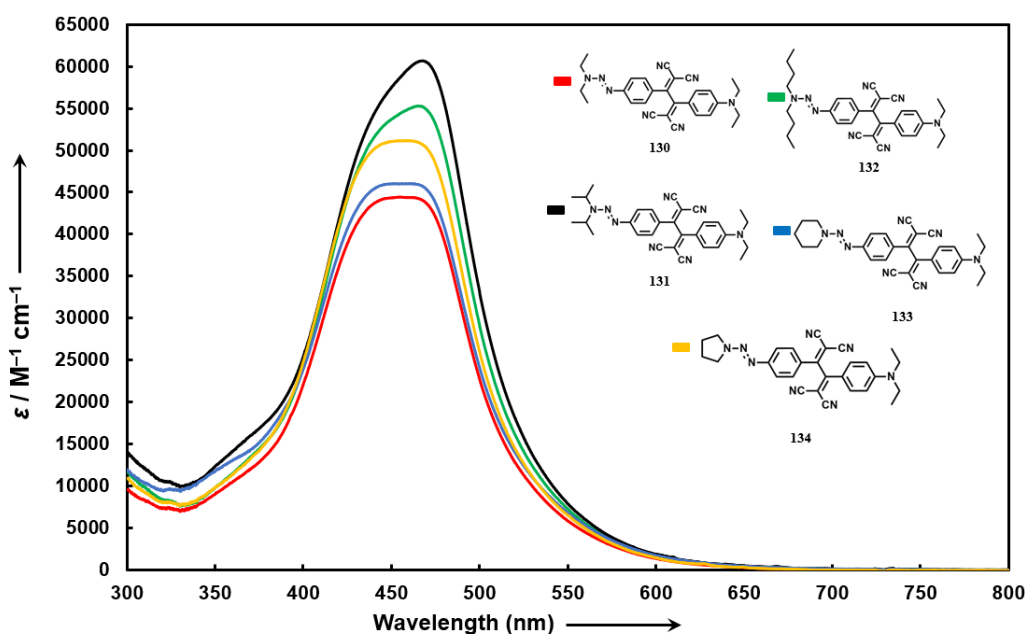
Figure 17. UV/Vis spectra of conjugated chromophores **130** (red line), **131** (black line), **132** (green line), **133** (blue line), **134** (yellow line) in CH₂Cl₂ at 298 K.

One of the most significant characteristics of push-pull chromophores is their ability to change the color of the solution due to differences in the polarity of the solvent which is known as solvatochromism.[108] Different fractions of DCM and *n*-hexane was used for the investigation of polarity effect on push-pull dye **130** (Figure 17). UV/Vis spectra displays bathachromic shift of the push-pull dye **130** due to increase in polarity of the solvent from *n*-hexane to DCM. Change of a color from orange to pale yellow is visual prove of this experimental data (Figure 17).
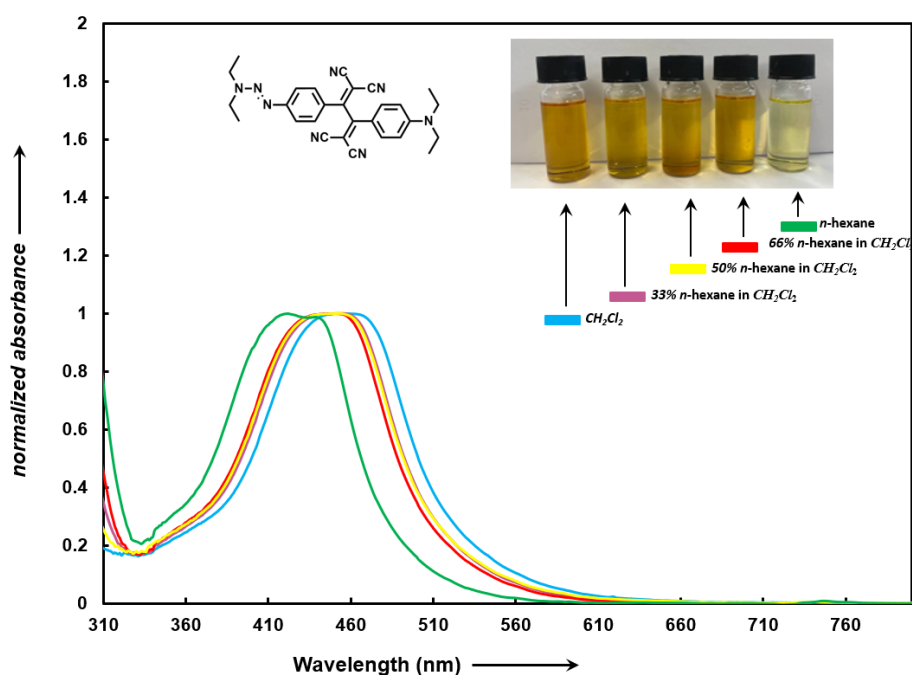
Figure 18. UV/Vis absorption spectra of push-pull dye **130** in CH_2Cl_2/*n*-hexane mixtures at 298 K.

TCNQ containing chromophores **135-139** show strong ICT properties too and their UV/Vis spectrum also approves that. Figure 18 below represents ICT bands for each push-pull dye. Different colors has been chosen for push-pull chromophores **135-139** as well. Molar extinction values changes for **135-139** between 37003–42798 M^{-1} cm^{-1}. The following data shows strongest photon absorption wavelength for each chromophore **135-139**, $\lambda_{max} = 691$ nm (40519 M^{-1} cm^{-1} for **135**), 691 nm

47

(42798 M^{-1} cm^{-1} for **136**), 692 nm (37003 M^{-1} cm^{-1} for **137**), 692 nm (42198 M^{-1} cm^{-1} for **138**), 690 nm (36158 M^{-1} cm^{-1} for **139**). There is no significant bathochromic or hypsochromic shift for compounds **135-139** either. For TCNQ products **135-139**, we applied solvatochromism to widen our investigation scope (Figure 19).
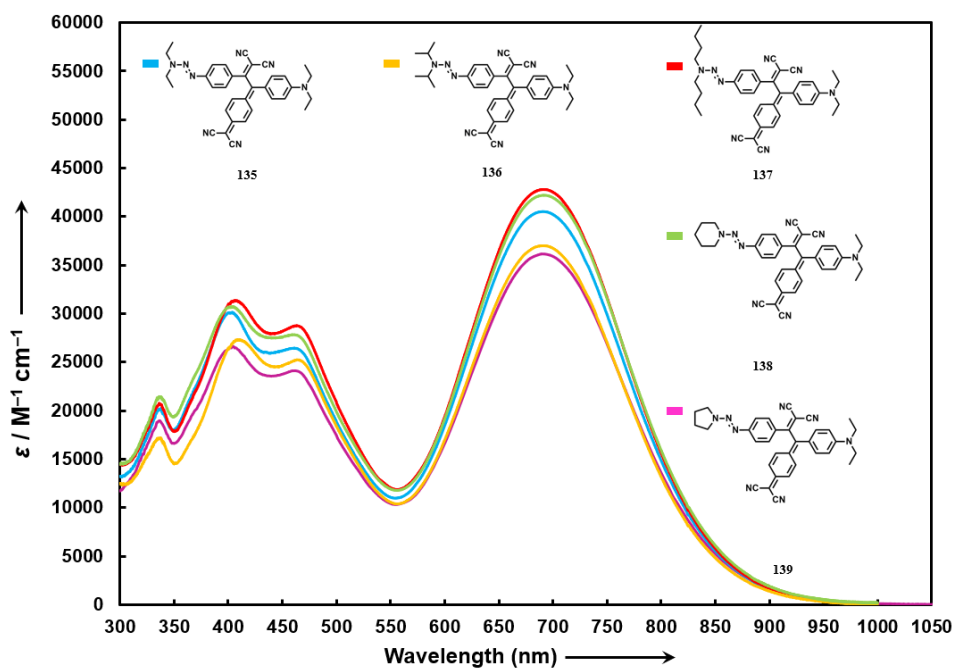
Figure 19. UV/Vis spectra of chromophores **135** (blue line), **136** (yellow line), **137** (red line), **138** (green line), **139** (purple line) in CH_2Cl_2 at 298 K.

135 was chosen as an example and dissolved in a solution DCM and *n*-hexane in different fractions. Figure 19 describes obtained data and change of a color of a solution from DCM to *n*-hexane. Bathochromic shift is observed here as well.
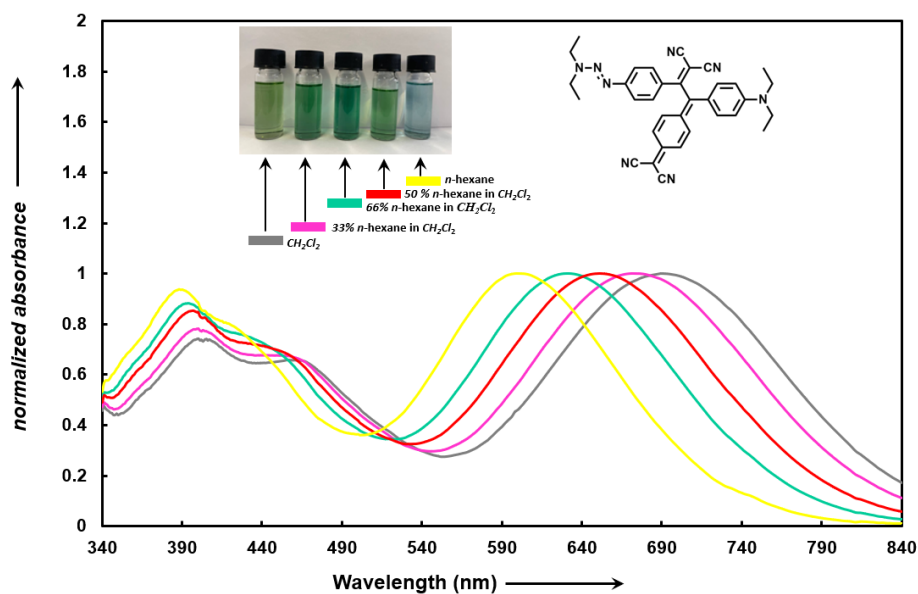
Figure 20. UV/Vis absorption spectra of push-pull dye **135** in CH_2Cl_2/*n*-hexane mixtures at 298 K.

3.5 Theoretical Studies

Computational chemistry is valid technique to investigate ICT properties of push-pull chromophores. For this reason synthesized TCNE and TCNQ products were investigated. As representative examples push-pull dyes **130** and **135** were chosen. For DFT and TD-DFT calculations, Gaussian-09 was utilized.[111] The following Figure displays theoretical extinction coefficient value of **130** and **135** (Figure 20a and 20b). B3LYP functional using basis set B3LYP/6–31++G(d,p) was used to obtain optimized molecular structures for **130** and **135**.[112] As a solvation model in CH_2Cl_2 the conductor-like polarizable continuum model (CPCM) was chosen.[109] Time dependent density theory (CAM-B3LYP/6-31-G(d)) was applied for the calculation of the vertical excitation energies at the S_0 level with the same solvent, CH_2Cl_2.[109]

As it occured in previous calculation in our structures **87-92** similar deviation for transition energies is observed.[113,114] Theoretical values were scaled by 1.43 and 1.17 for products **130** and **135** respectively to match experimental and computational spectra. For the product **130** experimental value is red-shifted by 0.4 eV and for the **135** it is only 0.2 eV. By taking into consideration all these theoretical investigation,we can conclude that experimental and theoretical values of extinction coefficient of push-pull chromophores **130** and **135** are in good agreement with each other.
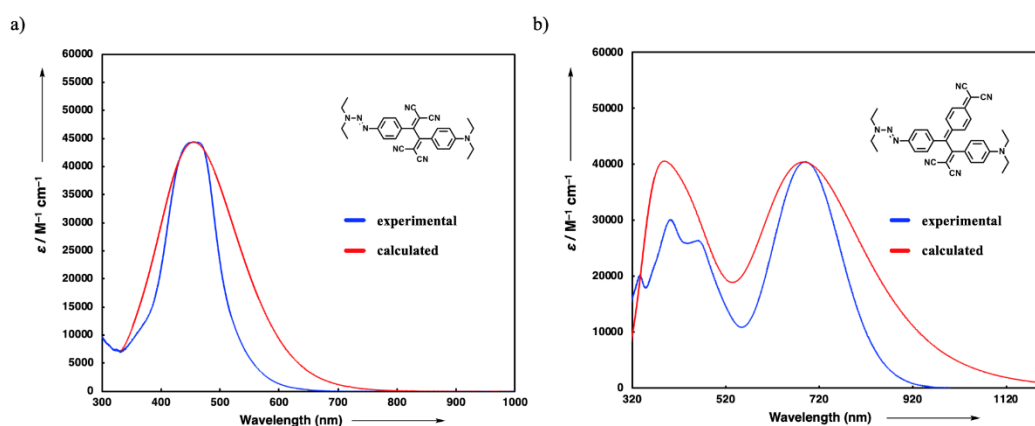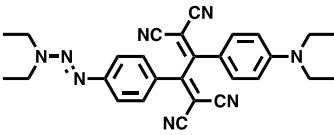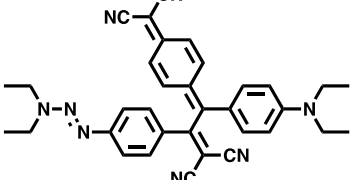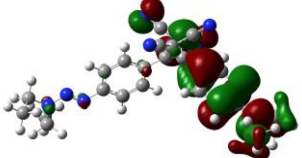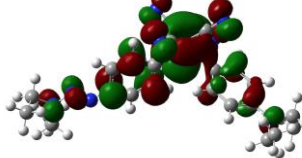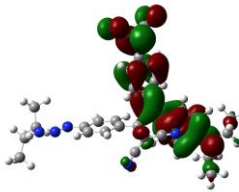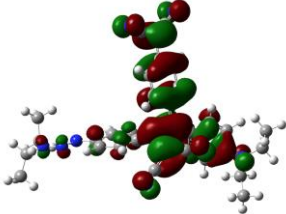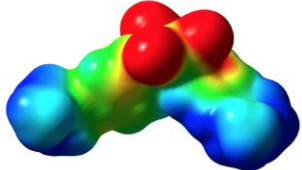
Figure 21. a) Calculated (red-shifted by 0.4 eV, scaled by 1.43, red line) TD-DFT:CAM-B3LYP/6–31G(d) level of theory in CH_2Cl_2 and experimental UV/Vis spectrum of **130** in CH_2Cl_2 (blue line). b) Calculated (red-shifted by 0.2 eV, scaled by 1.17, red line) TD-DFT:CAM-B3LYP/6–31G(d) level of theory in CH_2Cl_2 and experimental UV/Vis spectrum of **135** in CH_2Cl_2 (blue line).

Computational chemistry allowed us to elaborate ICT properties of obtained push-pull chromophores **130-139**. Structure **130** and **135** were chosen as an example to display ESP and distribution of HOMO-LUMO levels within the structure. The small overlap of HOMO and LUMO orbitals is proof of efficient electron charge transfer in push-pull chromophores **130** and **135**. Table 2 contains information about HOMO and LUMO depictions of the molecules **130** and **135** (Table 2).

50

Besides, ESP depictions allow to comment on electron density around the structures. As we expected, cyano-rich electron-acceptors pull the electrons and thus, the red middle area shows high electon density in the molecule. On the other hand, electron-donors triazene and diethylaniline groups are displayed by blue colors which is the sign of being electron-poor (Table 2).

Table 2. HOMO - LUMO representations of and ESP maps for structures **130** and **135**.

Orbital	130	135
Molecular Structure		
HOMO		
LUMO		
ESP		

As mentioned earlier energy value of HOMO-LUMO gap is critical in terms of investigation of intramolecular charge transfer bands. In the following table 3 energy values have been calculated at the CAM-B3LYP in CH_2Cl_2 (Table 3). For TCNE-attached push-pull dye $\Delta E(E_{HOMO} - E_{LUMO})$ value was calculated as 4.86 eV. For TCNQ-attached push-pull dye, it is 3.75 eV.

Table 3. E_{HOMO}, E_{LUMO} and $\Delta E(E_{HOMO} - E_{LUMO})$ of **130** and **135** at the CAM-B3LYP level of theory in CH_2Cl_2.

	130	135
Basis Set Solvent	**CAM-B3LYP DCM**	**CAM-B3LYP DCM**
E_{HOMO} (Ev)	-6.88	-6.38
E_{LUMO} (eV)	-2.02	-2.63
ΔE (eV)	4.86	3.75

CHAPTER 4

CONCLUSION

The first part of this thesis covers synthesizing triazene-substituted conjugated push-pull chromophores *via* click-type [2+2] CA-RE reactions. Six different push-pull dyes were obtained through the reaction between electron donor alkyne and electron acceptor alkene groups. Electron donating ability of triazene group was used to activate alkyne for targeted reaction. As an electron acceptor, TCNE **41** was chosen. Due to the instability of attained push-pull chromophores in silica, qNMR was applied to calculate the yields which were in between 42 and 96%. Since push-pull dyes are expected to have an excellent ICT properties in the visible region, UV/Vis spectroscopy was applied to investigate it. Furthermore, solvatochromism approved the validity of the ICT ability of six different substrates. Besides experimental investigations, theoretical calculations certified on electron donor ability of triazene group and optoelectronic properties of obtained push-pull chromophores.

The next chapter focus on widening substrate scope for the synthesis of push-pull chromophores. For that purpose, triazene-substituted non-terminal alkyne-containing molecules were synthesized *via* Sonogashira cross-coupling and Hay coupling reactions, respectively. Targeted push-pull chromophores could not be achieved either with TCNE or TCNQ electron acceptors; instead, the formation of diphenylacetylene and 1,4-diphenylbuta-1,3-diyne were observed. However, we stuck to the idea of obtaining push-pull chromophores with non-terminal alkynes, which is the subject of the following chapter.

By taking advantage of diethylaniline's strong electron-donating ability, non-terminal cross-coupling substrates and dimers were synthesized successfully. Substrates reacted with TCNE and TCNQ in a short period of time, purified easily by column chromatography, and gave high yields (95-99%) of push-pull chromophores. Spectroscopic techniques, such as ^{1}H and ^{13}C NMR analysis and HR-MS, allowed to characterize structures of obtained cross-coupling products, dimers, and push-pull chromophores. In addition, UV/Vis spectroscopy data and solvatochromism was utilized to investigate optoelectronic properties of push-pull dyes experimentally. Computational methods allowed the study of ICT properties obtained structures theoretically and compared them with experimental results.

CHAPTER 5

EXPERIMENTAL

5.1 Materials and Methods

Reagents were purchased as reagent grade and used without further purification. Commercially available chemicals were purchased by Merck, Fluka , Across, Abcr and Sigma Aldrich.

Solvents for extraction or Flash column chromatography were distilled.

Reactions on exclusion of air and moisture were performed in oven-dried glassware and under N_2 atmosphere.

Analytical thin layer chromatography (TLC) was performed on aluminum sheets coated with 0.2 mm silica gel 60 F254 (Merck) and visualized with a UV lamp (254 or 366 nm).

Evaporation in vacuo was performed at 25–60 °C and 900–10 mbar. Reported yields refer to spectroscopically and chromatographically pure compounds that were dried under high vacuum (0.1–0.05 mbar) before analytical characterization.

Nuclear magnetic resonance (NMR) spectra were recorded on Bruker Avance III Ultrashield 400 Hz NMR spectrometer in $CDCl_3$. Chemical shifts δ are reported in ppm downfield from tetramethylsilane (TMS) using the residual solvent signals as an internal reference ($CDCl_3$: $\delta_H = 7.26$ ppm, $\delta_C = 77.16$ ppm. For ^{1}H NMR, coupling constants J are reported in Hz and the resonance multiplicity is defined as s (singlet), d (doublet), t (triplet), q (quartet), quint (quintet), sext (sextet), sept (septet), m (multiplet), and br. (broad). All spectra were recorded at 298 K. NMR spectra were processed by using MestReNova program.

High-resolution mass spectrometry (HR-MS) was performed by the MS-service of the National Nanotechnology Research Center (UNAM) at Bilkent University and mass spectra recorded by LC-MS TOF electrospray ionization. Also, some HRMS result were obtained by MS-service of METU Central Laboratory. Spectra were processed in electro spray ionization with positive mode using Time of Flight mass analyzer. Masses are reported in m/z units as the molecule ion as $[M + H]^+$.

5.2 Synthetic Procedure

5.2.1 General Procedure of Conjugated Push-Pull Chromophores[20]

A solution of **86a–f** (1.5 mmol, 1 equiv.) and TCNE (1.5 mmol, 1 equiv.) in dichloromethane (8 mL) was stirred at 25 °C until complete consumption of starting material based on TLC analysis. After evaporation of the solvent, the obtained product was washed with hexanes (3 x 50 mL) to yield **87-92** in moderate to high 42–96% yields.

Compound 87:
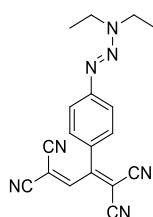
A dark-purple solid; 76%; $R_f = 0.27$ (SiO$_2$; DCM); ^{1}H NMR (400 MHz, CDCl$_3$, 298 K): $\delta = 1.24$ (t, $J = 7.0$ Hz, 3 H), 1.37 (t, $J = 7.0$ Hz, 3 H), 3.84 (q, $J = 7.0$ Hz, 4H), 7.46 (quasi d, $J = 8.7$ Hz, 2H), 7.61 (quasi d, $J = 8.7$ Hz, 2H), 8.03 ppm (s, 1 H); ^{13}C NMR (100 MHz, CDCl$_3$, 298 K): $\delta = 161.6, 156.7, 153.9, 130.7, 126.0, 122.0, 112.1, 111.8, 111.7, 108.8, 98.1, 88.0, 49.9, 42.1, 14.5, 11.3$ ppm; UV/Vis

(CH$_2$Cl$_2$): λ_{max} (ε) = 237 (9447), 305 (16583), 336 (19146), 508 nm (6080 M^{-1} cm^{-1}); HRMS: m/z calcd for C$_{18}$H$_{16}$N$_7$$^+$: 330.14617; found: 330.14529 [M + H]$^+$.

Compound 88:

A dark-purple solid; 96%; R$_f$ = 0.27 (SiO$_2$; DCM); ^{1}H NMR (400 MHz, CDCl$_3$, 298 K): δ = 1.27 (d, J = 6.8 Hz, 6H), 1.41 (d, J = 6.8 Hz, 6H), 4.09 (hept, J = 6.7 Hz, 1H), 5.38 (hept, J = 6.7 Hz, 1H), 7.47 (quasi d, J = 8.7 Hz, 2H), 7.59 ppm (quasi d, J = 8.7 Hz, 2H), 8.04 ppm (s, 1H); ^{13}C NMR (100 MHz, CDCl$_3$, 298 K): δ = 161.5, 157.2, 154.2, 130.8, 125.7, 121.8, 112.3, 111.80, 111.78, 108.8, 98.0, 87.3, 50.2, 47.4, 24.0, 19.4 ppm; UV/Vis (CH$_2$Cl$_2$): λ_{max} (ε) = 238 (12509), 303 (19862), 342 (24049), 524 nm (7965 M^{-1} cm^{-1}); HRMS: m/z calcd for C$_{20}$H$_{20}$N$_7$$^+$: 358.17747; found: 358.17724 [M + H]$^+$.
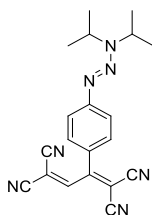
Compound 89:
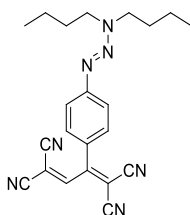
A dark-purple solid; 79%; R$_f$ = 0.41 (SiO$_2$; DCM); ^{1}H NMR (400 MHz, CDCl$_3$, 298 K): δ = 0.94–1.02 (m, 6H), 1.34–1.46 (m, 4H), 1.61–1.76 (m, 4H), 3.74–3.79 (m, 4H), 7.46 (quasi d, J = 8.7 Hz, 2H), 7.59 (quasi d, J = 8.7 Hz, 2H), 8.03 ppm

57

(s,1H); ^{13}C NMR (100 MHz, CDCl$_3$, 298 K): δ = 161.6, 156.7, 154.0, 130.7, 125.9, 121.9, 112.2, 111.8, 111.7, 108.8, 98.1, 87.7, 48.4, 47.5, 31.1, 28.1, 20.0, 19.9, 13.9, 13.8 ppm; UV/Vis (CH$_2$Cl$_2$): λ_{max} (ε) = 235 (18500), 303 (26450), 343 (31700), 521 nm (11300 M^{-1} cm^{-1}); HRMS: m/z calcd for C$_{22}$H$_{24}$N$_7^+$: 386.20877; found: 386.20909 [M + H]$^+$.

Compound 90:
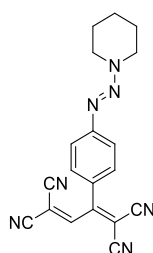
A dark-purple solid; 92%; R$_f$ = 0.24 (SiO$_2$; DCM); ^{1}H NMR (400 MHz, CDCl$_3$, 298 K): δ = 1.63–1.90 (m, 6H), 3.88–3.94 (m, 4H), 7.46 (quasi d, J = 8.7 Hz, 2H), 7.62 (quasi d, J = 8.7 Hz, 2H), 8.04 ppm (s, 1H); ^{13}C NMR (100 MHz, CDCl$_3$, 298 K): δ = 161.6, 156.3, 153.8, 130.7, 126.3, 122.0, 112.0, 111.8, 111.6, 108.7, 98.1, 88.3, 53.7, 44.1, 26.5, 24.7, 24.3 ppm; UV/Vis (CH$_2$Cl$_2$): λ_{max} (ε) = 234 (16616), 303 (27083), 337 (30691), 499 nm (9451 M^{-1} cm^{-1}); HRMS: m/z calcd for C$_{19}$H$_{16}$N$_7^+$: 342.14617; found: 342.14675 [M + H]$^+$.

Compound 91:
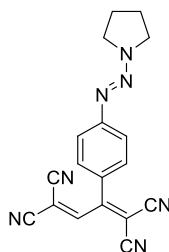
A dark-brown solid; 42%; $R_f = 0.09$ (SiO$_2$; DCM); ^{1}H NMR (400 MHz, CDCl$_3$, 298 K): $\delta = 2.04$–2.12 (m, 4H), 3.72 (t, $J = 6.4$ Hz, 2H), 3.99 (t, $J = 6.4$ Hz, 2H), 7.45 (quasi d, $J = 8.7$ Hz, 2H), 7.60 (quasi d, $J = 8.7$ Hz, 2H), 8.02 ppm (s, 1H); ^{13}C NMR (100 MHz, CDCl$_3$, 298 K): $\delta = 161.6$, 156.8, 153.8, 130.7, 126.1, 121.9, 112.1, 111.8, 111.7, 108.7, 98.1, 88.0, 51.9, 47.2, 24.0, 23.6 ppm; UV/Vis (CH$_2$Cl$_2$): λ_{max} (ε) = 228 (1829), 239 (12850), 336 (25090), 507 nm (8177 M^{-1} cm^{-1}); HRMS: m/z calcd for C$_{18}$H$_{14}$N$_7{}^+$: 328.13052; found: 328.13035 [M + H]$^+$.

**Compound 92:**
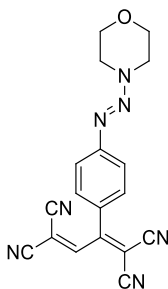
A dark-brown solid; 46%; $R_f = 0.11$ (SiO$_2$; DCM); ^{1}H NMR (400 MHz, CDCl$_3$, 298 K): $\delta = 3.80$–4.00 (m, 8 H), 7.46 (quasi d, $J = 8.6$ Hz, 2H), 7.64 (quasi d, $J = 8.6$ Hz, 2H), 8.03 ppm (s, 1H); ^{13}C NMR (100 MHz, CDCl$_3$, 298 K): $\delta = 161.7$, 155.2, 153.2, 130.6, 127.0, 122.4, 111.80, 111.79, 111.3, 108.6, 98.2, 89.7, 66.6 (2xC) ppm (13 out of 14 signals); UV/Vis (CH$_2$Cl$_2$): λ_{max} (ε) = 233 (14141), 322 (28849), 476 nm (6313 M^{-1} cm^{-1}); HRMS: m/z calcd for C$_{18}$H$_{14}$N$_7$O$^+$: 344.12543; found: 344.12583 [M + H]$^+$.

5.2.2 General Synthetic Procedures for Unsymmetrical and Symmetrical Sonogashira Cross-coupling Products

In a 100 mL round bottom flask compound **84** (0.50 mmol, 1 equiv.), bis (triphenylphosphine) palladium (II) dichloride (0.015 mmol, 0.03 equiv.) and copper

iodide (0.015 mmol, 0.03 equiv.) were added. The flask was flushed with nitrogen for 30 minutes, triethylamine (15 mL) added *via* syringe into flask and flushed with nitrogen for an additional 30 minutes, followed by addition of **86** (0.55 mmol, 1,1 equiv.). After stirring overnight at 25 °C, the solvents were removed under reduced pressure, target coupled alkynes **94-101** were isolated in 27-52% yields by performing column chromotograhy (CC) (SiO$_2$; 1:9 EtOAc : *c*-hexane).

Compound 94:
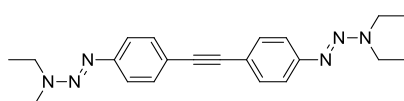
A yellow solid; 52%; CC: (SiO$_2$; 1:9 EtOAc : *c*-hexane); R$_f$ = 0.23 (SiO$_2$; 1:9 EtOAc : *c*-hexane); m.p. 106–108 °C; ^{1}H NMR (400 MHz, CDCl$_3$, 298K) δ= 1.28 (t, *J* = 6.3 Hz, 12H), 3.78 (q, *J* = 7.2 Hz, 8H), 7.40 (quasi d, *J* = 8.6 Hz, 4H), 7.50 ppm (quasi d, *J* = 8.6 Hz, 4H); ^{13}C NMR (100 MHz, CDCl$_3$, 298 K): δ = 151.0, 132.3, 120.5, 120.0, 89.9, 49.5, 42.5, 13.2 ppm.

Compound 95:
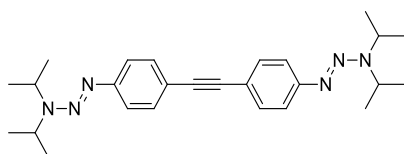
An orange solid; 35%; CC: (SiO$_2$; 1:9 EtOAc : *c*-hexane); R$_f$ = 0.61 (SiO$_2$; 1:9 EtOAc : *c*-hexane); m.p. 148–149 °C; ^{1}H NMR (400 MHz, CDCl$_3$, 298K) δ = 1.32 (br. s, 24H), 4.01 (br. s, 2H), 5.32 (br. s, 2H), 7.40 (quasi d, *J* = 8.5 Hz, 4H), 7.49

ppm (quasi d, J = 8.5 Hz, 4H); ^{13}C NMR (100 MHz, CDCl$_3$, 298 K): δ = 151.4, 132.3, 120.4, 119.6, 89.9, 48.9, 46.2, 23.8, 19.5 ppm.

Compound 96:
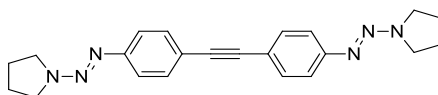
A shiny yellow solid; 28%; CC: (SiO$_2$; 1:2 EtOAc : c-hexane); R$_f$ = 0.74 (SiO$_2$; 1:9 EtOAc : c-hexane); m.p. 109–111 °C; ; ^{1}H NMR (400 MHz, CDCl$_3$, 298 K) δ = 2.02 (br. s, 8H), 3.50–4.00 (m, 8H), 7.16 (quasi d, J = 8.7 Hz, 4H), 7.61 ppm (quasi d, J = 8.7 Hz, 4H); ^{13}C NMR (100 MHz, CDCl$_3$, 298 K): δ = 151.2, 137.9, 122.5 (2 x C), 89.2, 51.0, 46.7, 23.9 ppm.

Compound 97:
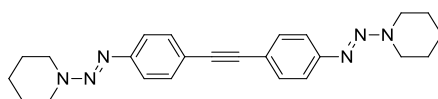
An orange liquid; 42%; CC: (SiO$_2$; 1:4 EtOAc : c-hexane); R$_f$ = 0.66 (SiO$_2$; 1:9 EtOAc : c-hexane); ^{1}H NMR (400 MHz, CDCl$_3$, 298 K) δ = 1.71 (br. s, 12H), 3.81 (br. s, 8H), 7.39 (quasi d, J = 8.6 Hz, 4H), 7.49 ppm (quasi d, J = 8.6 Hz, 4H); ^{13}C NMR (100 MHz, CDCl$_3$, 298 K): δ = 150.6, 137.8, 122.6 (2 x C), 89.8, 43.1, 25.4, 24.4 ppm.

Compound 98:
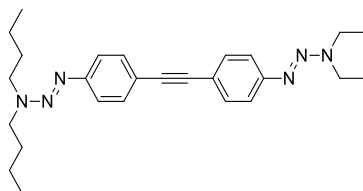
A brown liquid; 34%; CC: (SiO$_2$; 1:9 EtOAc : *c*-hexane); R$_f$ = 0.63 (SiO$_2$; 1:9 EtOAc : *c*-hexane); ^{1}H NMR (400 MHz, CDCl$_3$, 298 K) δ = 0.96 (t, *J* = 7.3 Hz, 6H), 1.21–1.31 (m, 6H), 1.32–1.41 (m, 4H), 1.61–1.73 (m, 4H), 3.66–3.82 (m, 8H), 7.38 (quasi d, *J* = 8.6 Hz, 2H), 7.39 (quasi d, *J* = 8.6 Hz, 2H), 7.48 (quasi d, *J* = 8.4 Hz, 2H), 7.49 ppm (quasi d, *J* = 8.6 Hz, 2H); ^{13}C NMR (100 MHz, CDCl$_3$, 298 K): δ = 150.92, 150.89, 132.3 (2 x C), 120.5 (2 x C), 119.9, 119.8, 89.94, 89.85, 65.6, 47.1, 20.3, 14.0 ppm.

Compound 99:
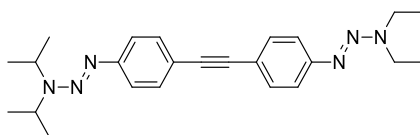
A shiny pale yellow solid; 27%; CC: (SiO$_2$; 1:9 EtOAc : *c*-hexane); R$_f$ = 0.3 (SiO$_2$; 1:9 EtOAc : *c*-hexane); m.p. 77–79 °C; ^{1}H NMR (400 MHz, CDCl$_3$, 298 K) δ = 1.19–1.43 (m, 18H), 3.78 (q, *J* = 7.1 Hz, 4H), 3.88–4.20 (m, 1H), 5.14–5.47 (m, 1H) 7.40 (quasi d, *J* = 8.5 Hz, 4H), 7.48 (quasi d, *J* = 8.6 Hz, 2H), 7.49 ppm (quasi d, *J* = 8.5 Hz, 2H); ^{13}C NMR (100 MHz, CDCl$_3$, 298 K): δ = 151.4, 150.9, 132.3 (2xC), 120.5, 120.3, 120.0, 119.5, 90.0, 89.8, 47.9, 23.8, 19.2, 12.9 ppm.

Compound 100:
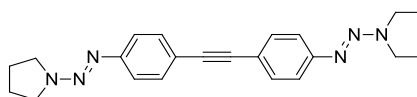
A dark brown solid; 32%; CC: (SiO$_2$; 1:9 EtOAc : c-hexane); R$_f$ = 0.51 (SiO$_2$; 1:9 EtOAc : c-hexane); m.p. 124–125 °C; ^{1}H NMR (400 MHz, CDCl$_3$, 298 K) δ = 1.20–1.35 (m, 6H), 1.96–2.10 (m, 4H), 3.70–3.88 (m, 8H), 7.42 (quasi d, J = 8.6 Hz, 4H), 7.50 ppm (quasi d, J = 8.5 Hz, 2H), 7.52 ppm (quasi d, J = 8.3 Hz, 2H); ^{13}C NMR (100 MHz, CDCl$_3$, 298 K): δ = 151.1, 150.9, 132.3, 132.2, 120.5, 120.4, 120.0, 199.0, 90.0, 89.9, 50.2, 52.1, 23.9 (2xC) ppm.

Compound 101:
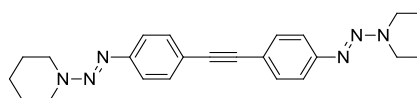
An orange liquid; 28%; CC: (SiO$_2$; 1:9 EtOAc : c-hexane); R$_f$ = 0.23 (SiO$_2$; 1:9 EtOAc : c-hexane); ^{1}H NMR (400 MHz, CDCl$_3$, 298 K) δ = 1.22–1.33 (m, 6H), 1.65–1.80 (m, 6H), 3.72–3.82 (m, 8H), 7.40 (quasi d, J = 8.5 Hz, 2H), 7.42 (quasi d, J = 8.5 Hz, 2H), 7.48 (quasi d, J = 8.5 Hz, 2H), 7.50 ppm (quasi d, J = 8.5 Hz, 2H); ^{13}C NMR (100 MHz, CDCl$_3$, 298 K): δ = 150.9, 150.5, 132.3 (2xC), 120.6, 120.5, 120.4, 119.8, 90.2, 89.8, 50.1, 42.7, 25.5, 24.5 ppm.

5.2.3 General Synthetic Procedure for Symmetrical Dimers

In a 50 ml round bottom flask CuI (0.005 mmol, 0.01 equiv.) was dissolved in 8 ml DCM, and when color of the reaction turned to blue, tetramethylethylenediamine (0.015 mmol, 0.03 equiv.), and **86** (1.00 mmol, 2 equiv.) was added subsequently. The reaction was stirred at 25 °C overnight, after removing solvent under reduced pressure, column chromatography (CC) (SiO$_2$; 1:9 EtOAc : c-hexane) gave **107-110** in 17-33% yields.[118]

Compound 107:
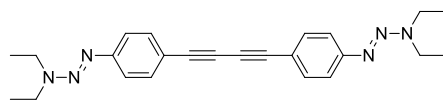
A dark yellow solid; 28%; CC: (SiO$_2$; 1:9 EtOAc : *c*-hexane); R$_f$ = 0.23 (SiO$_2$; 1:9 EtOAc : *c*-hexane); m.p. 119–122 °C; ^{1}H NMR (400 MHz, CDCl$_3$, 298 K) δ = 1.28 (t, *J* = 6.3 Hz, 12H); 3.78 (q, *J* = 7.2 Hz, 8H), 7.40 (quasi d, *J* = 8.5 Hz, 4H), 7.50 ppm (quasi d, *J* = 8.5 Hz, 4H); ^{13}C NMR (100 MHz, CDCl$_3$, 298 K): δ = 151.8, 133.3, 120.6, 118.0, 82.5, 74.1, 49.0, 42.0, 13.7, 12.1 ppm.

Compound 108:
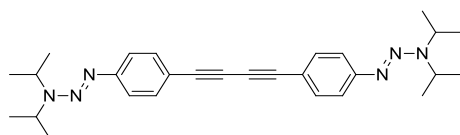
A brown solid; 33%; CC: (SiO$_2$; 1:9 EtOAc : *c*-hexane); R$_f$ = 0.5 (SiO$_2$; 1:9 EtOAc : *c*-hexane); m.p. 172–173 °C; ^{1}H NMR (400 MHz, CDCl$_3$, 298 K) δ = 1.20–1.42 (m, 24H), 4.01 (br. s, 2H), 5.30 (br. s, 2H), 7.37 (quasi d, *J* = 8.6 Hz, 4H), 7.48 ppm (quasi d, *J* = 8.6 Hz, 4H); ^{13}C NMR (100 MHz, CDCl$_3$, 298 K): δ = 152.3, 133.4, 120.4, 117.6, 82.5, 74.0, 49.0, 46.4, 27.0, 24.4, 19.5 ppm.

Compound 109:
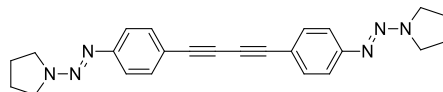
A dark yellow solid; 22%; CC: (SiO$_2$; 1:9 EtOAc : hexanes); R$_f$ = decomp. 233–235 °C; ^{1}H NMR (400 MHz, CDCl$_3$, 298 K) δ = 2.04 (br. s, 8H), 3.50–4.00 (m, 8H), 7.37 (quasi d, *J* = 8.6 Hz, 4H), 7.48 ppm (quasi d, *J* = 8.6 Hz, 4H); ^{13}C NMR

(100 MHz, CDCl$_3$, 298 K): δ = 152.0, 133.4, 133.2, 120.5, 82.5, 74.2, 51.3, 46.6, 29.8, 23.9 ppm.

Compound 110:
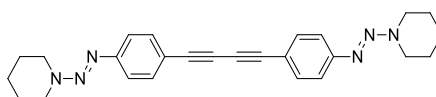
An orange solid; 17%; CC: (SiO$_2$; 1:9 EtOAc : c-hexane); R$_f$ = 0.43 (SiO$_2$; 1:9 EtOAc : c-hexane); decomp. 227–229 °C; ^{1}H NMR (400 MHz, CDCl$_3$, 298 K) δ = 1.71 (s, 12H), 3.81 (s, 8H), 7.39 (quasi d, J = 8.5 Hz, 4H), 7.49 ppm (quasi d, J = 8.5 Hz, 4H); ^{13}C NMR (100 MHz, CDCl$_3$, 298 K): δ = 151.4, 133.4, 120.7, 118.5, 82.4, 74.3, 37.1, 25.6, 24.5 ppm.

5.2.4 General Synthetic Procedures for Unsymmetrical Dimers

In a 50 ml round bottom flask CuI (0.005 mmol, 0.01 equiv.) was dissolved 8 ml CHCl$_3$: 1,4 dioxane mixture solvent (3 : 1 CHCl$_3$: 1,4 dioxane) and tetramethylethylenediamine (0.015 mmol, 0.03 equiv.) was added at 50 °C. Reagents **86c** and **86a** were added to the mixture and the reaction was left to be stirred overnight. The next day the resulting solution was cooled to room temperature and 8 ml of CHCl$_3$ was added. The mixture was washed with 6 ml of saturated NH$_4$Cl solution and dried over Mg$_2$SO$_4$. After purification with (CC) (SiO$_2$; 1:9 EtOAc : hexanes) the products **111**, and **112** were obtained in 36% and 22% yields respectively. Symmetrical product **107** yielded in a trace amount.

Compound 111:
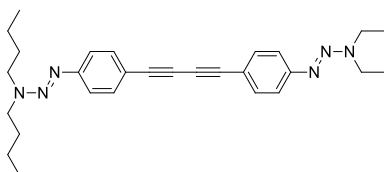
A brown liquid; 36%; CC: (SiO$_2$; 1:9 EtOAc : *c*-hexane); R$_f$ = 0.6 (SiO$_2$; 1:9 EtOAc : *c*-hexane); ^{1}H NMR (400 MHz, CDCl$_3$, 298 K) δ = 0.95 (t, *J* = 7.3 Hz, 6H), 1.20–1.30 (m, 6H), 1.31–1.41 (m, 4H), 1.61–1.73 (m, 4H), 3.66–3.72 (m, 4H), 3.75–3.81 (m, 4H), 7.34 (quasi d, *J* = 8.3 Hz, 2H), 7.37 (quasi d, *J* = 8.3 Hz, 2H), 7.49 ppm (quasi d, *J* = 8.3 Hz, 4H); ^{13}C NMR (100 MHz, CDCl$_3$, 298 K): δ = 151.78, 151.76, 133.4 (2xC), 120.54, 120.52, 118.0, 117.8, 83.0, 82.5, 74.11, 74.06, 54.90, 54.54, 46.9(2xC), 20.4, 20.0, 13.95(2xC) ppm.

Compound 112:
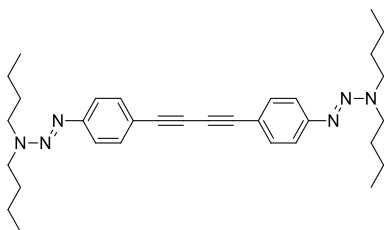
A brown oily liquid; 22%; CC: (SiO$_2$; 1:9 EtOAc : *c*-hexane); R$_f$ = 0.75 (SiO$_2$; 1:9 EtOAc : *c*-hexane); ^{1}H NMR (400 MHz, CDCl$_3$, 298 K) δ = 0.95 (t, *J* = 7.3 Hz, 12H), 1.30–1.40 (m, 8H), 1.60–1.70 (m, 8H), 3.70 (t, *J* = 7.0 Hz, 8H), 7.32 ppm (quasi d, *J* = 8.6 Hz, 4H), 7.46 ppm (quasi d, *J* = 8.5 Hz, 4H).

66

5.2.5 Synthetic Procedure for Diphenylacetylene

In a 100 mL round bottom flask compound **104** (0.50 mmol, 1 equiv.), bis (triphenylphosphine) palladium (II) dichloride (0.015 mmol, 0.03 equiv.) and copper iodide (0.015 mmol, 0.03 equiv.) were added. The flask was flushed with nitrogen for 30 minutes, triethylamine (15 mL) added *via* syringe into flask and flushed with nitrogen for an additional 30 minutes, followed by addition of **105** (0.55 mmol, 1.1 equiv.). After stirring overnight at 25 °C, the solvents were removed under reduced pressure, target coupled alkyne **103** were isolated in 81% yield by performing column chromotograhy (CC) (SiO$_2$; 1:9 EtOAc : hexanes). Spectral data is in consistent with literature.[119]

Compound 103:
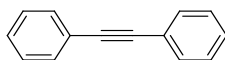
A yellow solid; 81%; CC: (SiO$_2$; 1:9 EtOAc : hexanes); R$_f$ = 0.71 (SiO$_2$; 1:9 EtOAc : hexanes); ^{1}H NMR (400 MHz, CDCl$_3$, 298 K) δ = 7.34–7.36 (m, 6H), 7.53–7.55 ppm (m, 4H); ^{13}C NMR (100 MHz, CDCl$_3$, 298 K) δ 131.7, 128.5, 128.4, 123.4, 89.5 ppm.

5.2.6 Synthetic Procedure for 1,4-diphenylbuta-1,3-diyne

In a 50 ml round bottom flask CuI (0.005 mmol, 0.01 equiv.) was dissolved in 8 ml DCM, and when color of the reaction turned to blue, tetramethylethylenediamine (0.015 mmol, 0.03 equiv.), and **105** (1.00 mmol, 2 equiv.) were added subsequently. The reaction was stirred at 25 °C overnight, after removing solvent under reduced pressure, column chromatography (CC) (SiO$_2$; 1 : 9 EtOAc : hexanes) gave **114** in 86% yield.[122] Spectral data is in consistent with literature.[120]

Compound 114:
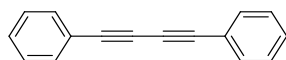
A white crystal solid; 86%; CC: (SiO$_2$; 1:9 EtOAc : hexanes); R$_f$ = 0.71 (SiO$_2$; 1:9 EtOAc : hexanes); ^{1}H NMR (400 MHz, CDCl$_3$, 298 K) δ = 7.52–7.54 (m, 6H), 7.32–7.40 ppm (m, 4H); ^{13}C NMR (100 MHz, CDCl$_3$, 298 K) δ = 132.6, 129.4, 128.6, 121.9, 81.7, 74.0 ppm

5.2.7 Synthetic procedures for CA-RE products

Compound 122
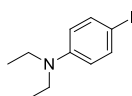
Target synthesis was carried out by following the literature. 4-iodoaniline **83** (1.00 g, 4.57 mmol), iodoethane (1.51 mL, 18.86 mmol) and sodium carbonate (1.14 g, 10.73 mmol) mixed in DMF (15 mL) at 70 °C for 14 h. Then, the solution was diluted with water (50 mL) and extracted with EtOAc (50 mL). After the organic phase was washed with brine (50 mL), it was dried over MgSO$_4$ and evaporated under vacuum. The target product **122** was obtained after column chromatography (SiO$_2$; hexanes) as pale yellow oil. [(1.11 g, 88%; R$_f$ = 0.72 (SiO$_2$; hexanes)]. ^{1}H NMR (400 MHz, CDCl$_3$, 298 K) δ = 1.14 (t, *J* = 7.1 Hz, 6H), 3.32 (q, *J* = 7.1 Hz, 4H), 6.45 (quasi d, *J* = 9.0 Hz, 2H), 7.43 ppm (quasi d, *J* = 9.0 Hz, 2H); ^{13}C NMR (100 MHz, CDCl$_3$, 298 K) δ = 147.7, 138.2, 114.6, 76.1, 44.8, 12.8 ppm. Spectral data were consistent with literature.[121]

Compound 123
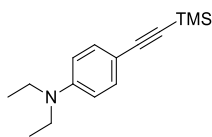
In a 100 mL round bottom flask compound **122** (1.00 mmol, 1 equiv.), bis (triphenylphosphine) palladium (II) dichloride (0.03 mmol, 0.03 equiv.) and copper iodide (0.03 mmol, 0.03 equiv.) were added. The flask was flushed with nitrogen for 30 minutes, triethylamine (15 mL) added *via* syringe into flask and flushed with nitrogen for an additional 30 minutes, followed by addition of trimethylsilyacetylene (1.1 mmol, 1.1 equiv.). After stirring overnight at 25 °C, the solvents were removed under reduced pressure, target TMS-protected alkynes **123** were isolated in 86% yields by performing column chromotograhy (CC) (SiO$_2$; 1:9 EtOAc : hexanes). [(211 mg, 86%; R$_f$ = 0.4 (SiO$_2$; 1:9 EtOAc:hexanes)]. ^{1}H NMR (400 MHz, CDCl$_3$, 298 K): δ = 0.23 (s, 9H), 1.16 (t, J = 7.1 Hz, 6H), 3.35 (q, J = 7.1 Hz, 4H), 6.55 (quasi d, J = 9.0 Hz, 2H), 7.31 ppm (quasi d, J = 9.0 Hz, 2H). Spectral data was consistent with literature.[121]

Compound 124
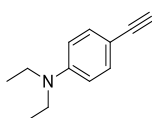
TMS-protected alkyne **123** (1.00 mmol, 1 equiv.) were dissolved in methanol (15 mL). Then, potassium carbonate (3.30 mmol, 3.30 equiv.) was added to this solution. After filtration, evaporation, and column chromatography (CC) (SiO$_2$; 1:9 EtOAc : hexanes) terminal alkyne **124** were obtained in 81% yields. ^{1}H NMR (400 MHz, CDCl$_3$, 298 K): δ = 1.17 (t, J = 7.0 Hz, 6H), 2.97 (s, 1H), 3.35 (q, J = 7.1 Hz, 4H), 6.58 (quasi d, J = 9.0 Hz, 2H), 7.34 ppm (quasi d, J = 9.0 Hz, 2H). Spectral data was consistent with literature.[121]

5.2.8 General Synthetic Procedures for DEA-substituted Coupling Products

In a 100 mL round bottom flask compound **84a-e** (1.00 mmol, 1 equiv.), bis (triphenylphosphine) palladium (II) dichloride (0.03 mmol, 0.03 equiv.) and copper iodide (0.03 mmol, 0.03 equiv.) were added. The flask was flushed with nitrogen for 30 minutes, triethylamine (15 mL) added *via* syringe into flask and flushed with nitrogen for an additional 30 minutes, followed by addition of **124** (1.10 mmol, 1.10 equiv.). After stirring overnight at 25 °C, the solvents were removed under reduced pressure, target coupled alkynes **125-129** were isolated in 56-78% yields by performing column chromotograhy (CC) (SiO$_2$; 1:9 EtOAc : hexanes).

Compound 125
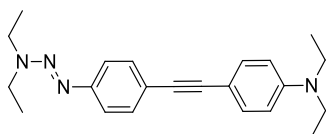
A yellow solid; 56%; CC: (SiO$_2$; 1:9 EtOAc : hexanes); R$_f$ = 0.51 (SiO$_2$; 1:9 EtOAc : hexanes); m.p. 116–118 °C; ^{1}H NMR (400 MHz, CDCl$_3$, 298 K) δ = 1.18 (t, *J* = 7.1 Hz, 6H), 1.27 (t, *J* = 7.0 Hz, 6H), 3.37 (q, *J* = 7.0 Hz, 4H), 3.77 (q, *J* = 7.1 Hz, 4H), 6.61 (quasi d, *J* = 8.7 Hz, 2H), 7.37 (quasi d, *J* = 8.7 Hz, 4H), 7.45 ppm (quasi d, *J* = 8.7 Hz, 2H); ^{13}C NMR (100 MHz, CDCl$_3$, 298 K) δ = 150.5, 147.6, 133.0, 132.0, 120.8, 120.5, 111.5, 109.6, 90.6, 87.8, 44.5, 12.7 ppm; HRMS: m/z calcd for C$_{22}$H$_{28}$N$_4^+$: 349.2392; found: 349.2392 [M + H]$^+$.

Compound 126
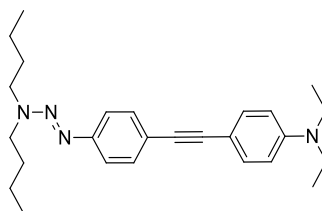
A brown solid; 67%; CC: (SiO$_2$; 1:9 EtOAc : hexanes); R$_f$ = 0.61 (SiO$_2$; 1:9 EtOAc : hexanes); m.p. 120–121 °C; ^{1}H NMR (400 MHz, CDCl$_3$, 298 K) δ = 0.97 (t, J = 7.4 Hz, 6H), 1.18 (t, J = 7.1 Hz, 6H), 1.32–1.44 (m, 4H), 1.61–1.70 (m, 4H), 3.37 (q, J = 7.1 Hz, 4H), 3.70 (t, J = 7.4 Hz, 4H), 6.62 (quasi d, J = 8.9 Hz, 2H), 7.37 (quasi d, J = 8.9, Hz, 4H), 7.45 ppm (quasi d, J = 8.9 Hz, 2H); ^{13}C NMR (100 MHz, CDCl$_3$, 298 K) δ = 150.5, 147.5, 133.0, 132.0, 120.6, 120.4, 111.4, 109.5, 90.6, 87.8, 44.5, 29.3, 20.4, 20.4, 14.0, 12.7 ppm; HRMS: m/z calcd for C$_{26}$H$_{36}$N$_4$$^+$: 405.3018; found: 405.3018[M + H]$^+$.

Compound 127

A pale yellowish green solid; 71%; CC: (SiO$_2$; 1:9 EtOAc : hexanes); R$_f$ = 0.46 (SiO$_2$; 1:9 EtOAc : hexanes); 130–131 °C; ^{1}H NMR (400 MHz, CDCl$_3$, 298 K) δ = 1.18 (t, J = 7.1 Hz, 6H), 2.00–2.10 (m, 4H), 3.37 (q, J = 7.0 Hz, 4H), 3.75–3.85 (m, 4H), 6.61 (quasi d, J = 8.8 Hz, 2H), 7.36-7.39 (m, 4H), 7.46 ppm (quasi d, J = 8.8 Hz, 2H); ^{13}C NMR (100 MHz, CDCl$_3$, 298 K) δ = 150.6, 147.5, 133.0, 132.1, 120.8, 120.4, 111.4, 109.5, 90.7, 87.7, 44.5, 23.9, 12.7 ppm; HRMS: m/z calcd for C$_{22}$H$_{26}$N$_4$$^+$: 347.2236; found: 347.2236 [M + H]$^+$.
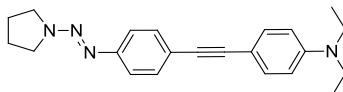
Compound 128
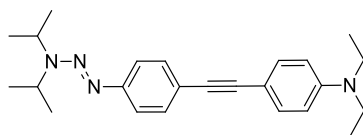
A pale yellow solid; 58%; CC: (SiO$_2$; 1:9 EtOAc : hexanes); R$_f$ = 0.53 (SiO$_2$; 1:9 EtOAc : hexanes); m.p. 101–102 °C; ^{1}H NMR (400 MHz, CDCl$_3$, 298 K) δ = 1.18 (t, J = 7.1 Hz, 6H), 1.22–1.40 (m, 12H), 3.37 (q, J = 7.1 Hz, 4H), 4.00–4.10 (m, 1H), 5.20–5.35 (m, 1H), 6.62 (quasi d, J = 8.6 Hz, 2H), 7.38 (quasi d, J = 8.6 Hz, 4H), 7.46 ppm (quasi d, J = 8.6 Hz, 2H); ^{13}C NMR (100 MHz, CDCl$_3$, 298 K) δ = 151.0, 147.5, 133.0, 132.0, 120.3, 120.1, 111.4, 109.5, 90.4, 87.9, 56.9, 44.5, 20.0, 12.7 ppm; HRMS: m/z calcd for C$_{24}$H$_{32}$N$_4$$^+$: 377.2701; found: 377.2705 [M + H]$^+$.

Compound 129

A pale yellow solid; 78%; CC: (SiO$_2$; 1:9 EtOAc : hexanes); R$_f$ = 0.52 (SiO$_2$; 1:9 EtOAc : hexanes); m.p. 133–134 °C; ^{1}H NMR (400 MHz, CDCl$_3$, 298 K) δ = 1.18 (t, J = 7.0 Hz, 6H), 1.71 (br. s, 6H), 3.37 (q, J = 6.9, 4H), 3.70–3.85 (m, 4H), 6.61 (quasi d, J = 8.5 Hz, 2H), 7.39 (quasi d, J = 8.7 Hz, 4H), 7.46 ppm (quasi d, J = 8.5 Hz, 2H); ^{13}C NMR (100 MHz, CDCl$_3$, 298 K) δ = 150.0, 147.6, 133.0, 132.1, 121.3, 120.6, 111.4, 109.5, 90.9, 87.7, 60.7, 44.5, 25.5, 24.5, 12.7 ppm; HRMS: m/z calcd for C$_{23}$H$_{28}$N$_4$$^+$: 361.2392; found: 361.2392 [M + H]$^+$.
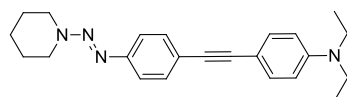
5.2.9 General Synthetic Procedures for CA-RE Products 130-134

A solution of **125-129** (1.5 mmol, 1 equiv.) and TCNE (1.5 mmol, 1 equiv.) in dichloromethane (8 mL) was stirred at 25 °C until complete consumption of starting material based on TLC analysis. After evaporation of the solvent, the obtained product **130-134** was purified by column chromatography (CC) (SiO$_2$; DCM) and yielded in between 95-99%.

Compound 130
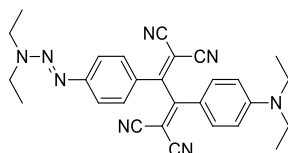
Yield : 97%; dark red; CC: (SiO$_2$; DCM); R$_f$ = 0.34 (SiO$_2$; DCM); m.p. 96–97 °C; ^{1}H NMR (400 MHz, CDCl$_3$, 298 K) δ = 1.20–1.30 (m, 9H), 1.36 (t, J = 6.9 Hz, 3H), 3.48 (q, J = 7.1 Hz, 4H), 3.83 (q, J = 7.2 Hz, 4H), 6.68 (quasi d, J = 9.4 Hz, 2H), 7.51 (quasi d, J = 8.9 Hz, 2H), 7.70-7.90 ppm (m, 4H); ^{13}C NMR (100 MHz, CDCl$_3$, 298 K) δ = 168.1, 163.9, 156.6, 152.7, 133.1, 131.4, 127.8, 121.6, 118.1, 114.8, 113.7, 113.3, 112.4, 112.0, 82.44, 73.74, 49.91, 45.23, 42.19, 14.50, 12.68, 11.29 ppm; λ_{max} (ε) = 454 (44432); (HRMS: m/z calcd for C$_{28}$H$_{28}$N$_8^+$: 477.2515; found: 477.2502 [M + H]$^+$.

Compound 131
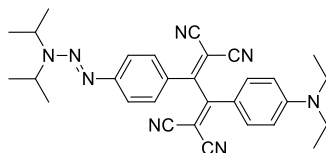
Yield : 99%; dark red; CC: (SiO$_2$; DCM); R$_f$ = 0.6 (SiO$_2$; DCM); m.p. 108–109 °C; ^{1}H NMR (400 MHz, CDCl$_3$, 298 K) δ = 1.22–1.28 (m, 12H), 1.40 (d, J = 6.5 Hz,

6H), 3.48 (q, J = 7.1 Hz, 4H), 4.05–4.11 (m, 1H), 5.34–5.40 (m, 1H), 6.68 (quasi d, J = 9.4 Hz, 2H), 7.51 (quasi d, J = 8.9 Hz, 2H), 7.75–7.84 ppm (m, 4H); ^{13}C NMR (100 MHz, CDCl$_3$, 298 K) δ = 168.0, 163.9, 157.1, 152.7, 133.0, 131.4, 127.40, 121.4, 118.0, 114.8, 113.7, 113.4, 112.5, 112.0, 82.0, 73.7, 50.3, 47.6, 45.2, 24.0, 19.4, 12.7 ppm; λ_{max} (ε) = 465 (55254); HRMS: m/z calcd for C$_{30}$H$_{32}$N$_8^+$: 505.2828; found: 505.2811 [M + H]$^+$.

Compound 132
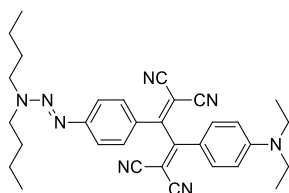
A dark red; 99%; CC: (SiO$_2$; DCM); R$_f$ = 0.81 (SiO$_2$; DCM); m.p. 135–136 °C; ^{1}H NMR (400 MHz, CDCl$_3$, 298 K) δ = 0.94–0.98 (m, 6H), 1.24 (t, J = 7.1 Hz, 6H), 1.33–1.40 (m, 4H), 1.59–1.70 (m, 4H), 3.48 (q, J = 7.1 Hz, 4H), 3.76 (t, J = 7.3 Hz, 4H), 6.68 (quasi d, J = 9.4 Hz, 2H), 7.50 (quasi d, J = 8.9 Hz, 2H), 7.70–7.85 ppm (m, 4H); ^{13}C NMR (100 MHz, CDCl$_3$, 298 K) δ = 168.0, 163.8, 156.6, 152.7, 133.0, 131.3, 127.5, 121.5, 117.9, 114.8, 113.8, 113.3, 112.4, 112.0, 82.2, 73.5, 55.2, 47.5, 45.2, 30.9, 28.1, 20.6, 19.9, 13.8, 13.7, 12.6 ppm; λ_{max} (ε) = 467 (60651); HRMS: m/z calcd for C$_{32}$H$_{36}$N$_8^+$: 533.3141; found: 533.3125 [M + H]$^+$.

Compound 133

A dark red; 96%; CC: (SiO$_2$; DCM); R$_f$ = 0.44 (SiO$_2$; DCM); m.p. 108–109 °C; ^{1}H NMR (400 MHz, CDCl$_3$, 298 K) δ = 1.25 (t, J = 7.1 Hz, 6H), 1.70–1.85 (m,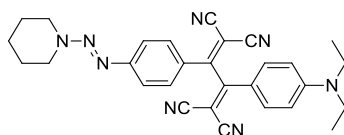 6H), 3.48 (q, J = 7.1 Hz, 4H), 3.80–4.00 (m, 4H), 6.68 (quasi d, J = 9.4 Hz, 2H), 7.52 (quasi d, J = 8.8 Hz, 2H), 7.78–7.80 ppm (m, 4H); ^{13}C NMR (100 MHz, CDCl$_3$, 298 K) δ = 168.1, 163.8, 156.3, 152.7, 133.0, 131.3, 128.0, 121.6, 118.0, 114.8, 113.7, 113.2, 112.3, 112.0, 82.7, 73.7, 53.9, 45.2, 44.4, 26.6, 24.8, 24.3, 12.7 ppm; λ$_{max}$ (ε) = 461 (46016); HRMS: m/z calcd for C$_{29}$H$_{28}$N$_8^+$: 489.2499; found: 489.2515 [M + H]$^+$.

Compound 134
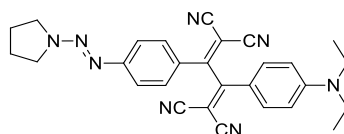
Yield : 96%; dark red; CC: (SiO$_2$; DCM); R$_f$ = 0.34 (SiO$_2$; DCM); m.p. 127–128 °C; ^{1}H NMR (400 MHz, CDCl$_3$, 298 K) δ = 1.25 (t, J = 7.1 Hz, 6H), 2.13–2.01 (m, 4H), 3.48 (q, J = 7.1 Hz, 4H), 3.71 (t, J = 6.1 Hz, 2H), 3.98 (t, J = 5.8 Hz, 2H), 6.68 (quasi d, J = 8.9 Hz, 2H), 7.50 (quasi d, J = 8.9 Hz, 2H), 7.78 ppm (quasi d, J = 8.9 Hz, 4H); ^{13}C NMR (100 MHz, CDCl$_3$, 298 K) δ = 168.0, 163.9, 156.8, 152.7, 133.0, 131.4, 127.8, 121.5, 118.1, 114.8, 113.7, 113.2, 112.4, 112.0, 82.5, 73.8, 51.9, 47.2, 45.2, 24.0, 23.6, 12.7 ppm; λ$_{max}$ (ε) = 459 (51149); HRMS: m/z calcd for C$_{28}$H$_{26}$N$_8^+$: 475.2359; found: 475.2360 [M + H]$^+$.

5.2.10 General Synthetic Procedures for CA-RE Products 135-139

A solution of **125-129** (1.5 mmol, 1 equiv.) and TCNQ (1.5 mmol, 1 equiv.) in dichloromethane (8 mL) was stirred at 25 °C until complete consumption of starting material based on TLC analysis. After evaporation of the solvent, the obtained

product **135-139** was purified by column chromatography (CC) (SiO$_2$; DCM) and yielded in between 95-99%.

Compound 135
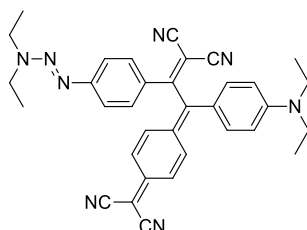
A dark green; 97%; CC: (SiO$_2$; DCM); R$_f$ = 0.38 (SiO$_2$; DCM); m.p. 220–221 °C; ^{1}H NMR (400 MHz, CDCl$_3$, 298 K) δ = 1.23–1.26 (m, 9H), 1.32–1.36 (m, 3H), 3.47 (q, J = 7.0 Hz, 4H), 3.81 (q, J = 7.0 Hz, 4H), 6.69 (quasi d, J = 9.1 Hz, 2H), 6.96 (dd, J = 9.5, 1.9 Hz, 1H), 7.12 (dd, J = 9.5, 1.9 Hz, 1H), 7.20–7.35 (m, 3H), 7.45 (quasi d, J = 9.1 Hz, 2H); 7.54 (dd, J = 9.6, 1.9 Hz, 1H), 7.70 ppm (quasi d, J = 9.1 2H); ^{13}C NMR (100 MHz, CDCl$_3$, 298 K) δ = 171.8, 155.9, 154.5, 153.2, 151.3, 136.0, 135.1, 134.7, 131.5, 131.0, 130.5, 124.9, 124.5, 123.5, 121.4, 115.4, 115.2, 113.9, 113.1, 112.4, 83.5, 69.9, 49.8, 45.1, 42.1, 14.5, 12.8, 11.3 ppm; λ$_{max}$ (ε) = 338 (20100), 404 (30098), 461 (26434), 691 nm (40519 M^{-1} cm^{-1}); HRMS: m/z calcd for C$_{34}$H$_{32}$N$_8{}^+$: 553.2828; found: 553.2829 [M + H]$^+$.

Compound 136
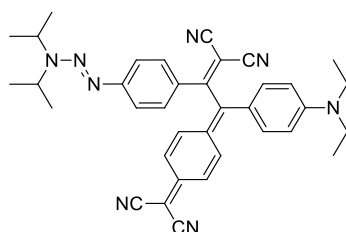
A dark green; 99%; CC: (SiO$_2$; DCM); R$_f$ = 0.26 (SiO$_2$; DCM); m.p. 166–168 °C; ^{1}H NMR (400 MHz, CDCl$_3$, 298 K) δ = 1.10–1.30 (m, 12H), 1.37 (t, J = 7.4 Hz, 6H), 3.40–3.55 (m, 4H), 4.03–4.09 (m, 1H), 5.31–5.38 (m, 1H), 6.69 (quasi d, J = 9.2, 2H); 6.97 (dd, J = 9.5, 1.8 Hz, 1H), 7.12 (dd, J = 9.5, 1.8 Hz, 1H), 7.24–7.31 (m, 3H), 7.46 (quasi d, J = 8.8, 2H), 7.54 (dd, J = 9.5, 1.9 Hz, 1H), 7.70 ppm (quasi d, J = 8.8, 2H); ^{13}C NMR (100 MHz, CDCl$_3$, 298 K) δ = 171.7, 156.4, 154.5, 153.3, 151.3, 136.0, 135.1, 134.8, 131.5, 131.0, 130.2, 124.9, 124.5, 123.5, 121.2, 115.4, 115.2, 114.0, 113.2, 112.4, 83.1, 70.0, 50.1, 47.4, 45.1, 31.1, 24.0, 19.4, 12.8 ppm; λ$_{max}$ (ε) = 337 (20631), 406 (31361), 463 (28758), 691 nm (42798 M^{-1} cm^{-1}); HRMS: m/z calcd for C$_{36}$H$_{36}$N$_8{}^+$: 581.3141; found: 581.2789 [M + H]$^+$.

Compound 137
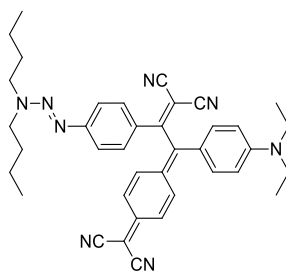
A dark green; 99%; CC: (SiO$_2$; DCM); R$_f$ = 0.28 (SiO$_2$; DCM); m.p. 227–229 °C; ^{1}H NMR (400 MHz, CDCl$_3$, 298 K) δ = 0.92–0.96 (m, 6H), 1.24 (t, J = 6.6 Hz, 6H), 1.22–1.39 (m, 4H), 1.55–1.73 (m, 4H), 3.47 (q, J = 6.6 Hz, 4H), 3.73–3.74 (m, 4H), 6.69 (quasi d, J = 7.7, 2H), 6.97 (d, J = 9.5 Hz, 1H), 7.11 (d, J = 9.5 Hz, 1H), 7.24–7.30 (m, 3H), 7.41–7.48 (m, 2H), 7.54 (d, J = 9.5 Hz, 1H), 7.70 ppm (quasi d, J = 8.6, 2H); ^{13}C NMR (100 MHz, CDCl$_3$, 298 K) δ = 171.7, 156.0, 154.5, 153.3, 151.3, 136.0, 135.1, 134.7, 131.5, 131.0, 130.4, 124.9, 124.5, 123.5, 121.4, 115.4, 115.2, 114.0, 113.2, 112.4, 83.3, 69.7, 55.2, 47.4, 45.1, 31.0, 28.1, 20.6, 19.9, 13.9, 13.8,

12.7 ppm; λ_{max} (ε) = 338 (17142), 409 (27303), 464 (25246), 692 nm (37003 M^{-1} cm^{-1}); HRMS: m/z calcd for $C_{38}H_{40}N_8^+$: 609.3454; found: 609.3426 [M + H]$^+$.

Compound 138
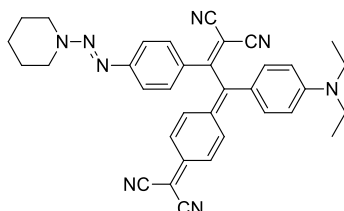
A dark green; 96%; CC: (SiO$_2$; DCM); (SiO$_2$; DCM); R$_f$ = 0.19 (SiO$_2$; DCM); m.p. 233–234 °C; ^{1}H NMR (400 MHz, CDCl$_3$, 298 K) δ = 1.24 (t, J = 6.8 Hz, 6H), 1.65-1.82 (m, 6H), 3.46 (q, J = 6.8 Hz, 4H), 3.86 (br. s, 4H), 6.68 (quasi d, J = 8.8, 2H), 6.96 (d, J = 9.5 Hz, 1H), 7.11 (d, J = 9.5 Hz, 1H), 7.20–7.30 (m, 3H), 7.46 (quasi d, J = 8.3, 2H), 7.53 (d, J = 9.5 Hz, 1H), 7.69 ppm (quasi d, J = 8.5, 2H); ^{13}C NMR (100 MHz, CDCl$_3$, 298 K) δ = 171.8, 155.6, 154.4, 153.1, 151.2, 136.0, 135.1, 134.7, 131.5, 131.2, 130.9, 125.0, 124.6, 123.6, 121.4, 115.3, 115.2, 113.9, 113.1, 112.4, 83.8, 70.2, 53.7, 45.2, 44.1, 31.1, 26.6, 24.7, 24.3, 12.8 ppm; λ_{max} (ε) = 336 (21457), 405 (30689), 460 (27829), 692 nm (42198 M^{-1} cm^{-1}); HRMS: m/z calcd for $C_{35}H_{32}N_8^+$: 565.2828 ; found: 565.2830 [M + H]$^+$.
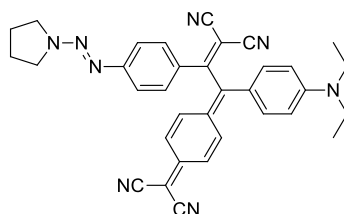
Compound 139

A dark green; 95%; CC: (SiO$_2$; DCM); R$_f$ = 0.15 (SiO$_2$; DCM); m.p. 229–230 °C;
^{1}H NMR (400 MHz, CDCl$_3$, 298 K) δ = 1.24 (t, J = 7.1 Hz, 6H), 2.02–2.12 (m, 4H),
3.47 (q, J = 7.1 Hz, 4H), 3.68 (t, J = 5.8 Hz, 2H), 3.96 (t, J = 5.7 Hz, 2H), 6.69 (quasi
d, J = 9.2, 2H), 6.96 (dd, J = 9.5, 1.8 Hz, 1H), 7.12 (dd, J = 9.5, 1.8 Hz, 1H), 7.24–
7.30 (m, 3H), 7.45 (quasi d, J = 9.2, 2H), 7.53 (dd, J = 9.6, 1.9 Hz, 1H), 7.69 ppm
(quasi d, J = 8.2, 2H); ^{13}C NMR (100 MHz, CDCl$_3$, 298 K) δ = 171.5, 155.9, 154.2,
152.9, 151.0, 135.7, 134.9, 134.5, 131.3, 130.9, 130.4, 124.7, 124.3, 123.3, 121.1,
115.1, 114.9, 113.7, 112.9, 112.1, 83.3, 69.9, 51.6, 46.9, 44.9, 23.7, 23.4, 12.5 ppm;
λ$_{max}$ (ε) = 337 (18958), 400 (26365), 462 (24124) 690 nm (36158 M^{-1} cm^{-1}); HRMS:
m/z calcd for C$_{34}$H$_{30}$N$_8$$^+$: 551.2672; found: 551.2648 [M + H]$^+$.

REFERENCES

1. Shirota, Y. Organic Materials for Electronic and Optoelectronic Devices. *J. Mater. Chem.* **2000**, *10* (1), 1–25. DOI: 10.1039/A908130E

2. Forrest, S. R.; Thompson, M. E. Introduction: Organic Electronics and Optoelectronics. *Chem. Rev.* **2007**, *107* 923–925. DOI: 10.1021/cr0501590

3. Gompper, R.; Wagner, H.-U. Donor-Acceptor-Substituted Cyclic π-Electron Systems—Probes for Theories and Building Blocks for New Materials. *Angew. Chem. Int. Ed.* **1988**, *27* 1437–1455. DOI: 10.1002/anie.198814371

4. Silvestri, F.; Jordan, M.; Howes, K.; Kivala, M.; Rivera-Fuentes, P.; Boudon, C.; Gisselbrecht, J. P.; Schweizer, W. B.; Seiler, P.; Chiu, M.; Diederich, F. Regular Acyclic and Macrocyclic [Ab] Oligomers by Formation of Push–Pull Chromophores in the Chain-Growth Step. *Chem. A Eur. J.* **2011**, *17*, 6088–6097. DOI: 10.1002/chem.201003672

5. Marder, S. R.; Kippelen, B.; Jen, A. K.-Y.; Peyghambarian, N. Design and Synthesis of Chromophores and Polymers for Electro-Optic and Photorefractive Applications. *Nature* **1997**, *388*, 845–851. DOI: 10.1038/42190

6. Kato, S.-ichiro; Kivala, M.; Schweizer, W. B.; Boudon, C.; Gisselbrecht, J.-P.; Diederich, F. Origin of Intense Intramolecular Charge-Transfer Interactions in Nonplanar Push-Pull Chromophores. *Chem. A Eur. J.* **2009**, *15*, 8687–8691. DOI: 10.1002/chem.200901630

7. Michinobu, T.; Boudon, C.; Gisselbrecht, J.-P.; Seiler, P.; Frank, B.; Moonen, N. N.; Gross, M.; Diederich, F. Donor-Substituted 1,1,4,4-Tetracyanobutadienes (Tcbds): New Chromophores with Efficient Intramolecular Charge-Transfer Interactions by Atom-Economic Synthesis. *ChemInform.* **2006**, *37*, 1889-1905. DOI: 10.1002/chem.200501113

8. Raimundo, J.-M.; Blanchard, P.; Gallego-Planas, N.; Mercier, N.; Ledoux-Rak, I.; Hierle, R.; Roncali, J. Design and Synthesis of Push−Pull Chromophores for Second-Order Nonlinear Optics Derived from Rigidified Thiophene-Based π-Conjugating Spacers. *J. Org. Chem.* **2001**, *67*, 205–218. DOI: 10.1021/jo010713f

9. Chérioux, F.; Attias, A.-J.; Maillotte, H. Symmetric and Asymmetric Conjugated 3,3′-Bipyridine Derivatives as a New Class of Third-Order NLO Chromophores with an Enhanced Non-Resonant, Nonlinear Refractive Index in the Picosecond Range. *Adv. Funct. Mater.* **2002**, *12*, 203. DOI: 10.1002/1616-3028(200203)12

10. Gauthier, S.; Porter, A.; Achelle, S.; Roisnel, T.; Dorcet, V.; Barsella, A.; Le Poul, N.; Guevara Level, P.; Jacquemin, D.; Robin-Le Guen, F. Mono- and Diplatinum Polyynediyl Complexes as Potential Push–Pull Chromophores: Synthesis, Characterization, TD-DFT Modeling, and Photophysical and NLO Properties. *Organometallics* **2018**, *37*, 2232–2244. DOI: 10.1021/acs.organomet.8b00223

11. Pigot, C.; Noirbent, G.; Bui, T.-T.; Péralta, S.; Gigmes, D.; Nechab, M.; Dumur, F. Push-Pull Chromophores Based on the Naphthalene Scaffold: Potential Candidates for Optoelectronic Applications. *Mater.* **2019**, *12*, 1342. DOI: 10.3390/ma12081342

12. Bureš, F. Fundamental Aspects of Property Tuning in Push–Pull Molecules. *RSC Adv.* **2014**, *4*, 58826–58851. DOI: 10.1039/C4RA11264D

13. Breiten, B.; Biaggio, I.; Diederich, F. Nonplanar Push–Pull Chromophores for Opto-Electronic Applications. *Chimia* **2010**, *64*, 409–413. DOI: 10.2533/chimia.2010.409

14. Malytskyi, V.; Simon, J.-J.; Patrone, L.; Raimundo, J.-M. Thiophene-Based Push–Pull Chromophores for Small Molecule Organic Solar Cells (Smoscs). *RSC Adv.* **2015**, *5*, 354–397. DOI: 10.1039/C4RA11664J

15. Raj, M. R.; Ramkumar, S.; Anandan, S. Photovoltaic Studies on Perylene Diimide-Based Copolymers Containing Electronic Push–Pull Chromophores. *RSC Adv*. **2013**, *3*, 5108. DOI: 10.1039/C3RA23383A

16. Chen, G.; Qiu, Z.; Tan, J.-H.; Chen, W.-C.; Zhou, P.; Xing, L.; Ji, S.; Qin, Y.; Zhao, Z.; Huo, Y. Deep-Blue Organic Light-Emitting Diodes Based on Push-Pull π-Extended Imidazole-Fluorene Hybrids. *Dyes Pigm.* **2021**, *184*, 108754. DOI: 10.1016/j.dyepig.2020.108754

17. Kato, S.-ichiro; Diederich, F. Non-Planar Push–Pull Chromophores. *Chem. Commun.* **2010**, *46*, 1994. DOI: 10.1039/B926601A

18. Raheem, A. A.; Kamaraj, S.; Sannasi, V.; Praveen, C. New D–π-a Push–Pull Chromophores as Low Band Gap Molecular Semiconductors for Organic Small Molecule Solar Cell Applications. *Org. Chem. Front.* **2018**, *5*, 777–787. DOI: 10.1039/C7QO00920H

19. Rout, Y.; Chauhan, V.; Misra, R. Synthesis and Characterization of Isoindigo-Based Push–Pull Chromophores. *J. Org. Chem.* **2020**, *85*, 4611–4618. DOI: 10.1021/acs.joc.9b03267

20. Mammadova, F.; Ozsinan, S.; Okutan, M.; Dengiz, C. Synthesis, Characterization, and Theoretical Investigation of Optical and Nonlinear Optical (NLO) Properties of Triazene-Based Push–Pull Chromophores. *J. Mol. Struct.* **2020**, *1220*, 128726. DOI: 10.1016/j.molstruc.2020.128726

21. Bureš, F.; Čermáková, H.; Kulhánek, J.; Ludwig, M.; Kuznik, W.; Kityk, I. V.; Mikysek, T.; Růžička, A. Structure-Property Relationships and Nonlinear Optical Effects in Donor-Substituted Dicyanopyrazine-Derived Push-Pull Chromophores with Enlarged and Varied π-Linkers. *Eur. J. Org. Chem.* **2011**, *2012*, 529–538. DOI: 10.1002/ejoc.201101226

22. Hajipour, A. R.; Abolfathi, P.; Tavangar-Rizi, Z. Iron-Catalyzed Cross-Coupling Reaction: Heterogeneous Palladium and Copper-Free Heck and Sonogashira Cross-Coupling Reactions Catalyzed by a Reusable Fe(III) Complex. *Appl. Organomet. Chem.* **2018**, *32*, e4353. DOI: 10.1002/aoc.4353

23. Fihri, A.; Luart, D.; Len, C.; Solhy, A.; Chevrin, C.; Polshettiwar, V. Suzuki–Miyaura Cross-Coupling Coupling Reactions with Low Catalyst Loading: A Green and Sustainable Protocol in Pure Water. *Dalton Trans.* **2011**, *40*, 3116. DOI: 10.1039/C0DT01637C

24. Kolb, H. C.; Finn, M. G.; Sharpless, K. B. Click Chemistry: Diverse Chemical Function from a Few Good Reactions. *Angew. Chem. Int. Ed.* **2001**, *40*, 2004–2021. DOI: 10.1002/1521-3773(20010601)40

25. Dürr, H.; Gleiter, R. Spiroconjugation. *Angew. Chemi. Int. Ed.* **1978**, *17*, 559–569. DOI: 10.1002/anie.197805591

26. Meier, H.; Gerold, J.; Kolshorn, H.; Mühling, B. Extension of Conjugation Leading to Bathochromic or Hypsochromic Effects in OPV Series. *Chem. Eur. J.* **2004**, *10*, 360–370. DOI: 10.1002/chem.200305447

27. García, R.; Calbo, J.; Viruela, R.; Herranz, M. Á.; Ortí, E.; Martín, N. The Role of Planarity versus Nonplanarity in the Electronic Communication of TCAQ-Based Push-Pull Chromophores. *ChemPlusChem* **2018**, *83*, 300–307. DOI: 10.1002/cplu.201700553

28. Moonen, N. N.; Pomerantz, W. C.; Gist, R.; Boudon, C.; Gisselbrecht, J.-P.; Kawai, T.; Kishioka, A.; Gross, M.; Irie, M.; Diederich, F. Donor-Substituted Cyanoethynylethenes: π-Conjugation and Band-Gap Tuning in Strong Charge-Transfer Chromophores. *Chem. Eur. J.* **2005**, *11*, 3325–3341. DOI: 10.1002/chem.200500082

29. Michinobu, T.; May, J. C.; Lim, J. H.; Boudon, C.; Gisselbrecht, J.-P.; Seiler, P.; Gross, M.; Biaggio, I.; Diederich, F. A New Class of Organic Donor–Acceptor Molecules with Large Third-Order Optical Nonlinearities. *Chem. Commun.* **2005**, *6*, 737–739. DOI: 10.1039/b417393g

30. Frank, B. B.; Camafort Blanco, B.; Jakob, S.; Ferroni, F.; Pieraccini, S.; Ferrarini, A.; Boudon, C.; Gisselbrecht, J.-P.; Seiler, P.; Spada, G. P.; Diederich, F. N-Arylated 3,5-Dihydro-4H-Dinaphtho[2,1-C:1′,2′-e]Azepines: Axially Chiral Donors with High Helical Twisting Powers for

Nonplanar Push-Pull Chromophores. *Chem. Eur. J.* **2009**, *15* (36), 9005–9016. DOI: 10.1002/chem.200900913

31. Moonen, N. N.; Pomerantz, W. C.; Gist, R.; Boudon, C.; Gisselbrecht, J.-P.; Kawai, T.; Kishioka, A.; Gross, M.; Irie, M.; Diederich, F. Donor-Substituted Cyanoethynylethenes: π-Conjugation and Band-Gap Tuning in Strong Charge-Transfer Chromophores. *Chem. Eur. J.* **2005**, *11*, 3325–3341. DOI: 10.1002/chem.200500082

32. Kolb, H. C.; Sharpless, K. B. The Growing Impact of Click Chemistry on Drug Discovery. *Drug Discov.* **2003**, *8*, 1128–1137. DOI: 10.1016/S1359-6446(03)02933-7

33. Manetsch, R.; Krasiński, A.; Radić, Z.; Raushel, J.; Taylor, P.; Sharpless, K. B.; Kolb, H. C. In Situ Click Chemistry: Enzyme Inhibitors Made to Their Own Specifications. *J. Am. Chem. Soc.* **2004**, *126*, 12809–12818. 10.1021/ja046382g

34. Wu, P.; Malkoch, M.; Hunt, J. N.; Vestberg, R.; Kaltgrad, E.; Finn, M. G.; Fokin, V. V.; Sharpless, K. B.; Hawker, C. J. Multivalent, Bifunctional Dendrimers Prepared by Click Chemistry. *Chem. Commun.* **2005**, *46*, 5775. DOI: 10.1039/B512021G

35. Gothelf, K. V.; Jørgensen, K. A. Asymmetric 1,3-Dipolar Cycloaddition Reactions. *Chem. Rev.* **1998**, *98* (2), 863–910. DOI: 10.1021/cr970324e

36. Diels, O.; Alder, K. Synthesen in Der Hydroaromatischen Reihe. *Liebig's Annalen* **1928**, *460*, 98–122.

37. Nicolaou, K. C.; Snyder, S. A.; Montagnon, T.; Vassilikogiannakis, G. The Diels-Alder Reaction in Total Synthesis. *Angew. Chem. Int. Ed.* **2002**, *41*, 1668–1698. DOI: 10.1002/jlac.19284600106

38. Gacal, B.; Durmaz, H.; Tasdelen, M. A.; Hizal, G.; Tunca, U.; Yagci, Y.; Demirel, A. L. Anthracene−Maleimide-Based Diels−Alder "Click Chemistry" as a Novel Route to Graft Copolymers. *Macromolecules* **2006**, *39*, 5330–5336. DOI: 10.1021/ma060690c

39. Kim, T.-D.; Luo, J.; Tian, Y.; Ka, J.-W.; Tucker, N. M.; Haller, M.; Kang, J.-W.; Jen, A. K.-Y. Diels−Alder "Click Chemistry" for Highly Efficient Electrooptic Polymers. *Macromolecules* **2006**, *39*, 1676–1680. DOI: 10.1021/ma052087k

40. Becer, C. R.; Hoogenboom, R.; Schubert, U. S. Click Chemistry beyond Metal-Catalyzed Cycloaddition. *Angew. Chem. Int. Ed.* **2009**, *48*, 4900–4908. DOI: 10.1002/anie.200900755

41. Michinobu, T.; Diederich, F. The [2+2] Cycloaddition-Retroelectrocyclization (CA-RE) Click Reaction: Facile Access to Molecular and Polymeric Push-Pull Chromophores. *Angew. Chem. Int. Ed.* **2018**, *57*, 3552–3577. DOI: 10.1002/anie.201711605

42. Nishiyabu, R.; Anzenbacher, P. 1,3-indane-based Chromogenic Calixpyrroles with Push-Pull Chromophores: Synthesis and anion sensing. *Org. Lett.* **2006**, *8*, 359–362. DOI: 10.1021/ol0521782

43. Noirbent, G.; Pigot, C.; Bui, T.-T.; Péralta, S.; Nechab, M.; Gigmes, D.; Dumur, F. Synthesis, Optical and Electrochemical Properties of a Series of Push-Pull Dyes Based on the 2-(3-Cyano-4,5,5-Trimethylfuran-2(5H)-Ylidene)Malononitrile (TCF) Acceptor. *Dyes Pigm.* **2021**, *184*, 108807. DOI: 10.1016/j.dyepig.2020.108807

44. Achelle, S.; Barsella, A.; Baudequin, C.; Caro, B.; Robin-le Guen, F. Synthesis and Photophysical Investigation of a Series of Push–Pull Arylvinyldiazine Chromophores. *J. Org. Chem.* **2012**, *77*, 4087–4096. DOI: 10.1021/jo3004919

45. Reisinger, C. M.; Rivera-Fuentes, P.; Lampart, S.; Schweizer, W. B.; Diederich, F. Cascade Pericyclic Reactions of Alleno-Acetylenes: Facile Access to Highly Substituted Cyclobutene, Dendralene, Pentalene, and Indene Skeletons. *Chem. - A Eur. J.* **2011**, *17*, 12906–12911. DOI: 10.1002/chem.201102852

46. Reekie, T. A.; Donckele, E. J.; Ruhlmann, L.; Boudon, C.; Trapp, N.; Diederich, F. Ester-Substituted Electron-Poor Alkenes for Cycloaddition-

Retroelectrocyclization (CA-RE) and Related Reactions. *Eur. J. Org. Chem.* **2015**, *2015*, 7264–7275. DOI:10.1021/acs.orglett.5b01598

47.   Donckele, E. J.; Finke, A. D.; Ruhlmann, L.; Boudon, C.; Trapp, N.; Diederich, F. The [2 + 2] Cycloaddition–Retroelectrocyclization and [4 + 2] Hetero-Diels–Alder Reactions of 2-(Dicyanomethylene)Indan-1,3-Dione with Electron-Rich Alkynes: Influence of Lewis Acids on Reactivity. *Org. Lett.* **2015**, *17*, 3506–3509. DOI: 10.1021/acs.orglett.5b01598

48.   Woodward, R. B.; Hoffmann, R. Stereochemistry of Electrocyclic Reactions. *J. Am. Chem. Soc.* **1965**, *87*, 395–397.

49.   Hoffmann, R.; Woodward, R. B. Orbital Symmetries and Endo-Exo Relationships in Concerted Cycloaddition Reactions. *J. Am. Chem. Soc.* **1965**, *87*, 4388–4389.

50.   Hoffmann, R.; Woodward, R. B. Selection Rules for Concerted Cycloaddition Reactions. *J. Am. Chem. Soc.* **1965**, *87*, 2046–2048.

51.   Palazzo, T. A.; Mose, R.; Jørgensen, K. A. Cycloaddition Reactions: Why Is It so Challenging to Move from Six to Ten Electrons? *Angew. Chemie - Int. Ed.* **2017**, *56*, 10033–10038. DOI: 10.1002/anie.201701085

52.   Vollmer, J. J.; Servis, K. L. Woodward-Hoffmann Rules: Cycloaddition Reactions. *J. Chem. Educ.* **1970**, *47*, 491.

53.   Alcaide, B.; Almendros, P.; Aragoncillo, C. Exploiting [2+2] Cycloaddition Chemistry: Achievements with Allenes. *Chem. Soc. Rev.* **2010**, *39*, 783–816. DOI: 10.1039/B913749A

54.   Sarkar, D.; Bera, N.; Ghosh, S. [2+2] Photochemical Cycloaddition in Organic Synthesis. *Eur. J. Org. Chem.* **2019**, *20*, 1310–1326. DOI: 10.1002/ejoc.201901143

55.   Eaton, P. E. The Tricyclo[5.3.0.02,6]Decane System. the Photodimers of Cyclopentenone. *J. Am. Chem. Soc.* **1962**, *84*, 2344–2348.

56.   Eaton, P. E. On the Mechanism of the Photodimerization of Cyclopentenone. *J. Am. Chem. Soc.* **1962**, *84*, 2454–2455.

57.   Corey, E. J.; Mitra, R. B.; Uda, H. Total Synthesis of D,L-Caryophyllene and D,L-Isocaryophyllene. *J. Am. Chem. Soc.* **1963**, *85*, 362–363.

58.   Cantrell, T. S.; Haller, W. S.; Williams, J. C. Photocycloaddition Reactions of Some 3-Substituted Cyclohexenones. *J. Org. Chem.* **1969**, *34*, 509–519. DOI: 10.1021/jo01255a007

59.   Cantrell, T. S. Photochemical Transformations of Some β-Substituted Enones. *Tetrahedron* **1971**, *27*, 1227–1237. DOI: 10.1021/jo01255a007

60.   Alibés, R.; Bourdelande, J. L.; Font, J.; Parella, T. Highly Efficient and Diastereoselective Approaches to (+)- and (−)-Grandisol. *Tetrahedron* **1996**, *52*, 1279–1292. DOI: 10.1016/0040-4020(95)00958-2

61.   White, J. D.; Gupta, D. N. The Total Synthesis of .Alpha.- and .Beta.-Bourbonene. *J. Am. Chem. Soc.* **1968**, *90*, 6171–6177. DOI: https://doi.org/10.1021/ja01024a040

62.   Ruider, S. A.; Sandmeier, T.; Carreira, E. M. Total Synthesis of (±)-Hippolachnin a. *Angew. Chem. Int. Ed.* **2014**, *54*, 2378–2382. DOI: 10.1002/anie.201410419

63.   Salomon, R. G.; Sachinvala, N. D.; Roy, S.; Basu, B.; Raychaudhuri, S. R.; Miller, D. B.; Sharma, R. B. Total Synthesis of Spatane Diterpenes: The Tricyclic Nucleus. *J. Am. Chem. Soc.* **1991**, *113*, 3085–3095. DOI: 10.1021/ja00008a043

64.   Reinhoudt, D. N. (2 + 2)-Cycloaddition and (2 + 2)-Cycloreversion Reactions of Heterocyclic Compounds. *Adv. Heterocycl. Chem.* **1977**, *21*, 253–321.

65.   Epiotis, N. D. Allgemeine Theorie Pericyclischer Reaktionen. *Angew. Chem.* **1974**, *86*, 825–855.

66.   Siebert, M. R.; Osbourn, J. M.; Brummond, K. M.; Tantillo, D. J. Differentiating Mechanistic Possibilities for the Thermal, Intramolecular [2 + 2] Cycloaddition of Allene−Ynes. *J. Am. Chem. Soc.* **2010**, *132*, 11952–11966. DOI: 10.1021/ja102848z

67.   Ohno, H.; Mizutani, T.; Kadoh, Y.; Miyamura, K.; Tanaka, T. Thermal Intramolecular [2+2] Cycloaddition of Allenenes and Allenynes:

Diasteroselective Access to Bicyclic Nitrogen Heterocycles. *Angew. Chem. Int. Ed.* **2005**, *44*, 5113–5115. DOI: 10.1002/anie.200501413

68. Kimura, M.; Horino, Y.; Wakamiya, Y.; Okajima, T.; Tamaru, Y. Pronounced Chemo-, Regio-, and Stereoselective [2 + 2] Cycloaddition Reaction of Allenes toward Alkenes and Alkynes. *J. Am. Chem. Soc.* **1997**, *119*, 10869–10870. DOI: 10.1021/ja105541r

69. Kato, S.-ichiro; Kivala, M.; Schweizer, W. B.; Boudon, C.; Gisselbrecht, J.-P.; Diederich, F. Origin of Intense Intramolecular Charge-Transfer Interactions in nonplanar Push-Pull Chromophores. *Chem. Eur. J.* **2009**, *15*, 8687–8691. DOI: 10.1002/chem.200901630

70. Trofimov, B.; Sobenina, L.; Stepanova, Z.; Ushakov, I.; Sinegovskaya, L.; Vakul'skaya, T.; Mikhaleva, A. Facile [2+2] Cycloaddition of DDQ to an Alkyne: Synthesis of Pyrrolyl- and Indolylbicyclo[4.2.0]Octadienes from C-Ethynylpyrroles or C-Ethynylindoles. *Synthesis* **2009**, *2010*, 470–476. DOI: 10.1055/s-0029-1217133

71. Trofimov, B. A.; Sobenina, L. N.; Stepanova, Z. V.; Ushakov, I. A.; Mikhaleva, A. I.; Tomilin, D. N.; Kazheva, O. N.; Alexandrov, G. G.; Chekhlov, A. N.; Dyachenko, O. A. Rearrangements of the [2+2]-Cycloadducts of DDQ and 2-Ethynylpyrroles. *Tetrahedron Lett.* **2010**, *51*, 5028–5031. DOI: 10.1055/s-0029-1217133

72. Kivala, M.; Boudon, C.; Gisselbrecht, J.-P.; Seiler, P.; Gross, M.; Diederich, F. A Novel Reaction of 7,7,8,8-Tetracyanoquinodimethane (TCNQ): Charge-Transfer Chromophores by [2 + 2] Cycloaddition with Alkynes. *Chem. Commun.* **2007**, *45*, 4731. DOI: 10.1039/B713683H

73. Husigen, R. Tetracyanoethylene and Enol Ethers. A Model for 2 + 2 Cycloadditions via Zwitterionic Intermediates. *Acc. Chem. Res.* **1977**, *10*, 117–124. DOI: 10.1002/Hlca.201200217

74. Hall, H. K.; Itoh, T.; Iwatsuki, S.; Padias, A. B.; Mulvaney, J. E. P-Phenylenetetramethylene Diradical and Zwitterion Intermediates in the

Spontaneous Copolymerizations of Electrophilic P-Quinodimethanes with Electron-Rich Olefins. *Macromolecules* **1990**, *23*, 913–917. DOI:

75. Bruce, M. I.; Rodgers, J. R.; Snow, M. R.; Swincer, A. G. Cyclopentadienyl-ruthenium and -osmium chemistry. Cleavage of tetracyanoethylene under mild conditions: X-ray crystal structures of [Ru{η3-C(CN)2cphc[double bond, length as m-dash]C(CN)2}(pph3)(η-C5H5)] and [Ru{C[[double bond, length as m-dash]C(CN)2]cph[double bond, length as m-dash]C(CN)2}-(cnbut)(pph3)(η-C5H5)]. *J. Chem. Soc., Chem. Commun.* **1981**, 271–272. DOI: 10.1039/C39810000271

76. Onitsuka, K.; Ose, N.; Ozawa, F.; Takahashi, S. Reactions of Acetylene-Bridged Diplatinum Complexes with Tetracyanoethylene. *J. Organomet. Chem.* **1999**, *578*, 169–177. DOI:

77. Wu, X., Wu, J., Liu, Y., & Jen, A. K.-Y. (1999). Highly efficient, thermally and chemically stable second order nonlinear optical chromophores containing a 2-phenyl-tetracyanobutadienyl acceptor. *J. Am. Chem. Soc.* **1999**, *121*, 472–473. DOI:10.1021/ja983537+

78. Cai, C.; Liakatas, I.; Wong, M.-S.; Bösch, M.; Bosshard, C.; Günter, P.; Concilio, S.; Tirelli, N.; Suter, U. W. Donor−Acceptor-Substituted Phenylethenyl Bithiophenes: Highly Efficient and Stable Nonlinear Optical Chromophores. *Org. Lett.* **1999**, *1*, 1847–1849. DOI: 10.1016/S0022-328X(98)01119-X

79. Morioka, Y.; Yoshizawa, N.; Nishida, J.-ichi; Yamashita, Y. Novel Donor–π–Acceptor Compounds Containing 1,3-Dithiol-2-Ylidene and Tetracyanobutadiene Units. *Chem. Lett.* **2004**, *33*, 1190–1191. DOI: 10.1246/cl.2004.1190

80. Chen, S.; Li, Y.; Liu, C.; Yang, W.; Li, Y. Strong Charge-Transfer Chromophores from [2+2] Cycloadditions of TCNE and TCNQ to Peripheral Donor-Substituted Alkynes. *Eur. J. Org. Chem.* **2011**, *2011*, 6445–6451. DOI: 10.1002/ejoc.201101009

81. Reutenauer, P.; Kivala, M.; Jarowski, P. D.; Boudon, C.; Gisselbrecht, J.-P.; Gross, M.; Diederich, F. Cheminform Abstract: New Strong Organic Acceptors by Cycloaddition of TCNE and TCNQ to Donor-Substituted Cyanoalkynes. *ChemInform* **2007**, *39*, 4898-4900. DOI: 10.1039/b714731g

82. Kivala, M.; Boudon, C.; Gisselbrecht, J.-P.; Enko, B.; Seiler, P.; Müller, I. B.; Langer, N.; Jarowski, P. D.; Gescheidt, G.; Diederich, F. Organic Super-Acceptors with Efficient Intramolecular Charge-Transfer Interactions by [2+2] Cycloadditions of TCNE, TCNQ, and F4-TCNQ to Donor-Substituted Cyanoalkynes. *Chem. Eur. J.* **2009**, *15*, 4111–4123. DOI: 10.1002/chem.200802563

83. Onitsuka, K.; Ose, N.; Ozawa, F.; Takahashi, S. Reactions of Acetylene-Bridged Diplatinum Complexes with Tetracyanoethylene. *J. Organomet. Chem.* **1999**, *578*, 169–177. DOI:

84. Erden, K.; Savaş, İ.; Dengiz, C. Synthesis of Triazene-Substituted Homoconjugated Push-Pull Chromophores by Formal [2 + 2] Cycloadditions. *Tetrahedron Lett.* **2019**, *60*, 1982–1985. DOI: 10.1016/j.tetlet.2019.06.046

85. Rijkers, D. T. S.; de Prada López, F.; Liskamp, R. M. J.; Diederich, F. A Convenient [2+2] Cycloaddition–Cycloreversion Reaction for the Synthesis of 1,1-dicyanobuta-1,3-Diene-Scaffolded Peptides as New Imaging Chromophores. *Tetrahedron Lett.* **2011**, *52*, 6963–6967. DOI: 10.1002/Chem.202001788

86. Silvestri, F.; Jordan, M.; Howes, K.; Kivala, M.; Rivera-Fuentes, P.; Boudon, C.; Gisselbrecht, J. P.; Schweizer, W. B.; Seiler, P.; Chiu, M.; Diederich, F. Regular Acyclic and Macrocyclic [Ab] Oligomers by Formation of Push–Pull Chromophores in the Chain-Growth Step. *Chem. Eur. J.* **2011**, *17*, 6088–6097. DOI: 10.1002/chem.201003672;

87. Jarowski, P. D.; Wu, Y.-L.; Boudon, C.; Gisselbrecht, J.-P.; Gross, M.; Schweizer, W. B.; Diederich, F. New Donor–Acceptor Chromophores by

Formal [2+2] Cycloaddition of Donor-Substituted Alkynes to Dicyanovinyl Derivatives. *Org. Bio. Chem.* **2009**, *7*, 1312. DOI: 10.1039/b821230a

88. Galán, E.; Andreu, R.; Garín, J.; Orduna, J.; Villacampa, B.; Diosdado, B. E.; Cycloaddition Reactions of Polyenic Donor–π-Acceptor Systems with an Electron-Rich Alkyne: Access to New Chromophores with Second-Order Optical Nonlinearities. *Org. Bio. Chem.* **2012**, *10*, 8684. DOI: 10.1039/c2ob26515j

89. Hopf, H.; Kreutzer, M.; Jones, P. G. On a Metathesis Reaction of Tetrathiafulvalene(Ttf). *Angew. Chem. Int. Ed.* **1991**, *30*, 1127–1128. DOI: 10.1002/anie.199111271

90. Kivala, M.; Boudon, C.; Gisselbrecht, J.-P.; Enko, B.; Seiler, P.; Müller, I. B.; Langer, N.; Jarowski, P. D.; Gescheidt, G.; Diederich, F. Organic Super-Acceptors with Efficient Intramolecular Charge-Transfer Interactions by [2+2] Cycloadditions of TCNE, TCNQ, and F4-TCNQ to Donor-Substituted Cyanoalkynes. *Chem. Eur. J.* **2009**, *15*, 4111–4123. DOI: 10.1002/chem.200802563

91. Jayamurugan, G.; Finke, A. D.; Gisselbrecht, J.-P.; Boudon, C.; Schweizer, W. B.; Diederich, F. One-Pot Access to Push–Pull Oligoenes by Sequential [2 + 2] Cycloaddition–Retroelectrocyclization Reactions. *J. Org. Chem.* **2013**, *79*, 426–431. DOI: 10.1021/ja312084s

92. Tang, X.; Liu, W.; Wu, J.; Lee, C.-S.; You, J.; Wang, P. Synthesis, Crystal Structures, and Photophysical Properties of Triphenylamine-Based Multicyano Derivatives. *J. Org. Chem.* **2010**, *75*, 7273–7278. DOI: 10.1021/jo101456v

93. Kato, S.-ichiro; Noguchi, H.; Jin, S.; Nakamura, Y. Synthesis and Electronic, Optical, and Electrochemical Properties of a Series of Tetracyanobutadiene-Substituted Carbazoles. *Asian J. Org. Chem.* **2015**, *5*, 246–256. DOI: 10.1002/ajoc.201500431

94. Dar, A. H.; Gowri, V.; Gopal, A.; Muthukrishnan, A.; Bajaj, A.; Sartaliya, S.; Selim, A.; Ali, M. E.; Jayamurugan, G. Designing of Push–Pull

Chromophores with Tunable Electronic and Luminescent Properties Using Urea as the Electron Donor. *J. Org. Chem.* **2019**, *84*, 8941–8947. DOI: 10.1021/acs.joc.9b00841

95. Shoji, T.; Higashi, J.; Ito, S.; Okujima, T.; Yasunami, M.; Morita, N. Synthesis of Redox-active, Intramolecular Charge-Transfer Chromophores by the [2+2] Cycloaddition of Ethynylated of 2H-cyclohepta[B]Furan-2-ones With Tetracyanoethylene. *Chem. Eur. J.* **2011**, *17*, 5116–5129. DOI: 10.1002/chem.201003628

96. Pesak, D. J.; Moore, J. S.; Wheat, T. E. Synthesis and Characterization of Water-Soluble Dendritic Macromolecules with a Stiff, Hydrocarbon Interior. *Macromolecules* **1997**, *30*, 6467–6482. DOI: 10.1021/ma970454p

97. Perrin, F. G.; Kiefer, G.; Jeanbourquin, L.; Racine, S.; Perrotta, D.; Waser, J.; Scopelliti, R.; Severin, K. 1-Alkynyltriazenes as Functional Analogues of Ynamides. *Angew. Chem.* **2015**, *127*, 13591–13594. DOI: 10.1002/ange.201507033

98. Jeanbourquin, L. N.; Scopelliti, R.; Fadaei Tirani, F.; Severin, K. Synthesis and Reactivity of 1-Allenyltriazenes. *Org. Lett.* **2017**, *19*, 2070–2073. 10.1021/acs.orglett.7b00671

99. Marchesi, F.; Turriziani, M.; Tortelli, G.; Avvisati, G.; Torino, F.; Devecchis, L.; F. Triazene Compounds: Mechanism of Action and Related DNA Repair Systems. *Pharmacol. Res.* **2007**, *56*, 275–287. DOI: 10.1016/j.phrs.2007.08.003

100. Mohammadi, A. Novel Triazene Dyes Based on N-Phenylpiperazine: Synthesis, Anti-Bacterial Activity and Solvatochromic Properties. *J. Mol. Liq.* **2014**, *193*, 69–73. DOI: 10.1016/j.molliq.2013.12.024

101. Kimball, D. B.; Haley, M.M.; *Angew. Chem. Int. Ed.* **2002**, 41, 3338-3351. DOI: 10.1002/1521-3773(20020916)41

102. Lazny, P.; Sienkiewicz M.; Sienkiewicz, Brase, S.; *Tetrahedron* 2001, *57*, 5825-5832. DOI:10.1016/S0040-4020(01)00495-1

103. Kimball, D. B.; Haley, M. M. Triazenes: A Versatile Tool in Organic Synthesis. *Angew. Chem. Int. Ed.* **2002**, *41* , 3338–3351. DOI: 10.1002/1521-3773(20020916)41

104. Block, M. A.; Hecht, S. Poly(Propylene Oxide)−Poly(Phenylene Ethynylene) Block and Graft Copolymers. *Macromolecules* **2008**, *41*, 3219–3227. DOI: 10.1021/ma702844w

105. Zarei, A.; Khazdooz, L.; Aghaei, H.; Azizi, G.; Chermahini, A. N.; Hajipour, A. R. Synthesis of Triazenes by Using Aryl Diazonium Silica Sulfates under Mild Conditions. *Dyes Pigm.* **2014**, *101*, 295–302. DOI: 10.1016/j.dyepig.2013.10.022

106. Bharti, S. K.; Roy, R. Quantitative ^{1}H NMR Spectroscopy. *TrAC Trends in Analyt. Chem.* **2012**, *35*, 5–26. DOI: 10.1016/j.trac.2012.02.007

107. Dengiz, C.; Dumele, O.; Kato, S.-ichiro; Zalibera, M.; Cias, P.; Schweizer, W. B.; Boudon, C.; Gisselbrecht, J.-P.; Gescheidt, G.; Diederich, F. From Homoconjugated Push-Pull Chromophores to Donor-Acceptor-Substituted Spiro Systems by Thermal Rearrangement. *Chem. Eur. J.* **2014**, *20*, 1279–1286. DOI: 10.1002/chem.201303533

108. Marini, A.; Muñoz-Losa, A.; Biancardi, A.; Mennucci, B. What Is Solvatochromism? *J. Phys. Chem.* **2010**, *114*, 17128–17135. DOI: 10.1021/jp1097487

109. Bureš, F.; Pytela, O.; Kivala, M.; Diederich, F. Solvatochromism as an Efficient Tool to Study N,N-Dimethylamino- and Cyano-Substituted π-Conjugated Molecules with an Intramolecular Charge-Transfer Absorption. *J. Phys. Chem.* **2010**, *24*, 274–281. DOI: 10.1002/poc.1744

110. Landman, I. R.; Suleymanov, A. A.; Fadaei-Tirani, F.; Scopelliti, R.; Chadwick, F. M.; Severin, K. Brønsted and Lewis Acid Adducts of Triazenes. *Dalton Trans.* **2020**, *49*, 2317–2322. DOI: 10.1039/D0DT00049C

111. Frisch, M.J., Trucks, G. W. , Schlegel, H. B., Scuseria, G. E., Robb, M. A., Cheeseman, J. R., Scalmani, G., Barone, V., Mennucci,B., Petersson, G. A., Nakatsuji, H., Caricato, M., Li, X., Hratchian, H. P., Izmaylov, A. F.,

Bloino, J., Zheng, G., Sonnenberg, J. L., Hada, M., Ehara, M., Toyota, K., Fukuda, R., Hasegawa, J., Ishida, M., Nakajima, T., Honda, Y., Kitao, O., Nakai, H., Vreven, T., Montgomery, J. A., Peralta, Jr., J. E., Ogliaro, F., Bearpark, M., Heyd, J. J., Brothers, E., Kudin, K. N., Staroverov, V. N., Kobayashi, R., Normand, J., Raghavachari, K., Rendell, A., Burant, J. C., Iyengar, S., S., Tomasi, J., Cossi, M., Rega, N., Millam, J. M., Klene, M., Knox, J. E., Cross, J. B., Bakken, V., Adamo, C., Jaramillo, J., Gomperts, R., Stratmann, R.E, Yazyev, O., Austin, A., J., Cammi, R., Pomelli, C., Ochterski, J. W., Martin, R. L., Morokuma, K., Zakrzewski, V. G. Voth, G. A., Salvador, P., Dannenberg, J. J., Dapprich, S., Daniels, A. D., Farkas, Ö., Foresman, J. B., Ortiz, J. V., Cioslowski, J., Fox, D. J.; Gaussian 09, Revision D.01.

112. Lee, C.; Yang, W.; Parr, R. G. Development of the Colle-Salvetti Correlation-Energy Formula into a Functional of the Electron Density. *Phys. Rev. B* **1988**, *37*, 785–789. DOI: 10.1103/PhysRevB.37.785

113. Jamorski Jödicke, C.; Lüthi, H. P. Time-Dependent Density-Functional Theory Investigation of the Formation of the Charge Transfer Excited State for a Series of Aromatic Donor–Acceptor Systems. Part II. *J. Chem. Phys.* **2002**, *117*, 4157–4167. DOI: 10.1063/1.1498817

114. Lokhande, P. K.; Patil, D. S.; Kadam, M. M.; Sekar, N. Theoretical Investigation of Optical and Nonlinear Optical (NLO) Properties of 3-Azabenzanthrone Analogues : DFT and TD-DFT Approach. *ChemistrySelect* **2019**, *4*, 10033–10045. DOI: 10.1002/slct.201901681

115. Zouaoui-Rabah, M.; Sekkal-Rahal, M.; Djilani-Kobibi, F.; Elhorri, A. M.; Springborg, M. Performance of Hybrid DFT Compared to MP2 Methods in Calculating Nonlinear Optical Properties of Divinylpyrene Derivative Molecules. *J. Phys. Chem.* **2016**, *120*, 8843–8852. DOI: 10.1021/acs.jpca.6b08040

116. Srinivasa Rao, P., Brixi, S., Shaikh, D. B., Al Kobaisi, M., Lessard, B. H., Bhosale, S. V., & Bhosale, S. V. (2021). The effect of TCNE and TCNQ

acceptor units on triphenylamine-naphthalenediimide push-pull chromophore properties. *Eur. J. Org. Chem.* **2021**, *18*, 2615–2624. DOI:10.1002/ejoc.202100198

117. Moonen, N. N.; Gist, R.; Boudon, C.; Gisselbrecht, J.-P.; Seiler, P.; Kawai, T.; Kishioka, A.; Gross, M.; Irie, M.; Diederich, F. Donor-Substituted Cyanoethynylethenes: Powerful Chromophores for Opto-Electronic Applicationselectronic. *Org. Biomol. Chem.* **2003**, *1*, 2032. DOI: 10.1039/ b303879c

118. Zhu, M.; Ning, M.; Fu, W.; Xu, C.; Zou, G. Gold-Catalyzed Homocoupling Reaction of Terminal Alkynes to 1,3-Diynes. *Bulletin of the Korean Chem. Soc.* **2012**, *33*, 1325–1328. DOI: 10.5012/bkcs.2012.33.4.1325

119. Su, L.; Dong, J.; Liu, L.; Sun, M.; Qiu, R.; Zhou, Y.; Yin, S.-F. Copper Catalysis for Selective Heterocoupling of Terminal Alkynes. *J. Am. Chem. Soc.* **2016**, *138*, 12348–12351. DOI: 10.1021/jacs.6b07984

120. Wardrop, D. J.; Komenda, J. P. Dehydrative Fragmentation of 5-Hydroxyalkyl-1h-Tetrazoles: A Mild Route to Alkylidenecarbenes. *Org. Lett.* **2012**, *14*, 1548–1551. DOI: 10.1021/ol300276p

121. Tancini, F.; Wu, Y. L.; Schweizer, W. B.; Gisselbrecht, J. P.; Boudon, C.; Jarowski, P. D.; Beels, M. T.; Biaggio, I.; Diederich, F. 1,1-Dicyano-4-[4-(diethylamino)phenyl]buta-1,3-dienes: Structure-Property Relationships. *Eur. J. Org. Chem.* **2012**, *2012*, 2756–2765. DOI: 10.1002/ejoc.201200111

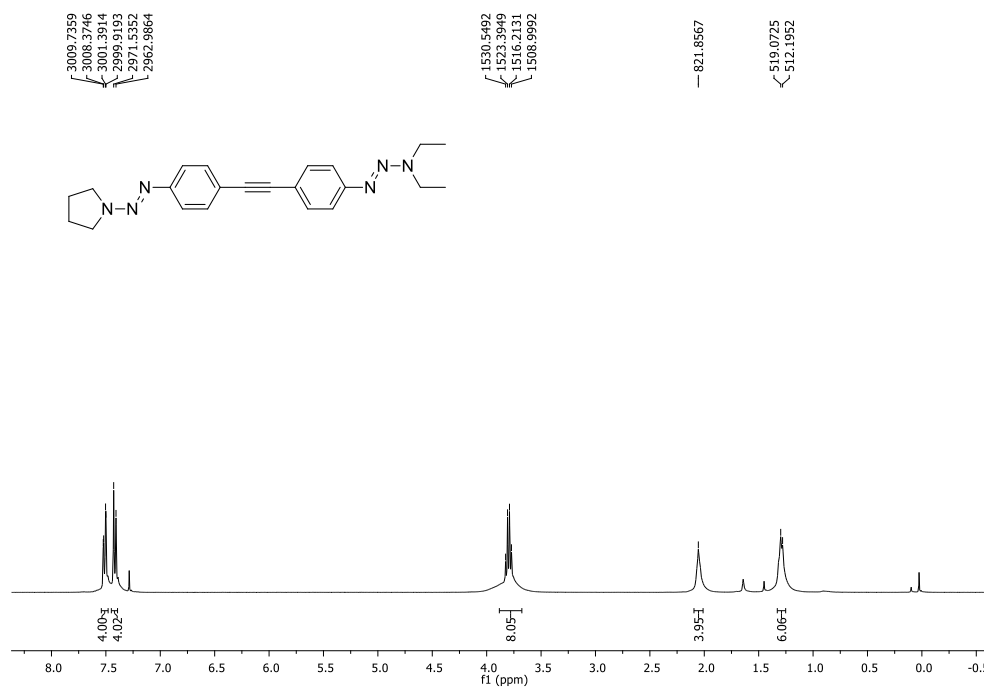## A. ¹H and ¹³C NMR Spectra
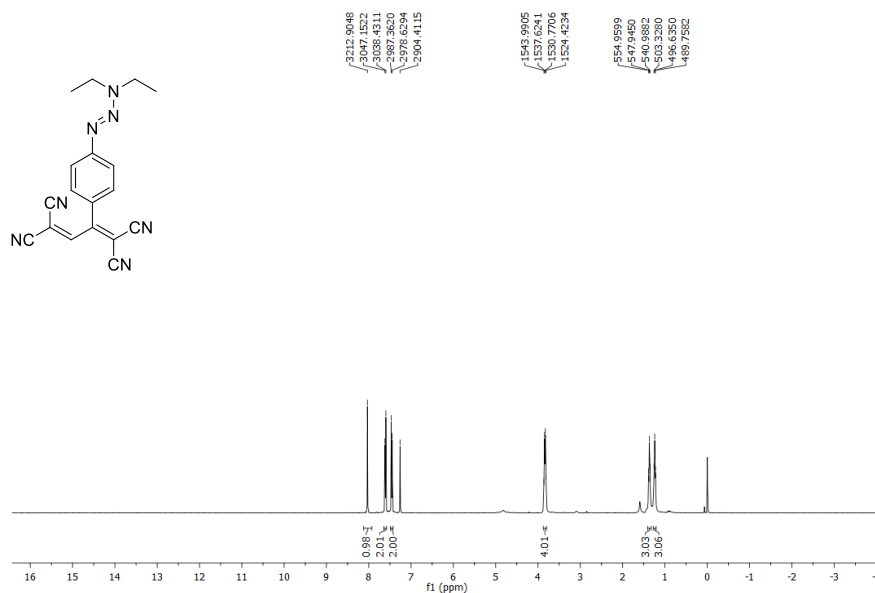
Figure 22. ¹H NMR spectrum of crude **87** in CDCl₃ solution (400 MHz).
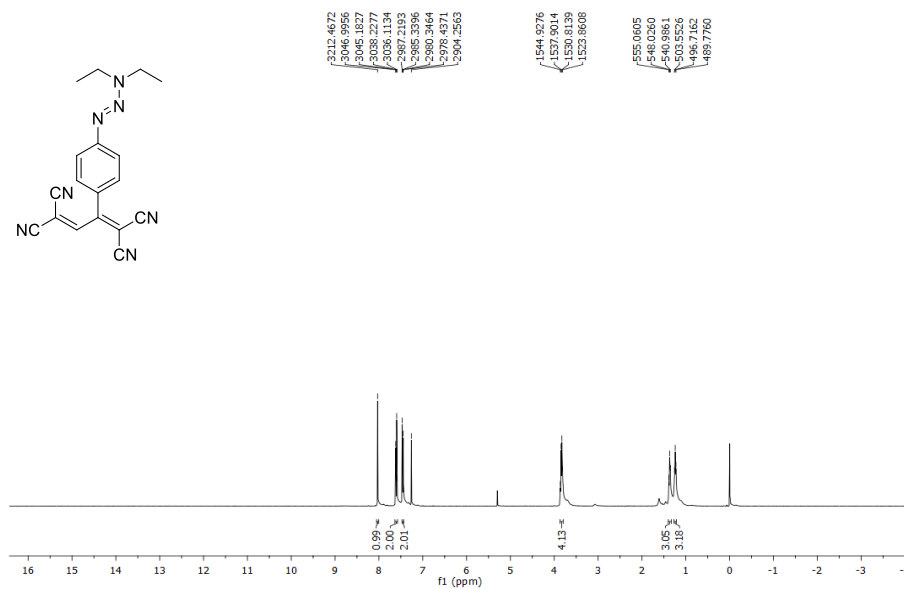
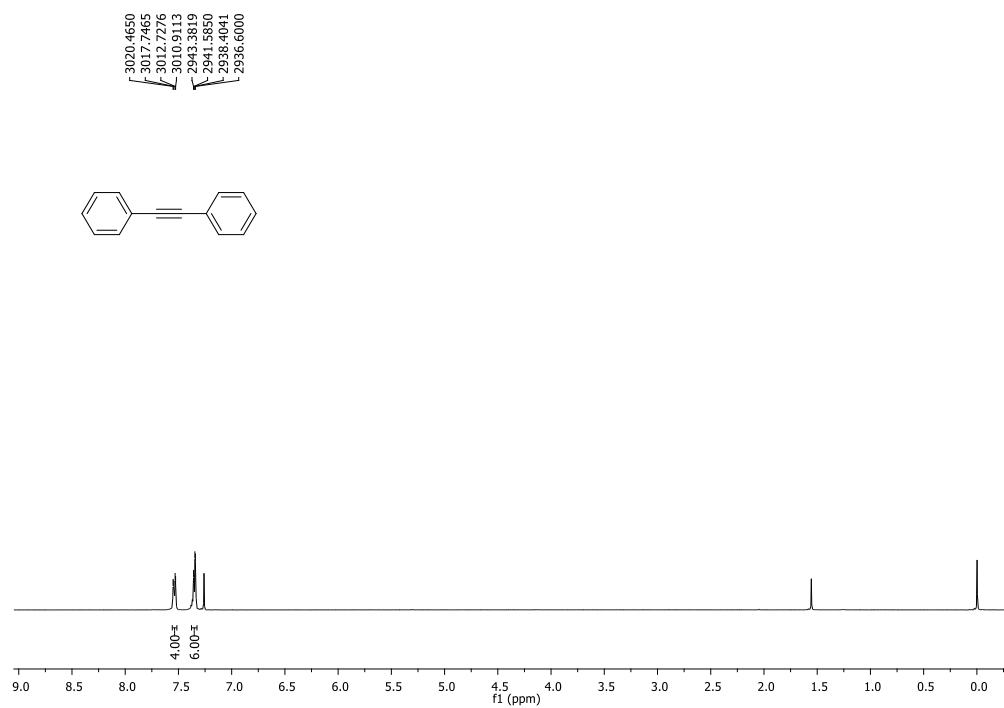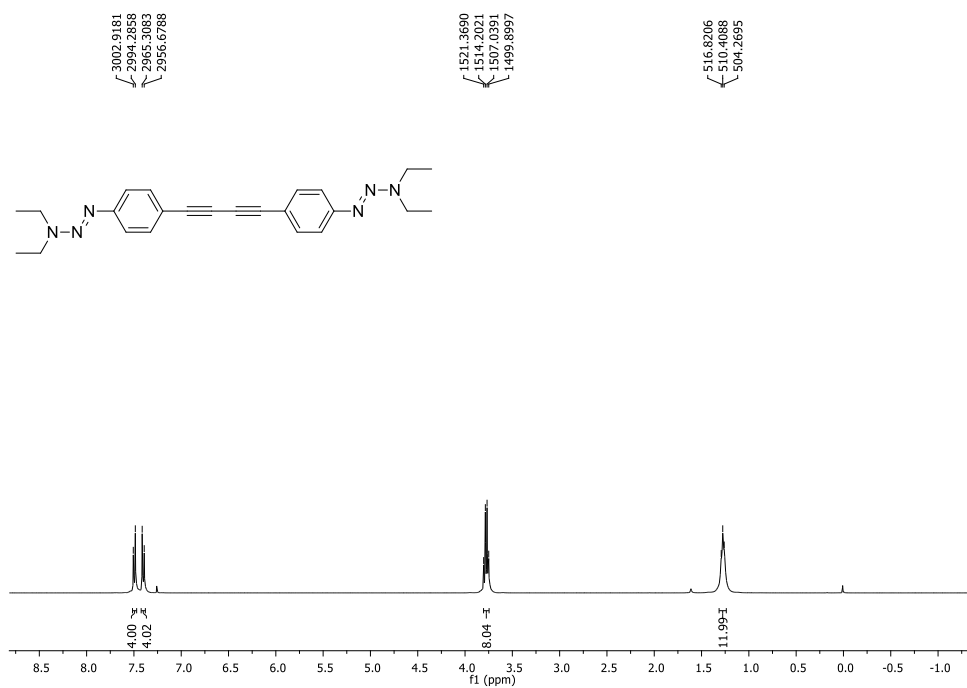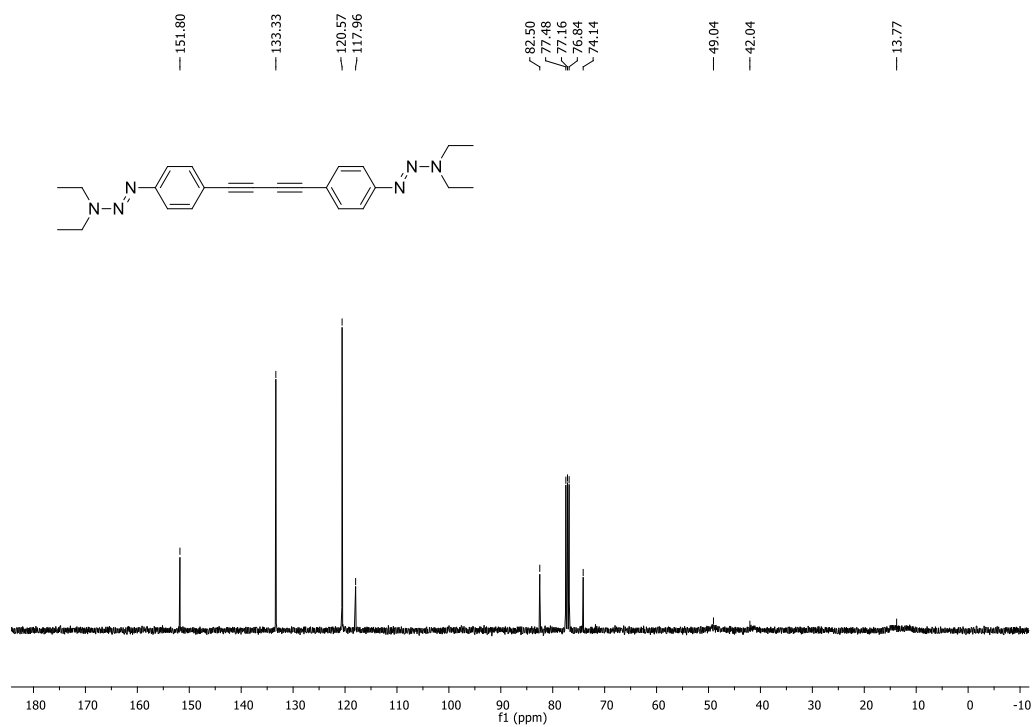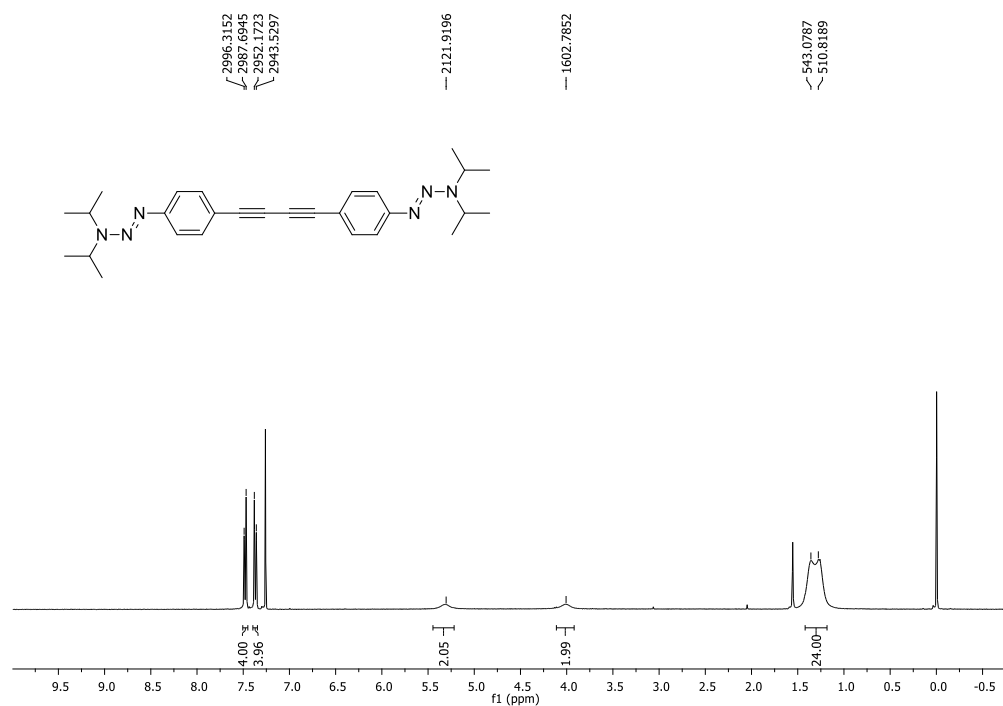**Figure 23**. ¹H NMR spectrum of **87** in CDCl₃ solution (400 MHz).
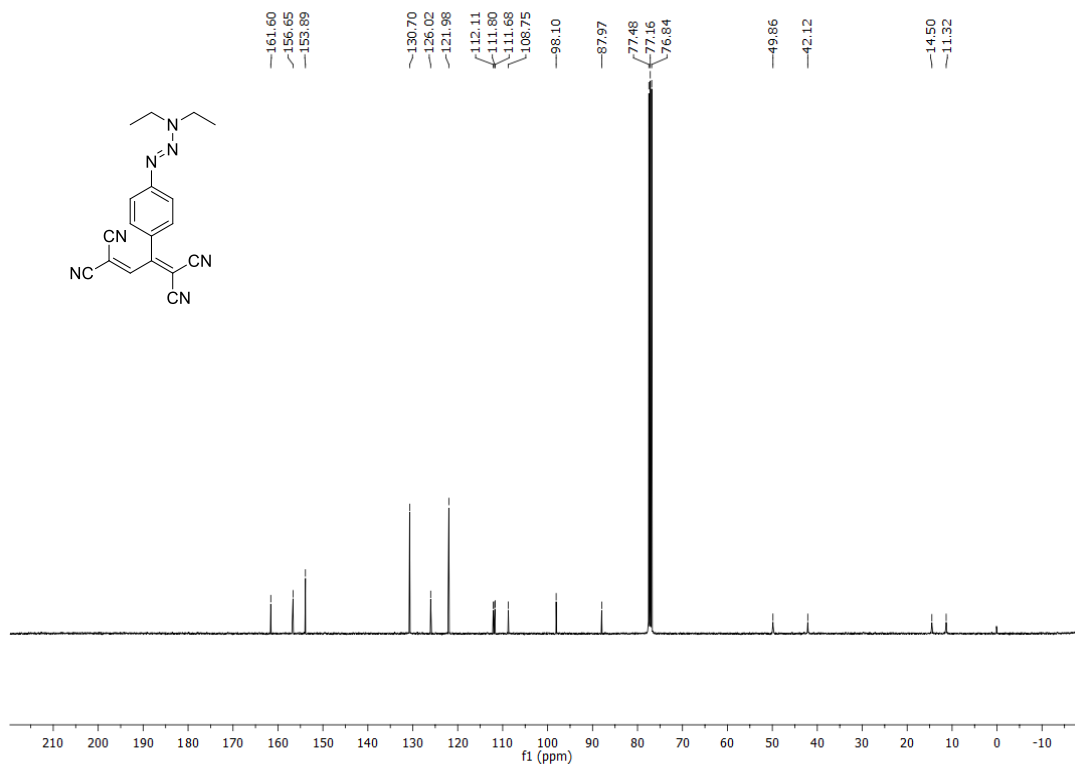
Figure 24. ^{13}C NMR spectrum of **87** in CDCl$_3$ solution (100 MHz).
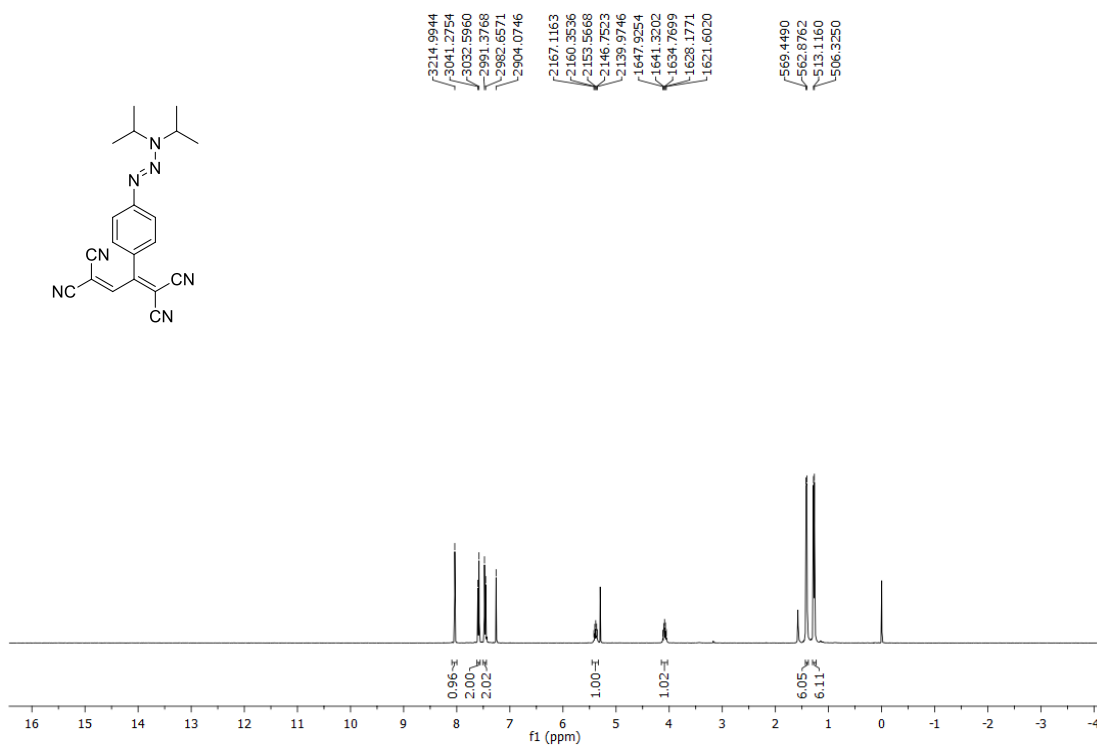
Figure 25. ^{1}H NMR spectrum of crude **88** in CDCl$_3$ solution (400 MHz).

98
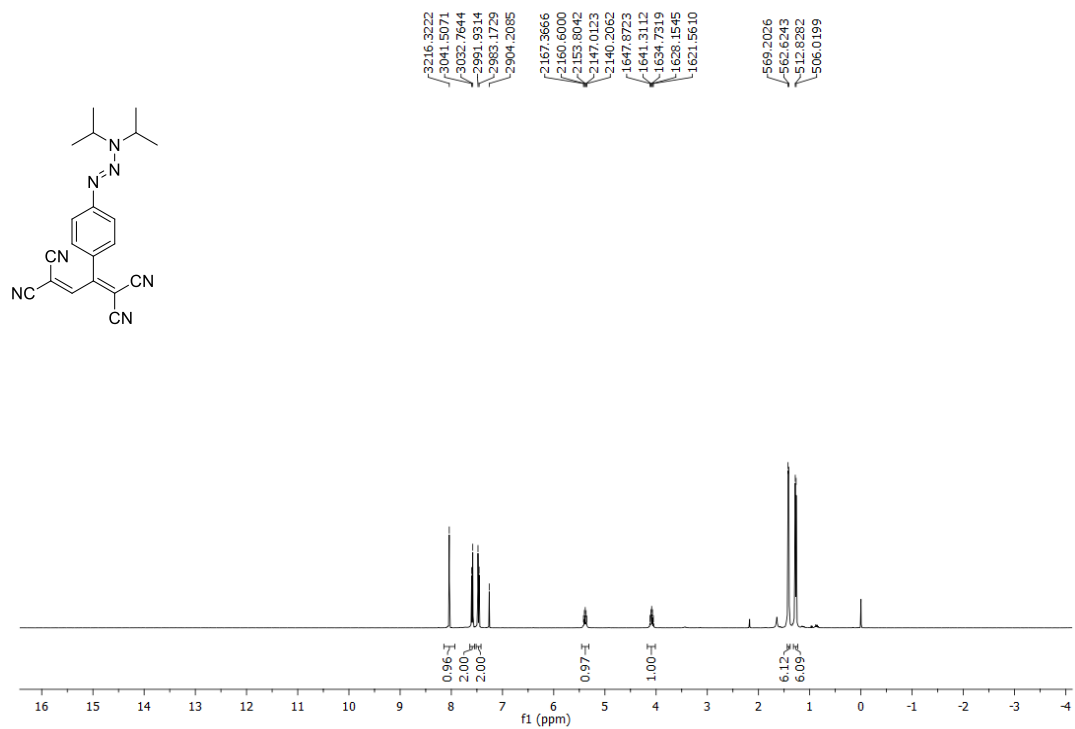
Figure 26. ^{1}H NMR spectrum of **88** in CDCl$_3$ solution (400 MHz).
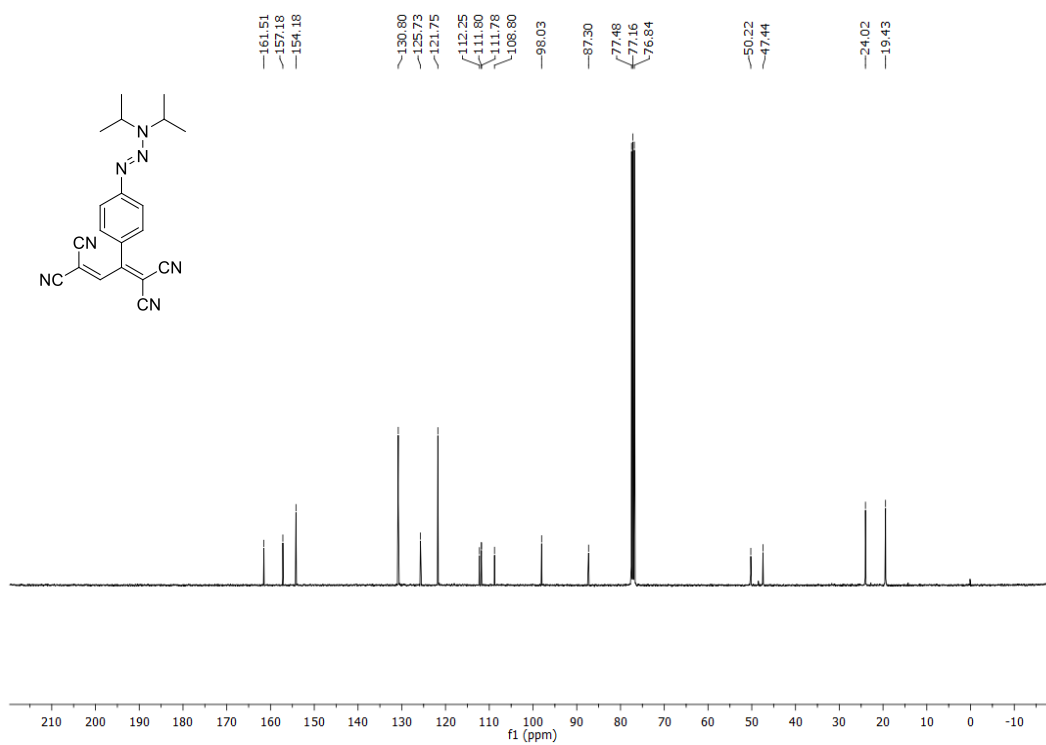
Figure 27 ^{13}C NMR spectrum of **88** in CDCl$_3$ solution (100 MHz).

99
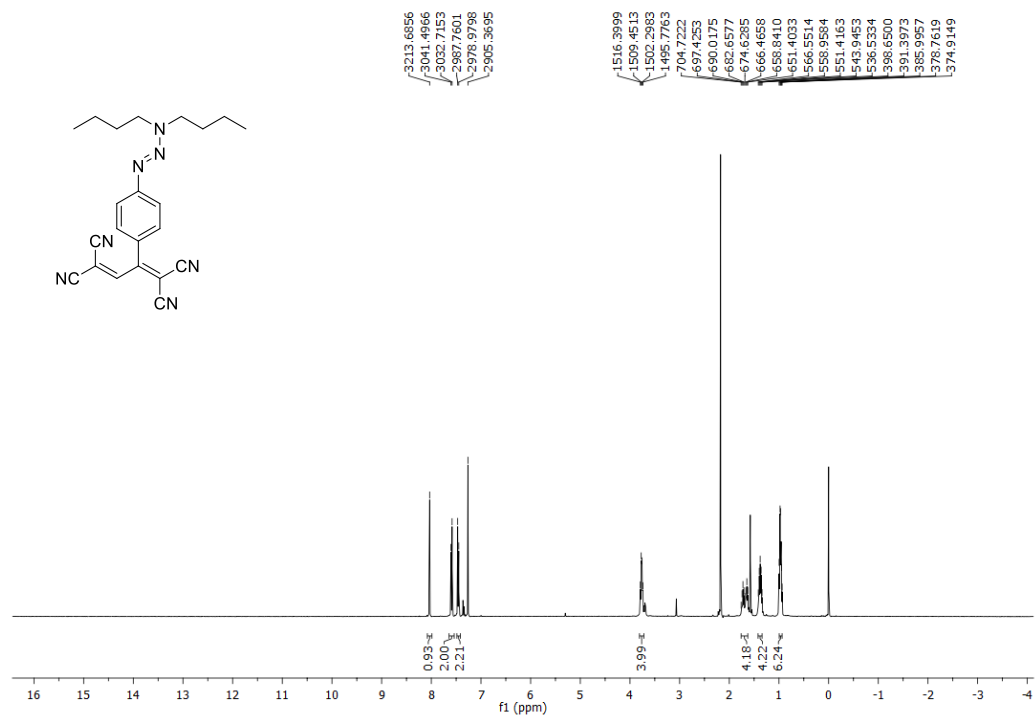
Figure 28. ^{1}H NMR spectrum of crude **89** in CDCl$_3$ solution (400 MHz).
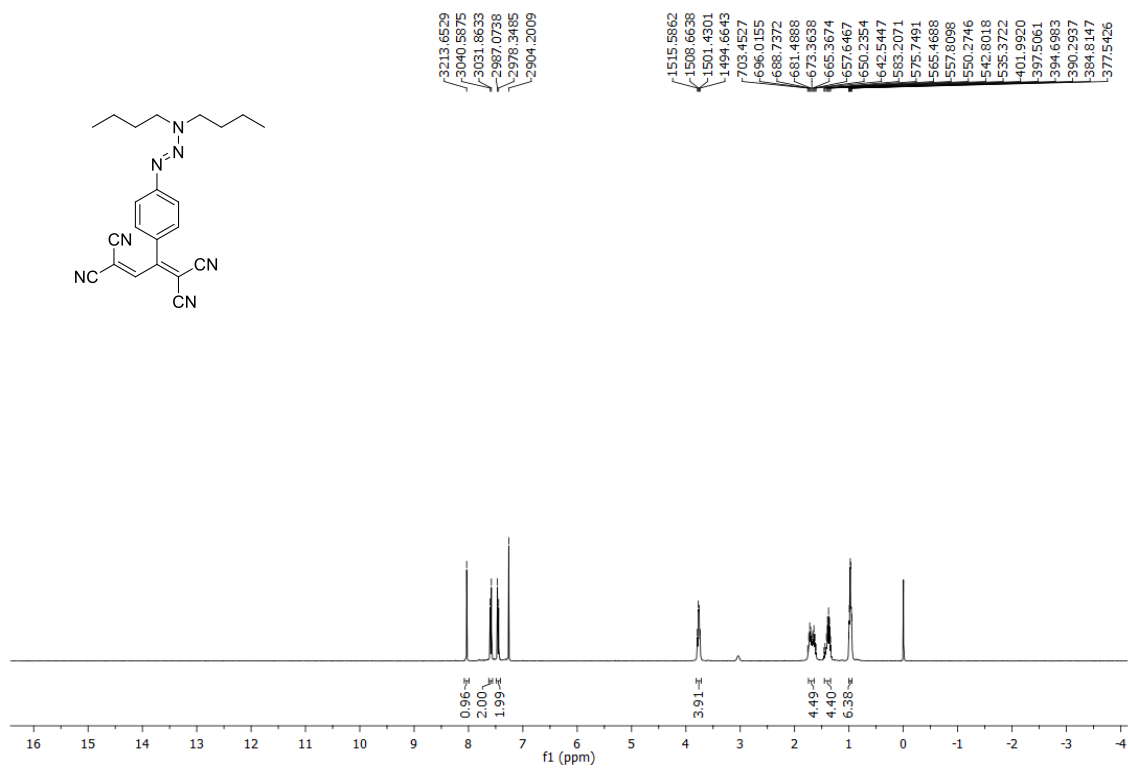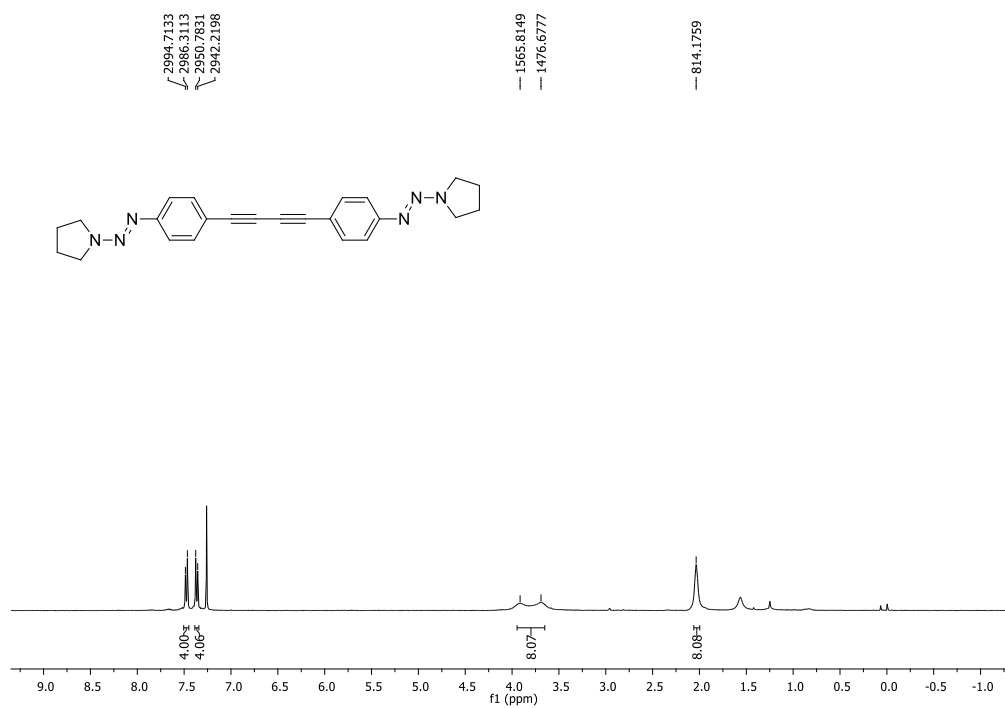

Figure 29. ^{1}H NMR spectrum of **89** in CDCl$_3$ solution (400 MHz).
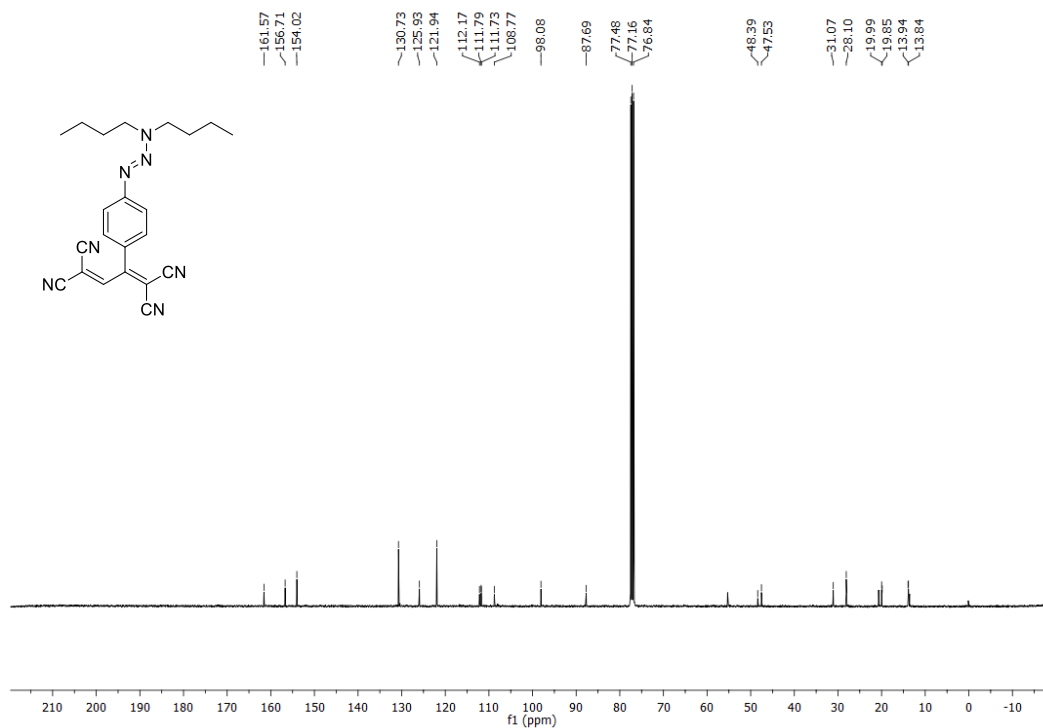
Figure 30. ^{13}C NMR spectrum of **89** in CDCl$_3$ solution (100 MHz).
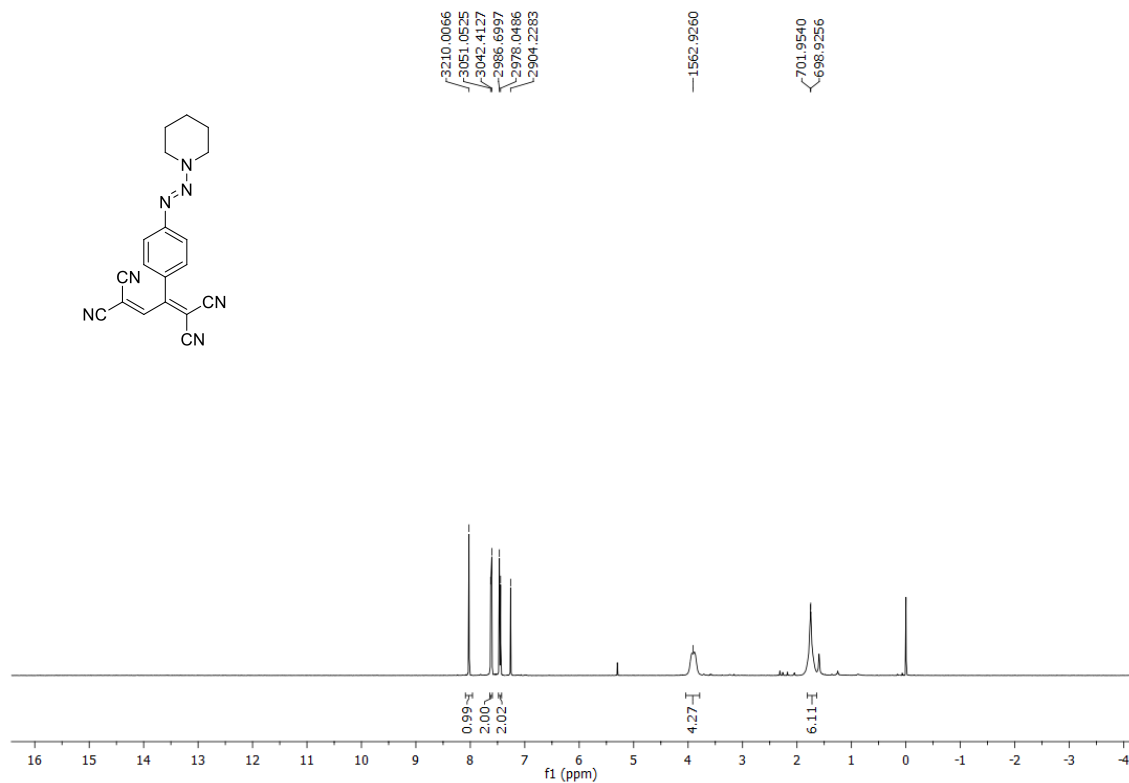
Figure 31. ^{1}H NMR spectrum of crude **90** in CDCl$_3$ solution (400 MHz).

101
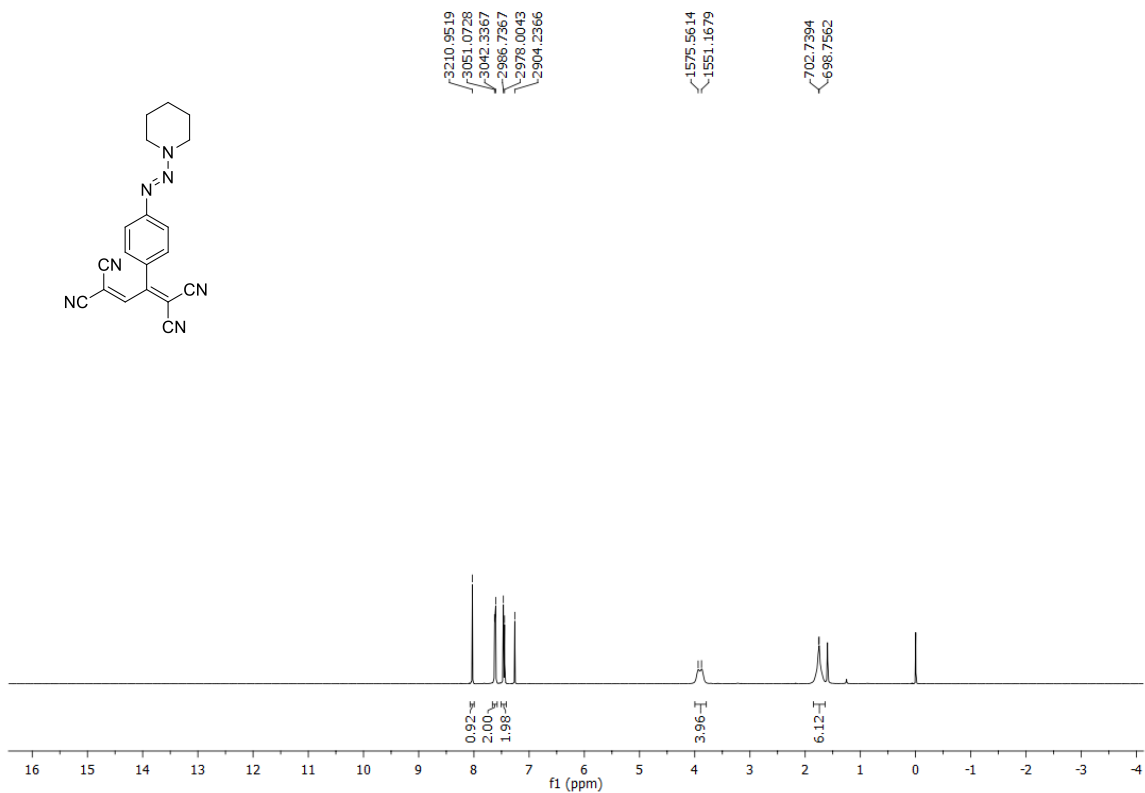
Figure 32. ^{1}H NMR spectrum of **90** in CDCl$_3$ solution (400 MHz).
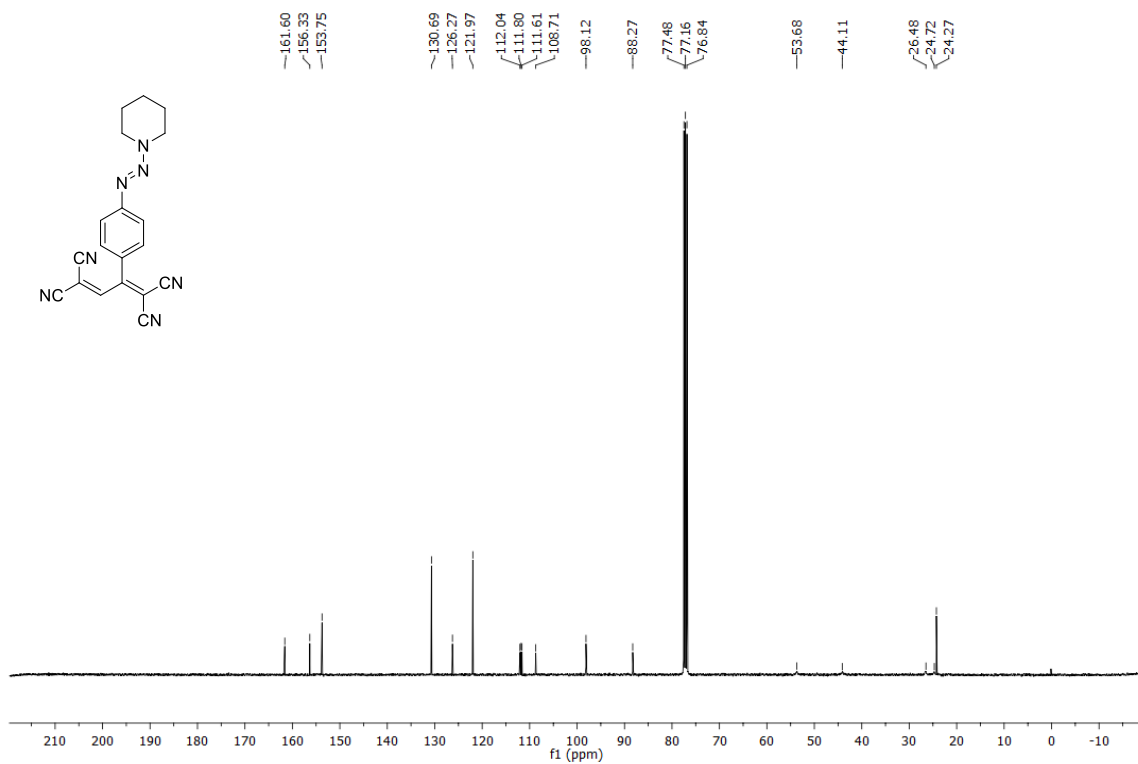
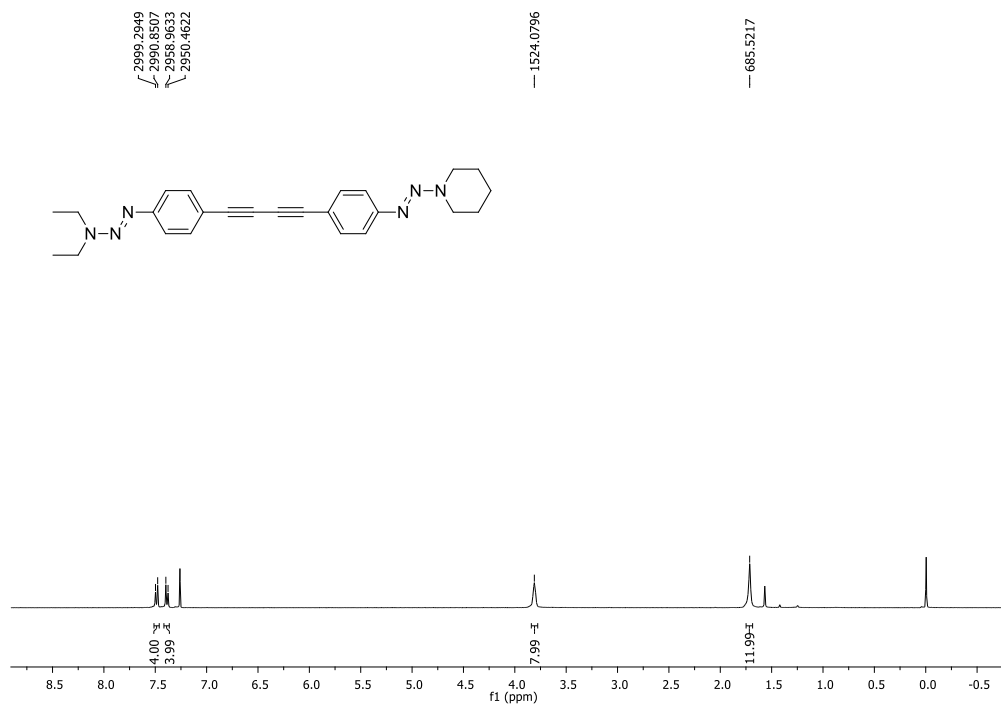**Figure 33.** ^{13}C NMR spectrum of **90** in CDCl$_3$ solution (100 MHz).
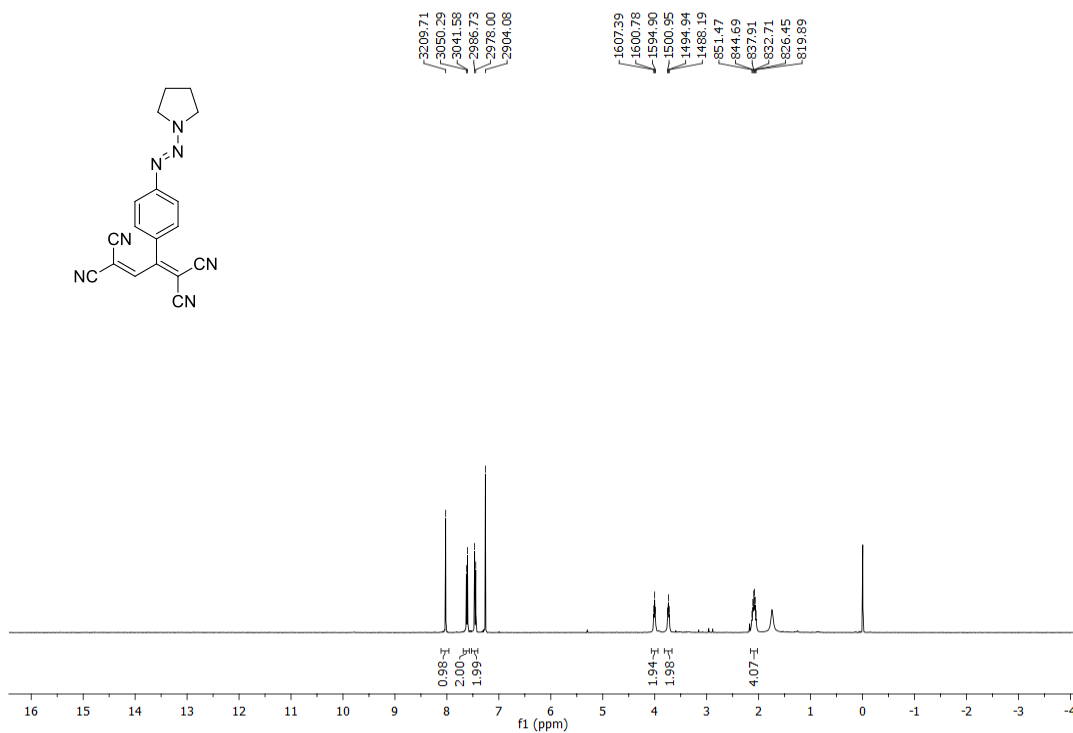
Figure 34. ^{1}H NMR spectrum of crude **91** in CDCl$_3$ solution (400 MHz).
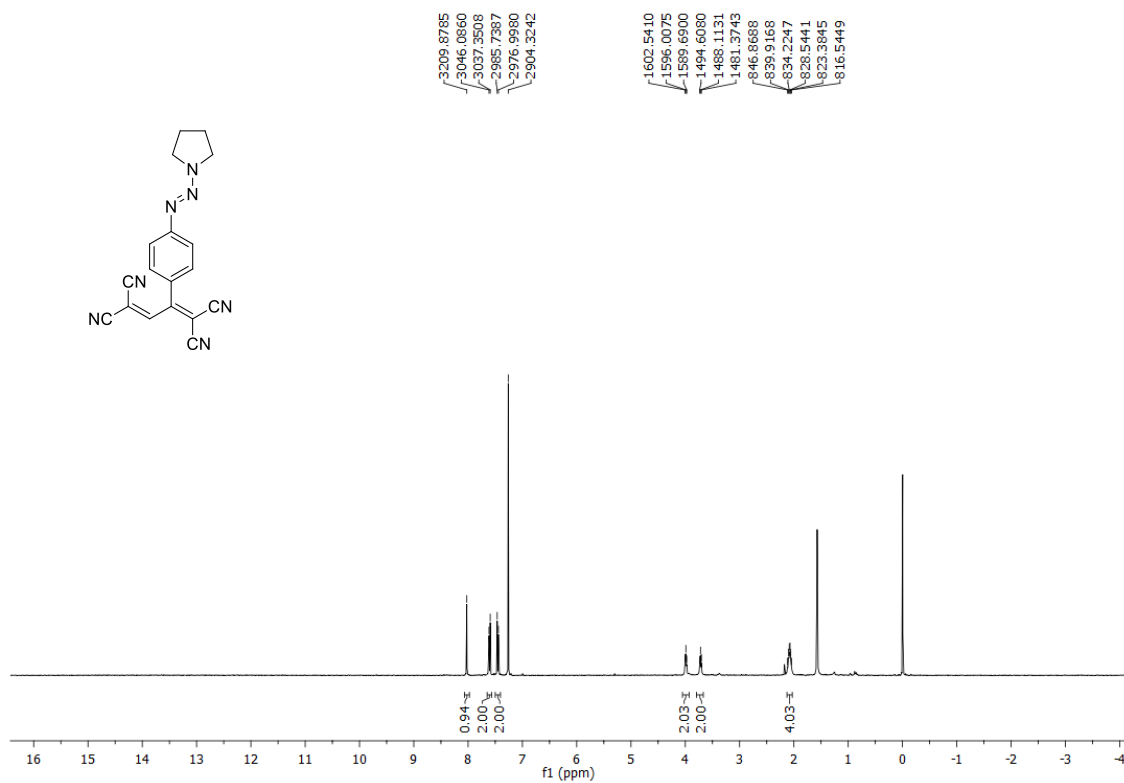
Figure 35. ^{1}H NMR spectrum of **91** in CDCl$_3$ solution (400 MHz).
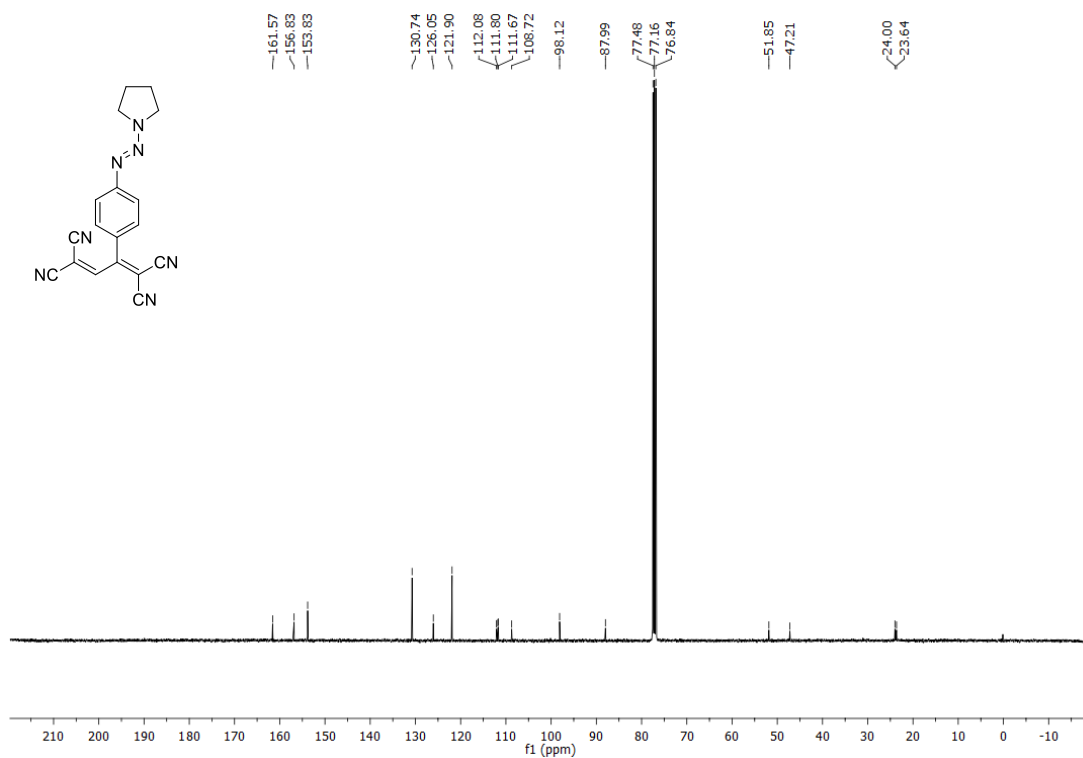
Figure 36. ^{13}C NMR spectrum of **91** in CDCl$_3$ solution (100 MHz).
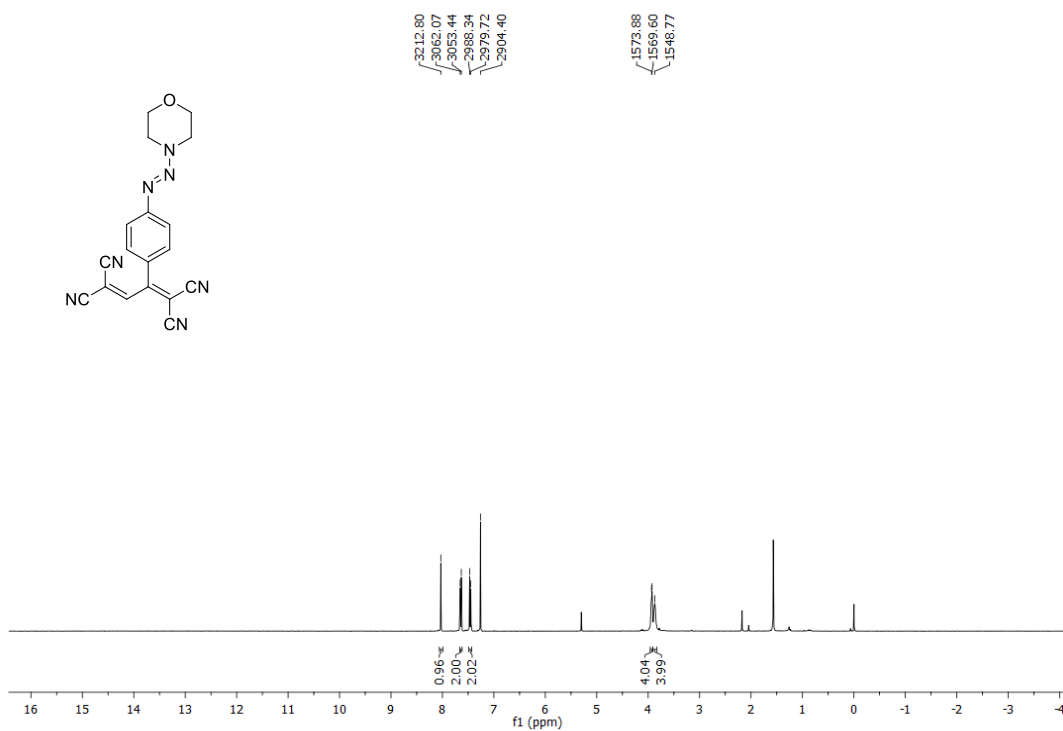
Figure 37. ^{1}H NMR spectrum of crude **92** in CDCl$_3$ solution (400 MHz).
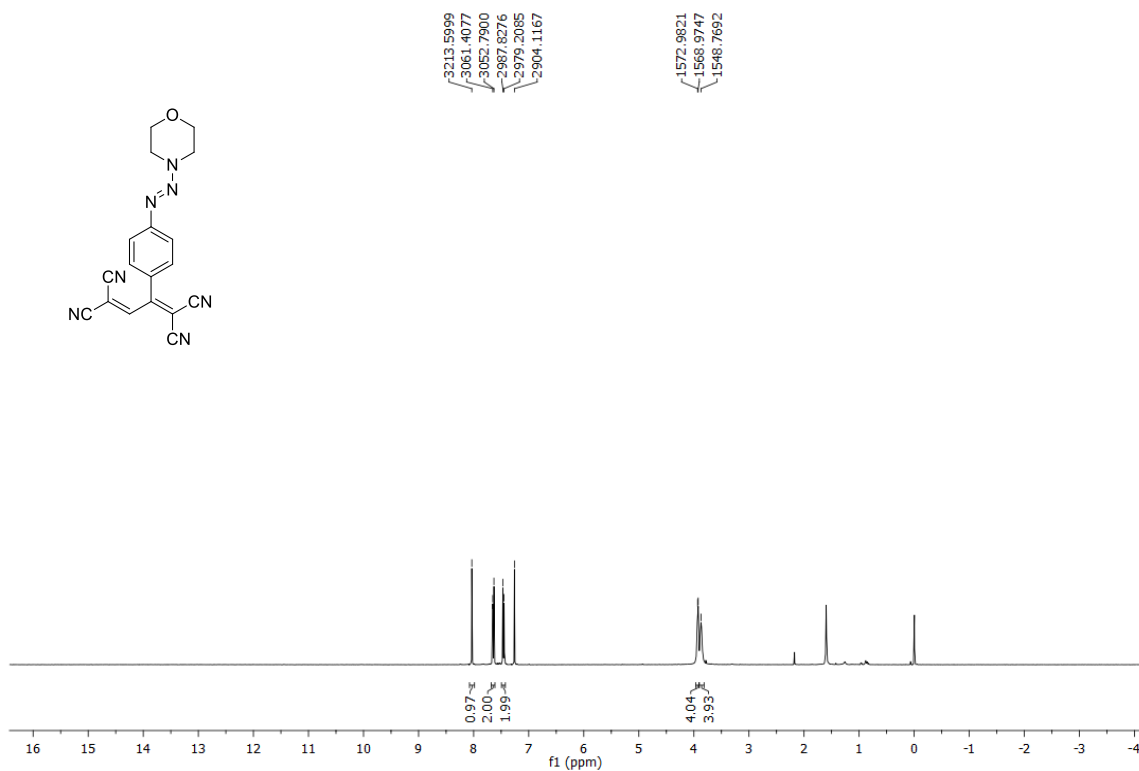
Figure 38. ^{1}H NMR spectrum of **92** in CDCl$_3$ solution (400 MHz).
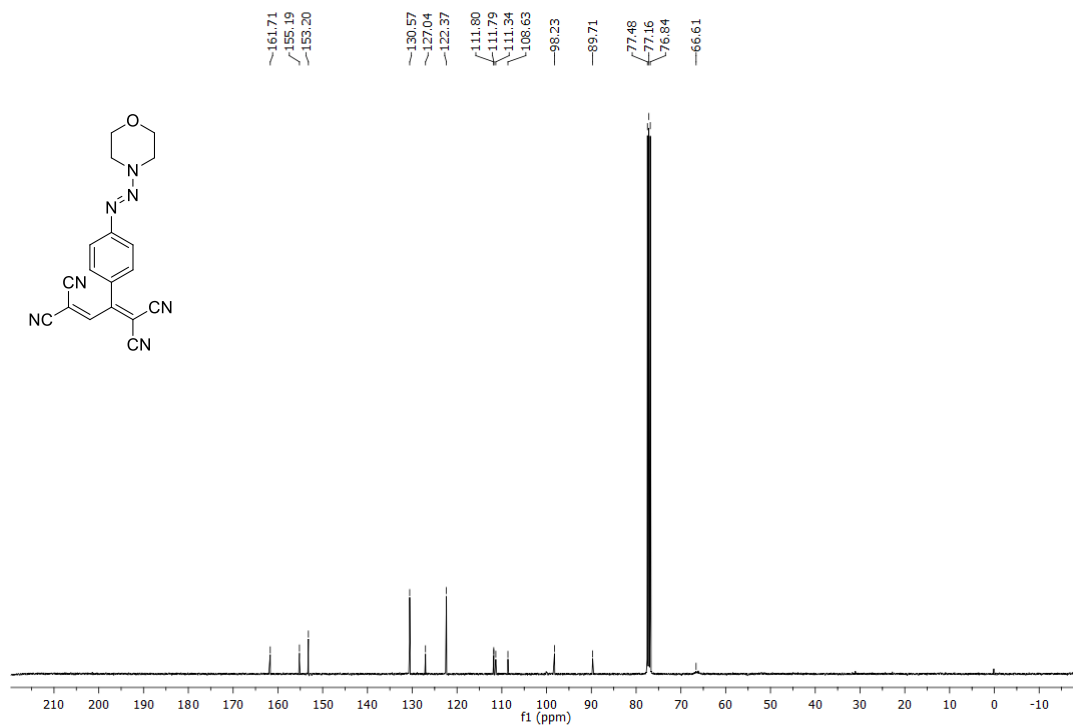
Figure 39. ^{13}C NMR spectrum of **92** in CDCl$_3$ solution (100 MHz).

105
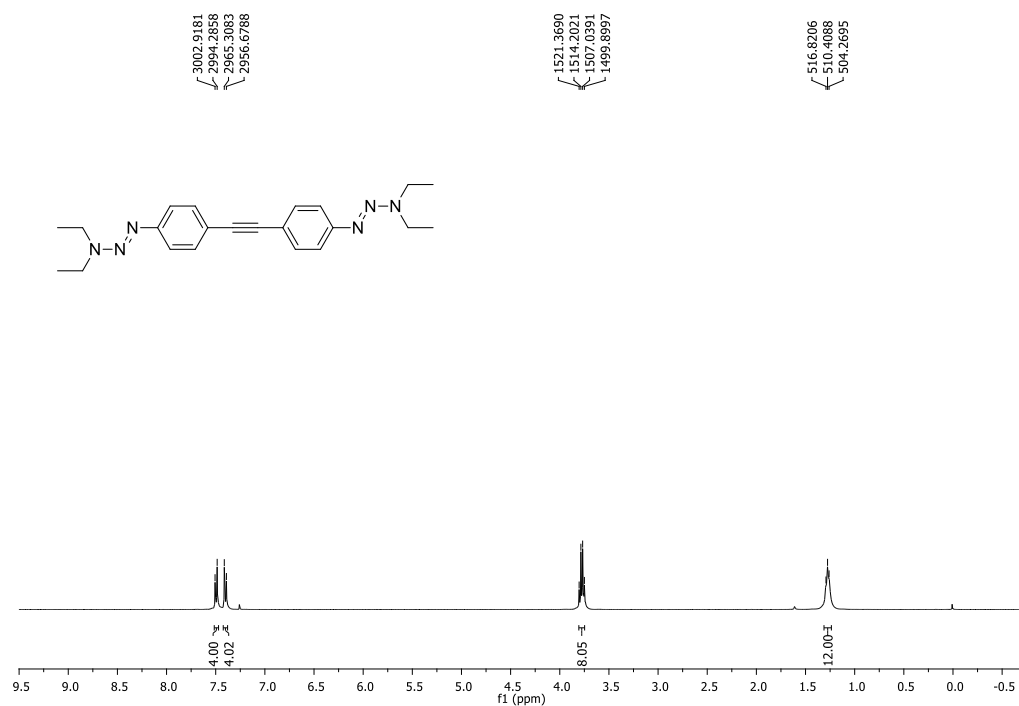
Figure 40. ^{1}H NMR spectrum of **94** in CDCl$_3$ solution (400 MHz).
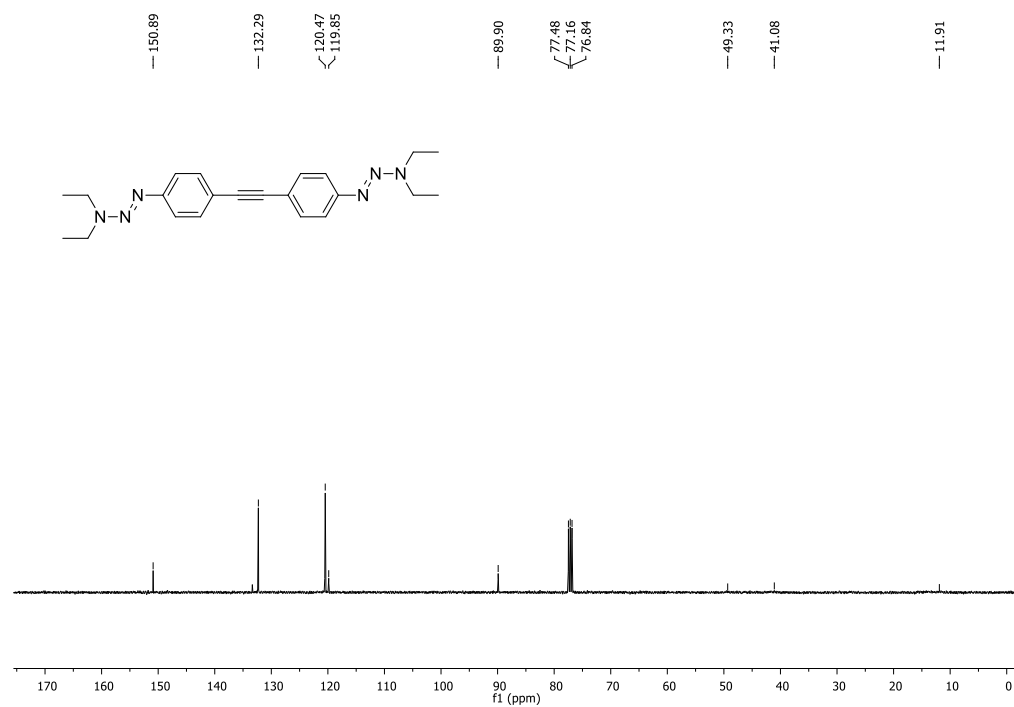
Figure 41. ^{13}C NMR spectrum of **94** in CDCl$_3$ solution (100 MHz).

106
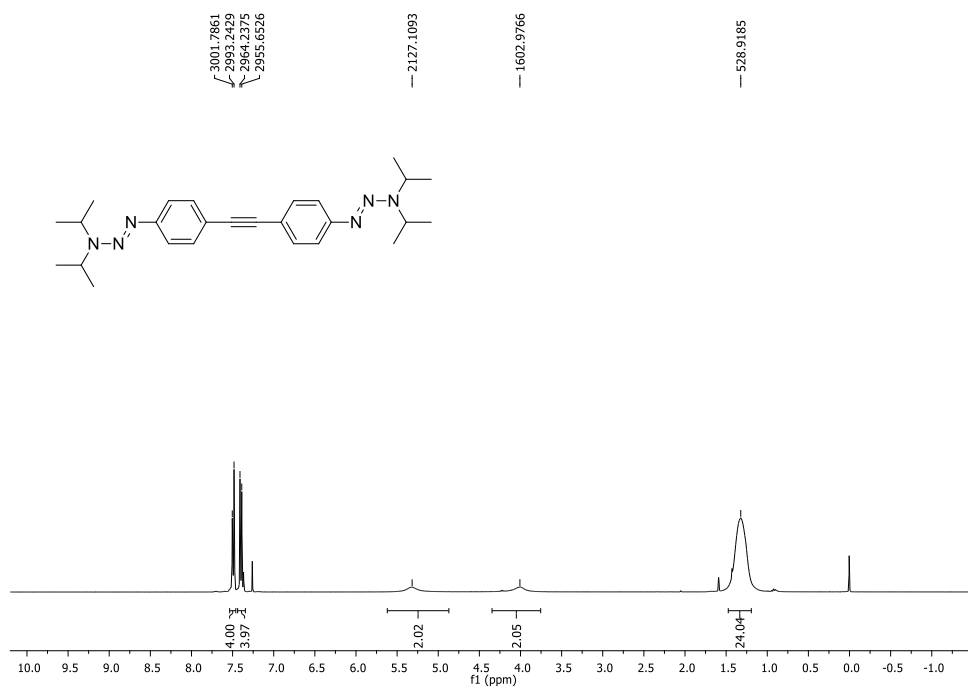
Figure 42. ^{1}H NMR spectrum of **95** in CDCl$_3$ solution (400 MHz).
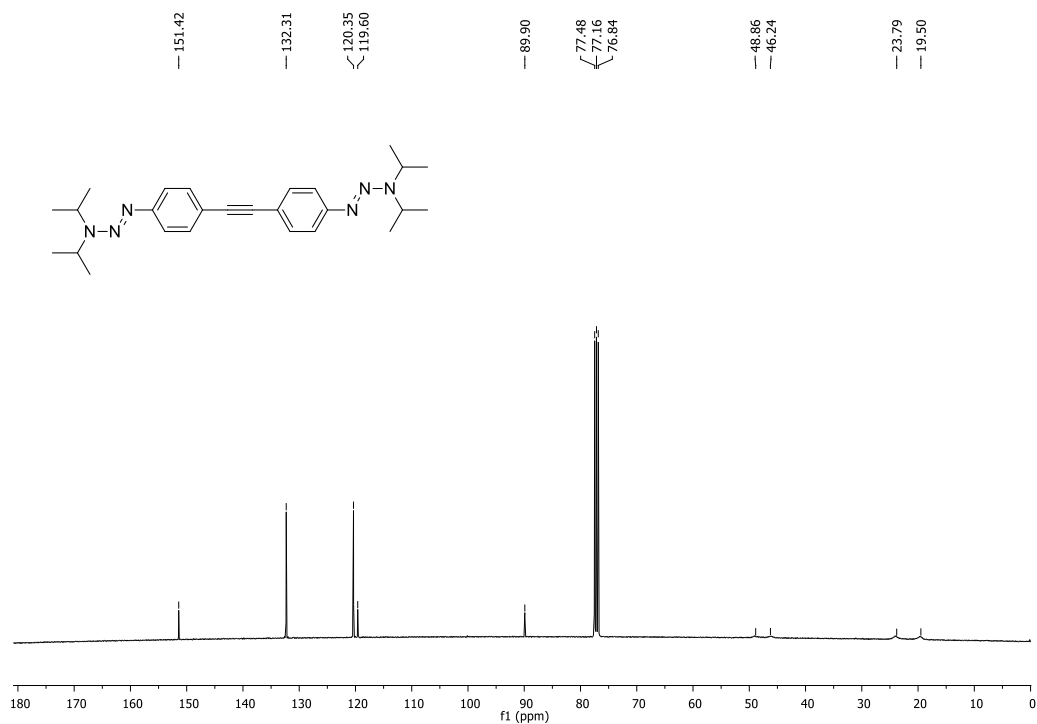
Figure 43. ^{13}C NMR spectrum of **95** in CDCl$_3$ solution (100 MHz).

107
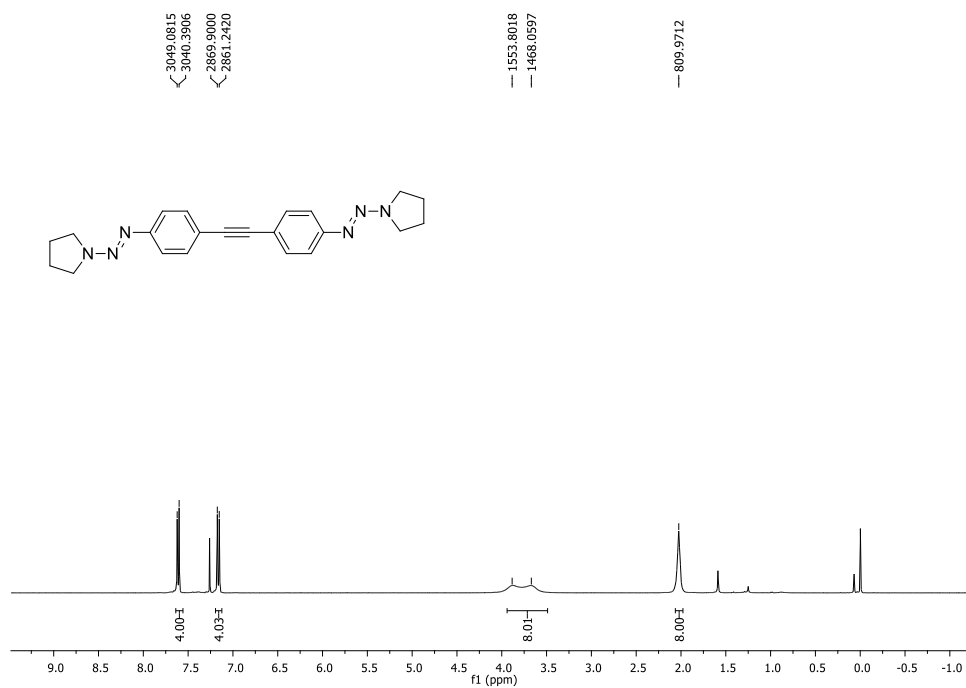
Figure 44. ^{1}H NMR spectrum of **96** in CDCl$_3$ solution (400 MHz).
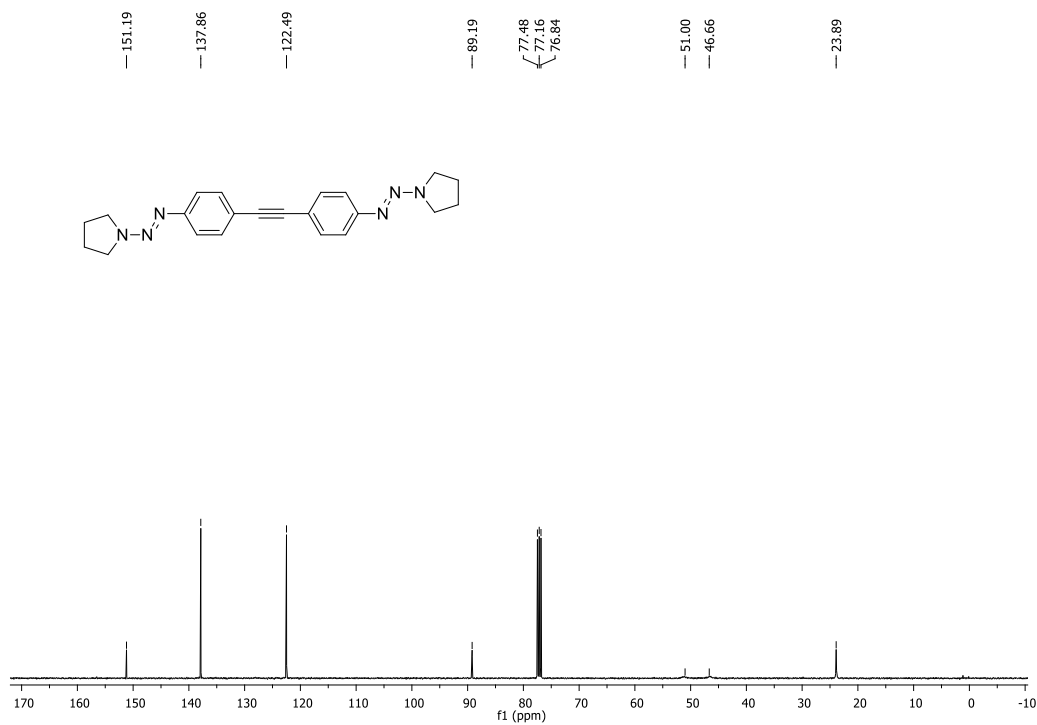
Figure 45. ^{13}C NMR spectrum of **96** in CDCl$_3$ solution (100 MHz).
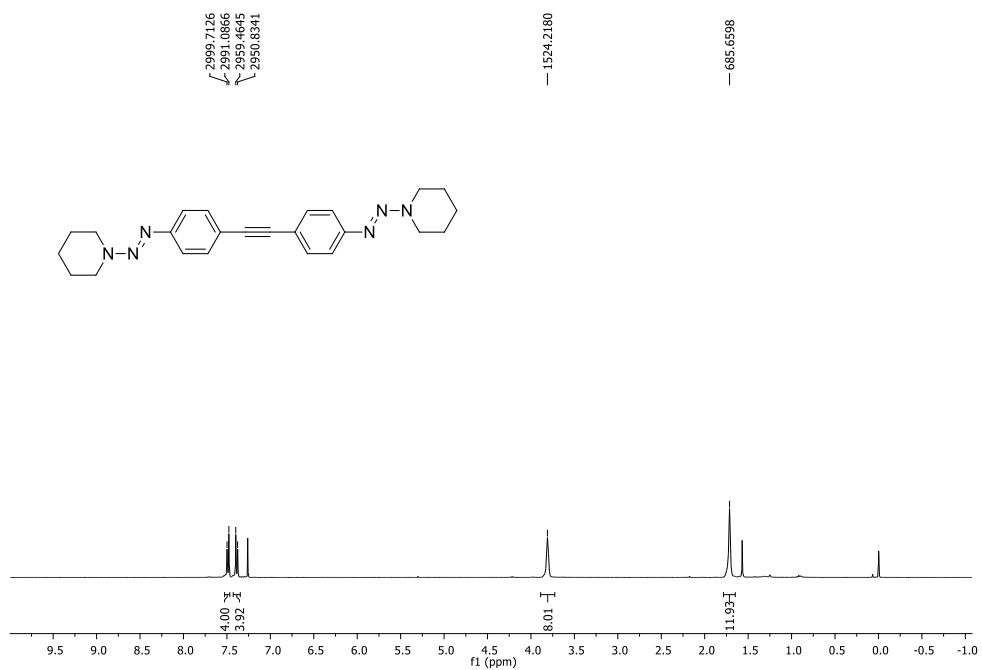
Figure 46. ^{1}H NMR spectrum of **97** in CDCl$_3$ solution (400 MHz).
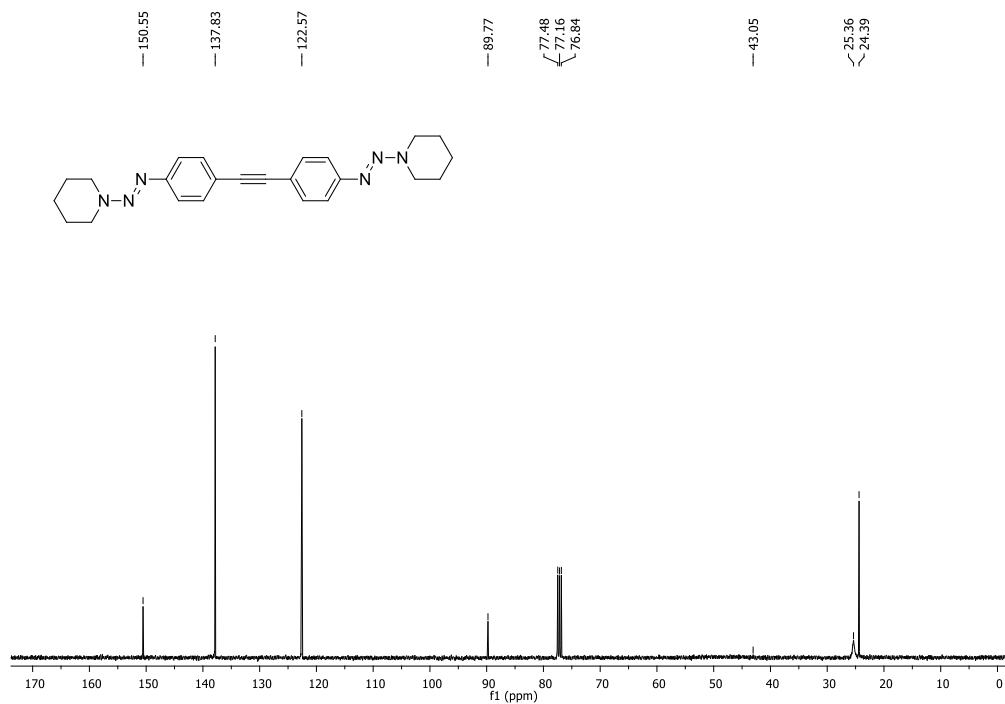
Figure 47. ^{13}C NMR spectrum of **97** in CDCl$_3$ solution (100 MHz).
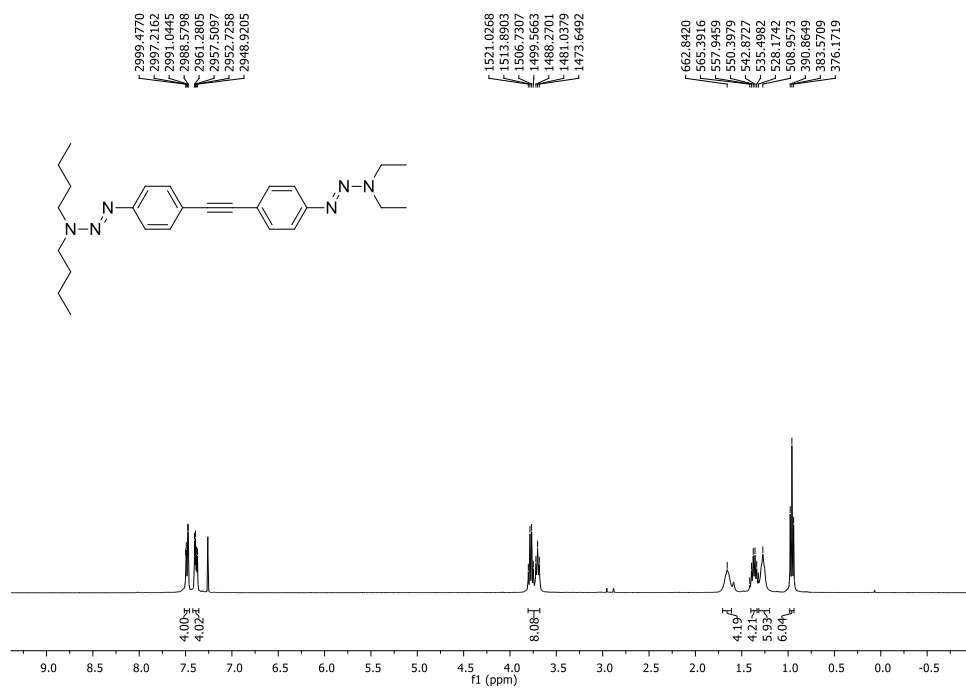
Figure 48. ^{1}H NMR spectrum of **98** in CDCl$_3$ solution (400 MHz).
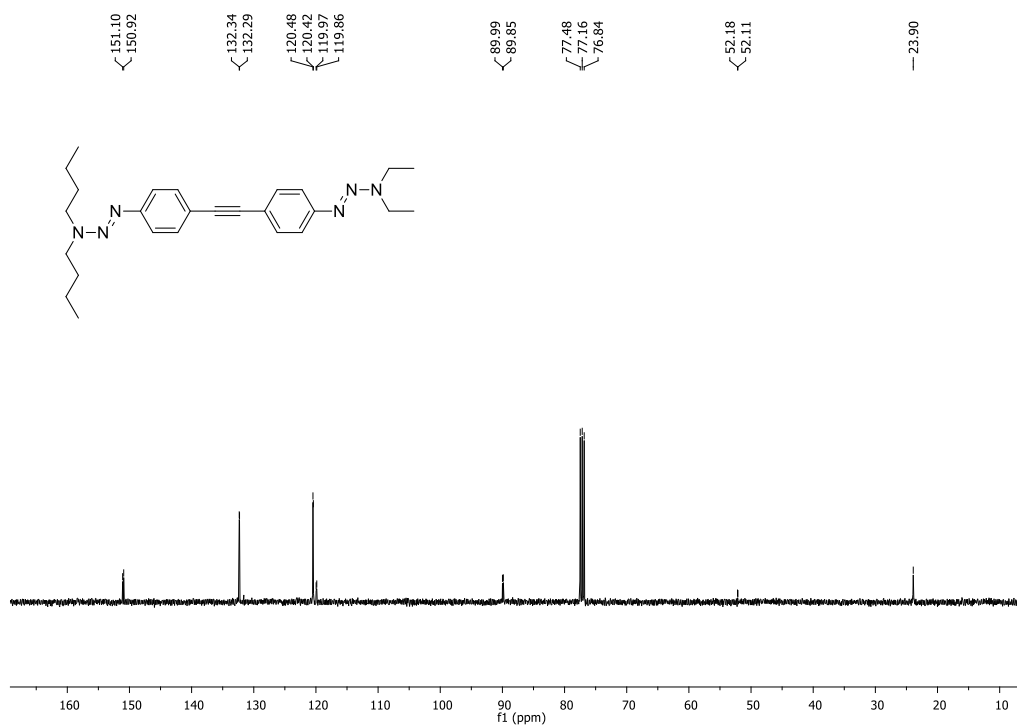
Figure 49. ^{13}C NMR spectrum of **98** in CDCl$_3$ solution (100 MHz).

110
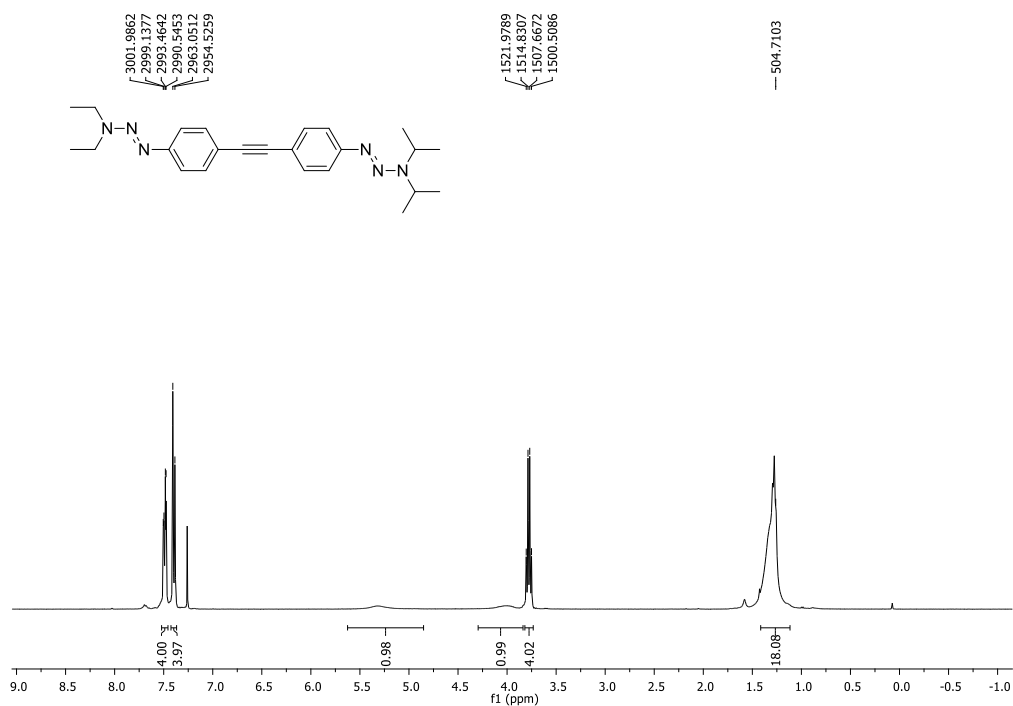
Figure 50. ^{1}H NMR spectrum of **99** in CDCl$_3$ solution (400 MHz).
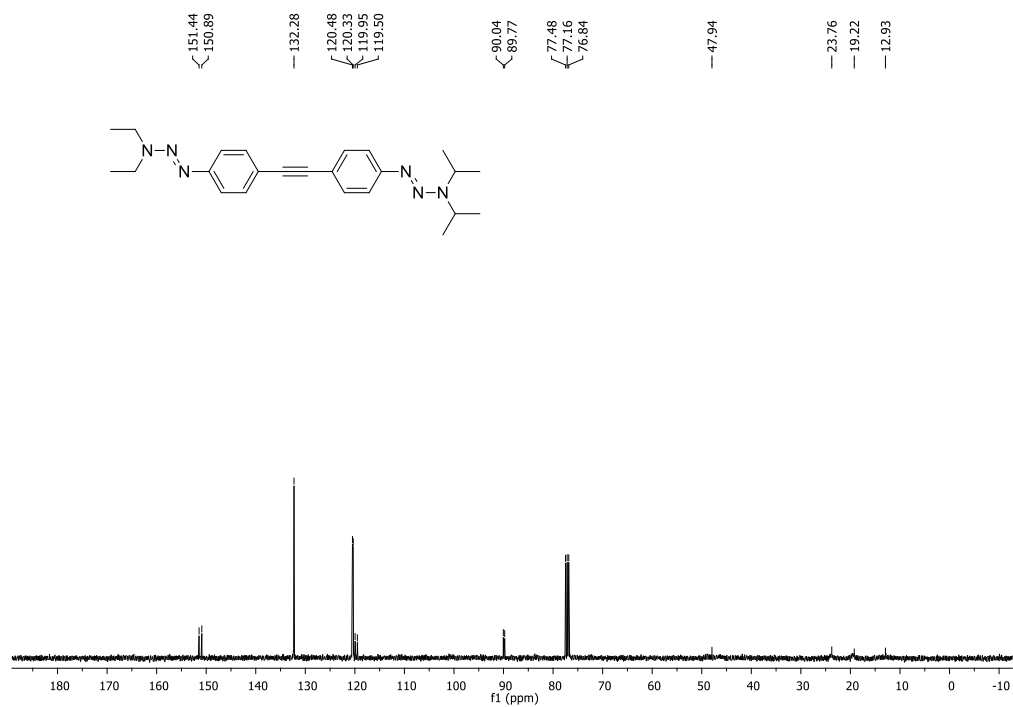
Figure 51. ^{13}C NMR spectrum of **99** in CDCl$_3$ solution (100 MHz).

111

Figure 52. ^{1}H NMR spectrum of **100** in CDCl$_3$ solution (400 MHz).
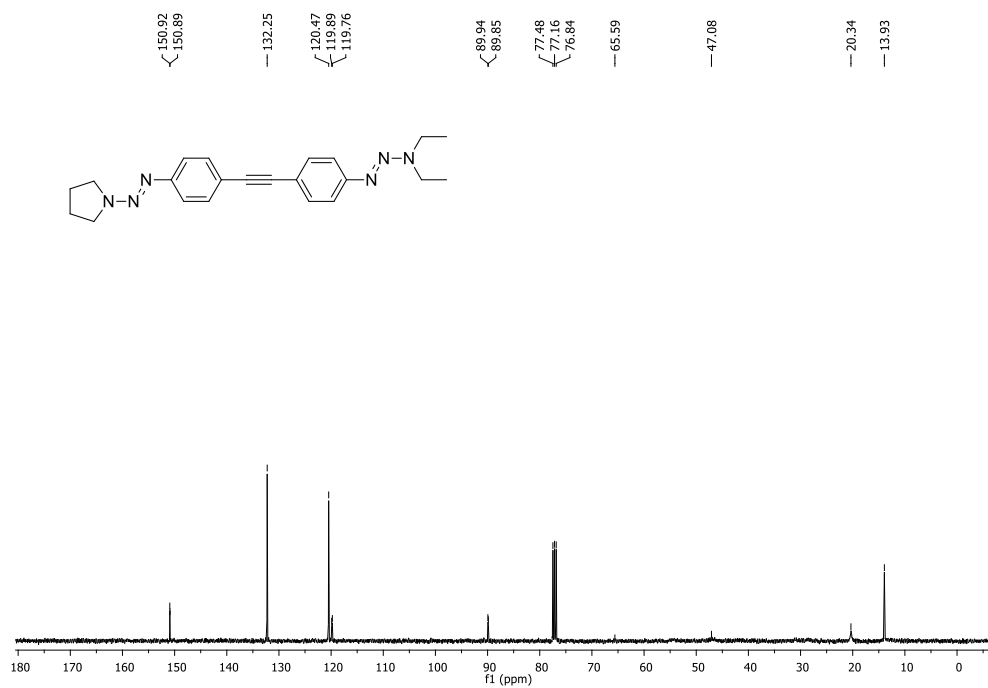
Figure 53. ^{13}C NMR spectrum of **100** in CDCl$_3$ solution (100 MHz).

112
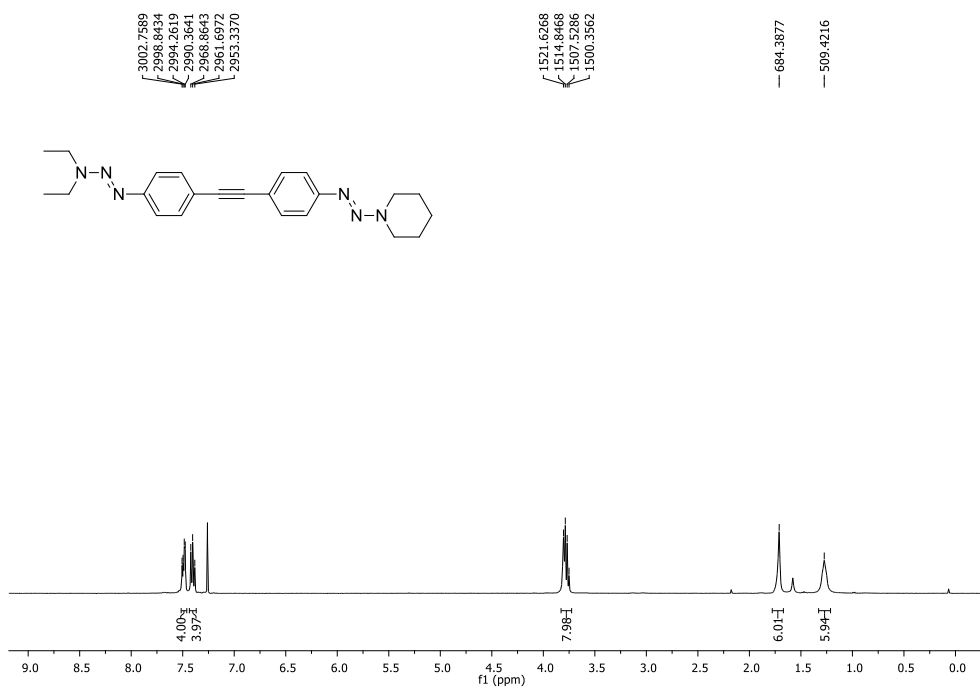
Figure 54. ^{1}H NMR spectrum of **101** in CDCl$_3$ solution (400 MHz).
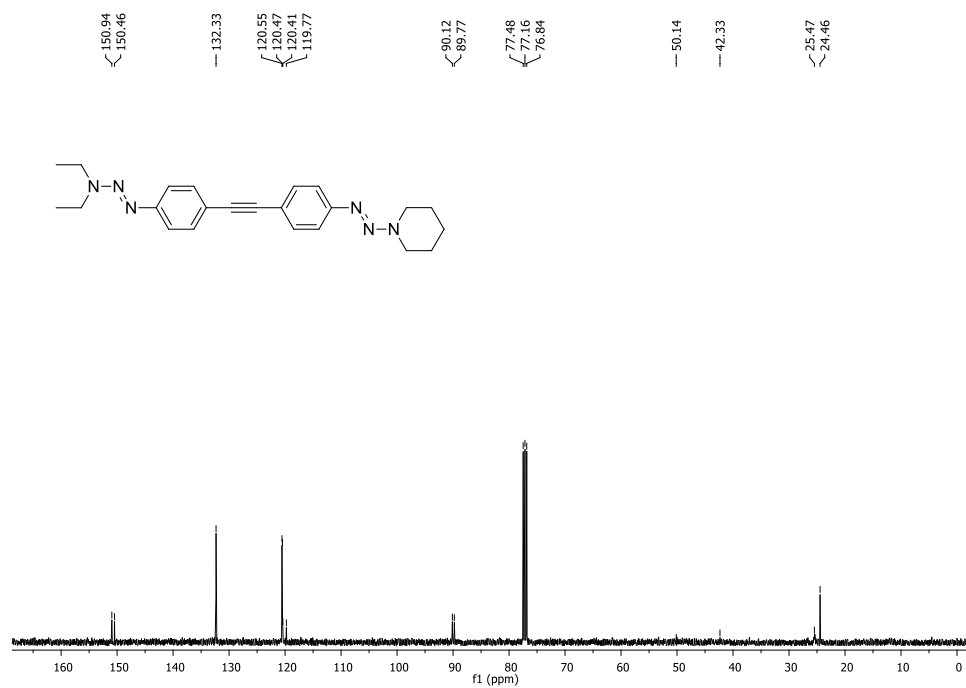
Figure 55. ^{13}C NMR spectrum of **101** in CDCl$_3$ solution (100 MHz).

113

3020.4650
3017.7465
3012.7276
3010.9113
2943.3819
2941.5850
2938.4041
2936.6000

4.00
6.00

9.0 8.5 8.0 7.5 7.0 6.5 6.0 5.5 5.0 4.5 4.0 3.5 3.0 2.5 2.0 1.5 1.0 0.5 0.0
f1 (ppm)

Figure 56. ^{1}H NMR spectrum of **103** in CDCl$_3$ solution (400 MHz).

131.73
128.48
128.39
123.37

89.49

77.48
77.16
76.84

160 150 140 130 120 110 100 90 80 70 60 50 40 30 20 10 0 -10
f1 (ppm)
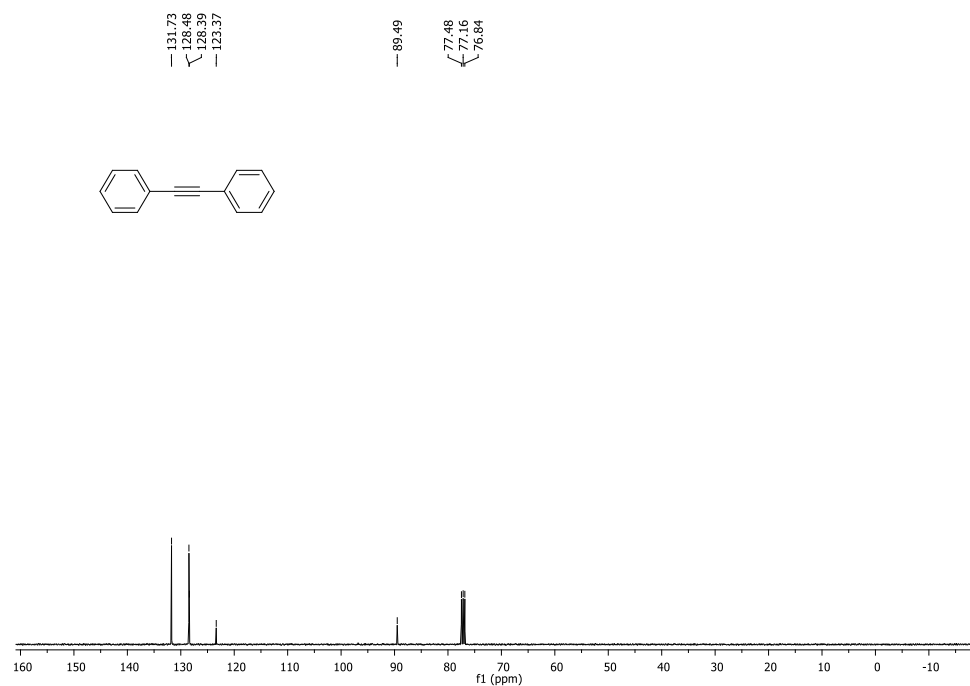
Figure 57. ^{13}C NMR spectrum of **103** in CDCl$_3$ solution (100 MHz).

114

Figure 58. ^{1}H NMR spectrum of **107** in CDCl$_3$ solution (400 MHz).

Figure 59. ^{13}C NMR spectrum of **107** in CDCl$_3$ solution (100 MHz).

115

Figure 60. ^{1}H NMR spectrum of **107** in CDCl$_3$ solution (400 MHz).
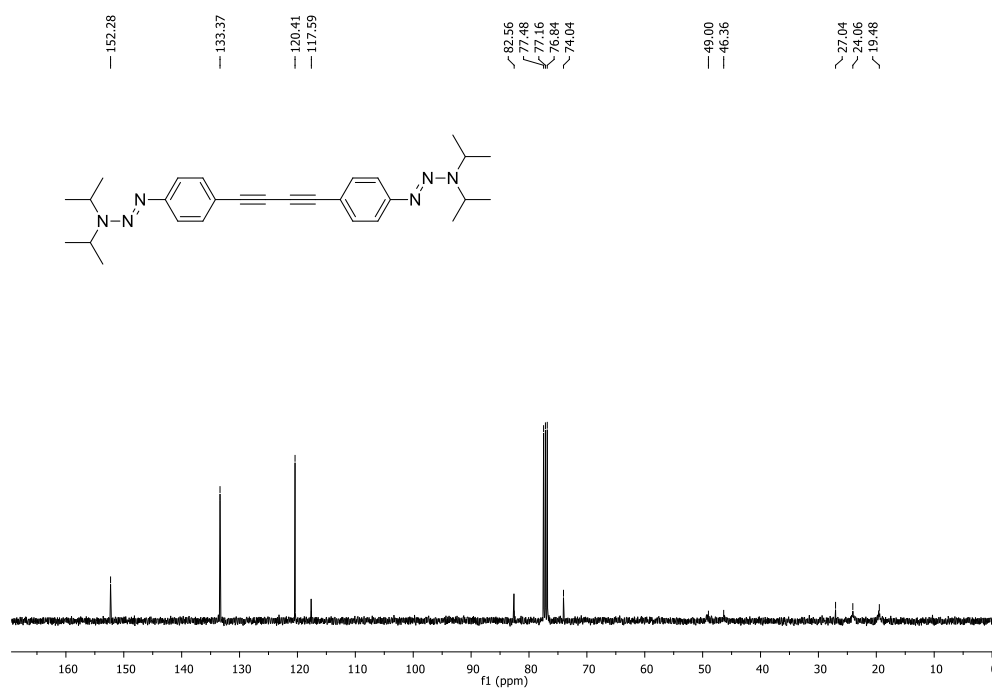
Figure 61. ^{13}C NMR spectrum of **108** in CDCl$_3$ solution (100 MHz).
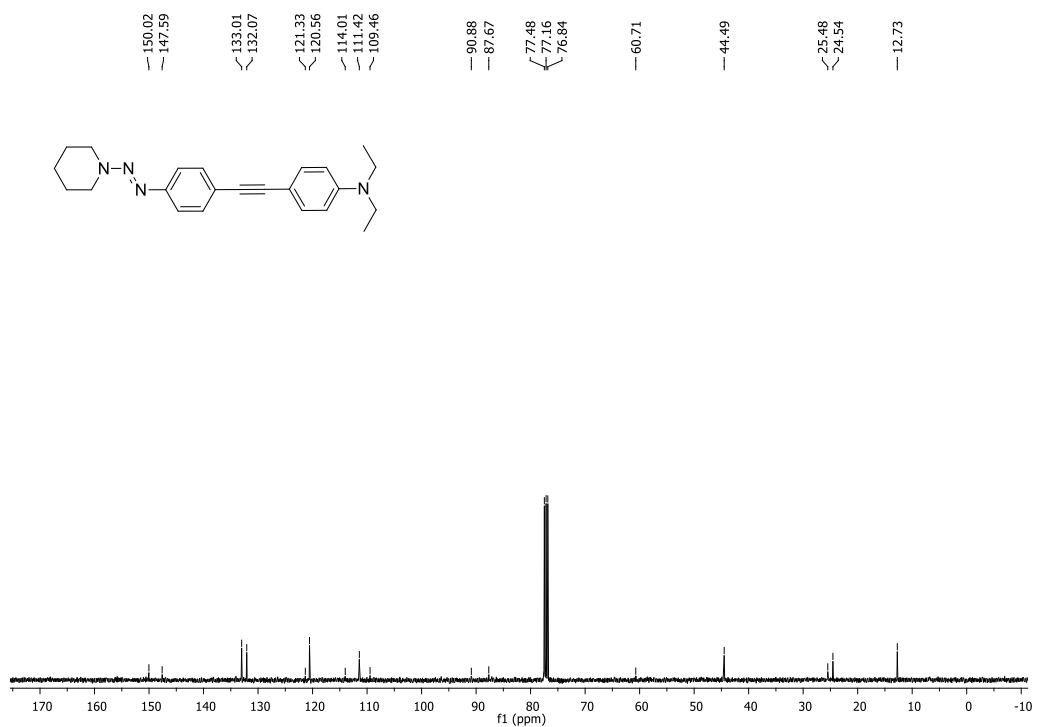
116

Figure 62. ^{1}H NMR spectrum of **109** in CDCl$_3$ solution (400 MHz).
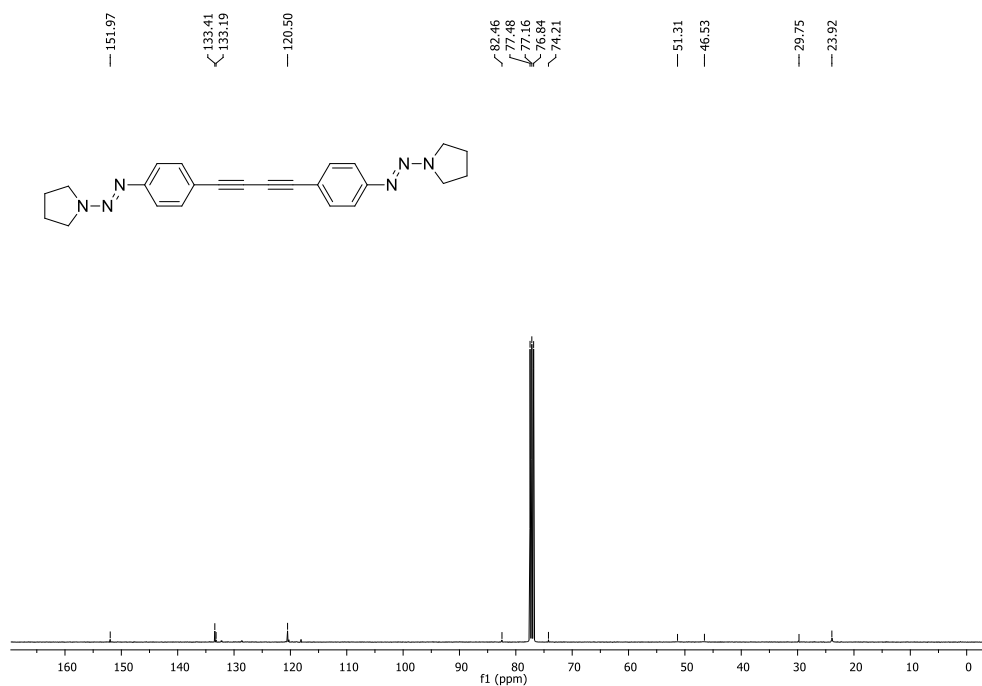
Figure 63. ^{13}C NMR spectrum of **109** in CDCl$_3$ solution (100 MHz).

117

Figure 64. ^{1}H NMR spectrum of **110** in CDCl$_3$ solution (400 MHz).
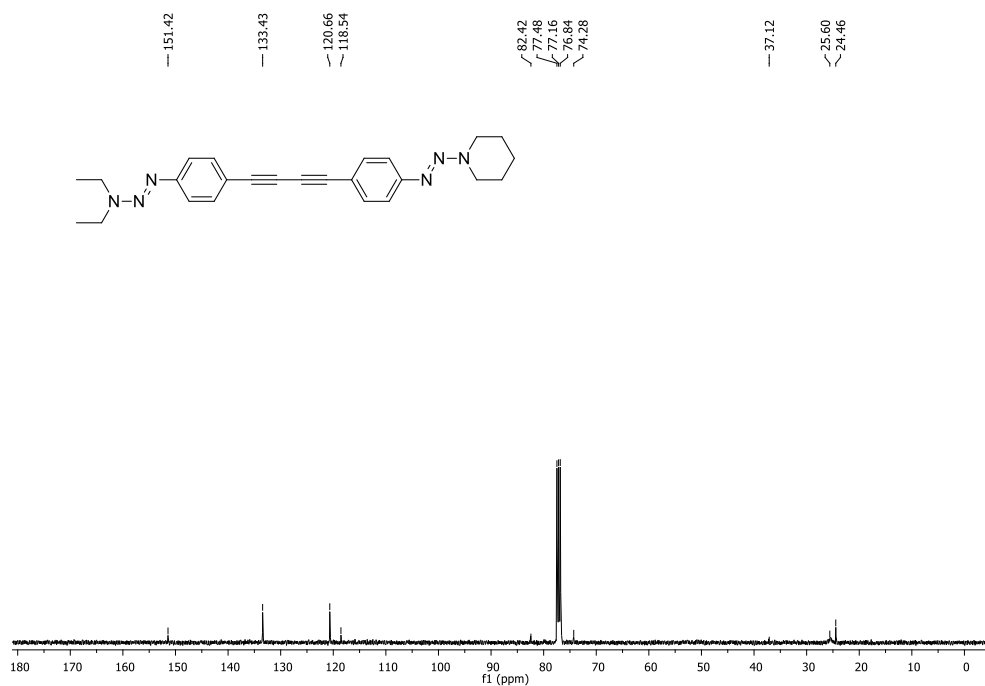
Figure 65. ^{13}C NMR spectrum of **110** in CDCl$_3$ solution (100 MHz).

118
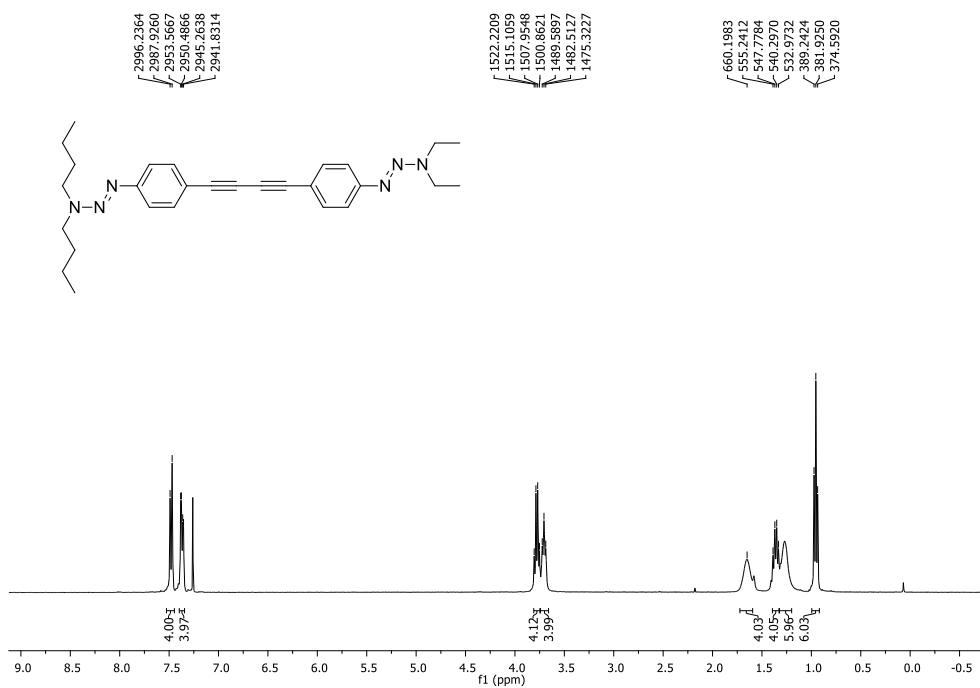
Figure 65. ^{1}H NMR spectrum of **111** in CDCl$_3$ solution (400 MHz).
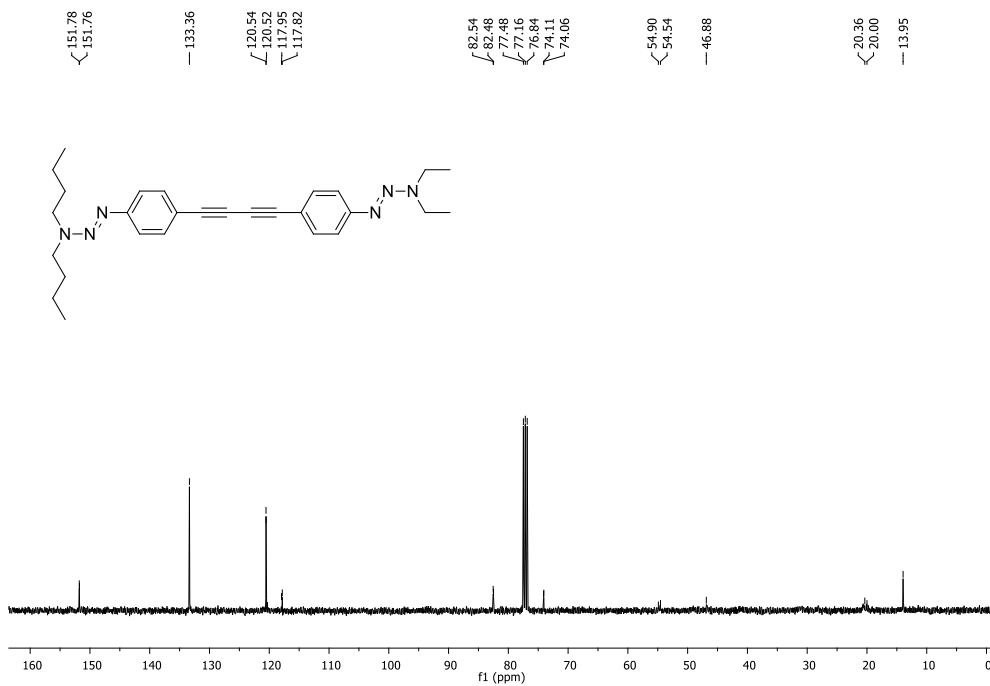
Figure 67. ^{13}C NMR spectrum of **111** in CDCl$_3$ solution (100 MHz).
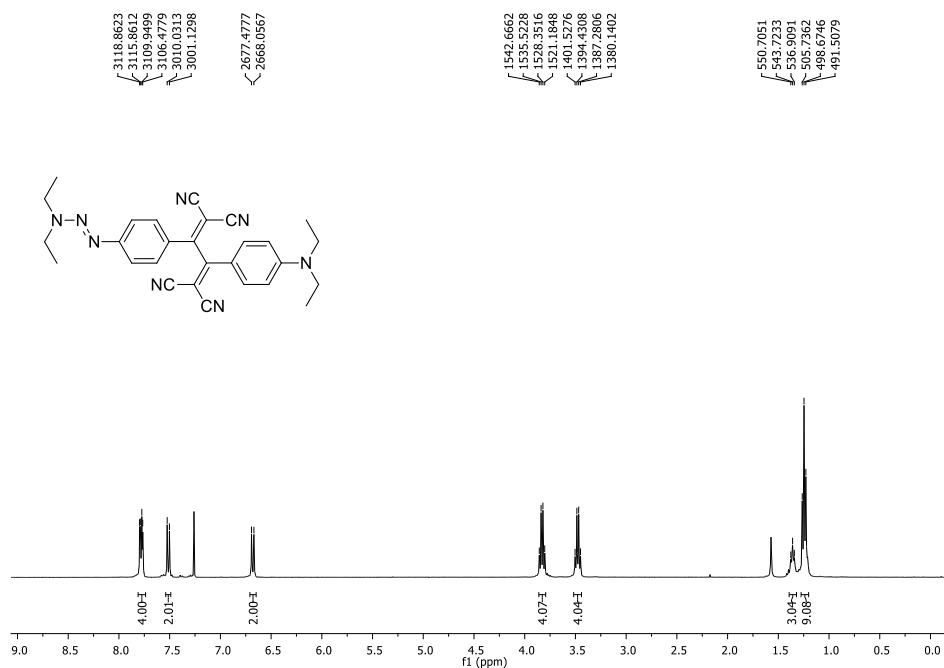
119
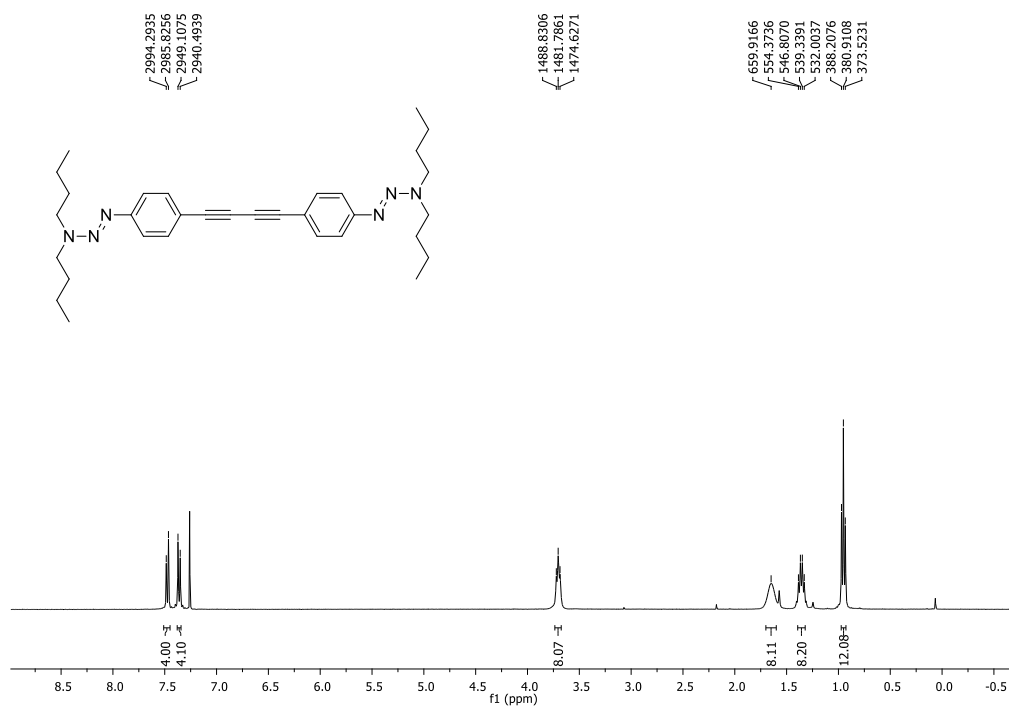
Figure 68. ^{1}H NMR spectrum of **112** in CDCl$_3$ solution (400 MHz).
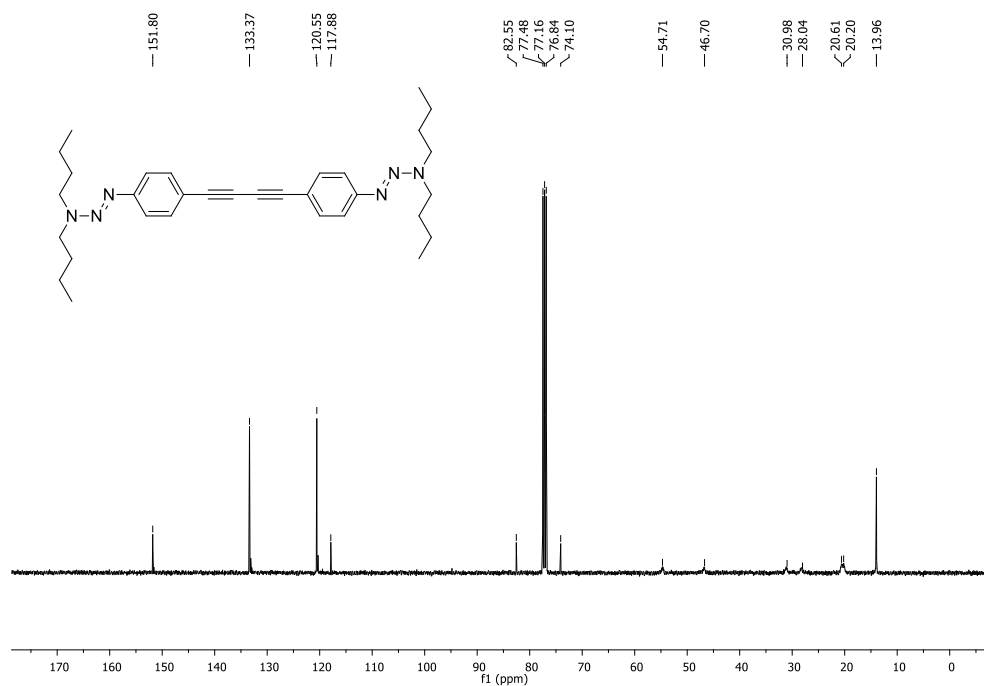
Figure 69. ^{13}C NMR spectrum of **112** in CDCl$_3$ solution (100 MHz).

120
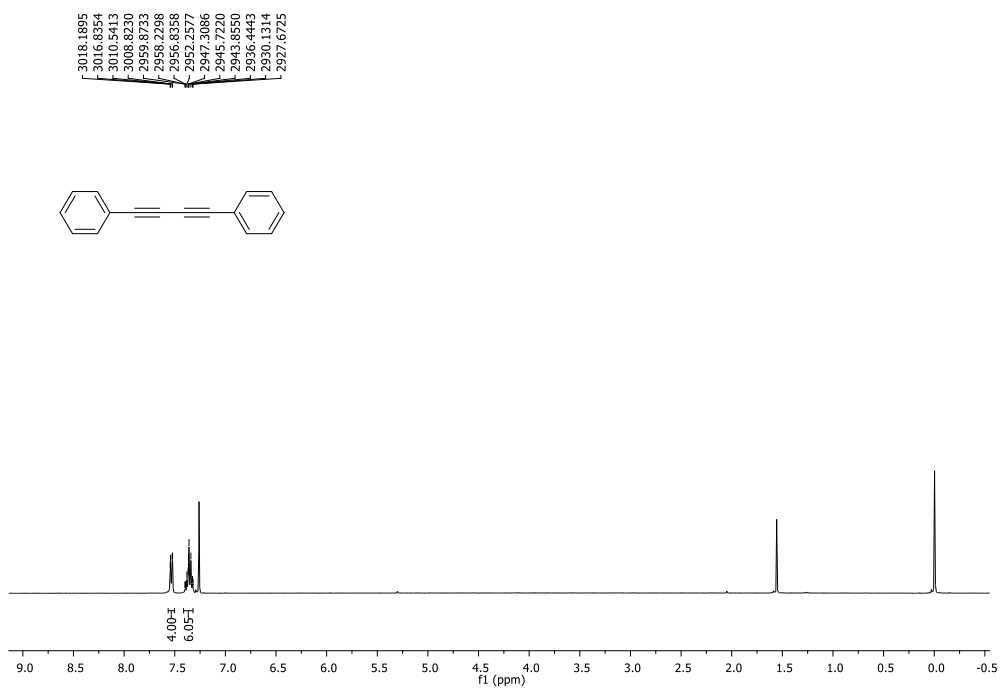
Figure 70. ^{1}H NMR spectrum of **114** in CDCl$_3$ solution (400 MHz).
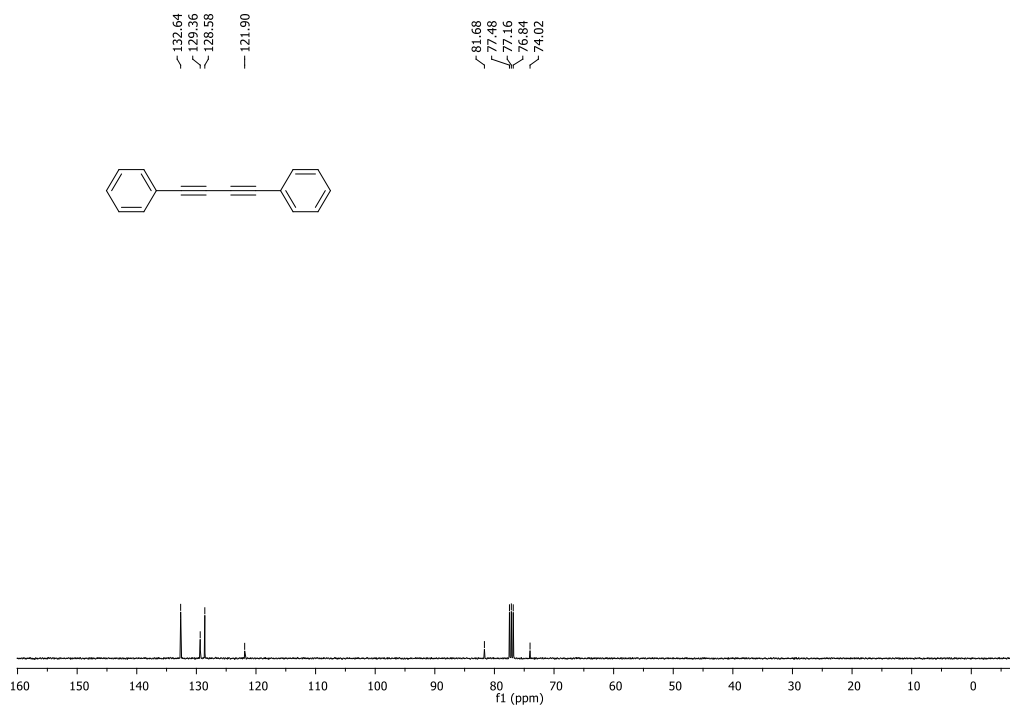
Figure 71. ^{13}C NMR spectrum of **114** in CDCl$_3$ solution (100 MHz).
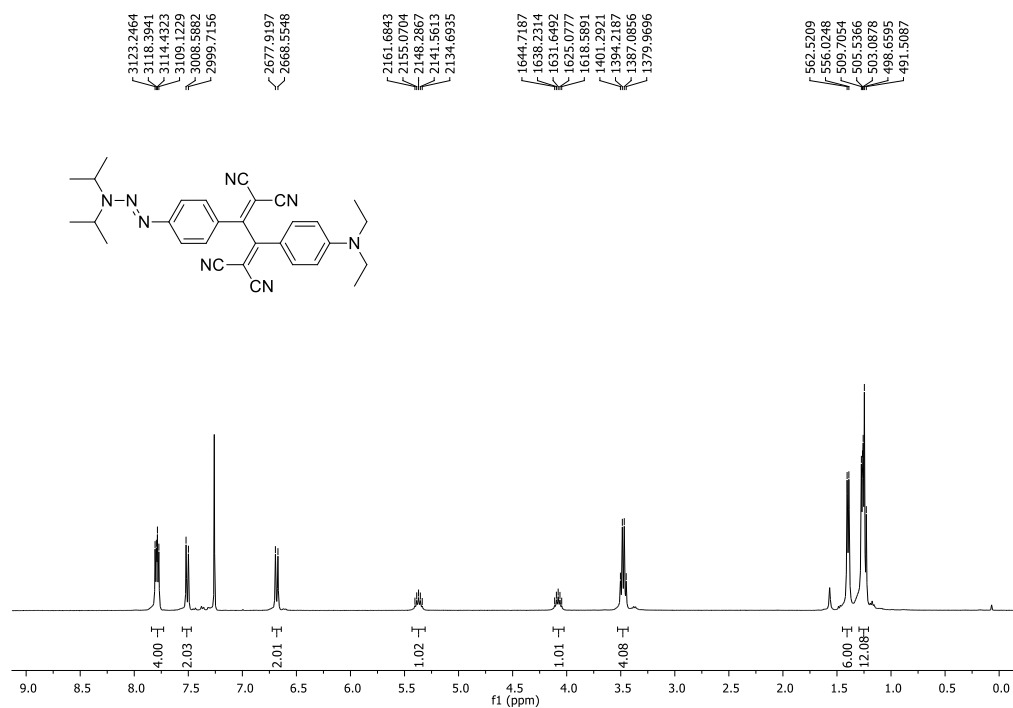
2985.1794
2976.6783
2952.6452
2944.0060
2649.0592
2640.1822
1518.5668
1511.4074
1504.2446
1497.0819
1359.7997
1352.7502
1345.6785
1338.6438
515.6523
508.6174
501.5759
477.3461
470.3195
463.2425
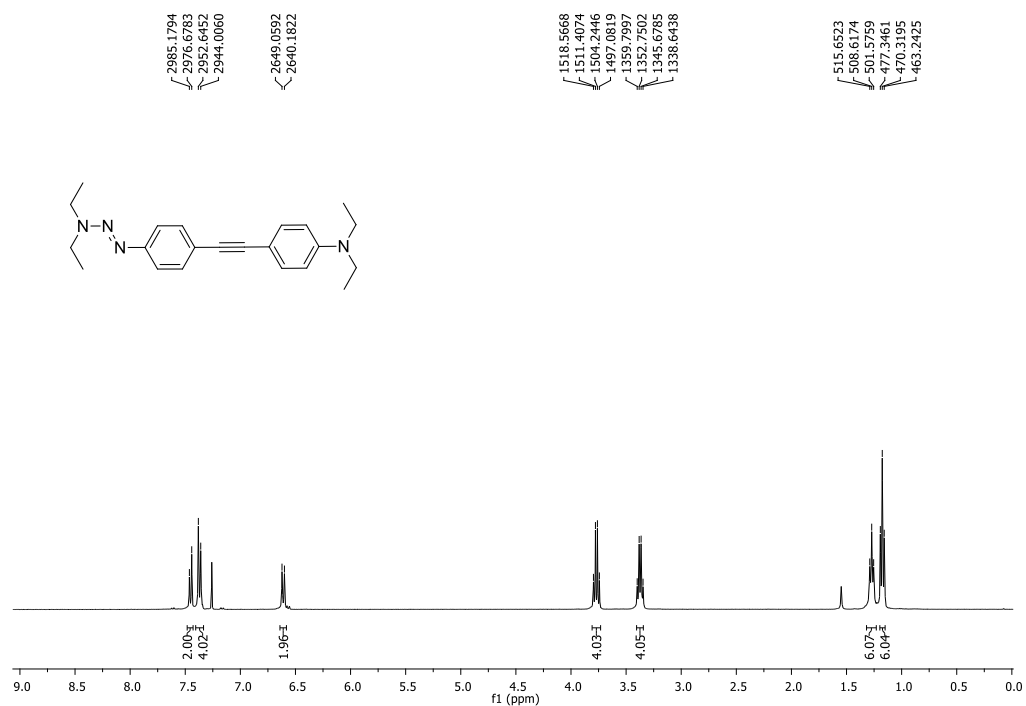
Figure 72 ^{1}H NMR spectrum of **125** in CDCl$_3$ solution (400 MHz).

150.5
147.6
133.0
132.0
120.8
120.5
111.4
109.6
90.6
87.8
77.5
77.2
76.8
44.5
12.7
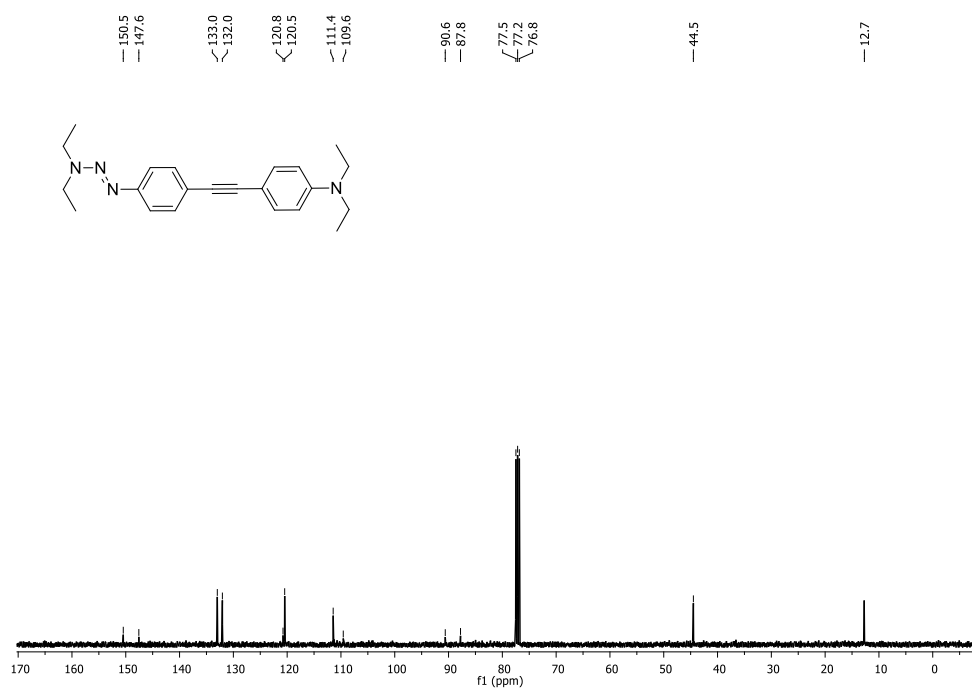
Figure 73. ^{13}C NMR spectrum of **125** in CDCl$_3$ solution (100 MHz).

122
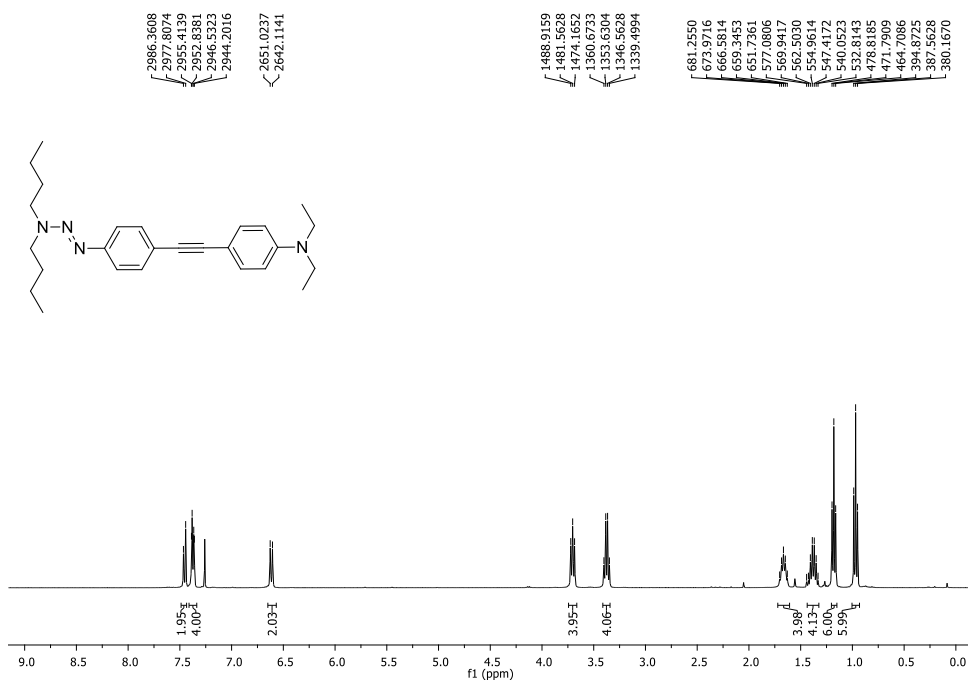
Figure 74. ^{1}H NMR spectrum of **126** in CDCl$_3$ solution (400 MHz).
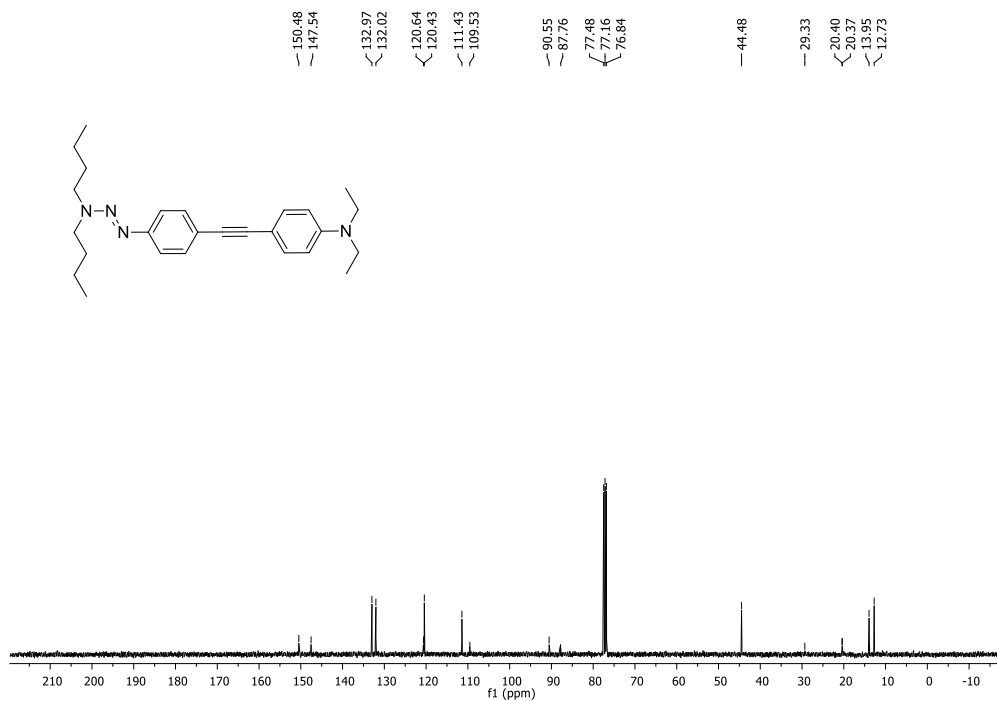
Figure 75. ^{13}C NMR spectrum of **126** in CDCl$_3$ solution (100 MHz).

123
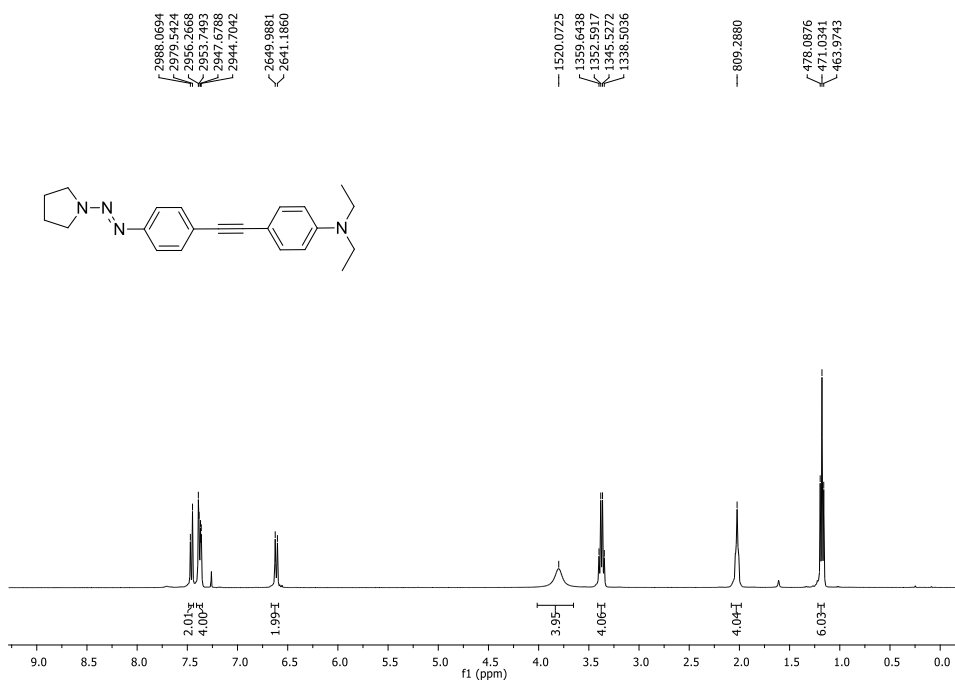
Figure 76. ^{1}H NMR spectrum of **127** in CDCl$_3$ solution (400 MHz).
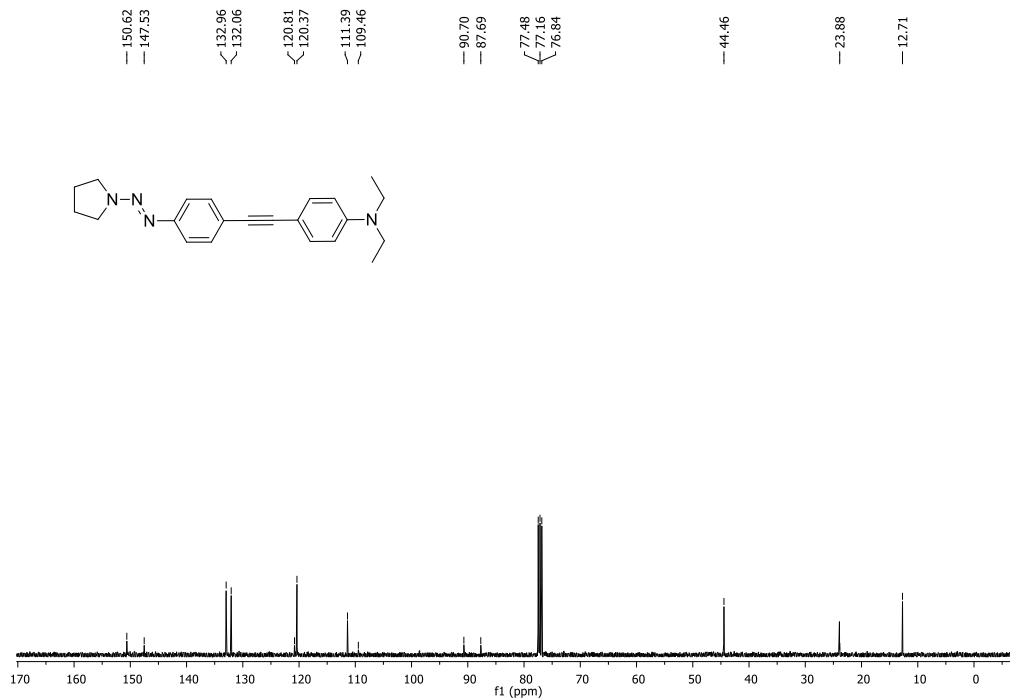
Figure 77. ^{13}C NMR spectrum of **127** in CDCl$_3$ solution (100 MHz).
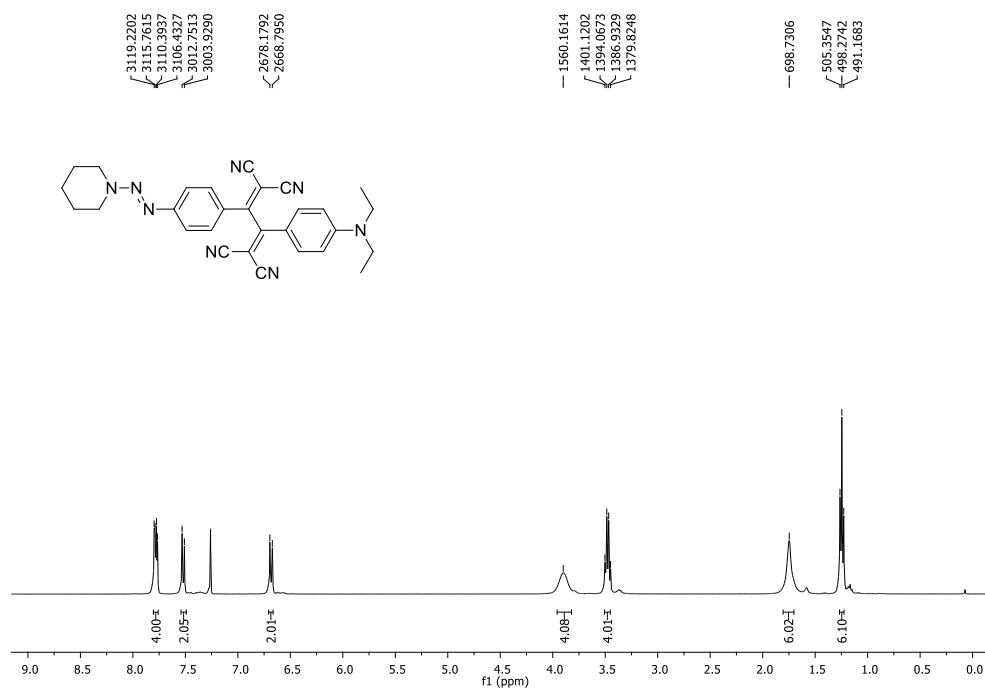
124
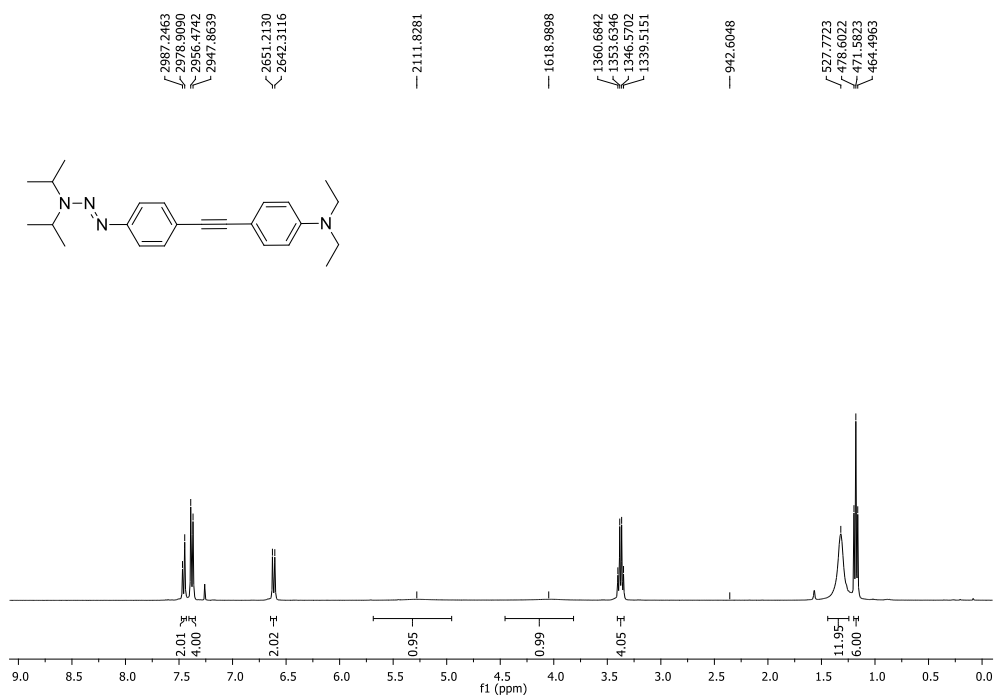
Figure 78. ^{1}H NMR spectrum of **128** in CDCl$_3$ solution (400 MHz).
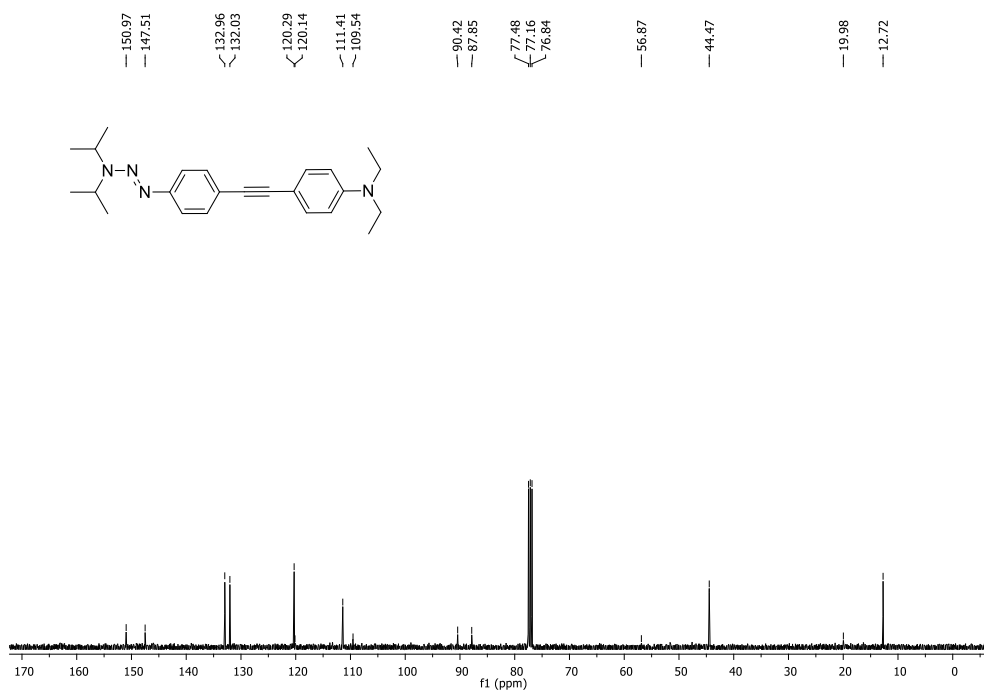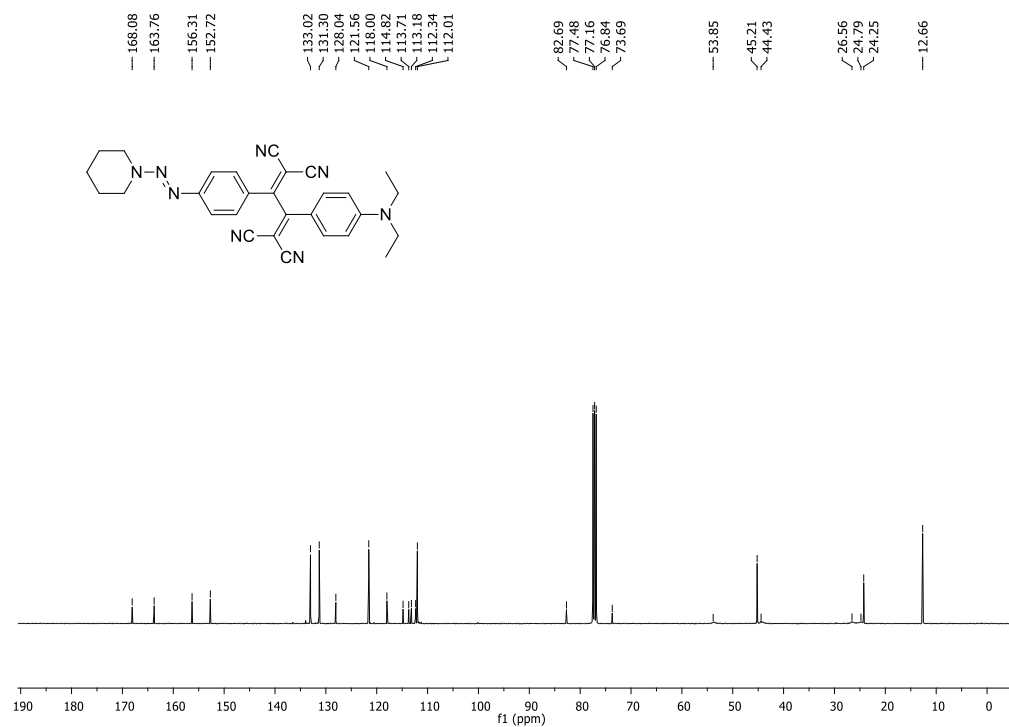

Figure 79. ^{13}C NMR spectrum of **128** in CDCl$_3$ solution (100 MHz).

125

Figure 80. ^{1}H NMR spectrum of **129** in CDCl$_3$ solution (400 MHz).

Figure 81. ^{13}C NMR spectrum of **129** in CDCl$_3$ solution (100 MHz).

126
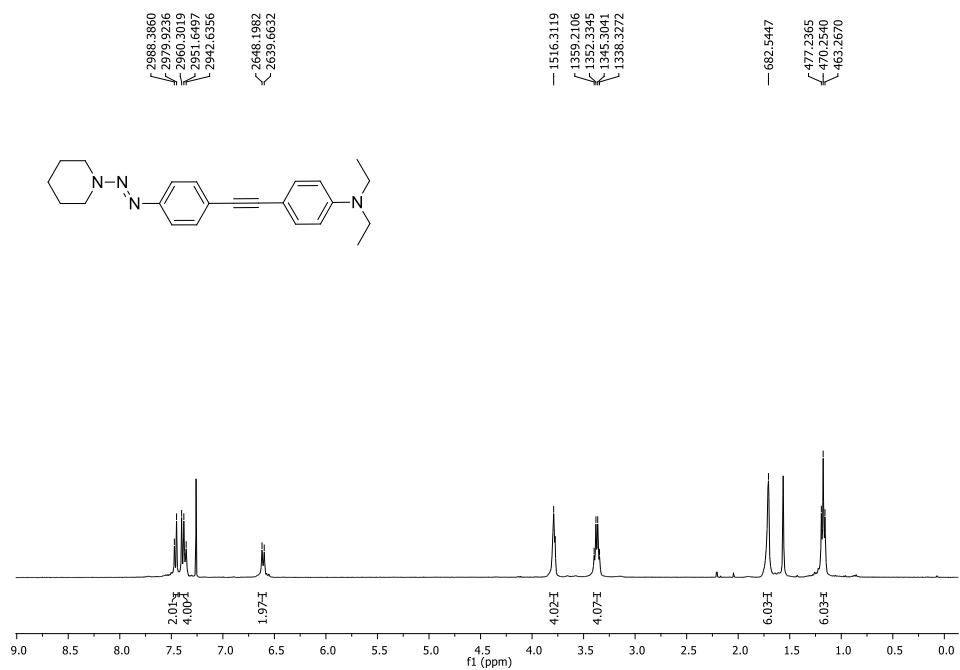
Figure 82. ^{1}H NMR spectrum of **130** in CDCl$_3$ solution (400 MHz).
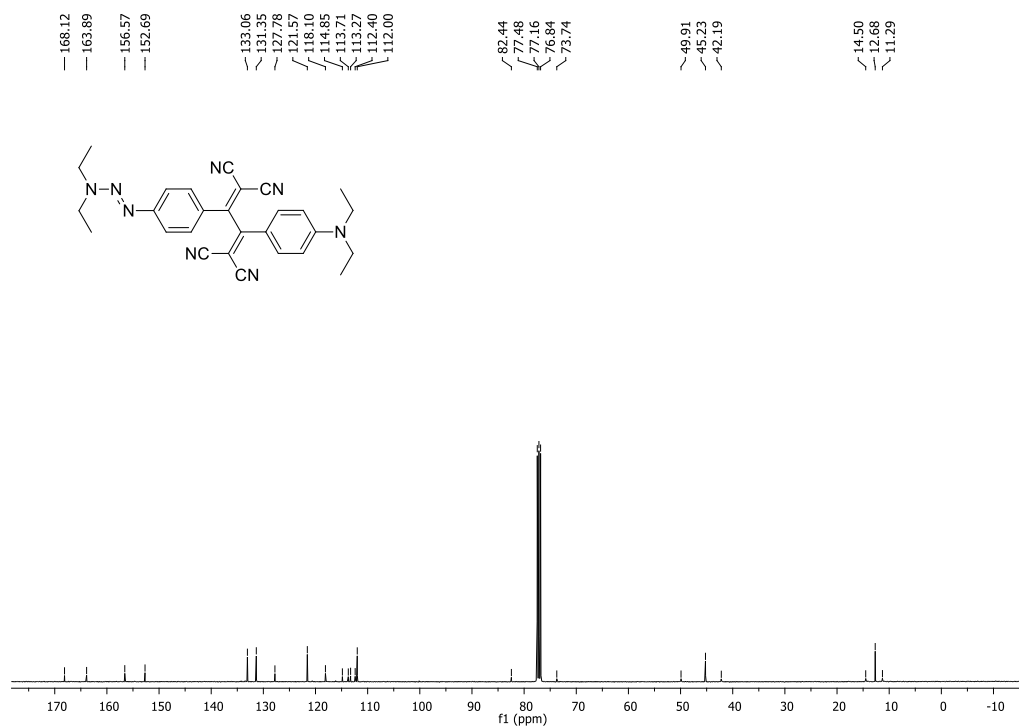
Figure 83. ^{13}C NMR spectrum of **130** in CDCl$_3$ solution (100 MHz).

127

3123.2464
3118.3941
3114.4323
3109.1229
3008.5882
2999.7156
2677.9197
2668.5548
2161.6843
2155.0704
2148.2867
2141.5613
2134.6935
1644.7187
1638.2314
1631.6492
1625.0777
1618.5891
1401.2921
1394.2187
1387.0856
1379.9696
562.5209
556.0248
509.7054
505.5366
503.0878
498.6595
491.5087

4.00 2.03 2.01 1.02 1.01 4.08 6.00 12.08

Figure 84. ^{1}H NMR spectrum of **131** in CDCl$_3$ solution (400 MHz).

168.00
163.93
157.08
152.70
133.02
131.38
127.40
121.37
118.03
114.84
113.74
113.36
112.48
111.99
81.95
77.48
77.16
76.84
73.66
50.29
47.55
45.20
23.95
19.38
12.65
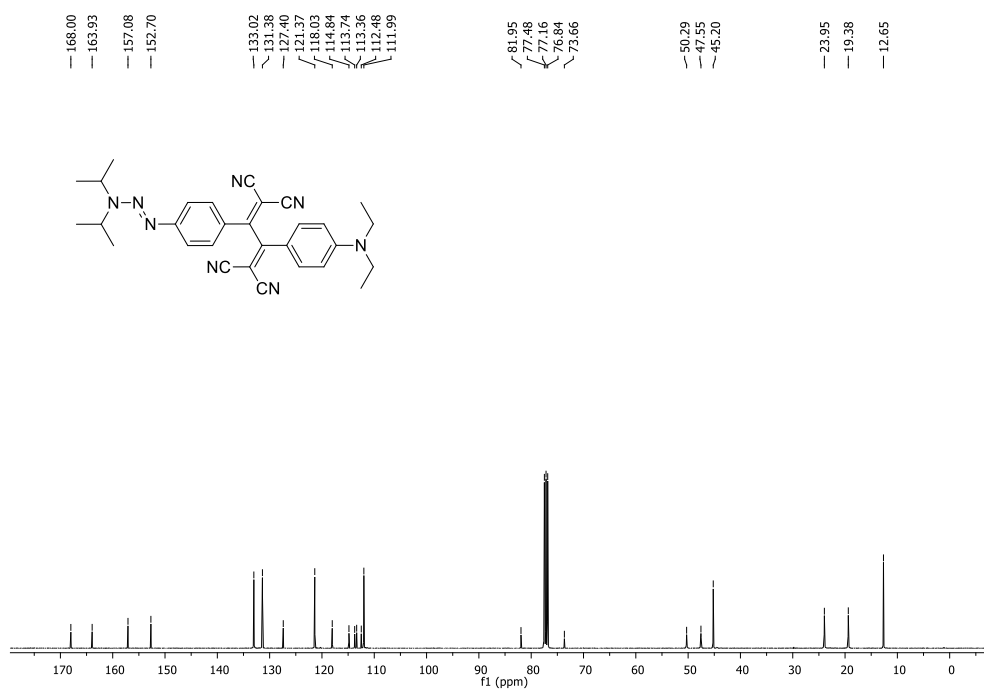
Figure 85. ^{13}C NMR spectrum of **131** in CDCl$_3$ solution (100 MHz).

128
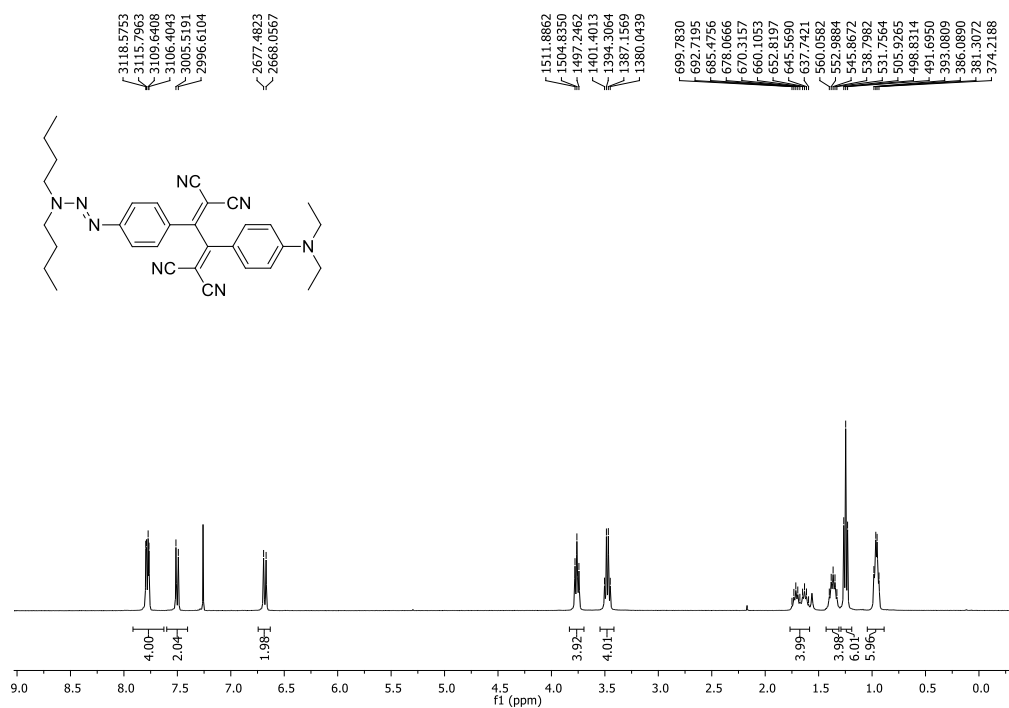
Figure 86. ^{1}H NMR spectrum of **132** in CDCl$_3$ solution (400 MHz).
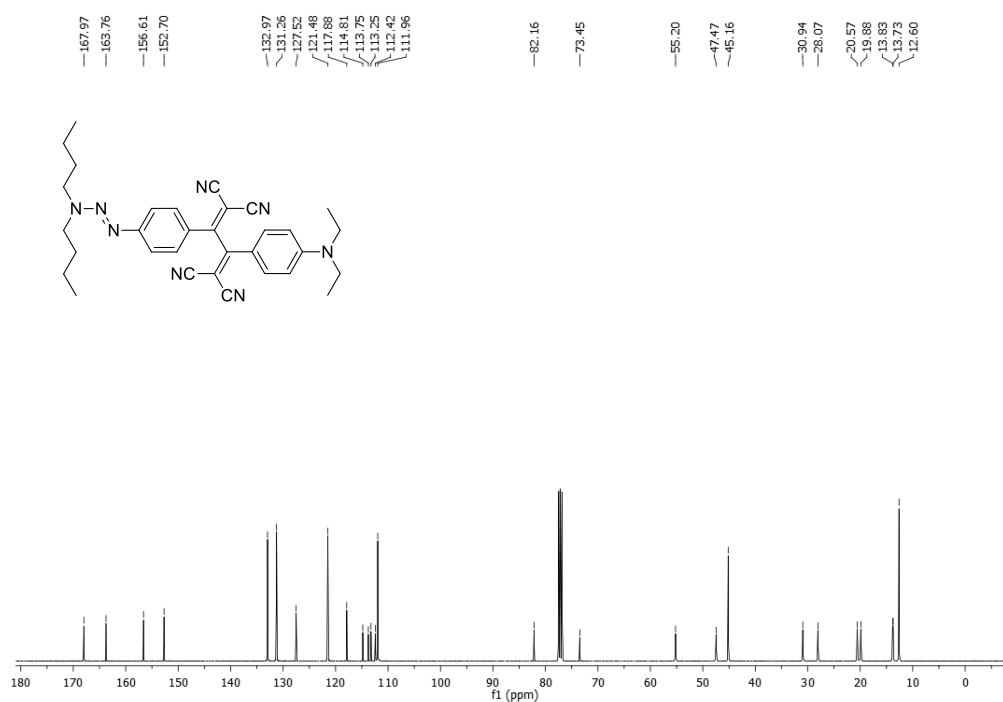
Figure 87. ^{13}C NMR spectrum of **132** in CDCl$_3$ solution (100 MHz).

129

Figure 88. ^{1}H NMR spectrum of **133** in CDCl$_3$ solution (400 MHz).

Figure 89. ^{13}C NMR spectrum of **133** in CDCl$_3$ solution (100 MHz).

130
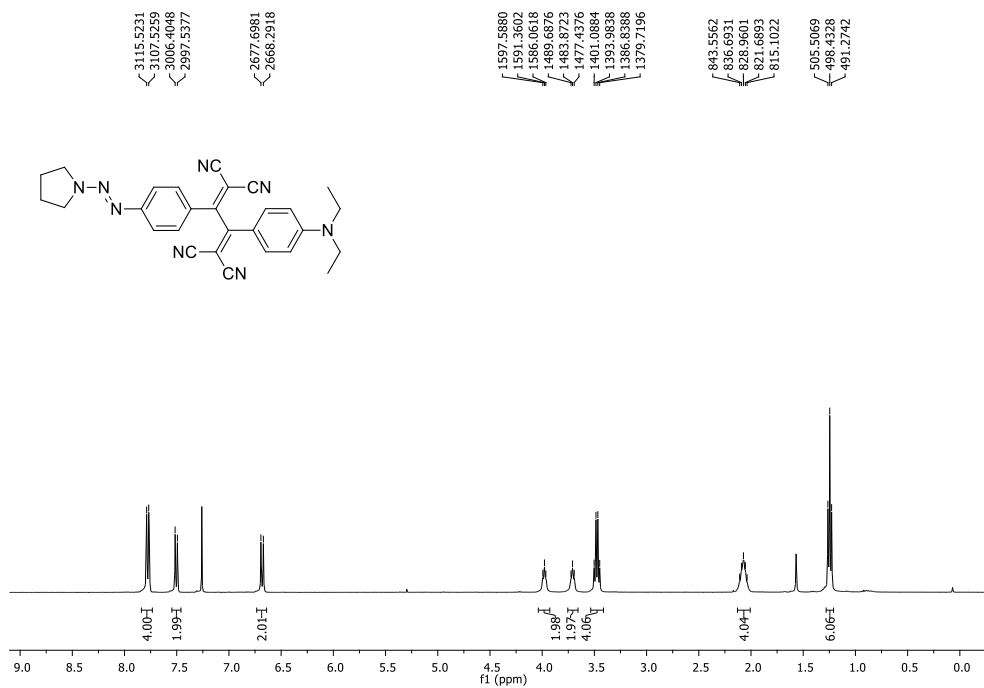
Figure 90. ^{1}H NMR spectrum of **134** in CDCl$_3$ solution (400 MHz).
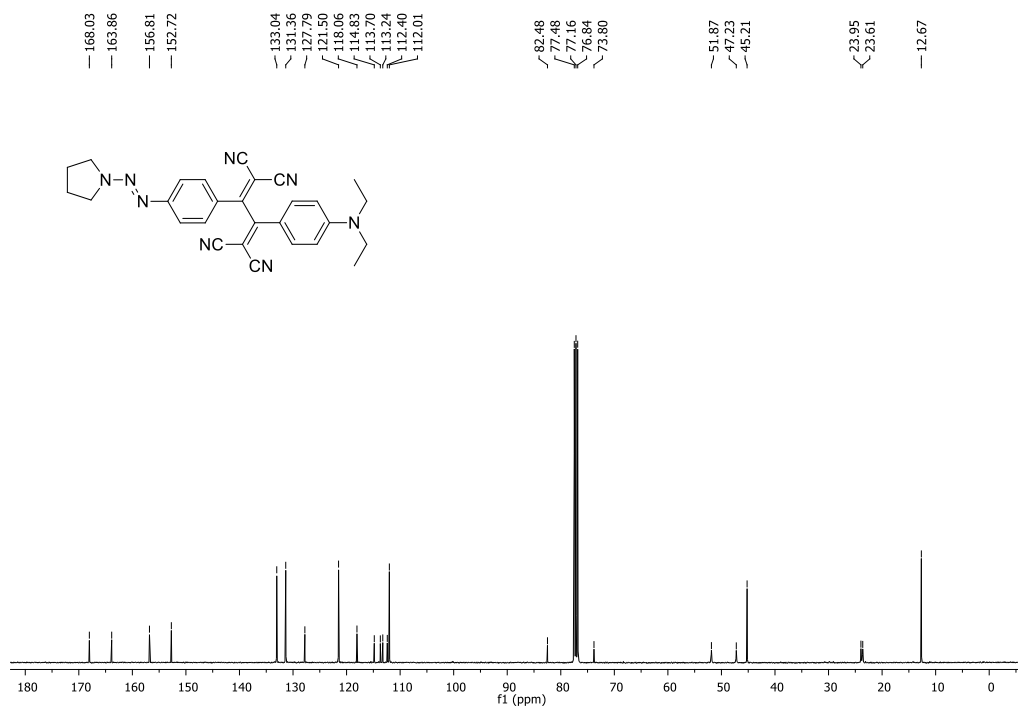
Figure 91. ^{13}C NMR spectrum of **134** in CDCl$_3$ solution (100 MHz).
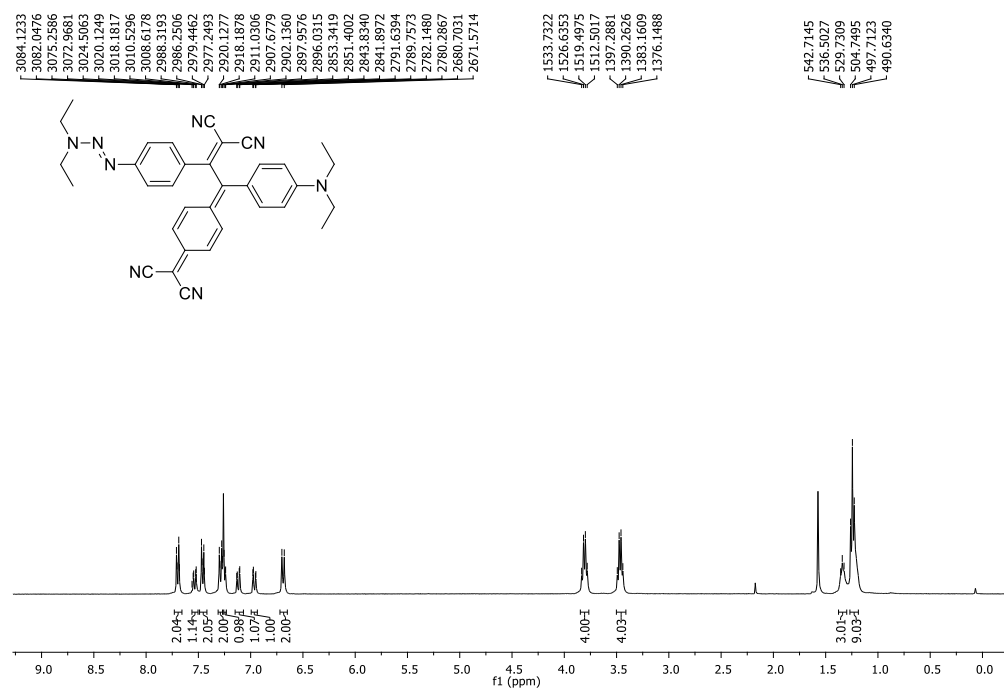
Figure 92. ^1H NMR spectrum of **135** in CDCl$_3$ solution (400 MHz).
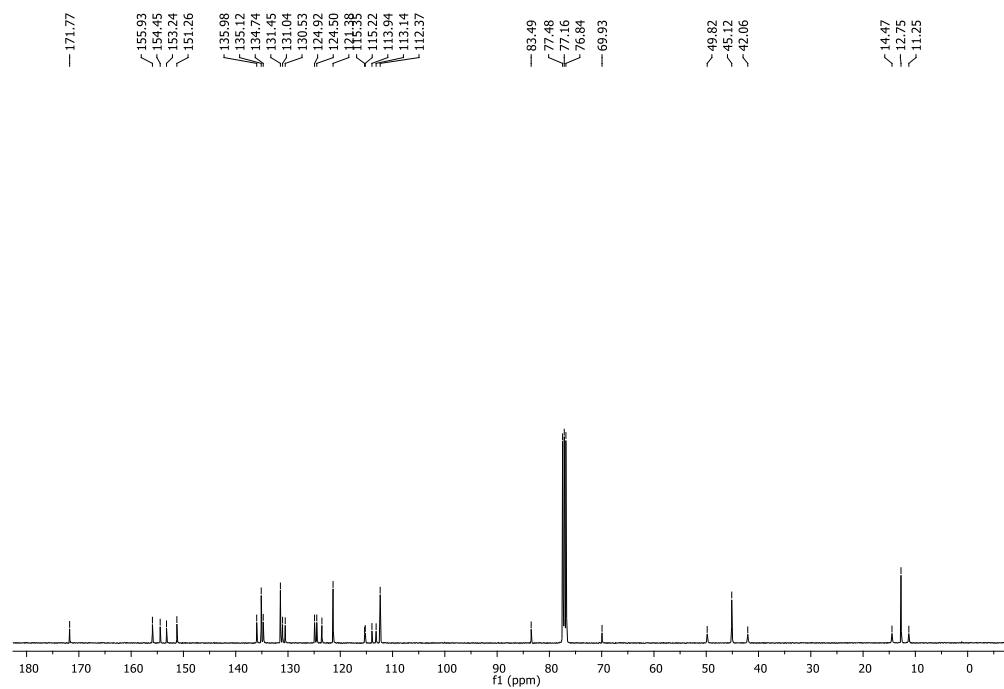
Figure 93. ^{13}C NMR spectrum of **135** in CDCl$_3$ solution (100 MHz).

132
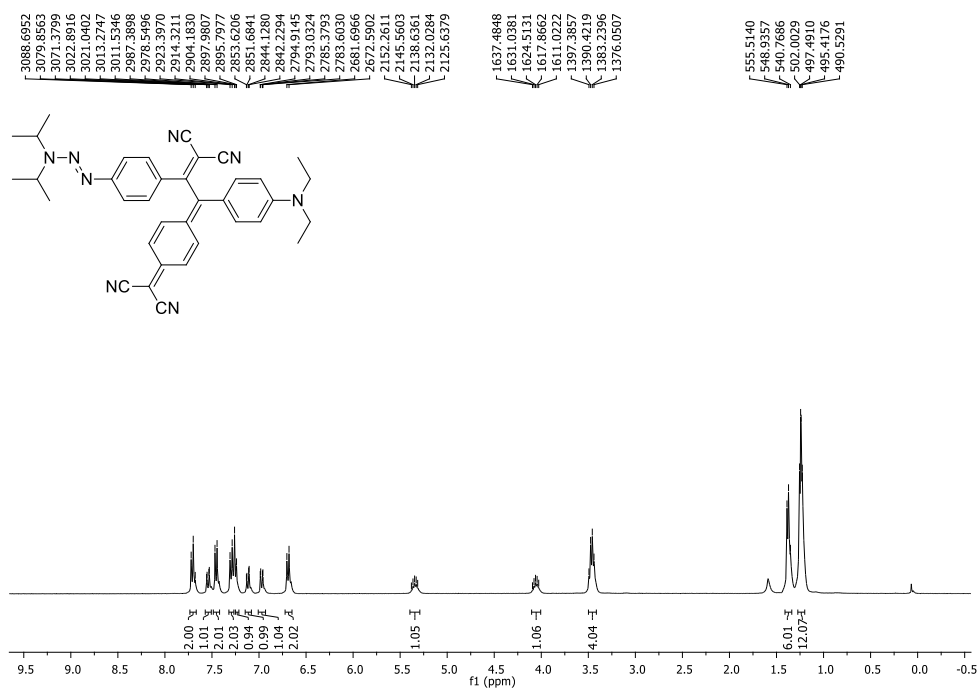
Figure 94. ^{1}H NMR spectrum of **136** in CDCl$_3$ solution (400 MHz).
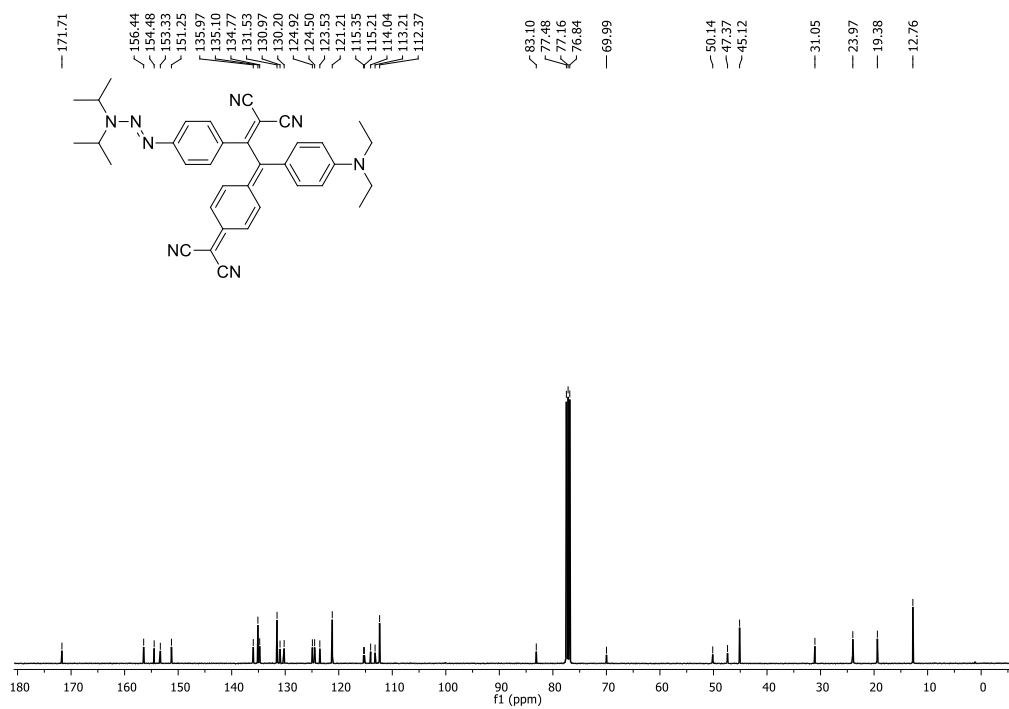
Figure 95. ^{13}C NMR spectrum of **136** in CDCl$_3$ solution (100 MHz).

133
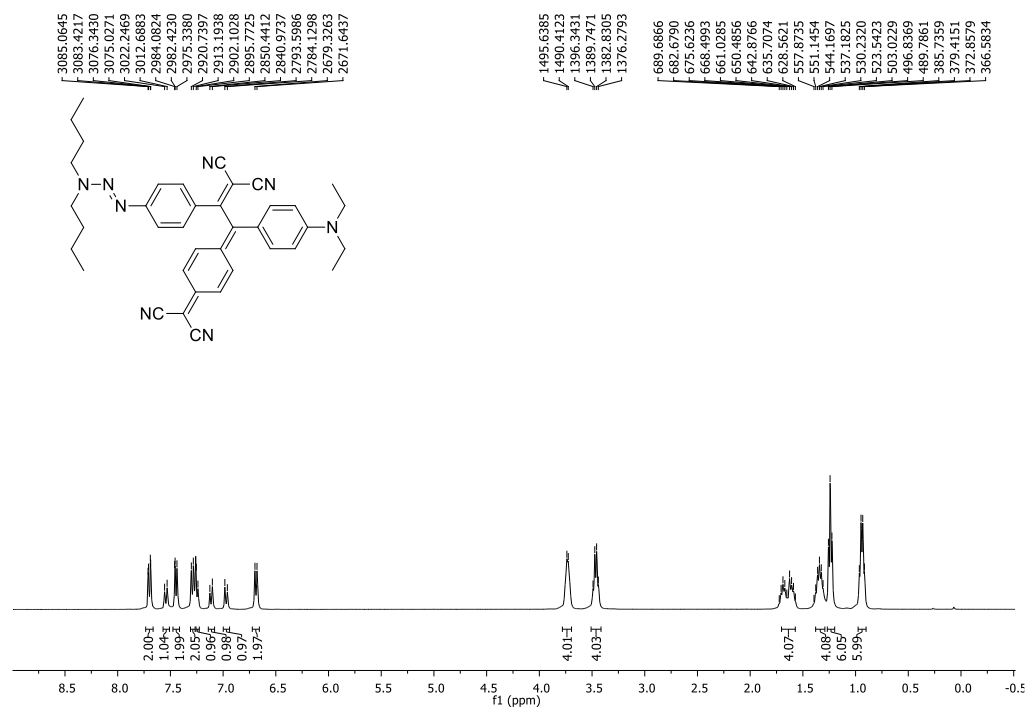
Figure 96. ^{1}H NMR spectrum of **137** in CDCl$_3$ solution (400 MHz).
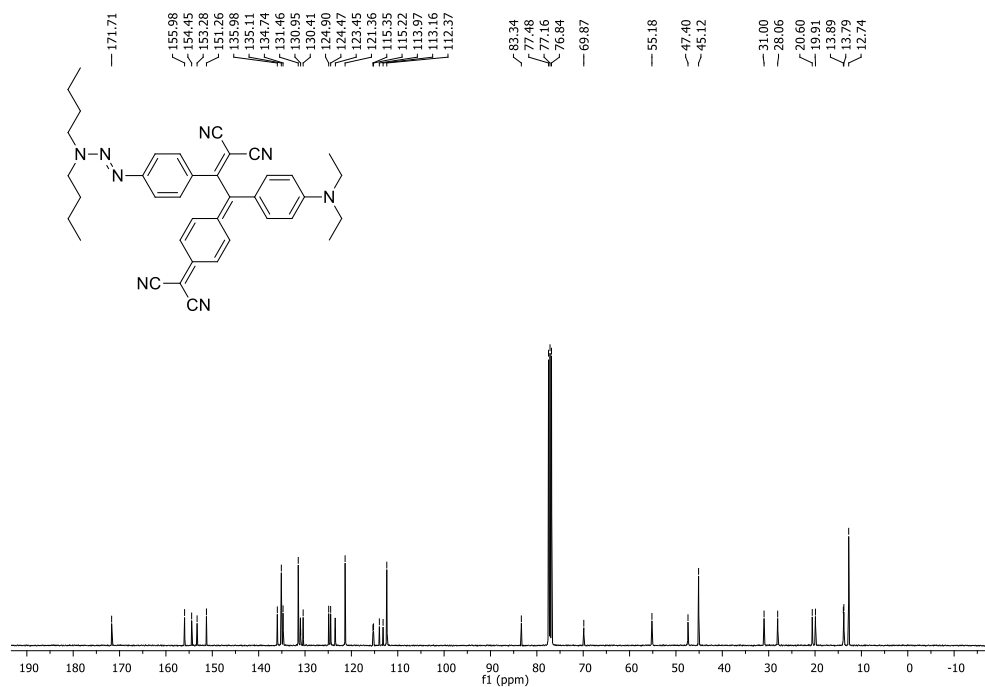
Figure 97. ^{13}C NMR spectrum of **137** in CDCl$_3$ solution (100 MHz).

134
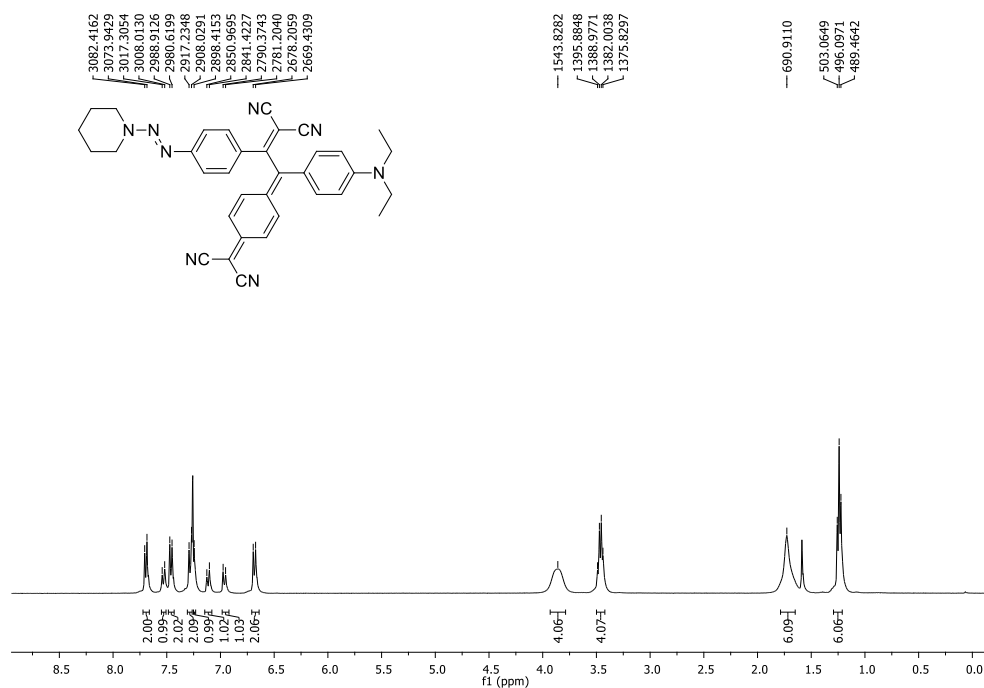
Figure 98. ^{1}H NMR spectrum of **138** in CDCl$_3$ solution (400 MHz).
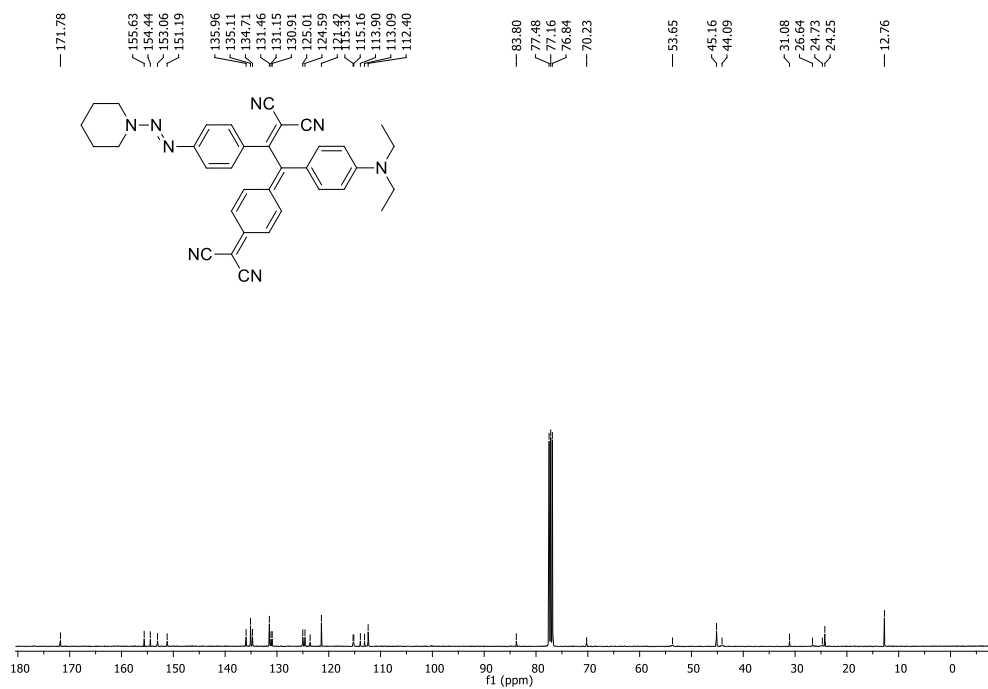
Figure 99. ^{13}C NMR spectrum of **138** in CDCl$_3$ solution (100 MHz).
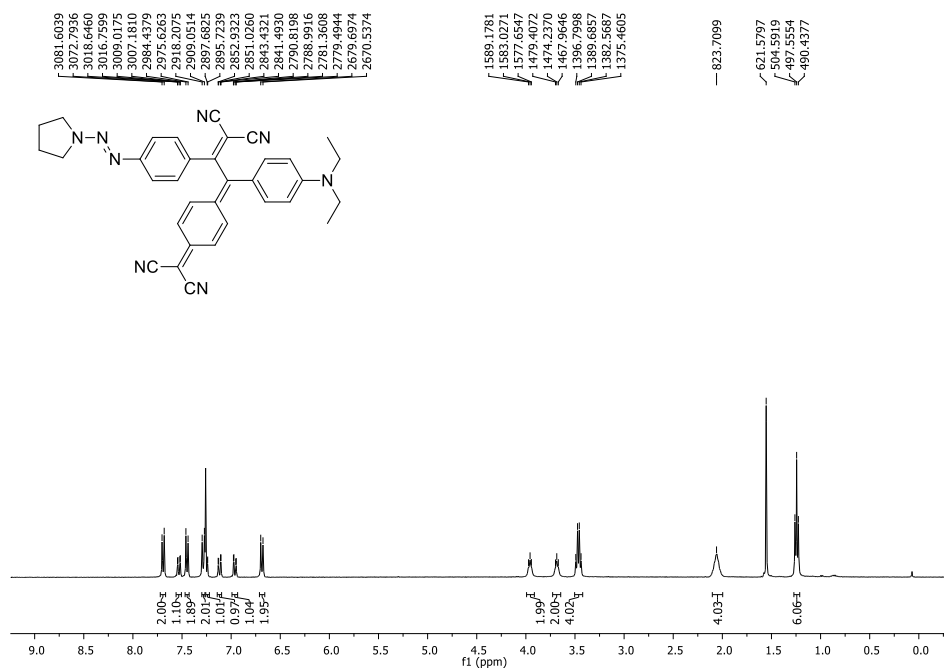
135

Figure 100. ^{1}H NMR spectrum of **139** in CDCl$_3$ solution (400 MHz).s
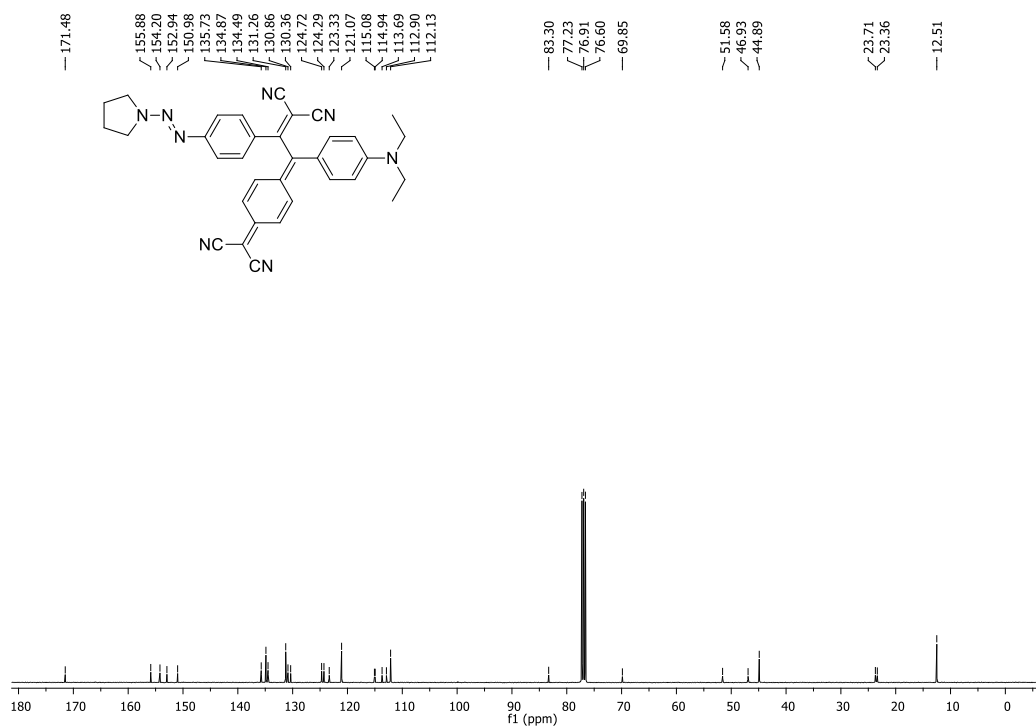

Figure 101. ^{13}C NMR spectrum of **139** in CDCl$_3$ solution (100 MHz)

136

B. HR-MS

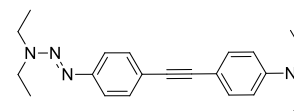**Elemental Composition Report** Page 1

Single Mass Analysis
Tolerance = 1000.0 PPM / DBE: min = -5.5, max = 1000.0
Element prediction: Off
Number of isotope peaks used for i-FIT = 9

Monoisotopic Mass, Even Electron Ions
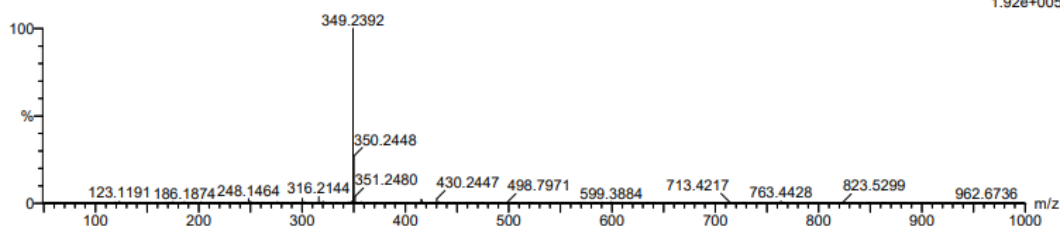1 formula(e) evaluated with 1 results within limits (all results (up to 1000) for each mass)
Elements Used:
C: 22-22   H: 28-29   N: 4-4
Flora Mammadova
34685_20211230_01-05 13 (0.518) Cm (7:17)

1: TOF MS ES+
1.92e+005

Mass	Calc. Mass	mDa	PPM	DBE	i-FIT	i-FIT (Norm)	Formula
349.2392	349.2392	0.0	0.0	10.5	1359.6	0.0	C22 H29 N4

Minimum: -5.5
Maximum: 1000.0 1000.0 1000.0

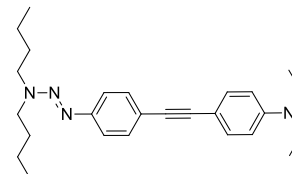---

Elemental Composition Report Page 1

Single Mass Analysis
Tolerance = 1000.0 PPM / DBE: min = -5.5, max = 1000.0
Element prediction: Off
Number of isotope peaks used for i-FIT = 3

Monoisotopic Mass, Even Electron Ions
1 formula(e) evaluated with 1 results within limits (all results (up to 1000) for each mass)
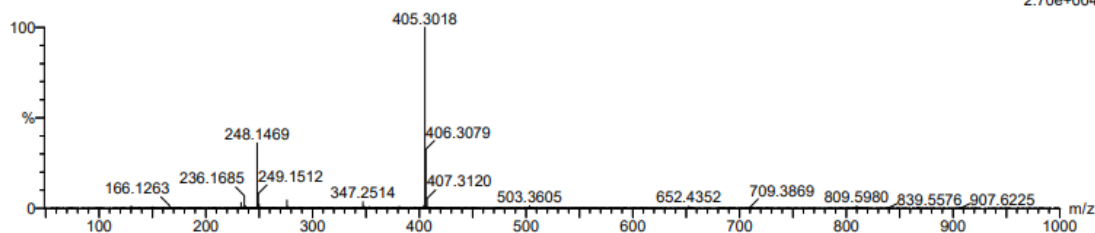Elements Used:
C: 26-26   H: 36-37   N: 4-4
Cagatay Dengiz
34143_20211103_11-03 1 (0.070) Cm (1:18)

1: TOF MS ES+
2.70e+004

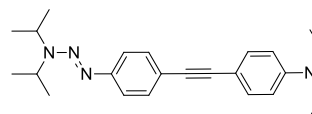| Mass	Calc. Mass	mDa	PPM	DBE	i-FIT	i-FIT (Norm)	Formula
405.3018	405.3018	0.0	0.0	10.5	354.6	0.0	C26 H37 N4

Minimum: -5.5
Maximum: 1000.0 1000.0 1000.0

137

Single Mass Analysis
Tolerance = 1000.0 PPM   /   DBE: min = -5.5, max = 1000.0
Element prediction: Off
Number of isotope peaks used for i-FIT = 9

Monoisotopic Mass, Even Electron Ions
1 formula(e) evaluated with 1 results within limits (all results (up to 1000) for each mass)
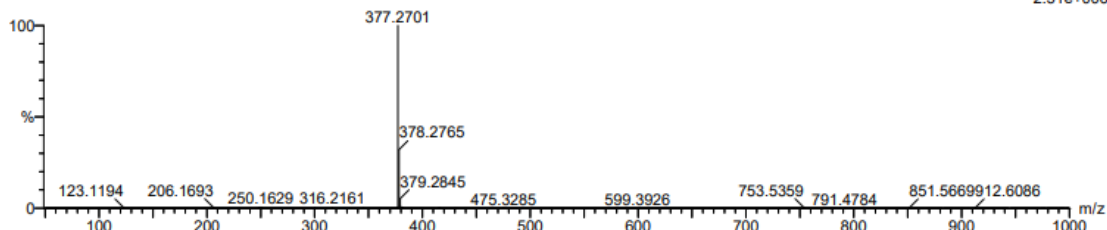Elements Used:
C: 24-24   H: 32-33   N: 4-4
Flora Mammadova
34685_20211230_02-03 20 (0.775) Cm (10:20)   1: TOF MS ES+
                                                              2.51e+006

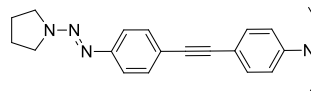| Minimum: | | | | -5.5 | | | |
Maximum:		1000.0	1000.0	1000.0			
Mass	Calc. Mass	mDa	PPM	DBE	i-FIT	i-FIT (Norm)	Formula
377.2701	377.2705	-0.4	-1.1	10.5	1808.1	0.0	C24 H33 N4

Single Mass Analysis
Tolerance = 1000.0 PPM   /   DBE: min = -5.5, max = 1000.0
Element prediction: Off
Number of isotope peaks used for i-FIT = 9

Monoisotopic Mass, Even Electron Ions
1 formula(e) evaluated with 1 results within limits (all results (up to 1000) for each mass)
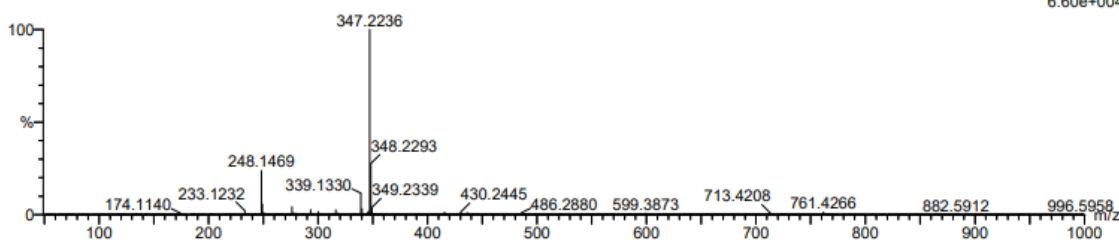Elements Used:
C: 22-22   H: 26-27   N: 4-4
Flora Mammadova
34685_20211230_04-01 20 (0.775) Cm (13:23)   1: TOF MS ES+
                                                              6.60e+004

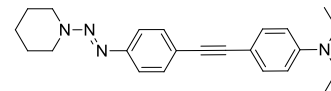| Minimum: | | | | -5.5 | | | |
Maximum:		1000.0	1000.0	1000.0			
Mass	Calc. Mass	mDa	PPM	DBE	i-FIT	i-FIT (Norm)	Formula
347.2236	347.2236	0.0	0.0	11.5	1146.0	0.0	C22 H27 N4

138

Elemental Composition Report

Single Mass Analysis
Tolerance = 1000.0 PPM   /   DBE: min = -5.5, max = 1000.0
Element prediction: Off
Number of isotope peaks used for i-FIT = 9

Monoisotopic Mass, Even Electron Ions
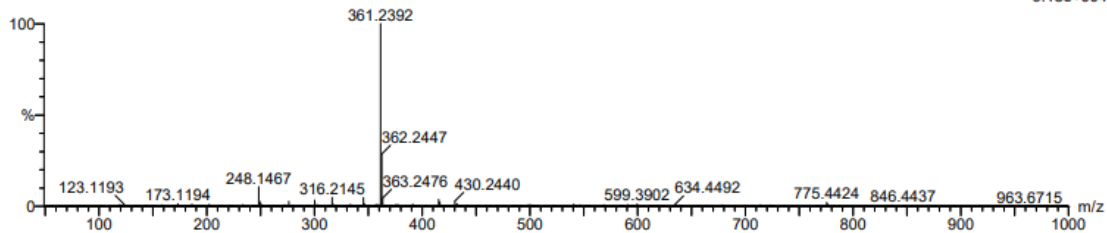1 formula(e) evaluated with 1 results within limits (all results (up to 1000) for each mass)
Elements Used:
C: 23-23   H: 28-29   N: 4-4
Flora Mammadova
34685_20211230_03-02 15 (0.586) Cm (5:18)

1: TOF MS ES+
9.18e+004

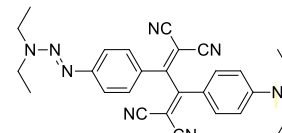| Minimum:				-5.5			
Maximum:		1000.0	1000.0	1000.0			
Mass	Calc. Mass	mDa	PPM	DBE	i-FIT	i-FIT (Norm)	Formula
361.2392	361.2392	0.0	0.0	11.5	1231.1	0.0	C23 H29 N4

Elemental Composition Report

Single Mass Analysis
Tolerance = 1000.0 PPM   /   DBE: min = -5.5, max = 1000.0
Element prediction: Off
Number of isotope peaks used for i-FIT = 3

Monoisotopic Mass, Odd and Even Electron Ions
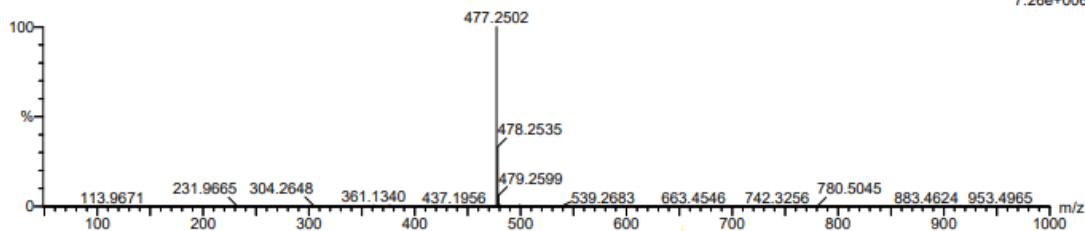1 formula(e) evaluated with 1 results within limits (all results (up to 1000) for each mass)
Elements Used:
C: 28-28   H: 28-29   N: 8-8
Cagatay Dengiz
34143_20211103_01-02 6 (0.260) Cm (1:8)

1: TOF MS ES+
7.26e+006

Minimum:				-5.5			
Maximum:		1000.0	1000.0	1000.0			
Mass	Calc. Mass	mDa	PPM	DBE	i-FIT	i-FIT (Norm)	Formula
477.2502	477.2515	-1.3	-2.7	18.5	640.6	0.0	C28 H29 N8

139

Single Mass Analysis
Tolerance = 1000.0 PPM   /   DBE: min = -5.5, max = 1000.0
Element prediction: Off
Number of isotope peaks used for i-FIT = 3
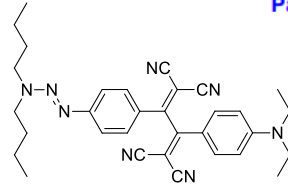
Monoisotopic Mass, Even Electron Ions
1 formula(e) evaluated with 1 results within limits (all results (up to 1000) for each mass)
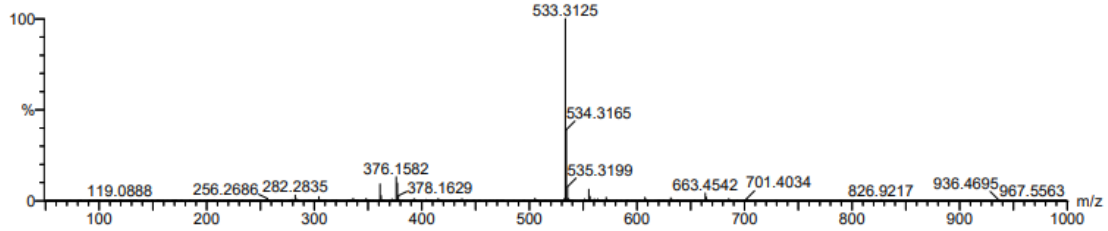Elements Used:
C: 32-32   H: 36-37   N: 8-8
Cagatay Dengiz
34143_20211103_03-05 11 (0.450) Cm (8:21)

1: TOF MS ES+
2.38e+005

Mass	Calc. Mass	mDa	PPM	DBE	i-FIT	i-FIT (Norm)	Formula
533.3125	533.3141	-1.6	-3.0	18.5	426.9	0.0	C32 H37 N8

Single Mass Analysis
Tolerance = 1000.0 PPM   /   DBE: min = -5.5, max = 1000.0
Element prediction: Off
Number of isotope peaks used for i-FIT = 3
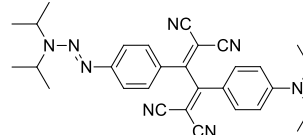
Monoisotopic Mass, Even Electron Ions
1 formula(e) evaluated with 1 results within limits (all results (up to 1000) for each mass)
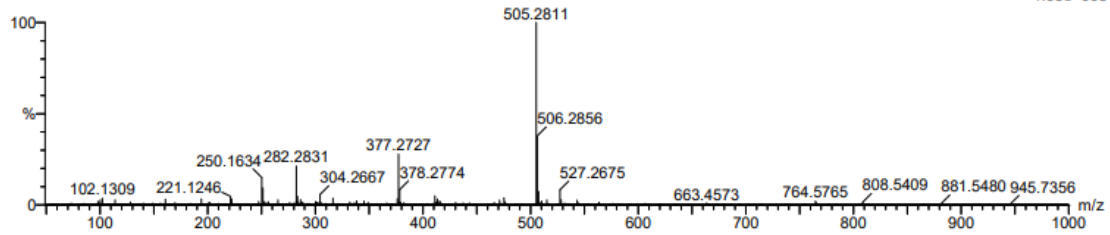Elements Used:
C: 30-30   H: 32-33   N: 8-8
Cagatay Dengiz
34143_20211103_02-06 23 (0.897) Cm (15:24)

1: TOF MS ES+
1.03e+005

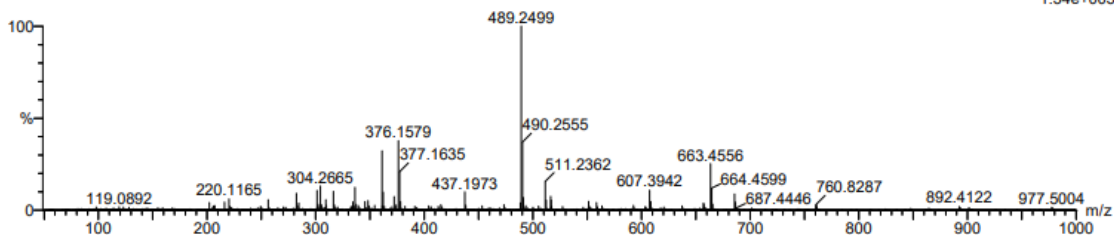| Mass	Calc. Mass	mDa	PPM	DBE	i-FIT	i-FIT (Norm)	Formula
505.2811	505.2828	-1.7	-3.4	18.5	386.6	0.0	C30 H33 N8

Single Mass Analysis
Tolerance = 1000.0 PPM   /   DBE: min = -5.5, max = 1000.0
Element prediction: Off
Number of isotope peaks used for i-FIT = 3
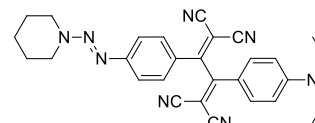
Monoisotopic Mass, Even Electron Ions
1 formula(e) evaluated with 1 results within limits (all results (up to 1000) for each mass)
Elements Used:
C: 29-29   H: 28-29   N: 8-8
Cagatay Dengiz
34143_20211103_05-03 6 (0.260) Cm (1:10)
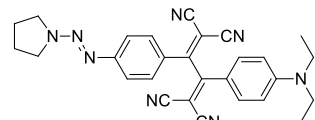
1: TOF MS ES+
1.34e+005

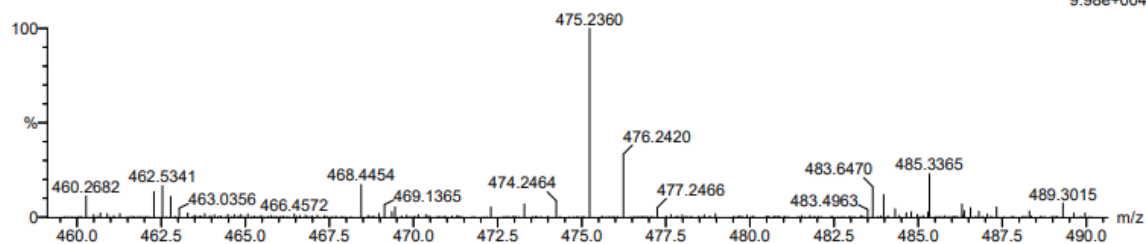| Minimum:				-5.5			
Maximum:		1000.0	1000.0	1000.0			
Mass	Calc. Mass	mDa	PPM	DBE	i-FIT	i-FIT (Norm)	Formula
489.2499	489.2515	-1.6	-3.3	19.5	430.1	0.0	C29 H29 N8

Single Mass Analysis
Tolerance = 1000.0 PPM   /   DBE: min = -5.5, max = 1000.0
Element prediction: Off
Number of isotope peaks used for i-FIT = 9

Monoisotopic Mass, Even Electron Ions
1 formula(e) evaluated with 1 results within limits (all results (up to 1000) for each mass)
Elements Used:
C: 28-28   H: 26-27   N: 8-8
Flora Mammadova
34685_20211230_09-04 11 (0.450) Cm (6:16)

1: TOF MS ES+
9.98e+004

Minimum:				-5.5			
Maximum:		1000.0	1000.0	1000.0			
Mass	Calc. Mass	mDa	PPM	DBE	i-FIT	i-FIT (Norm)	Formula
475.2360	475.2359	0.1	0.2	19.5	715.4	0.0	C28 H27 N8

141

Elemental Composition Report

Single Mass Analysis
Tolerance = 1000.0 PPM / DBE: min = -5.5, max = 1000.0
Element prediction: Off
Number of isotope peaks used for i-FIT = 3

Monoisotopic Mass, Even Electron Ions
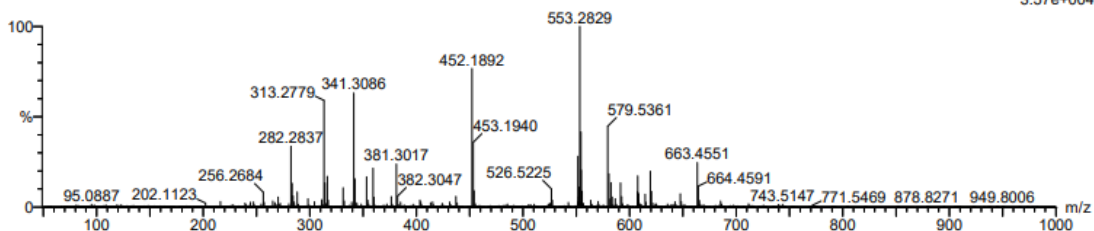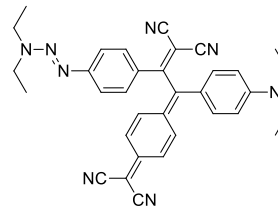1 formula(e) evaluated with 1 results within limits (all results (up to 1000) for each mass)
Elements Used:
C: 34-34   H: 32-33   N: 8-8

Cagatay Dengiz
34143_20211103_06-05 1 (0.070) Cm (1:15)

1: TOF MS ES+
3.57e+004

Minimum:				-5.5			
Maximum:		1000.0	1000.0	1000.0			
Mass	Calc. Mass	mDa	PPM	DBE	i-FIT	i-FIT (Norm)	Formula
553.2829	553.2828	0.1	0.2	22.5	262.0	0.0	C34 H33 N8

Elemental Composition Report

Single Mass Analysis
Tolerance = 1000.0 PPM / DBE: min = -5.5, max = 1000.0
Element prediction: Off
Number of isotope peaks used for i-FIT = 3

Monoisotopic Mass, Even Electron Ions
1 formula(e) evaluated with 1 results within limits (all results (up to 1000) for each mass)
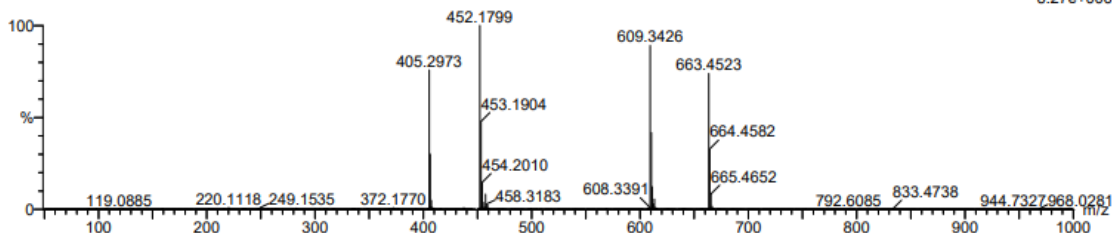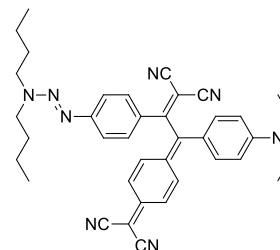Elements Used:
C: 38-38   H: 40-41   N: 8-8

Cagatay Dengiz
34143_20211104_08-06 4 (0.172) Cm (1:8)

1: TOF MS ES+
8.27e+006

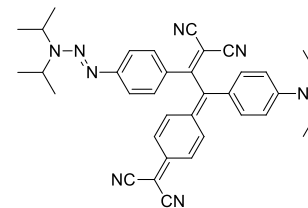| Minimum:				-5.5			
Maximum:		1000.0	1000.0	1000.0			
Mass	Calc. Mass	mDa	PPM	DBE	i-FIT	i-FIT (Norm)	Formula
609.3426	609.3454	-2.8	-4.6	22.5	374.4	0.0	C38 H41 N8

142

Single Mass Analysis
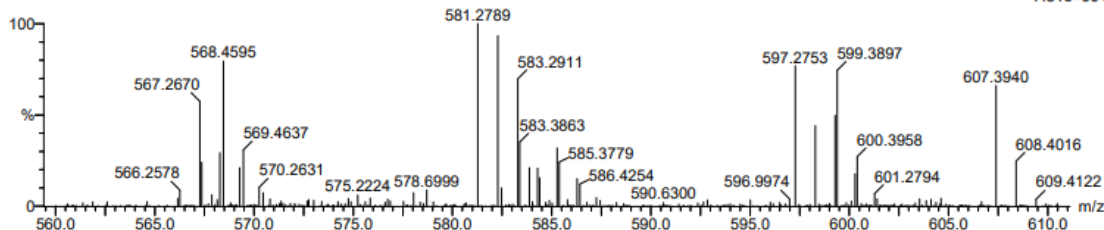Tolerance = 1000.0 PPM / DBE: min = -5.5, max = 1000.0
Element prediction: Off
Number of isotope peaks used for i-FIT = 9

Monoisotopic Mass, Even Electron Ions
1 formula(e) evaluated with 1 results within limits (all results (up to 1000) for each mass)
Elements Used:
C: 36-36 H: 36-37 N: 8-8
Flora Mammadova
34685_20211230_10-08 9 (0.362) Cm (1:15)   1: TOF MS ES+
                     7.81e+004

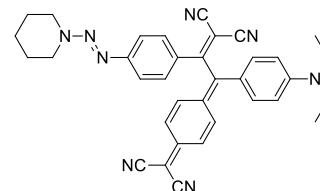| Minimum:				-5.5			
Maximum:		1000.0	1000.0	1000.0			
Mass	Calc. Mass	mDa	PPM	DBE	i-FIT	i-FIT (Norm)	Formula
581.2789	581.3141	-35.2	-60.6	22.5	708.4	0.0	C36 H37 N8

Single Mass Analysis
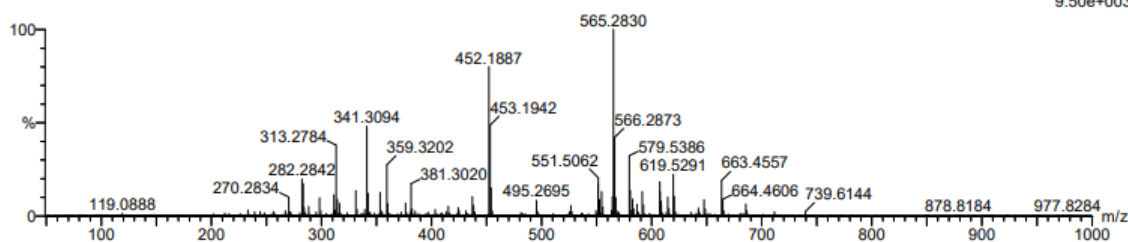Tolerance = 1000.0 PPM / DBE: min = -5.5, max = 1000.0
Element prediction: Off
Number of isotope peaks used for i-FIT = 3

Monoisotopic Mass, Even Electron Ions
1 formula(e) evaluated with 1 results within limits (all results (up to 1000) for each mass)
Elements Used:
C: 35-35 H: 32-33 N: 8-8
Cagatay Dengiz
34143_20211103_10-04 22 (0.863) Cm (13:25)   1: TOF MS ES+
                     9.50e+003

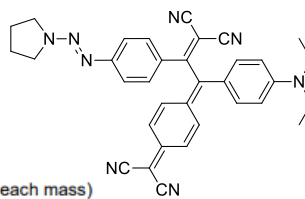| Minimum:				-5.5			
Maximum:		1000.0	1000.0	1000.0			
Mass	Calc. Mass	mDa	PPM	DBE	i-FIT	i-FIT (Norm)	Formula
565.2830	565.2828	0.2	0.4	23.5	245.6	0.0	C35 H33 N8

Single Mass Analysis
Tolerance = 1000.0 PPM   /   DBE: min = -5.5, max = 1000.0
Element prediction: Off
Number of isotope peaks used for i-FIT = 3

Monoisotopic Mass, Even Electron Ions
1 formula(e) evaluated with 1 results within limits (all results (up to 1000) for each mass)
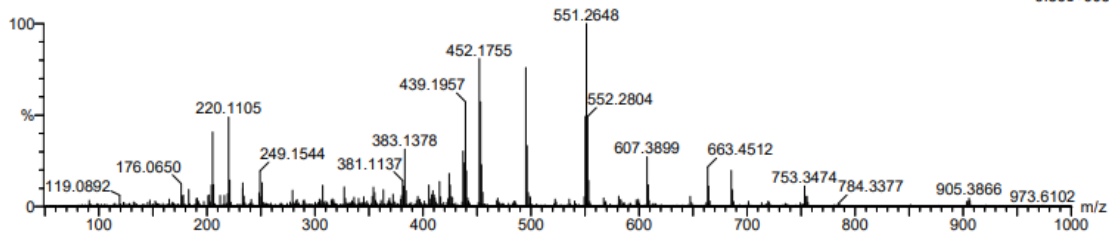Elements Used:
C: 34-34   H: 30-31   N: 8-8
Cagatay Dengiz
34143_20211104_09-03 5 (0.206) Cm (1:8)

1: TOF MS ES+
9.86e+003

Minimum:				-5.5			
Maximum:		1000.0	1000.0	1000.0			
Mass	Calc. Mass	mDa	PPM	DBE	i-FIT	i-FIT (Norm)	Formula
551.2648	551.2672	-2.4	-4.4	23.5	255.9	0.0	C34 H31 N8

144